



Universitat Autònoma de Barcelona

ADVERTIMENT. L'accés als continguts d'aquesta tesi queda condicionat a l'acceptació de les condicions d'ús establertes per la següent llicència Creative Commons:  http://cat.creativecommons.org/?page_id=184

ADVERTENCIA. El acceso a los contenidos de esta tesis queda condicionado a la aceptación de las condiciones de uso establecidas por la siguiente licencia Creative Commons:  <http://es.creativecommons.org/blog/licencias/>

WARNING. The access to the contents of this doctoral thesis it is limited to the acceptance of the use conditions set by the following Creative Commons license:  <https://creativecommons.org/licenses/?lang=en>



Universitat Autònoma de Barcelona

***Physiopathological and Molecular Characterization
of a Transgenic Mouse Overexpressing
TNFalpha in Schwann Cells
Reveals a Model for
Chronic Peripheral Neuropathy***

Belén García-Lareu

ACADEMIC DISSERTATION

To obtain the degree of PhD in Biochemistry, Molecular Biology and
Biomedicine by the Universitat Autònoma de Barcelona

Bellaterra, 2017

Supervised by

Dr. Assumpció Bosch i Merino

The research described in this thesis was conducted at the Department of Biochemistry and Molecular Biology – Center of Animal Biotechnology and Gene Therapy (CBATEG) – Institute of Neurosciences (INc), at the Universitat Autònoma de Barcelona (UAB) in the Group of Gene therapy strategies for neuropathies, directed by Dr. Assumpció Bosch i Merino.

All the studies were financially supported by the Formación de Profesorado Universitario (FPU AP2010-4559) Fellowship from the Gobierno de España and the grant support by the Centro de Investigación Biomédica en Red sobre Enfermedades Neurodegenerativas (CIBERNED), Instituto de Salud Carlos III.

Supervisor:

ASSUMPCIÓ BOSH I MERINO

PhD candidate:

BELÉN GARCÍA-LAREU



A

AD	Alzheimer diseases
ADAM	a disintegrin and metalloproteinase
AGE	Advanced glycation end products
Akt	protein kinase B (PKB)
ALS	Amyotrophic lateral sclerosis
ANS	Autonomic nervous system
Arg1	Arginase 1
ATF3	Activating Transcription Factor 3

B

B6	Black 6 inbred mouse strain
BDNF	Brain-derived neurotrophic factor
BKS	C57BLKS/J inbred mouse strain
BNB	Blood nerve barrier

C

c57/Bl6	Inbred mouse strain Black 6
c57/BJ	Inbred mouse strain Black 6
CAM	cell adhesion molecules
CCL2	chemokine (C-C motif) ligand 2
CCL3	chemokine (C-C motif) ligand 3
cDNA	complementary DNA
cJun	Jun proto-oncogene, AP-1 transcription factor subunit
CMAP	Compound muscle action potential
CMT	Charcot-Marie-Tooth disease
CNAP	Compound nerve action potential
CNS	Central nervous system
Cq	Quantification cycle value (Threshold cycle)
CCR2	C-C chemokine receptor type 2

D

db/db	diabetes spontaneous mutation (Lepr db) mice
DM	Diabetes Mellitus
DN	Diabetic neuropathy
DNA	Deoxyribonucleic acid
DPN	Diabetic peripheral neuropathy
dpl	days post lesion
DRG	Dorsal root ganglia
DSS	Dejerine–Sottas disease

E

E(number)	Embryonic day
EAE	Experimental autoimmune encephalomyelitis
ECM	Extracellular matrix molecules
Egr2	Early growth response protein 2
ELISA	Enzyme-Linked Immunosorbent Assay
ErbB	Epidermal growth factor receptor family
ERK	Extracellular Signal-regulated Kinase

LIST OF ABBREVIATIONS

F

F0	Founder animals
F1	First transgenic animal generation
F4/80	EGF like module-containing mucin-like hormone receptor-like 1

G

GAP43	Growth Associated Protein 43
GBS	<i>Guillain-Barré</i> syndrome
GDNF	Glial cell-derived neurotrophic factor
GFAP	Glial fibrillary acidic protein
GM-CSF	Granulocyte Macrophage Colony-Stimulating Factor

H

HIV	Human immunodeficiency virus
HMG-CoA	3-hydroxy-3-methylglutaryl coenzyme A reductase
HNPP	Hereditary neuropathy with liability to pressure palsies
hpl	Hours post lesion
h	Hours

I

Iba1	Ionized calcium binding adaptor molecule 1
IF	Immunofluorescence
IHC	Immunohistochemistry
IL	Interleukin
ILR	Interleukin receptor
IL1RA	Interleukin-1 receptor antagonist
INOS	Nitric oxide synthases
IP	Intraperitoneal
IR	Insulin receptor
IRS1	Insulin receptor substrate 1
iSC	immature Schwann cell

J

JAK	Janus Kinase
JNK	c-Jun N-terminal kinases

K

kDa	Kilo Dalton
KO	Knock Out

L

L	Transgenic Animal Line
LPS	Lipopolysaccharide

M

ug	microgram
-----------	-----------

LIST OF ABBREVIATIONS

uL	microliter
um	micrometer
M1	Macrophage phenotype 1
M2	Macrophage phenotype 2
MAG	Myelin-associated glycoprotein
MAPK	Mitogen-Activated Protein Kinase
MBP	Myelin Basic Protein
MCP-1	Monocyte chemoattractant protein-1
MCSF	Macrophage colony-stimulating factor
MEK	MAPK/ERK kinase
MIP-1	Macrophage Inflammatory Proteins
miRNA	microRNA
mL	miliLiter
MNCV	Motor Nerve Conduction Velocity
MPZ	Myelin protein zero
mRNA	Messenger RNA
MS	Multiple esclerosis
mSC	mature Schwann cell
mTOR	mammalian Target of Rapamycin
 N	
Nav	Sodium voltage channel
NFATc4	Nuclear factor of activated T-cells, cytoplasmic 4
NFkB	Nuclear factor kappa-light-chain-enhancer of activated B cells
NGF	Nerve growth factor
NO	Nitric oxide
NOD	Non-obese diabetic
NP	Neuropathic pain
NRG	Neuregulin
ns	non-statistically significant
NSC	Non-myelinated Schwann cell
 O	
ob/ob	obese mouse
Oct6	octamer transcription factor 6
 P	
P(number)	Post-natal day
p75NTR	neurotrophin receptor p75
pb	pair base
PCR	polymerase chain reaction
PD	Parkinson disease
pg	picogram
PI	Phosphatidylinositol
PI3K	Phosphatidylinositol-4,5-bisphosphate 3-kinase
PKA	Protein kinase A
PI	Print length
PMP22	peripheral myelin protein 22
PN	peripheral neuropathy

LIST OF ABBREVIATIONS

PNS	peripheral nervous system
P0	myelin protein zero
Q	
qPCR	real-time quantitative polymerase chain reaction
R	
RNA	Ribonucleic acid
ROS	Reactive oxygen species
S	
SC	Schwann cell
SCP	Schwann cell precursors
SFI	Sciatic Functional Index
SNVC	Sensory nerve velocity conduction
Sox10	SRY-related HMG-box transcription factor 10
SPPL2b	Signal peptide peptidase-like 2B
STAT3	Signal transducer and activator of transcription 3
STZ	Streptozotocin
T	
TACE	Tumor necrosis factor-alpha converting enzyme
Tg	Transgenic
TNF	Tumor necrosis factor
TNFR	Tumor necrosis factor receptor
Trk	tyrosine receptor kinase
Ts	Toe spread
W	
WD	Wallerian degeneration
Wpl	weeks post lesion
wt	wild type

LIST OF ABBREVIATIONS	I-IV
I. INTRODUCTION	
1. The nervous system	1
1.1 The peripheral nervous system (PNS)	2
1.1.1 <u>Peripheral nerves</u>	4
1.2 The myelin	8
1.2.1 <u>Structure of myelin sheaths</u>	10
1.2.2 <u>Composition of myelin membranes</u>	11
1.3 The biology of Schwann cells (SCs)	12
1.3.1 <u>The myelination process & development</u>	12
1.3.2 <u>The myelin factors</u>	13
2. Damage in the PNS	16
2.1 Wallerian degeneration (WD): implication after injury	16
2.1.1 <u>The origin of macrophages in WD</u>	18
2.1.2 <u>Cytokines involved in WD</u>	18
2.2 Peripheral nerve injuries	19
2.1.2 <u>Peripheral neuropathies: Classification</u>	21
3. Regeneration in the PNS	22
3.1 The process of regeneration	22
3.1.1 <u>Tropic & trophic cues</u>	25
3.2 Molecular pathways	26
3.2.1 <u>The PI3K/Akt/mTOR pathway</u>	26
3.2.2 <u>The p38/MAPK pathway</u>	27
3.2.3 <u>The ERK pathway</u>	28
3.2.4 <u>The NRG1/ErbB signalling pathway & regeneration</u>	28
3.3 Regenerative neurotrophic factors	29
4. Neuroinflammation in PNS injury	32
4.1 Proinflammatory cytokines	34
4.1.1 <u>Tumor Necrosis Factor alpha (TNFα)</u>	□□
□□□□□□□□ <i>The TNFα receptor (TNFR) family</i>	
38	
4.2 Antiinflammatory cytokines	39
4.3 The macrophages activation in the PNS	40
4.4 Neuropathic pain after peripheral injury	42
5. Animal models for peripheral neuropathies	43
5.1 Diabetic Peripheral Neuropathy (DPN)	46
5.2 Animal models for cytokines	48

II. OBJECTIVES	50
III. RESULTS	
1. Generating a transgenic P0TNFα mice line	51
1.1 Molecular characterization of L1 & L4 lines	54
2. Crush protocol: Inducing peripheral injury	56
2.1 Sciatic Functional Index (SFI) calculation	56
3. Molecular characterization of P0TNFα mice	60
3.1 TNF α detection in intact animals	60
3.2 TNF α detection in injured animals	62
3.3 Compensatory mechanism: TNFR1/RII detection	65
3.4 Antinflammatory responses: IL10 detection	67
3.5 Myelination process characterization	69
3.6 Demyelination & remyelination characterization	71
3.6.1 <u>Egr2 detection</u>	71
3.6.2 <u>Myelin protein detection</u>	72
3.6.3 <u>Short timing study</u>	76
4. Morphometric characterization of P0TNFα mice	78
5. Phenotype of SCs in P0TNFα mice	86
5.1 Immature SCs: p75NTR detection	86
5.1.1 <u>SCs primary cultures</u>	90
6. Macrophages & inflammation in P0TNFα mice	93
6.1 Chemoattractive environment: CCL2 detection	93
6.2 Macrophages markers: Iba1 & GFAP detection	94
6.2.1 <u>Detection in peripheral nerves</u>	94
6.2.2 <u>Short-time study of macrophage infiltration</u>	97
6.2.3 <u>Detection in spinal cord</u>	97
7. WD delay & pain initiation in P0TNFα mice	101
7.1 Molecular pathways	101
7.2 p75NTR & WD: spinal cord detection	102
7.3 Ion channels & pain: Nav1.7 & Nav1.8 detection	104
7.4 Molecular factors related to injury	105
7.4.1 <u>ATF3 detection</u>	105
7.4.2 <u>BDNF</u>	106
7.4.3 <u>GAP43</u>	106

7.4.4 <u>Short-time study after peripheral injury</u>	107
8. Cytokines pattern after injury: WD & pain implications	109
8.1 Macrophages role: F4/80 detection	109
8.2 Pro-inflammatory cytokines	110
8.2.1 <u>IL1β detection</u>	110
8.2.2 <u>IL6 detection</u>	111
8.2.3 <u>IL1RA detection</u>	112
8.2.4 <u>Caspase3 detection</u>	112
9. Algesimetry tests characterization in P0TNFα mice	114
10. Electrophysiology study in P0TNFα mice	116
IV. DISCUSSION	
1. A transgenic P0TNFα mouse model	118
2. P0TNFα model stressed by sciatic nerve <i>crush</i> injury	132
3. TNFα and DM	151
V. CONCLUSIONS	156
VI. MATERIALS & METHODS	
1. Materials	158
1.1 Plasmidic vectors	158
1.2 Mice	158
1.3 Primer pair sequence	158
1.3.1 <u>DNA primers sequence</u>	158
1.3.2 <u>mRNA primers sequence</u>	158
1.4 Antibodies & counterstaining reagents	159
1.5 Buffer solutions	159
1.6 Imaging equipment	159
2. Methods	162
2.1 Mouse handling	162
2.1.1 <u>Surgical procedures</u>	162
2.1.1.1 <i>Sciatic nerve injury: crush protocol</i>	162
2.1.1.2 <i>SCs primary culture</i>	163
2.1.1.3 <i>Anesthesia & Euthanasia</i>	164
2.1.2 <u>SFI determination</u>	165
2.1.2.1 <i>Walking tracks</i>	165

2.1.3 <u>Functional tests</u>	166
2.1.3.1 <i>Electrophysiology & nerve conduction tests</i>	166
2.1.3.2 <i>Algesimetry & sensory threshold measurement</i>	166
2.1.4 <u>Sample extraction & collection</u>	167
2.2 Biochemical techniques: DNA obtaining & manipulation	168
2.2.1 <u>Genomic DNA extraction & quantification</u>	168
2.2.2 <u>Genotyping by Genomic DNA PCR</u>	168
2.2.3 <u>Genotyping by Genomic DNA qPCR</u>	169
2.2.3.1 <i>qPCR from genomic DNA</i>	169
2.2.3.2 <i>Transgene copy number determination</i>	169
2.2.3.3 <i>Zygoty of transgenic animals</i>	170
2.3 Biochemical techniques: RNA obtaining & manipulation	170
2.3.1 <u>RNA extraction & quantification</u>	170
2.3.1.1 <i>Automated electrophoresis – ExperionTM</i>	171
2.3.2 <u>Retrotranscription</u>	171
2.3.4 <u>qPCR procedure</u>	171
2.3.4.1 <i>qPCR data analysis</i>	172
2.4 Biochemical techniques: Protein obtaining & manipulation	172
2.4.1 <u>Protein extraction and quantification</u>	172
2.4.1.1 <i>Protein extraction</i>	172
2.4.1.2 <i>Protein quantification</i>	173
2.4.2 <u>Western blot</u>	173
2.4.2.1 <i>Sample preparation</i>	174
2.4.2.2 <i>Denaturing gel electrophoresis</i>	174
2.4.2.3 <i>Transfer and blocking</i>	175
2.4.2.4 <i>Immunoblotting</i>	175
2.4.2.5 <i>Chemiluminescent detection and quantification</i>	176
2.4.2.6 <i>Membrane stripping</i>	176
2.4.3 <u>ELISA</u>	177
2.4.3.1 <i>mouse TNFα ELISA</i>	177
2.4.3.1 <i>mouse IL10 ELISA</i>	178
2.5 Histological analysis	178
2.5.1 <u>Morphometrical analysis</u>	178
2.5.1.1 <i>Sample preparation</i>	178
2.5.1.2 <i>Morphometric procedure</i>	178
2.5.2 <u>Immunohistochemistry</u>	178
2.5.2.1 <i>Sample processing</i>	179

TABLE OF CONTENTS

2.5.2.2 <i>Peripheral nerves, spinal cord and DRG</i>	179
2.5.2.3 <i>mouse hind paw skin</i>	180
2.6 Cellular cultures techniques	181
2.6.1 <u>SCs primary cultures</u>	181
2.7 Statistical analysis	182
VII. BIBLIOGRAPHY	183

SUMMARY

Tumor Necrosis Factor (TNF) alpha has been implicated in the pathogenesis of diabetic peripheral neuropathy (DPN), among other inflammatory demyelinating diseases and neuropathic pain. TNF- α is a pro-inflammatory cytokine that can act at several steps in the demyelination process. It is produced by Schwann cells in the peripheral nervous system (PNS) after nerve injury and released into the local environment to attract and activate macrophages at the site of injury, contributing to Wallerian degeneration and demyelination.

An important observation in different peripheral neuropathies is the increased levels of TNF- α in plasma, being implicated in the onset and/or malignant progression of peripheral nerve diseases. In vivo studies demonstrated a local inflammation in the sciatic nerve of rats after injection of TNF- α , followed by demyelination and axonal degeneration. Furthermore, the administration of TNF- α resulted in acute mechanical hyperalgesia, a main characteristic of neuropathic pain and therefore TNF- α is postulated as a biomarker for painful alterations after nerve injury.

Nowadays, there is not an effective therapy to stop and reverse the axonal degeneration and pain that characterize peripheral neuropathies. Unfortunately, the preclinical data using animal models demonstrated the lack of optimum models and outcome measures to underlay the pathogenesis of the disease. An appropriate animal model is critical for replicating the essential features of peripheral neuropathies, understanding DPN pathophysiology and to develop effective strategies.

Although the increasing worldwide prevalence of diabetes has fueled the development of several mouse models, the main discrepancies related to the proper generation of a mouse model for the study of peripheral neuropathies, and complications of DM, like diabetic peripheral neuropathy, are a consequence of the anatomical differences and the incomparable life expectancies between humans and rodents.

With the aim to characterize TNF- α effects in the development of peripheral neuropathy and chronic neuropathic pain, a transgenic mouse model overexpressing TNF- α in Schwann cells, under the peripheral myelin protein P0 promoter, was generated.

Here we characterized the overexpression of TNF- α in myelinated Schwann cells at different steps of myelination (postnatal days 5, 21 and 65) showing that high levels of TNF- α in sciatic nerve leads to the downregulation of the major PNS myelin proteins (P0, MBP, PMP22, MAG) compared to wild type mice, correlating with the loss of structured myelin and an increase in p75NTR in the sciatic nerve, a marker for immature and non-myelinated Schwann cells. Local inflammation was also demonstrated by high levels of macrophage infiltration in both sciatic nerve and spinal cord, compared with wild type animals.

Furthermore, stress conditions were induced by sciatic nerve crush after which recovery and subsequent remyelination were delayed in the transgenic mice, as evaluated by the Sciatic Functional Index and electrophysiological tests. On the other hand, algesimetrical tests revealed unaltered mechanical nociception, with or without injury, although transgenic animals showed thermal hypersensitivity, higher after peripheral injury, correlating with the microglial and astrocyte activation in the spinal cord. Moreover, high expression of BDNF and CCL2, as well as overexpression of Nav1.7 and Nav1.8 channels, all related to the maintenance of chronic inflammatory pain, were detected in DRGs of TNF- α transgenic mice.

A morphometrical study of tibialis nerves showed no differences in the total nerve surface between genotypes and injury. However, transgenic mice exhibited a slight reduction in the axonal diameter and a significant thinner myelin sheath than wild type animals.

This model could be helpful in the characterization of the role TNF- α in pain development, injury and DPN as well as in developing efficient therapeutic strategies to modulate such pathological conditions.

RESUMEN

Se ha relacionado la implicación de Tumor Necrosis Factor (TNF) α en la patogénesis de la neuropatía diabética periférica (DPN) así como en otras enfermedades inflamatorias cursadas con desmielinización y dolor neuropático. TNF- α es una citoquina proinflamatoria que puede actuar a diferentes niveles en el proceso de desmielinización. Tras una lesión en el nervio periférico, las células de Schwann producen esta citoquina en el sistema nervioso periférico (PNS) y se secreta localmente para atraer y activar a los macrófagos circulantes hacia la lesión, contribuyendo así a la degeneración Walleriana.

En diferentes neuropatías periféricas conocidas, el incremento de los niveles de TNF- α en plasma se encuentran implicados en la progresión maligna de la enfermedad. Estudios en ratas inyectadas con TNF- α directamente en el nervio ciático, demuestran una inflamación local seguida de desmielinización y degeneración axonal. Además, la administración de TNF- α ocasiona hiperalgesia mecánica aguda, una de las principales características del dolor neuropático, así como se ha postulado a TNF- α como biomarcador de dolor tras lesión nerviosa.

Hoy en día no existen terapias efectivas para frenar y revertir la degeneración axonal y el dolor que cursan las neuropatías. Datos preclínicos obtenidos con los modelos animales actuales demuestran la carencia de un modelo óptimo y de los parámetros adecuados para establecer la patogénesis de la enfermedad. La obtención de un modelo animal apropiado es crítico para mimetizar las neuropatías periféricas humanas.

Aunque el incremento mundial de la prevalencia de la diabetes ha potenciado el desarrollo de numerosos modelos, las principales discrepancias para la obtención de un correcto modelo in vivo para las neuropatías asociadas a la Diabetes Mellitus, residen en las importantes diferencias anatómicas y la esperanza de vida entre humanos y roedores.

Con el objetivo de caracterizar los efectos de TNF- α en el desarrollo de neuropatía periférica crónica y dolor neuropático, se generó un ratón

transgénico que sobreexpresa TNF- α en células de Schwann, bajo control del promotor de la proteína de la mielina P0.

En el trabajo que se presenta a continuación se caracteriza la sobreexpresión de TNF- α en las células de Schwann pro-mielinizantes en diferentes estadios de mielinización (a 5, 21 y 65 días de vida), reflejando que los altos niveles alcanzados en los nervios ciáticos transgénicos ocasionan una desregulación de las principales proteínas de la mielina (P0, MBP, PMP22, MAG), correlacionando con una desestructuración de la vaina de mielina y el incremento de células positivas para p75NTR, marcador específico de células de Schwann inmaduras y no-mielinizantes. También detectamos una inflamación local debido a una alta infiltración de macrófagos en nervios ciáticos y médula espinal en estos animales.

Tras la lesión del nervio ciático, la recuperación de la función motora y posterior remielinización se retrasa en los ratones transgénicos, como demuestra la evaluación mediante el *Sciatic Functional Index*, y los test electrofisiológicos. Sin embargo, estudios de algosimetría muestran inalterada la nocicepción frente a estímulos mecánicos, aunque los ratones transgénicos presentan hipersensibilidad ante estímulos térmicos, incrementada tras la lesión y correlacionada con la activación microglial y astrocitaria en la médula espinal. Además, se detectaron altos niveles de BDNF and CCL2, junto con una sobreexpresión de los canales iónicos Nav1.7 y Nav1.8, relacionados con dolor.

Estudios morfométricos no reflejan diferencias en el tamaño de los nervios, ni siquiera tras la lesión, aunque los animales transgénicos sí presentan una ligera reducción en el diámetro axonal y un menor grosor de la mielina.

Por consiguiente, este modelo podría ayudar a elucidar el papel de TNF- α en el desarrollo de dolor, la regeneración y las neuropatías periféricas, así como en el desarrollo de nuevas terapias eficientes para paliar estas patologías.

I. INTRODUCTION

1. The nervous system

The human nervous system is formed by the central (CNS) and the peripheral nervous system (PNS). **CNS** can be divided in two major structures: brain (cerebrum, cerebellum and brainstem) and spinal cord. **PNS** consists of the nerves (cranial, spinal and autonomus) and ganglia, a nerve cell cluster of afferent nerve cell bodies. Unlike CNS, PNS is not protected by bones, but it is protected by a fused double layer of membranes. (Ariza L. 2010, Homs J. 2010, Dorland´s Medical Dictionary, White J.S 2008).

Nervous tissue is the main component of the nervous system and it is composed by neurons (Fig 1.) and neuroglial cells (Fig 2.). **Neurons**, or nerve cells, are specialized and excitable cells which receive and facilitate the transmission of electrochemical nerve impulses to the next neuron (Byrne, 2004;

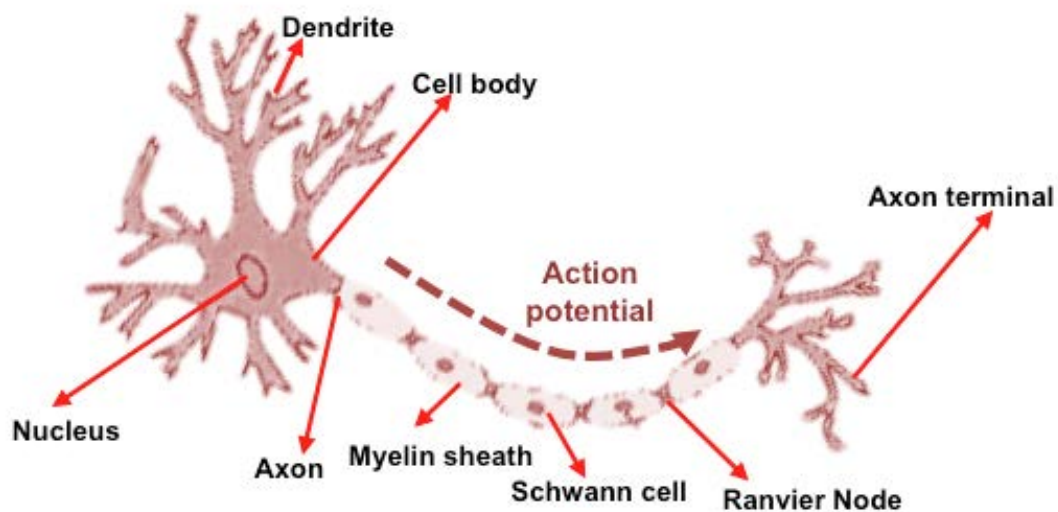


Figure 1. A typical neuron possess three well-defined structures: the receptor part of the synaptic signals that is form by soma or cell body and dendrites, the transmission part where the axon of each neuron is specialized in the propagation of the information rapidly along the axon to branches axonal terminals or the action part, activating synapses onto other neurons. A synapsis is, then, a contact between the axon of one neuron and a dendrite or soma of another. (Adapted from OpenStax College, Biology and Molecular cell biology, 4th edition, W.H. Freeman, 2000).

Kandel, 2000).

Neuroglia (1856 by Rudolf Virchow) can be divided into microglia and macroglia cells (Fig2.). Neuroglia, also known as glial cells or just glia, assist in the propagation of the nerve impulses and provide mechanical and metabolic supportive functions, protection and synthesize the specific axonal myelin. Glial

cells are smaller than neurons and vary in structure according to their function (Swenson R. 2015). Although it was believed, initially, that only neurons were excitable cells, nowadays there seems to be evidences to support that glial cells could have a role in the transmission of nerves impulses. (D'Antoni, 2008; Yang, 2008; Gomez-Gonzalo, 2010; Kimelberg, 2010).

In PNS, **macroglia** include **Schwann Cells** (SCs) in nerves and satellite glial cells in ganglia, preferently. The SCs (Fig2.) are neuroglial cells helping to maintain axons and form myelin sheaths in peripheral nerves, while oligodendrocytes develop this role in the CNS. **Satellite glial cells** (Fig.2.) are small cells that surround neurons in sensory ganglia, and regulate the external chemical enviroment by increasing intracellular concentration of calcium ions. These cells are highly sensitivie to injury and inflammation contributing to pathological states such as chronic pain (Hanani, 2005).

Microglia (Fig 2.), are specialized phagocytic macrophages capable of protecting and support neurons. These cells are able to phagocyte cellular debris, playing relevant functions in the immflamatory process after injury of the nervous system (Sofroniew, 2009; Brodal, 2010; Waymire, 2015; Verkhatsky, 2013). Microglial cells are small relative to macroglial cells, with changing shapes after activation, and are found in all regions of the brain and the spinal cord (Kettenmann, 2008). Many neurodegenerative disorders, such as Alzheimer disease (AD), Parkinson disease (PD), Amyotrophic lateral sclerosis (ALS) and Multiple sclerosis (MS); are associated with abnormal overactivated microglia playing destructive roles through direct and indirect inflammatory attack. They have been recently described as a target to treat neuroinflammation and have been also implicated in neuropathic pain (Hains, 2006; Tsuda, 2003).

1.1 The peripheral nervous system (PNS)

According to functional criteria, there are two types of neurons in the PNS: the sensory and motor neurons. **Sensory neurons** are also called afferent, and they relay sensory information of a large variety of stimulous of differents parts of the organism in form of an action potential from the PNS to the CNS. The soma of sensory neurons is localized into a structure called dorsal root ganglion (DRG), or spinal ganglion (Fig3.). **Motor neurons** are the efferent neurons that relay an action potential out from the CNS to the proper effector, such as

muscles, body organs or glands. The cell body of these neurons is located in the ventral region of the spinal cord (**Fig3.**) (Waymire, 2015).

Thus, the PNS is divided into motor and sensory peripheral nervous system. The efferents motor neurons are part of the **motor-PNS** that it is divided into

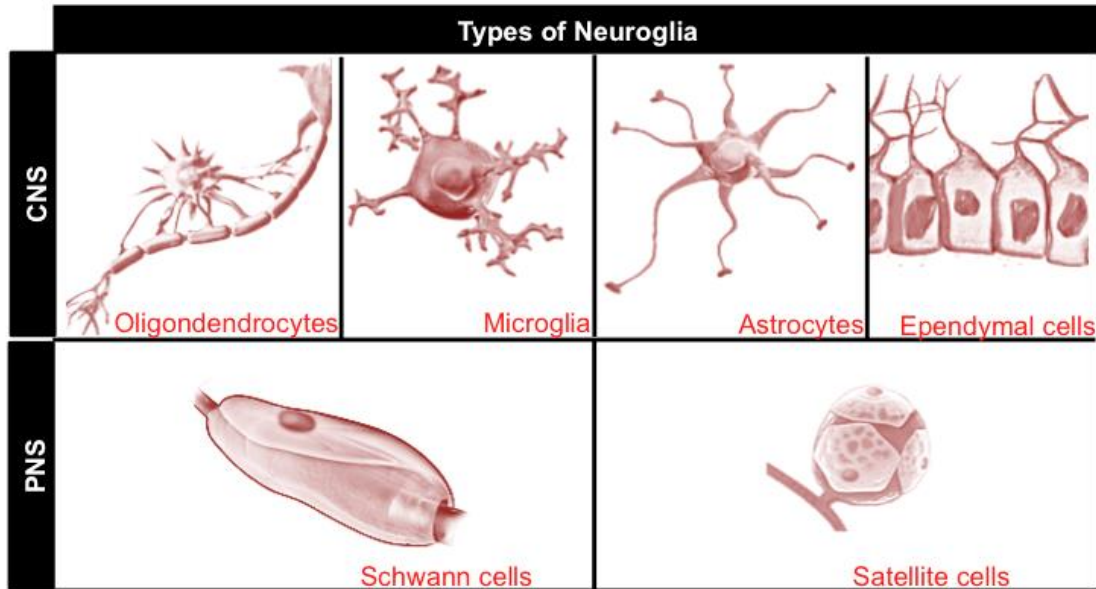


Figure 2. Types of neuroglial cells found in central and peripheral nervous system. Neuroglial cells are classified as: microglial cells (specialized macrophages capable of phagocytosis), astrocytes (star-shaped macroglial cells found in the CNS), oligodendrocytes (CNS cells that form myelin sheaths on the axons of neurons) and their precursors (NG2 glia), Schwann cells (SCs, PNS cells that help to maintain axons and form myelin sheaths in the PNS) and satellite glial cells (localized in the surface of ganglia). (Adapted from OpenStax College, Biology, Neuroscience 2nd edition, Sinauer associates, 2001 and “Medical gallery of Balusen Medical 2014).

somatic nervous system and **autonomic nervous system** (ANS) (**Fig3.**). The **ANS**, subdivided into sympathetic and parasympathetic, influences the function of internal organs which have a no voluntary and unconsciously control and regulates involuntary responses to maintain the physiological functions. In fact, sympathetic and parasympathetic division normally act in the same organs but have opposite effects, and it is the equilibrium between them that allows the internal homeostasis of the body. Neurons of the **sympathetic system** are often considered the “fight or flight” system, like a quick response mobilizing the system against an emergency, whereas the **parasympathetic division** is known as the “feed and breed” one, such as a more slowly activated dampening system to save the energy (**Fig.3.**) (Laight, 2013; Matic, 2014, Costanzo, 2007).

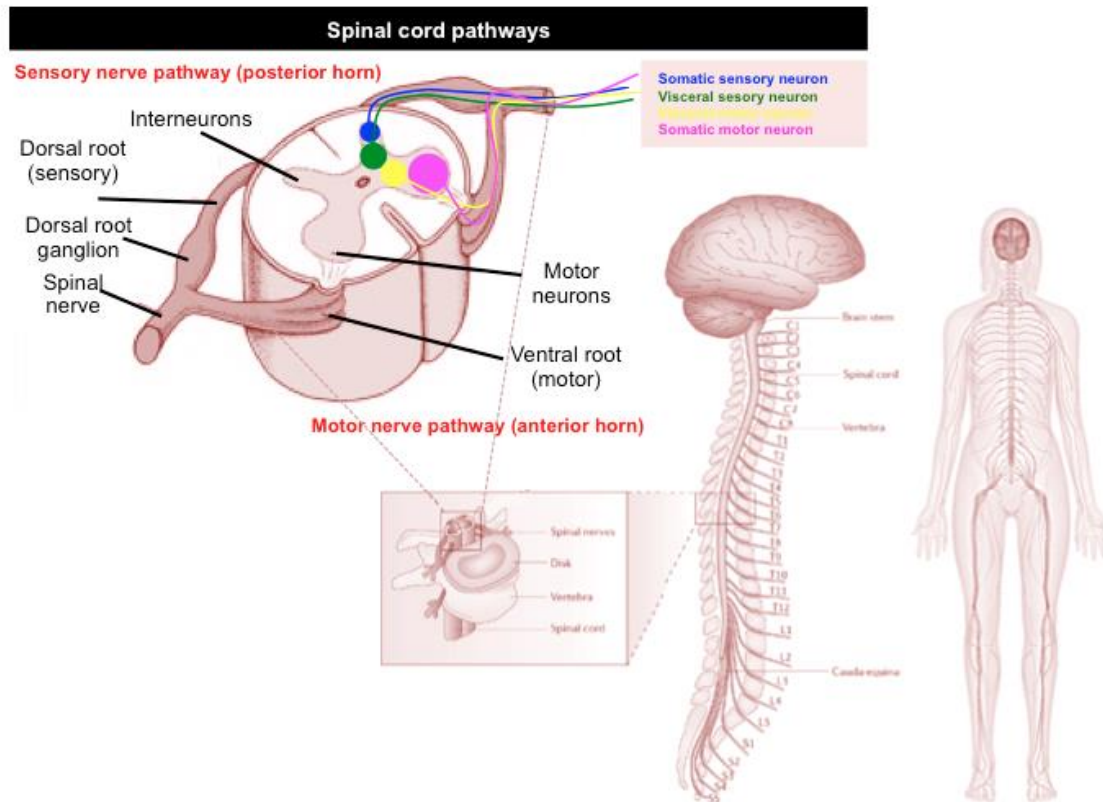


Figure 3. The organization of the peripheral nervous system and the somato motor-sensory pathways. Afferent and efferent signals are integrated in spinal cord, ventral or anterior horn destined to motor neurons, while in posterior or dorsal horn the sensory pathways are localized. (Adapted from Nervous control of skeletal muscles, Journal Of Neurophysiology; and OpenStax College, The function of Nervous System; Bradbury, 2006).

Nowadays, is often more common to speak about the **somato motor-sensory nervous system**, formed by both types of neurons: motor and sensory ones and it includes the transmission of sensory signals from sensory receptors, such as the five special senses, temperature, pain and pressure, and the proprioception to the spinal cord and brain by afferent via (Swenson, 2008). The somatosensory information generates a voluntary motor output stimulus to control the skeletal muscle contraction as answer to a previous sensory input (Fig3. & Fig4.).

1.1.1 Peripheral nerves

Neurons are also called nerve cells as axons of different neuron are enclosed in cable-like bundle and form **nerve fibers** (Fig4.) in the PNS, and provide a common pathway for the electrochemical impulse transmission along each of the axons to the peripheral organs. However, the nerve cell term is potentially

misleading since many neurons do not form nerves, and nerves also include non-neuronal Schwann cells.

Peripheral nerves can be formed by efferent (CNS to PNS) or afferent (from PNS to CNS) axons. These axons can be myelinated or non-myelinated, and are limited by connective tissue sheaths, to confer physical support, and blood and lymphatic vessels. Each nerve is covered externally by 3 layers (Fig 4.): the most external is the epineurium, a dense sheath of connective tissue; the perineurium which subdivide the nerve into several bundles of fibers surrounding by the endoneurium that consists in an inner sheath of glycochlyx and an outer layer of collagen fibers to form an tube that it is known as endoneurial tube. Within the endoneurium, the individual nerve fiber is surrounded by the endoneurial fluid that acts in a similar way to the cerebrospinal fluid in the CNS and constitutes a blood-nerve barrier (BNB) similar to the blood-brain barrier in the CNS (Kanda, 2013).

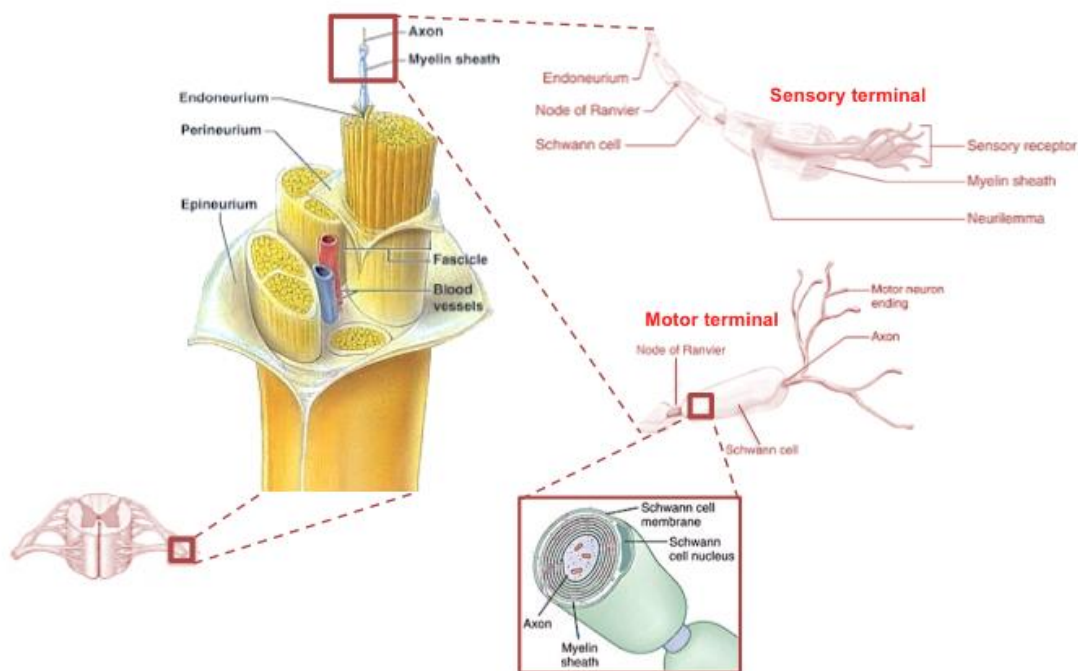


Figure 4. A sectional view of a spinal nerve showing its connective tissue layers and a representative picture of myelinated sensory (above) and motor (below) axons, and the multilayer membrane of SCs which wrap these axons. (Adapted from Benjamin Cummings, 2001 and S. McReynolds, 2017).

A

Cranial Nerves	Name	Nerve type	Function
I	Olfactory	Sensory	Smell
II	Optic	Sensory	Vision
III	Oculomotor	Motor	Eye movement
IV	Trochlear	Motor	Moves eye
V	Trigeminal	Both	Face sensation, mastication
VI	Abducens	Motor	Abducts the eye
VII	Facial	Both	Facial expression, taste
VIII	Vestibulocochlear	Sensory	Hearing, balance
IX	Glossopharyngeal	Both	Taste, gag reflex
X	Vagus	Both	Gag reflex, parasympathetic innervation
XI	Accessory	Motor	Shoulder shrug
XII	Hypoglossal	Motor	Swallowing, speech

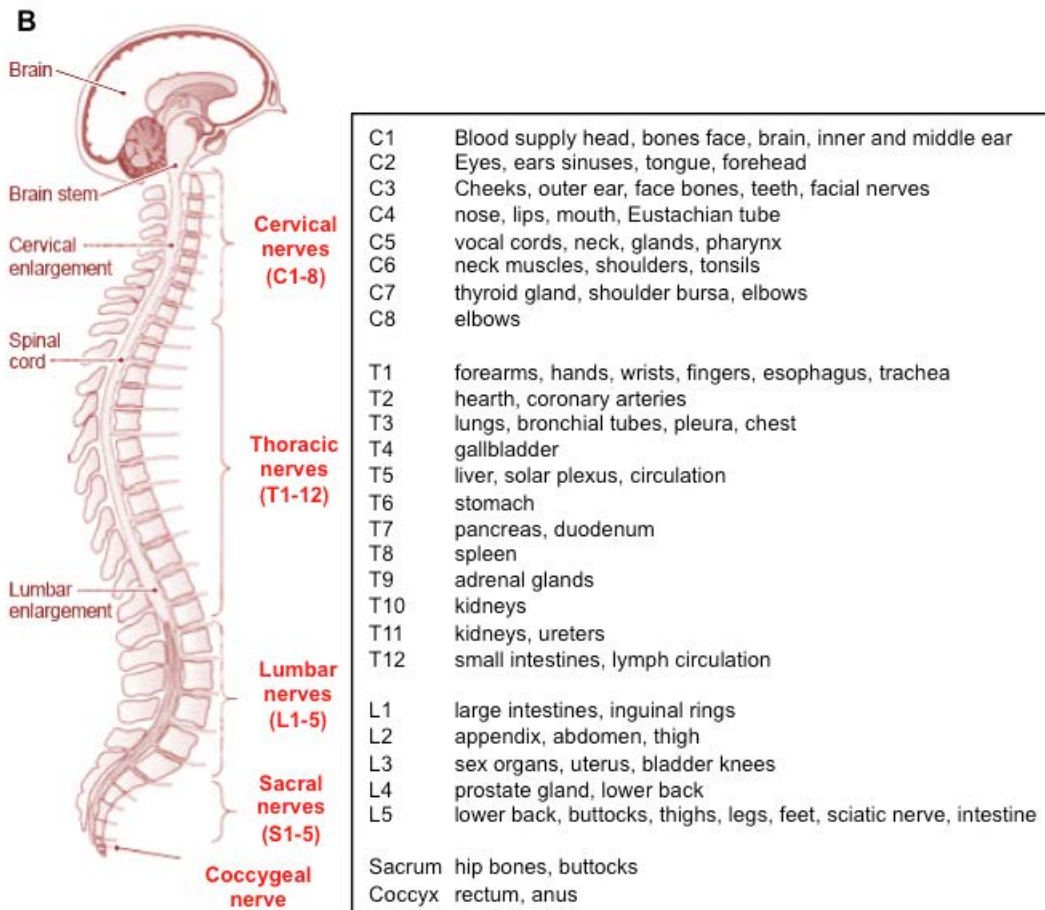


Figure 5. (A) There are 12 cranial nerves, 10 of which originate from brainstem: oculomotor, trochlear, trigeminal, abducens, facial, vestibulocochlear, glossopharyngeal, vagus, accessory and hypoglossal. The nuclei of the olfactory and optic nerves arise in the forebrain and thalamus, respectively. **(B)** Classification of the spinal nerves. There are 31 pairs of spinal nerves: 8 cervical, 12 thoracic, 5 lumbar, 5 sacral and 1 coccygeal; and their nerve root is named according to the spinal vertebra which they are associated. Adapted from Withwan, 1976 and Peripheral nervous system anatomy, Chawla J, 2016).

The somato motor-sensory PNS is formed by cranial nerves, in the head and neck, and spinal nerves for the rest of the body (Fig5.). **Cranial nerves** carry sensory and received motor data from neck and head to CNS and viceversa (Fig5.A.). **Spinal nerves** arise from the spinal cord to control the functions (Fig5.B.) and are associated by two spinal cord roots, the ventral or anterior and the dorsal or posterior root. The ventral roots are preferently formed by efferents/motor fibers, while afferents or sensory fibers project to the dorsal area of the spinal cord (Fig3.).

There are three types of peripheral nerve fibers based on their diametre: A, B and C groups and these fibers can be myelinated or unmyelinated (Fig6.).

Fibre Type	Subtype	Myelin	Diameter (µm)	Conduction Speed (m/s)	Location	Function
A	α	yes	12-20	30-120	Efferent	Motor, somatic nerve
	β	yes	5-15	30-70	Afferent	Tactile, proprioception, pressure
	γ	yes	3-6	15-35	Efferent	Muscle tone
	δ	yes	1-4	5-25	Afferent	Pain, cold temperature, touch
B		yes	<3	3-15	Preganglionic	Autonomic functions
C	sC	none	0.3-1.3	0.7-1.3	Postganglionic	Autonomic functions
	dC	none	0.4-1.2	0.1-2	Afferent	Pain, warm temperature, reflex

Figure 6. Classification of nerve fibres. Motor fibers that innervate skeletal muscles (fibers of the A group) have around 10-17 µm of axonal diameter and the highest conduction velocity of 1,2-40 m/s.; Afferent A fibers are also classified in different groups according to their functions and target tissue: A alpha (Ia and Ib), A beta (II fibers) and A delta (III fibers). There are also various types of A efferents fibers: A Alpha, A beta and A gamma. And motor fibers to smooth muscles of the ANS (B group fibers) have lower diameters, typical of 3-8 µm and lower conduction speed (3-14 m/s aproximatly). Sensory are 2-20 µm of axonal diameter myelinated (A group) and/or unmyelinized fibers (C group with low diameter and conduction velocity diameter, on average 0.2-1.5 µm, and velocity, on the order of 0,3-1,2 m/s. (Adapted from Whitwan, 1976; Schalow, 1995).

On one hand, diameter of **motor nerve fibers** depends on organs or body areas and are always myelinated. Myelinated fibers are present in higher numbers in human body and have bigger diametres and faster velocities of conduction speeds thanks to the myelin sheaths. **The A fibers** have the largest diameter and the highest conduction velocity and can be subdivided into sensory/afferent A fibers and motor/efferents A fibers. Afferent A fibers are also classificated in different groups according to thier functions and target tissue. However, **B group** contains the sensory and motor fibers to smooth muscles of

the ANS, with a small diameter and low conduction velocity as a consequence of a less myelinated state than group A (Julius, 2001; Martini, 2016).

On the other hand, **the sensory nerve fibers**, having their cell bodies in the DRG, carry the sensory information through type A myelinated and/or unmyelinated fibers.

The axons from C group fibers are surrounded by unmyelinated Schwann cells and grouped close together into a Remak bundles. This kind of fibers are in a minor proportion, have a smaller diameter, and the lack of myelination causes these fibers to respond slowly but deeper and spread out over an unspecific area, to stronger intensities stimulus. Normally, C fibers are nociceptives (pain), but some of them exhibit polymodal reactions to thermal, mechanical or chemical stimuli.

1.2. The myelin

The myelin sheaths (discovered by Rudolf Virchow in 1854) are formed by a modified proteolipidic plasma membrane wrapped around the axon in a concentric-spiral fashion (Fig7.), to bioelectrically isolate, protect and allow the fast transmission of stimuli. In addition, myelin confers an evolutive advantage allowing decreased reaction times to different stimulus in the nervous system by a factor of 10, compared to unmyelinated fibers of the same diameter (Fig.6.). Furthermore, myelin provides several improvements in metabolic efficiency for recovering the energy cost of traffic the nerve impulse and allows for a more compact nervous system by decreasing axonal length and size. This phenomenon is called: the economy of space (Zalc, 2000; Zalc, 2008; Lenz, 2012, Wilson, 2011; Zalc, 2006).

The myelin membrane is originated from and synthesized by multiple membrane layers of myelinating glial cells: oligodendrocytes in the CNS and SCs in the PNS (Fig7.). Myelin is maintained as a dynamic plasma membrane specialization in response to reciprocal signalling and physical interaction between the axon and the glial cell. It is reasonable to predict that, therefore, any intervention for lipid and protein synthesis may affect the myelination process. Some types of these myelin proteins are CNS or PNS specific (Xiaoyu, 2016; Kangas, 2016).

Each **myelin-generating SCs** provide myelin for only one segment of any given axon, although several SCs can interact with the same neuron (**Fig8.**). Within the broader nerve microenvironment many other cell types including endothelial cells, fibroblasts, and macrophages provide support, surveillance, and other functions for proper structural and functional maintenance of the peripheral nerve (Martini, 2016).

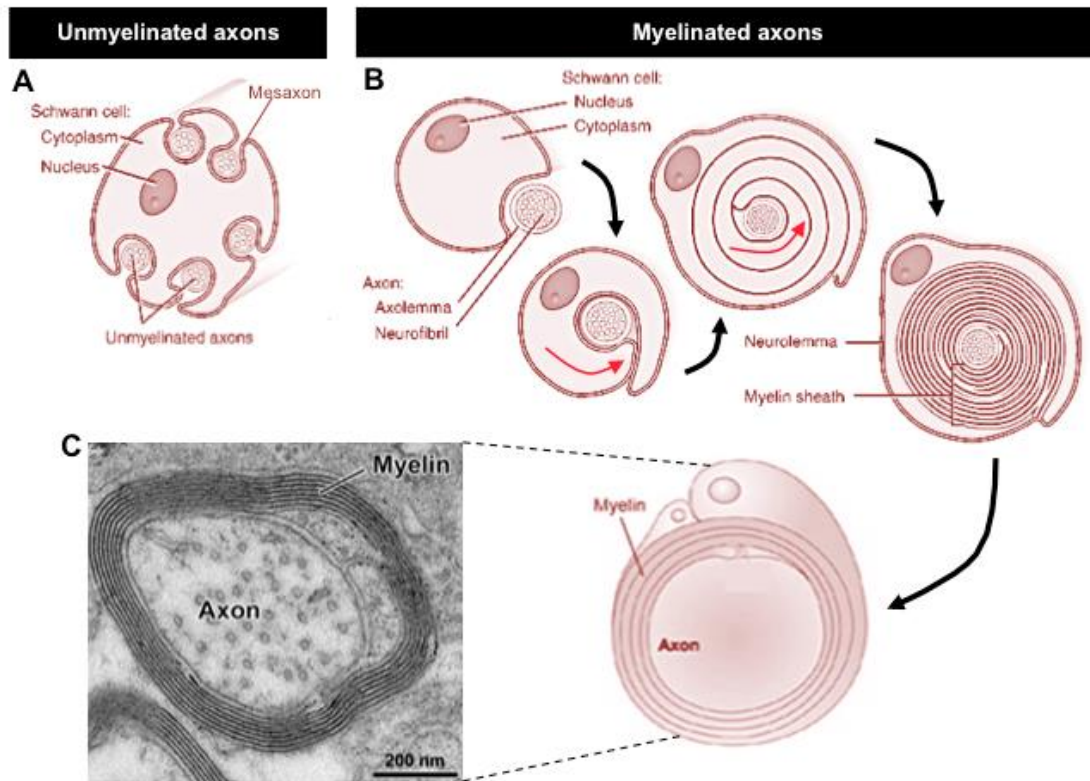


Figure 7. Myelin formation in PNS by SCs. Transversal sections of **(A)** unmyelinated and **(B)** myelinated axons and the mechanism through SCs wrap up the axons to form concentric layers of myelin membrane. **(C)** represents the ultrastructure of axon myelinated by electronic microscopy. (OMA:Outer mesaxons; IMA: Inner mesaxon) In the myelin sheath there are possible two different density layers about the density. The darkest line represents the major dense line (period line) and the lightest is the minor denser lines (or intraperiod line). (Adapted from Susuki K., 2010).

The nodes of Ranvier (**Fig8.**) are the periodic interruptions, critical to the functioning of myelin, where short portions of the axon, are left uncovered by myelin and in contact with the extracellular media. It is possible to find about 100 or more of these segments along the axon to allow a saltatory conduction in the propagation of action potentials, “jumping” from one node to the next, increasing the conduction velocity, (Xiaoyu, 2016). In the internodal space the ions are exchanged across the axon membrane thanks to the highly enriched

presence of Na⁺/K⁺ ATPases, Na⁺/Ca²⁺ exchangers and high density of voltage-gated Na⁺ channels that regenerate action potentials (Fig8.) (Morell, 1999).

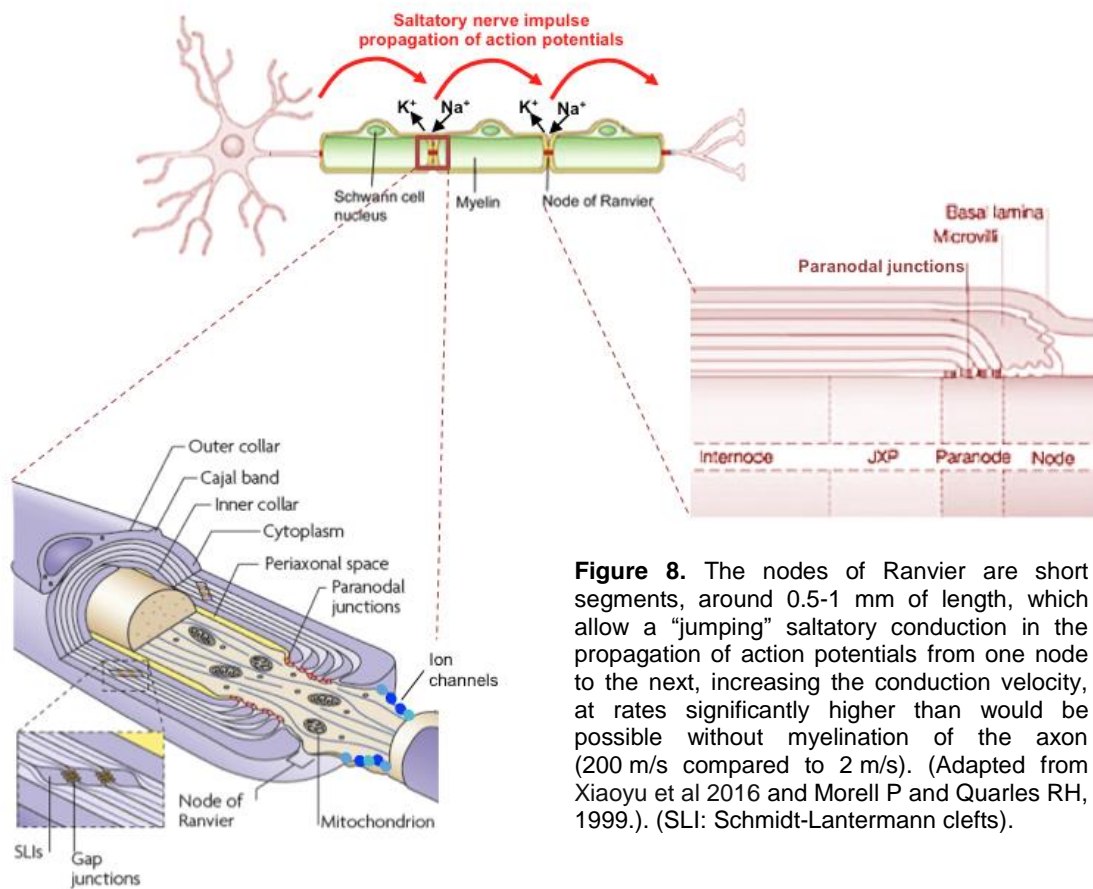


Figure 8. The nodes of Ranvier are short segments, around 0.5-1 mm of length, which allow a “jumping” saltatory conduction in the propagation of action potentials from one node to the next, increasing the conduction velocity, at rates significantly higher than would be possible without myelination of the axon (200 m/s compared to 2 m/s). (Adapted from Xiaoyu et al 2016 and Morell P and Quarles RH, 1999). (SLI: Schmidt-Lantermann clefts).

1.2.1 Structure of myelin sheaths

Myelin characteristic ultrastructure visualizes the myelin sheath as a series of multiple protein-lipid-protein-lipid-protein structure layers that are wound radially around the long axis of the axon (Fig7.). These layers are generally uniform and continuous. However due to imperfect nature of the wrapping process by which SCs enclose the nerve axon, this process can sometimes leave behind small pockets of residual cytoplasm displaced to the periphery during the formation of the myelin sheath. These pockets, myelin incisures or **Schmidt-Lantermann clefts** (Fig8.), provide communication channels between layers by connecting the cytoplasm of the SCs to the deepest layer of myelin sheath. These regions are common in peripheral myelinated axons but rare in the CNS (Morell, 1999).

The myelin sheath forms complex structures analogous to the neuromuscular junction. It has two regions, compact and noncompact domains, with distinct molecular structures and biological functions (Fig7.). **The compact region** contains the multiple layers of SCs which participate in forming the highly organized myelin sheath and the electrically insulating axons. **Non-compact myelin** contains substantially more cytoplasm than compact myelin. It is found in the nodes of Ranvier and Schmidt-Lanterman incisures, being critical for myelin functions and signaling (Spiegel, 2002).

1.2.2 Composition of myelin membranes

One of the prominent biochemical characteristics that distinguishes myelin from other membranes is its high lipid to protein ratio: lipids account for at least 80% of the dry weight of myelin membranes, composed by hydrocarbon chains, cholesterol, phospholipids, and glycolipids, in an approximately 4:3:2 ratio (Barkovicha, 2000; Ryu, 2008; Xiaoyu, 2016). In addition, proteins are another main constituent of myelin, around 20%, that allow the maintenance of structural and functional architecture of myelin (Xiaoyu, 2016).

PNS and CNS myelin lipids are qualitatively similar. Nevertheless, these differences are not as dramatic as the differences in protein composition. Thus, in the PNS, MPZ also called P0, (myelin protein zero) is the major protein. Others proteins could be found, such as MBP (myelin basic protein), PMP22 (peripheral myelin protein-22), MAG (myelin-associated glycoprotein) and MP11 (myelin protein-11) (Morell,1999; Yin, 2008).

Consistent with the compact myelin domain, most proteins in this region are relatively small, having molecular weights below 30 kDa, such as MPZ, PMP22 and MBP, which are also the major myelin structural proteins. On the other hand, noncompact regions often feature adhesion molecules, such as cadherins and catenins, and transport protein complexes.

P0 accounts for more than half of the PNS myelin protein. P0 is a transmembrane protein (28kDa), member of the immunoglobulin supergene family it is also posttranslationally modified. This protein stabilizes the layers of PNS myelin through both, protein-protein and protein-carbohydrate

interactions (Kirschner, 2004). Furthermore, a critical dosage of P0 has an apparently essential role to form stoichiometric complexes for normal myelin formation and maintenance (Gallego, 2001).

MBPs are a family of alternatively spliced gene to generated 4 different isoforms: 21, 18.5, 17 and 14 kDa; which are highly charged (Greenfield, 1993; Zeller, 1984) binding negatively charged lipids to maintain myelin functional stability and promotes the myelination process. It appears that MBP does not play a critical role in myelin structure in the PNS as P0 or PMP22.

Compact PNS myelin contains also a 22 kDa protein, **PMP22**, that accounts for less than 5% of the total proteins. However, unlike P0 which is nerve-specific, this protein is detected in motor neurons and during embryonic stages. The synthesis of PMP22 ceases when SCs begin to proliferate following nerve transection. For this reason, PMP22 is also known such as a “growth arrest protein”, suggesting an unknown role in regulation of growth or differentiation, and in SCs viability rather than a major structural role. PMP22 has been shown to form complexes with P0 and it may be relevant to its function (Jetten, 2000; Sancho, 2001; Amici, 2007).

MAG is a 100kDa single pass cell membrane glycoprotein and belong to the Ig superfamily. The cytoplasmic domain changes according with the alternative splicing processing. It represents around 0.1-1% of the total myelin protein in PNS (Sternberger, 1979; Trapp, 1982).

1.3. The biology of Schwann cells (SCs)

Most of the biomolecules contributing to the structural and functional properties of the myelin sheath have been identified and well characterized. In contrast, only a weak knowledge of the coordinated cellular and molecular events that regulate the formation and maintenance of the myelin sheath were demonstrated (Kangas, 2016).

1.3.1 The myelination process & development

The glial-axonal interactions have important relevance to **the myelination process** (Fig9.). During development, glia provides survival signals to neurons and determines the diameter of axons. In turn, axons provide signals that regulate the proliferation, survival and differentiation of glia, as well as myelin

formation. On the other hand, in adulthood, myelinating glia maintains axolemmal organization, axon diameter and neuronal health, while axons maintain glial differentiation and myelin integrity (Taveggia, 2010).

SCs can provide myelination to regenerating axons in the PNS, and also have phagocytotic activity to clear cellular debris that allows regrowth of PNS neurons (Jessen, 2005).

In the early development in mice (Fig.9.), the **neural crest stem cells** (NSCS) migrate into gliogenesis areas such as sciatic nerve and DRG (Hagedorn, 1999; Morrison, 1999), where they become specialized in **SCs precursors** (SCP). SCPs from the neural crest migrate out and contact the developing peripheral axons, between E12/13 (Fig9.) They become **immature SCs** (iSCs) around E15/16, and ensheath bundles of developing axons (Fig9.) (Dong, 1999). All iSCs have the potential to become either myelinating or nonmyelinating SCs and this process is directed by axons: SCs that establish a one to one association with an axon, called the promyelinating stage, initiate the program of myelination and become **myelinating SCs**. In contrast, SCs that do not establish this relationship with an axon do not activate the program of myelin gene expression, and become **non-myelinating Schwann cells** (Shy, 2000).

Generation of **mature SC** (mSC) involves several molecular changes in basal lamina and receptors from extracellular matrix, integrins and promyelin factors such as Oct6, Krox20/Egr2, Sox10 and NRG1 (Fig9.); all of them critical in myelination process and regulation (Birchmeier, 2008).

The different stages of SCs development can be detected by expression of specific molecular markers. The developmental progress of myelination varies between regions and species. In humans, portions of the PNS myelinate first, then the spinal cord, and the brain last.

1.3.2 The myelination factors

In the PNS, axons directly control the thickness of their myelin sheath via the regulation of the expression of **the neuregulin** (NRG) family of proteins and their receptors, which belong to the ErbB family of tyrosine kinase receptors (heterodimeric ErbB2–ErbB3 in SCs and ErbB4–ErbB3 in CNS oligodendrocytes), and are important regulators of most aspects of SCs

development (Michailov, 2004; Taveggia, 2008).

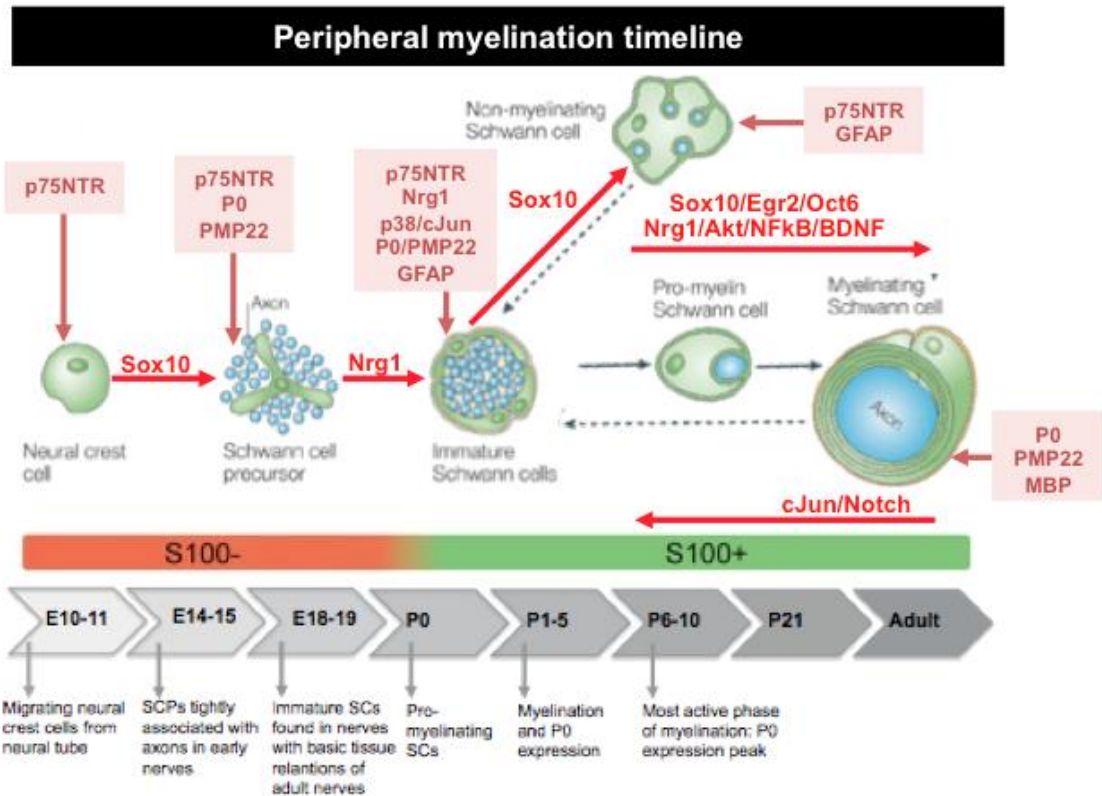


Figure 9. The embryonic phase of SCs development involve 3 transient cell populations: migrating neural crest cells, SCPs and immature SCs that have the same developmental potential that mature SCs. Myelination occurs only in SCs that by chance envelop large diameter axons. SCPs can differentiate from NCSC by expression of molecular markers, such as P0, that is not present in NCSC (Jessen and Mirsky, 2005). Moreover, different trophic factors, for example FGF and IGF, are necessary for SCPs to survive. However, NRG1 signalling is required by NCSC survival, but not SCPs. (Woodhoo *et al.*, 2004; Woodhoo and Sommer, 2008). iSCs overexpressed GFAP, S100 and p75NTR (Jessen and Mirsky, 2005). Egr2 is a typical marker for pro-myelin SCs (pro-mSC) and myelinating SCs. MBP is also a specific marker for mSCs. However, non-myelinating SCs don't express P0 or Oct6 (Liu Z. *et al.*, 2015). Sox10 is essential for SCs lineage and the NRG1 axonal contact is a survival factor for SCP.

NRGs are encoded by at least four genes (NRG1, NRG2, NRG3 and NRG4) of which Nrg1 was the first discovered and best characterized. Nrg1 encodes at least six major isoforms generated by alternate splicing or by use of several cell type-specific transcription initiation sites and perform a wide variety of functions (Britsch, 2007). The more relevant NRG1 isoforms are NRG1typeI, NRG1typeII and NRG1typeIII.

The NRG1/ErbB signalling pathway, related by myelin process, occurs with the PI3K/Akt/mTOR intracellular signalling pathway, that is necessary to promote growth and cellular proliferation over differentiation, specifically in NSC development and migration to initiate the myelination process and myelinating SCs (Meyer, 1997; Flores, 2008; Goebbels, 2010). Different mutations in NRG1,

ErbB2/ErbB3 genes cause embryo developmental problems, by altering the NSC migration (Britsch, 1998).

There are many other factors that enhance the myelin pathway by activation PI3K/AKT pathway to promote NSCs proliferation, including IGF1 and insulin, related thus the insulin implication between DM, neuropathy and demyelination (**Fig14.**) (Ojeda, 2011).

In PNS most signals that promote myelination act through different factors to drive the transition from iSCs to mSC and myelinating SCs (**Fig9. & Fig13. & Fig14.**), for example Oct6 (SCIP), Krox20 (EGR2) and Sox10 to promyelinated ones; and cJun and Sox2 as factors to control demyelination.

Oct6 is a transcription factor that initiates the transition from non- to promyelinating (Ghislain, 2002; Jagalur, 2011). Expression of Oct6 shows a peak right after birth in promyelinating SCs, as well as in the first steps of the regeneration process. Mice mutants for Oct6 have a delay in the myelination kinetics and show hypomyelinated phenotypes (Bermingham, 1996; Jaegle, 1996; Jaegle, 2003).

In normal human peripheral nerves, Oct6 is only present in the cytoplasm (Kawasaki, 2003; Nickols, 2003; Yoon, 2008). Moreover, during myelin formation and in the early phase of axonal degeneration after injury, Oct6 is upregulated and translocated to SCs nuclei to promote the transcription of myelin genes (**Fig9. & Fig13. & Fig14.**) (Kawasaki T, 2003).

Sox10 is expressed during all stages of SCs development, and continues to be present in myelinating SCs in adult PNS (Kuhlbrodt, 1998a). Specific Sox10 deletion in mouse model confirmed the importance of this factor for SCs development (Britsch, 2001). There is also evidence that Sox10, both to Krox20, controls the expression of several peripheral myelin genes, such as P0 or MAG (Peirano, 2000; Bondurand, 2001; Jones, 2007; LeBlanc, 2007). Furthermore, Sox10 has a dependent activation of Oct6, and defines a feedforward regulatory module that serves to amplify the onset of myelination in the PNS (**Fig9. & Fig13. & Fig14.**) (Ghislain, 2002; Jagalur, 2011).

The Oct6 and Sox10 synergize activate the expression of the major myelin related transcription factor **Krox20** (Jagalur, 2011), considered as the master regulator of PNS myelination (**Fig9. & Fig13. & Fig14.**) (Topilko, 1994; Nagarajan, 2001; Ghislain, 2006). Krox20 gene mutations block SCs at the promyelinating stage

(Topilko et al, 1994) and in vitro experiments showing that P0, MBP, PMP22 or MAG myelin genes are induced by this transcription factor (Bondurand, 2001; Nagarajan, 2001; Taveggia, 2004; Denarier, 2005; LeBlanc, 2006). Moreover, Krox20 is also implicated in the lipid biosynthesis necessary for myelin formation, (Leblanc, 2005). Consistently, Krox20 mutations have also been identified in patients from hereditary peripheral neuropathies, such as Charcote Marie Tooth 1 (CMT1) or Déjérine-Sottas syndrome (DSS) (Warner, 1998; Warner, 1999; Pareyson, 2000).

Sox10 also respond to NFATc4 (nuclear factor of activated T cells) and recently, it was demonstrated the calcineurin/NFAT pathway implication in myelination process, through NRG1/ErbB signals to activate Krox20 and P0 expression, synergistically with Sox10 (Fig.13) (Kao, 2009; Reiprich,2010).

2. Damage in the PNS

Different from CNS, PNS is able to regenerate after an injury due to the capacity to phagocytes cellular debris rapidly.

2.1 Wallerian degeneration (WD): implications after injury

Wallerian degeneration (WD) (described by Augustus Waller in 1850) is a uniform reaction of PNS that involves complex interactions of axonal and myelin structures with cellular elements such as SCs and macrophages (Fig.11). WD can be described as a macrophage-driven process (Perry et al., 1987) that proceeds from the site of nerve injury distally, culminating in phagocytosis of the injured axons and associated SCs (Brück, 1997; Stoll, 2002; Myers, 2011).

NRG1 are believed to be responsible for the rapid activation of WD mechanism in the PNS, through ErbB2 receptor activation in SCs resulting in the activation of the MAPK pathway (Fig14).

The pathology begins when axons separate from cell bodies after peripheral injury, and with interruption of the perineurial layer, hypertrophy of endothelial cells, and infiltration of macrophages.

Two hypotheses have been proposed for axon degeneration. The 'focal lesion hypothesis' triggers WD of the distal stump while the proximal stump remains intact. Alternatively, the 'dying-back hypothesis' postulates that the axons degenerate at the distal part with a retrograde progression. Elucidation of the

mechanisms of axon degeneration could help to gain insight into the peripheral neuropathies.

It is possible to differentiate two nerve segments when the WD starts (Fig10.). First, **the proximal stump** refers to the end of the injured neuron that is still attached to the neuron cell body; and it is the part that regenerates better.

In the **distal stump** of nerve fibers, at the end of the injured neuron, that is still attached to the end of the axon. In this segment, within 48 h following peripheral nerve injury, and after disintegration of the neuronal cytoskeleton, the axolemma also degenerates at the same time followed by myelin sheath break down to smaller segments (termed ovoids), and SCs retract their cytoplasm (Fig10.). This destruction of axons and myelin is initiated by a calcium-dependent process (Fig13.) (Schlaepfer, 1973; Oaklander, 1988; Kidd, 1991; Wu, 1994; Bruck, 1997).

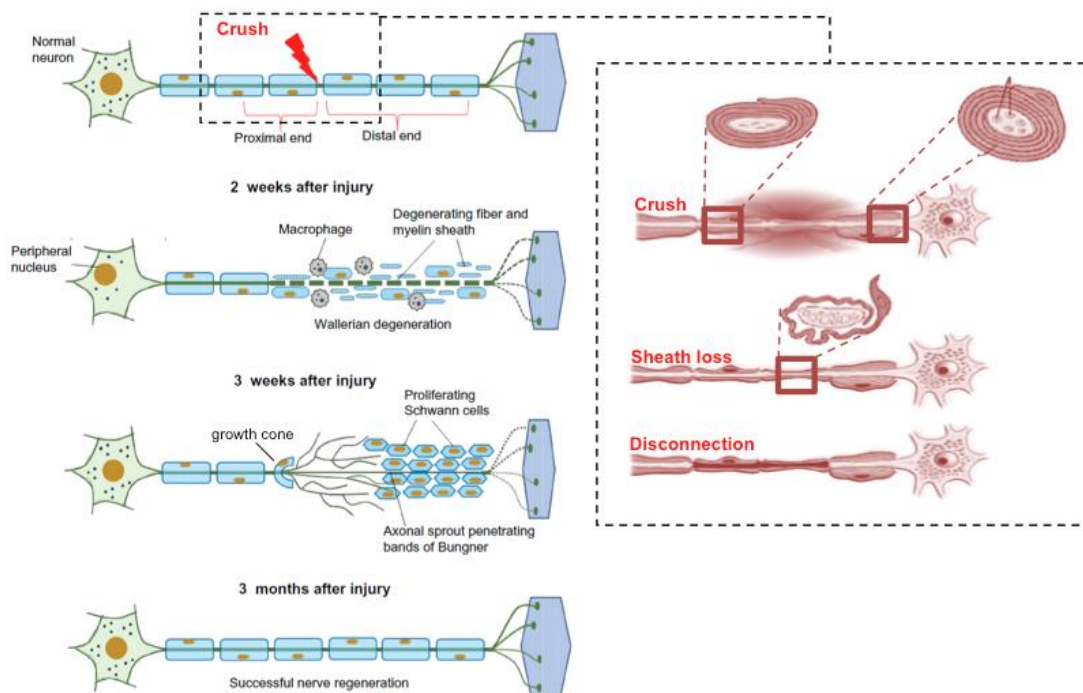


Figure 10. Wallerian degeneration (WD) occurs distally from the site of nerve injury distally, culminating in phagocytosis of the injured axons and associated SCs. Distal stump degenerates within 48 h following injury and the process is complete about 3-4 wpl. (Adapted from Svaren, 2016).

Within the next few days, circulating macrophages enter into the distal stump through the damaged Blood-Nerve-Barrier (BNB) and phagocyte axonal and myelin debris from degenerated fibers. The recruitment of resident macrophages start within hours while the infiltration of macrophages from blood

begins 2-3 dpl and peaks between 7 and 14 dpl, when myelin clearance is almost complete. The myelin debris are digested by hydrolytic enzymes in cytoplasmatic vacuoles after fusion with lysosomes (Han, 1989; Hirata, 1999; Holtzman, 1965).

2.1.1 The origin of macrophages in WD

The clearance by phagocytic elements of these injured tissue components and the removal of myelin debris is one of the most important and critical events preceding the regenerative process (Schubert, 1981; Beuche, 1984; Scheidt, 1987).

The origin of phagocytes appearing after nerve injury was controversial. Ramon y Cajal (1928) elaborated the details of the sequential process of cellular alteration following nerve injury and concluded of the exogenous origin of phagocytes. However, he did not exclude the possibility that SCs behave as true phagocytes, such as Weiss and Wang (1945) demonstrated from in vitro experimental, concluding that SCs are a major source of phagocytes.

Nowadays, it is known that in vivo, SCs also phagocytose myelin and axonal debris and infiltrating blood-borne macrophages are joined to complete the process. First of all, within 2 days after WD starts, SCs have already transformed from myelinating cells to myelin phagocytosing cells. However, at this time myelin-phagocytosis by macrophages is rarely detected (Sulaiman, 2010). Therefore, maintenance of healthy SCs is of vital importance in peripheral nerve biology (Hirata, 2000).

Moreover, while WD in the PNS is fast, taking 14-21 days to clear axonal and myelin debris, it is dramatically slow in CNS. This fact has suggested that slow or deficient debris clearance could create an inhibitory environment for axonal regeneration. In addition, the pro-regenerative response of SCs to nerve injury is facilitated by early intercellular interactions with fibroblasts through adhesion cell molecules (CAMs).

2.1.2 Cytokines involved in WD

According with the cytokine expression pattern during WD, some authors suggest that **cytokines are involved in the physiopathology of WD**, and they have classified WD in a two-stage process. The first one, is an inflammatory process when pro-inflammatory cytokines such as IL-1b and TNFalpha are

produced mainly by **resident** macrophages and SCs, followed by a second stage of WD which aims at resolution of inflammation with secretion of anti-inflammatory cytokines such as IL-10 by **infiltrated** macrophages and Schwann cells (**Fig15.** & **Fig16.**). TNFalpha has been identified in WD and also in others inflammatory demyelinating lesions of the PNS and CNS such as Multiple Sclerosis (MS).

Macrophages release pro-inflammatory molecules during injury to activate resident and migrating inflammatory cells and increase vascular permeability. For example, the role of these cytokines is the activation of T helper cells to activate B cells generating myelin-specific antibodies and macrophages to produce ROS. This combination of molecules damages the myelin sheath and axons. Finally, symptoms decrease with a full recovery in most cases, due to the downregulation of Tcells by antiinflammatory molecules and apoptosis pathways.

Moreover, the type of nerve injury is relevant to determine the successful of WD and regeneration process.

2.2 Peripheral nerve injuries

Peripheral nerve injuries can be caused by peripheral neuropathies or can occur as a result of trauma or acute compression, and may result in loss of motor function (skeletal muscle remains weakness and paralysed), sensory function (the sensory information is not sent to the CNS), or both; and depending on the severity and the degree of nerve injury, recovery of function occurs with remyelination, regeneration and reinnervation. It was demonstrated that motor and sensory pathways have distinct functional identities that regulate the regenerative sprouting of axons.

The severity of the damage is categorized in the Seddon classification (1943), based on the extent of structural and functional alterations of nerve fibers and the surrounding connective tissue (**Fig11.**). Thus, there are three different degrees of nerve injury: neurapraxia, axonotmesis and neurotmesis. The Sunderland classification, more complex and specific than Seddon types, can also be used to determine the severity of injury.

Classification of peripheral nerve injuries				
Seddon	Sunderland	Injury	Degeneration	Regeneration
Normal	Normal	Normal	Normal	Normal
Neuropraxia	I	Myelin sheath (M)	Conduction block	Complete recovery
Axonotmesis	II	M+ Axon(A)	Wallerian Degeneration	
Neurotmesis	III	M+A+ Endoneurium(E)		Incomplete recovery
	IV	M+A+E+ Perineurium(P)		
	V	M+A+E+P+ Epineurium		

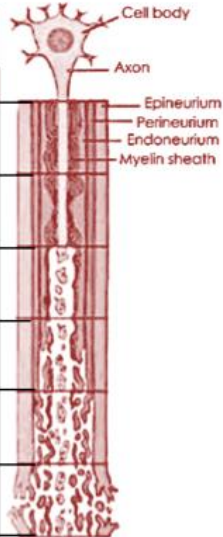


Figure 11. Types of peripheral nerve injuries using the classification of Seddon and Sunderland. The Sunderland classification uses five different degrees of nerve injury, the first one being the least severe and the equivalent to neurapraxia and the most severe being the fifth degree and having the same classification as neurotmesis. The second through fourth degrees are dependent on the variance of axon discontinuity and are classified under Seddon’s classification of axonotmesis (Adapted from Seddon, 1943; Suddenland, 1965 and Novak, 2016).

The lowest degree of nerve injury in which the nerve remains intact but its signaling ability is temporarily damaged is called neuropraxia (From Greek *apraxia* inaction: “loss or impairment of the ability to execute complex coordinated movements without muscular or sensory impairment”). Normally, neuropraxia is caused by pressure and as a result ischemia occurs and an edema is extending from the source of pressure. It blocks the action potential transmission and causes a reduction or loss of function in the downstream neural connection. As a result of intact and no transected nerve fibers, WD does not occur in neuropraxia (Campbell, 2008). Thus, neurapraxia is almost always followed by a quick and complete recovery period.

The second degree in which disruption of axon and nerve fibers is observed, but the majority of the SCs remain preserved, is called axonotmesis (in Greek *tmesis* signifies "to cut"). WD often occurs below in the distal section of nerve injury site and proximal sections are repaired by creating a sprout growth cone. The recovery depends also on the distance involved, and nerve regeneration may take several months.

The last and most serious degree in which both the axon and connective nerve sheath tissue are damaged, equivalent to physiologic disruption of the entire nerve, is called neurotmesis. While partial recovery may occur, complete recovery is impossible (Burnett, 2004).

2.1.2 Peripheral neuropathies: Classification

Peripheral neuropathies are diseases that course with peripheral nerve injury in which either the axon or SCs display dysfunction due to metabolic, toxic, infectious, or genetic causes. The cellular and molecular mechanisms involved in the development are diverse and only partially understood.

The patients often experience symptoms depending on the type of the nerve fiber affected: motor nerve fiber, autonomic nerve fibers, proprioceptive sensory fibers or other sensory fibers may lead to paresthesias, and sometimes pain. Diagnosis of peripheral neuropathy is often made based on examination of features that corroborate involvement of specific nerve fiber types, nerve conduction studies, electromyography, and blood tests to measure the neurotrophic factors levels. Nerve morphometric studies to determine axonal atrophy are more invasive, tedious and time consuming.

Based on these parameters, peripheral neuropathies are classified in hereditary peripheral neuropathies (PN), acquired PN and immune PN.

Although **hereditary neuropathies** include a variety of diseases with various aetiologies about clinical and genetical criteria (autosomal dominant, recessive or X-linked). The hereditary long-standing chronic sensorimotor polyneuropathy associated with demyelinating processes are the most common. They include all forms of Charcote-Marie-Tooth (CMT) hereditary neuropathy with liability to pressure palsy (HNPP) and DSS. CMT diseases are the most frequent inherited neuropathy with a prevalence of 4/10,000.

On the other hand, **acquired peripheral neuropathies** are one of the most common neurological disorders, affecting nearly 20 million people in the United States alone. In the developed countries, DM (Diabetic polyneuropathy, DPN) and alcoholism are the most common metabolic etiologies. However, the main cause in primary worldwide is leprosy. HIV-associated sensory neuropathy due to an infectious disease and chemotherapy-induced peripheral neuropathy

(CIPN), caused by a chemical agent, are some of the more common acquired diseases (prevalence 48% in 2016) (Tzatha, 2016).

The prototypic **immune neuropathy** is the heterogeneous Guillain-Barré syndrome (GBS), one of the most common disorders in industrialized countries (1-9/45000 incidence, 3-5% in Western countries but 30-50% in Asia and Latin America) (orphan.net, 2016). This disease is frequently preceded by viral infection, vaccination or serum injection leading to a humoral and cellular auto-immune response against the peripheral myelin.

3. Regeneration in the PNS

Generally, the processes of degeneration and **regeneration** occur simultaneously, although one process can predominate depending on intrinsic or extrinsic factors and it appears that a certain level of degeneration is necessary for regeneration, at least in vertebrate nerves (Hilliard, 2010).

Functional deficits caused by nerve injuries can be **recovered by three endogenous neural mechanisms**, which can be summarized as the '3Rs': by **regeneration** of injured axons reinnervating denervated targets; the **reinnervation** can be achieved by collateral sprouting of undamaged axons; and by **remodelling** of circuits within the CNS (Navarro, 2015).

3.1 The process of regeneration

The first phase may be subdivided into two steps, the emergence of sprouts from the transected axons and their growth across the injury and repair site, called the latency period, and the elongation of axons along the distal nerve segment (Witzel, 2005).

The axons that remain attached to the cell body, proximal to the nerve injury, are sustained with intact myelin (Fig10.). Axons that regenerate within the distal endoneurium will have a right reinnervation only if they reach an appropriate target tissue establishing functional connections. However, it does not always result in effective reinnervation, due to an increasing probability of misdirecting regrowth through a foreign distal branch and mismatching targets (Madison, 1996; Valero-Cabre, 2002a).

Following appropriate reinnervation, regenerated axons mature with an increase in size and myelin thickness that tend to restore normal conduction properties as well as movement and sensation. Finally, the restitution of complex functions requires also that the central connections return to normal pattern after being lost or reorganized due to the nerve injury (Munro, 1998; Valero-Cabre, 2002a; Nichols, 2005; Navarro, 2007).

However, functional recovery is usually not complete and the functional reinnervation of the target tissue is better in distal stumps (Gordon, 1982).

Functional analysis offers the most unequivocal way to demonstrate that a nerve has not only regenerated, but also had made appropriated end organ connections (Nichols, 2005; Vleggeert-Lankamp, 2007). In vivo electrophysiological studies after a nerve crush reported different timelines in the regeneration process according to the fibre diameter, and it depends of the type of peripheral nerve injury and different factors such as severity and site of nerve injury, age of the subject, and the distance axons have to grow until they reach distal targets (Krarup, 1988; Navarro, 1994; Verdú, 1997). In addition, histological data showed no evidence that myelinated fibres regenerate less well than unmyelinated fibres (Giannini, 1989).

Mature SCs have the remarkable capacity to reverse their phenotype and dedifferentiate when they lose contact with axons (Fig.9 & Fig12). Therefore, after a peripheral nerve injury, the molecular markers characteristic of mature SCs are dramatically downregulated, such as P0, as a consequence of axonal degeneration distal to the injury site, whereas markers of immature and non-myelinating SCs, such as p75NTR, are re-acquired. When these cells regain contact with the axons, they re-differentiate again (Jessen, 2008).

Between day 1 and 5 after injury, SCs start proliferating with a peak of activation around 3dpi and then there is a decrease during the following weeks. This proliferation plays a key role during WD since, in coordination with macrophages, SCs initiate the degradation of myelin debris. A second phase of proliferation occurs later to create a permissive pathway for regenerating axons (Schroder, 1972; Powers, 2013).

Both, the intrinsic capacity of neurons and SCs to switch to a proregenerative state and the trophic environment of the distal nerve are key factors to outcome nerve regeneration. SCs react robustly to injury by secreting a number of growth factors to support glial and neuronal survival, normally this release occurs in a fiber-type specific pattern (Fig12.).

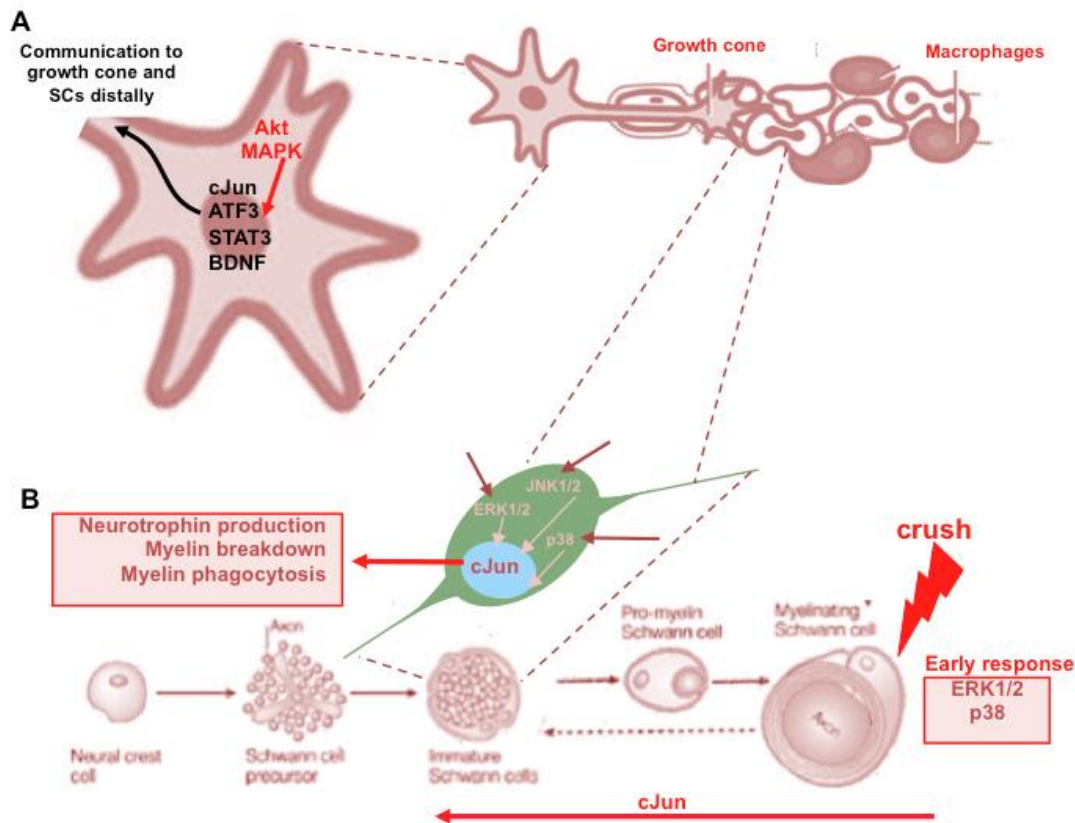


Figure 12. Scheme of nerve repair following peripheral nerve injury. **(A)** After injury, neurons also change the expression pattern of some transcription factors, and increase the novo synthesis of some of them, such as ATF3 and STAT3, to communicate both to SCs and basal lamina and ECM, **(B)** Following transection, ERK1/2 and p38MAPK signaling rapidly increase within SCs distal to the site of injury and cause them to proliferate and take on an undifferentiated repair phenotype that depend upon the transcription factor cJun, which direct both the breakdown of myelin and the production of neurotrophins, such as BDNF. (Adapted from Kim, 2013).

These results open the possibility of manipulating neurons using gene therapy techniques, to virus-based vectors or nanoparticles, to swicht their intrinsic growth capacities. Actually, this approach is being directly applicable for hereditary demyelinating peripheral neuropathies (Navarro, 1994; Verdu, 1997; Abe, 2010; Mitnacht, 2010; Ma, 2011; Guerout, 2011; Homs, 2014). Cell therapy in the PNS mainly focused on SCs (Rodriguez, 2000) and mesenchymal stem cells (McGrath, 2012) are also another alternative for therapy (Birnaskie, 2007; Martini, 2008; Khuong, 2014).

Moreover, improved artificial nerve guides adding neurotrophic factors or transplanting cells with genetic modifications has also been tested (Radtke, 2011).

3.1.1 Tropic & trophic cues

Tropic and trophic cues play important roles in the guidance of axons regrowing through the degenerated distal nerve towards the target tissues (Navarro, 2003).

After injury and WD, in order to achieve successful regeneration and to maintain the proper directionality, SCs and macrophages provide a permissive micro-environment for axonal re-growth by releasing cytokines and neurotrophic factors for promoting axonal outgrowth or by producing CAMs and their receptors necessary for axonal guidance through basal lamina and the extracellular matrix complex (ECM) (Griffin, 1992; DeFrancesco-Lisowitz, 2015). This process is known as chemotaxis, and cues can have both, chemoattractive and chemorepulsive properties to create a permissive environment for axonal growth or a molecular barrier that impairs axonal elongation. In addition, denervated SCs also express on its plasma membrane several receptors for neurotrophic factors, such as the p75 neurotrophin receptor (p75NTR) in the distal segment (Wen, 2006).

Once SCs regain the contact with axons, SCs return to a quiescent state and the expression of neurotrophic factors and their receptors is suppressed. In an intact peripheral nerve there are presence of inhibitory factors for regeneration, and these molecules are upregulated right after nerve injury (Wen, 2006). The sprouts that do not make peripheral connections undergo atrophy and finally disappear. If growth cones don't reach the distal stump, they may sprout within the proximal stump forming a neuroma (Mackinnon, 1991).

Interestingly, unmyelinated fibers remain unmyelinated independently of the origin of the SCs. Besides, the myelinating or unmyelinating phenotype, it was proposed a selective secretion of trophic factors by SCs of motor or sensory neurons, in accordance to the different phenotypes that have been observed in SCs (Martini, 1994; Saito, 2005). This capability is probably related to the expression of receptors in different populations of neurons. Properly, the "topography regeneration" term should complement the expression of "selective

regeneration”, due to that the reconnection of proximal neurons and distal end organ targets follows a determined topographic order that was created during development, disrupted after lesion and trying to be restored by the neurotrophic pattern expression in the extracellular environment (Hoke, 2006, Allody, 2012).

3.2 Molecular pathways

The molecular pathways involved in the production of these trophic factors are diverse (Fig13. & Fig14. & Fig15.).

3.2.1 The PI3K/Akt/mTOR pathway

PI3K/Akt/mTOR (phosphatidylinositol 3-kinase/Akt/mammalian target of rapamycin) signaling downstream of NRG1/ErbB can serve as an additional mechanism to promote myelination, even at later stages of development (Flores, 2008; Goebbels, 2010; Harrington, 2010; Sherman, 2012). Pharmacological inhibition of PI3K blocks myelination in vitro at an early stage whereas PI3K gain of function, results in hypermyelination in vivo with the occasional small-caliber axon switching to a myelinated fate (Maurel and Salzer, 2000; Goebbels, 2010).

Active AKT-phosphorylating (Fig14.) form can have a number of downstream effects activating Oct6 and Egr2 transcription factors, that affect the expression of myelin protein like P0 and also the cholesterol biosynthesis by the HMG-CoA activation, an essential lipidic component from cell membrane and myelin. Moreover, AKT may be involved in the axonal signal that drives production and deposition of ECM by SCs (Bunge, 1986; Innocenti, 2003; Porstmann, 2005; Taveggia, 2005; Chen, 2006; Quintes, 2010).

Recent data with transgenic knockout animals and in vitro studies to pharmacologically inhibit the Akt activity, indicates that this kinase is the major PI3K effector during myelination, promoting SCs wrapping and myelination via multiple distinct pathways (Fig14.) (Topilko, 1994; Zorick, 1996; Decker, 2006; Goebbels, 2010; Xu, 2012; Ebi, 2013; Sudheendra, 2016). The results also demonstrate that Akt is a key regulator of PNS myelination and NRG1III is the main driver of Akt activation (Michailov, 2004; Taveggia, 2005; Thurnherr, 2006; Benninger, 2007; Nodari, 2007; Flores, 2008; Heller, 2014).

mTOR also has a key role in SCs myelination and links nutrient availability and cell growth by regulating protein and lipid synthesis. In addition, insulin plays a major role as neurotrophin in PNS, and also activates mTOR via Akt-pathway (Porstmann, 2008; Laplante, 2009; Peterson, 2011; Sherman, 2012). Mice mTOR deficient have delayed myelination and hypomyelination in the adult due to impairment in lipid biosynthesis (Normen, 2014).

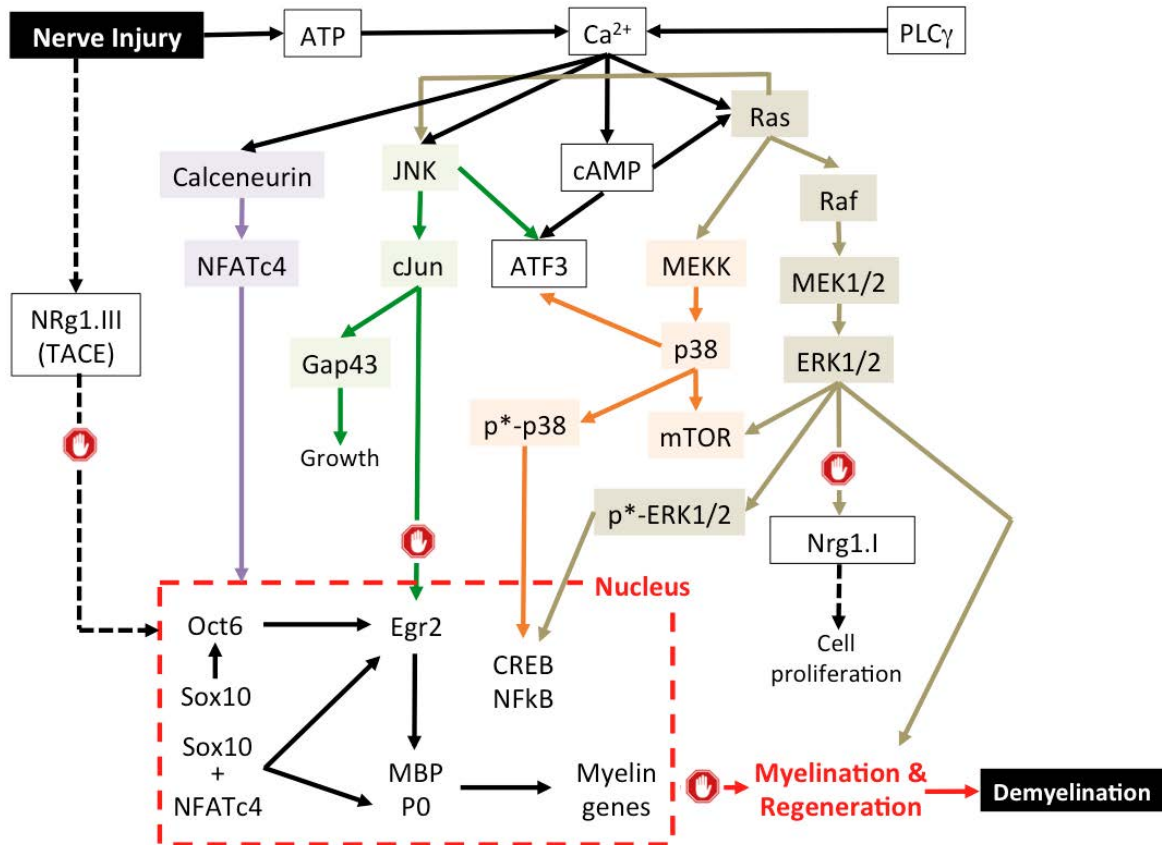


Figure 13. Activation of diverse molecular pathways following peripheral nerve injury.

Further studies of Akt-dependent pathways in myelination may identify more specific therapeutic targets for these neuropathies in the future, mainly as a therapies involved with negative or deficient myelination phenotype. However, Akt pathway seems not be the principal signaling cascade in response to myelin formation after peripheral injury (Caballi V, 2008; Yang, 2012).

3.2.2 The p38/MAPK pathway

The p38 MAPK pathway and the downstream effector c-Jun, are now being recognized as the critical molecules required for resetting SC fate towards a reparative phenotype and are also specifically important in axonal regeneration

(Fig.14.). (Cavalli, 2008; Arthur-Farraj, 2012; Yang, 2012). This signaling pathway also regulates cytokine expression by phosphorylation and enhances the activity of many transcription factors, such as NF κ B (Fig15.). Moreover, p38 MAPK inhibition reduces SC TNF α protein and increases the rate of regeneration in crushed nerve fibers (Myers, 2003). In spinal cord, p38 inhibition reduces TNF α synthesis and attenuates mechanical allodynia, 3 days after chronic constriction injury (Xu, 2007).

3.2.3 The ERK pathway

The ERK pathway is also involved, particularly by ERK1/2-MAPK, in the regulation of myelin thickness and promoting myelination after damage (Fig.14.). The ablation of ERK1/2 in SCs arrests their differentiation, resulting in dramatic hypomyelination (Newbern, 2011; Ishii, 2012). Through this pathway, TNF- α can directly modulate its own production (Fig15.) (Song, 2003).

There is also strong evidence that suggests a negative effect of increased activation of this pathway. For example, in vitro activation of ERK1/2 or upstream effectors prevents SCs differentiation, induces downregulation of myelin proteins and causes demyelination in SCs-DRG cocultures. Also in vivo overactivation of ERK1/2 in adult peripheral nerves leads to their dedifferentiation and demyelination (Harrisingh, 2004; Ogata, 2004; Napoli, 2012).

Future studies are required to determine whether PI3K/Akt/mTOR and Mek/ERK1/2-MAPK are independent parallel pathways or whether they cooperate to facilitate myelin growth.

3.2.4 The NRG1/ErbB signalling pathway & regeneration

After nerve injury, both axonal and SCs derived NRG1 are required for remyelination and axon regeneration, as suggested by findings in transgenic mice (Fricker, 2011; Pereira, 2011; Stassart, 2013; Boerboom, 2017). In addition, neuregulins produced by SCs may be partially responsible for SC proliferation during WD (Fig.14). The current understanding of the involvement of NRG in peripheral regeneration following injury is that axonal transmembrane NRG 1 type III repress soluble NRG 1 type I expression in SCs via ERK1/2 (Raphael, 2011; Luo, 2011; Fleck, 2013; Stassart, 2013; Mei, 2014). Moreover, NRG1 type III is upregulated in the regeneration phase of peripheral nerve injury (Ronchi, 2015).

The NRG1/ErbB pathway also has an extensive crosstalk with other signaling pathways and activates the MAPK/JNK/ERK cascade, PI3K, and other downstream pathways, including the calcineurin/NFATc4 pathway, which has been implicated as essential for proper myelination (**Fig.14**). (Pietri, 2004; Kao, 2009; Woodhoo, 2009; Newbern, 2010; Mogha, 2013; Schulz, 2014; Petersen, 2015). Moreover, AKT and p38 that have been recently described to exert early signalling responses although their roles are still controversial (Perlson, 2005; Michaelevski, 2010). These pathways change the nuclear localization and phosphorylation of different transcription factors such as cJun or ATF3 (will lead to changes in gene expression of the injured and regenerating neurons, with an increase o growth associated protein GAP43, and a decrease proteins involved in the neurotransmission machinery, such as of neurofilament proteins, ion channels (Jankowski, 2009, Mason, 2011).

The precise roles of these signaling pathways in the transcriptional and morphogenetic events of myelination, however, remain to be established nowadays.

3.3. Regenerative neurotrophic factors

Peripheral nerve regeneration is a challenging field nowadays: the enhancement or the inhibition of certain cell pathways previously described can modulate the regenerative capabilities of neurons after injury. Positive and negative signals coming from the injury site turn neurons to a pro-regenerative state, activating the regenerative machinery that involves expression of regeneration-associated genes and producing downstream changes on the extracellular environment in order to get a positive regenerative outcome (Van Kesteren, 2011).

Several growth factors and neurotrophins such as NRG1 type III or BDNF, activate this molecular pathway axes promoting myelination by integration of signals from multiple upstream factors and downstream substrates: transcription factors, epigenetics regulators, microRNAs, cytoskeletal proteins and receptors. (Roux, 2004; Du, 2006; Shahbazian, 2006; He, 2010; Steelman, 2011; Patzig, 2011; Xiao, 2012).

The expression of neurotrophic factors also play critical roles during development. The specific receptors for these family of molecules are called Trks (Tyrosine kinase receptors), a family of protooncogene receptors which mediate their effects on DRG neurons and in some motoneurons.

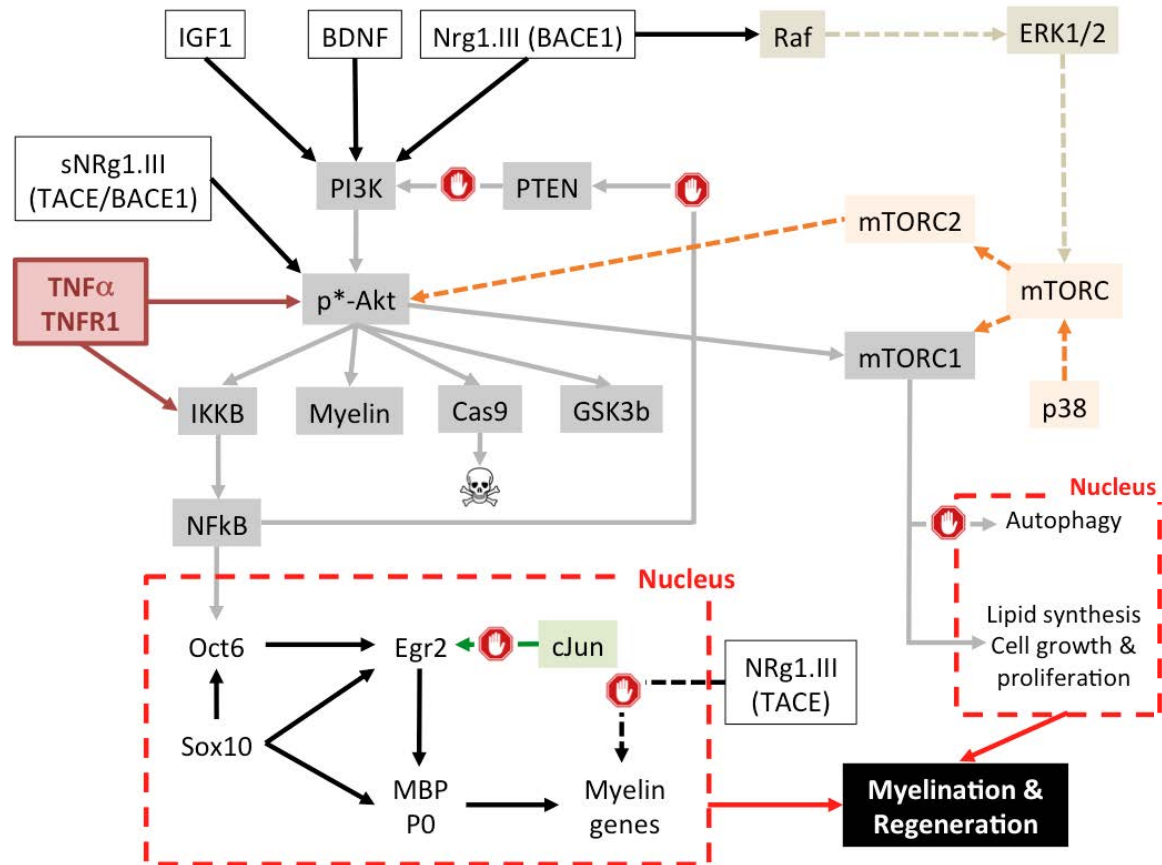


Figure 14. Schematic representation of the main signalling pathways related to myelination and regeneration after peripheral nerve damage.

TrkA is the high-affinity receptor for NGF and it is expressed in subpopulations of the small primary sensory neurons, but not in motoneurons. TrkB is the high-affinity receptor for BDNF and is normally found in spinal motoneurons and also in mid-size primary sensory neurons. TrkC is present in spinal motor neurons and in a subpopulation of large primary sensory neurons (Esper, 2009). p75NTR is a low-affinity receptor for neurotrophins and the role of this receptor is controversial as it can exert also pro-apoptotic functions. (Bennet, 1996a; Hoke, 2001; Hoke, 2006).

Following peripheral nerve injury, these receptors are upregulated mainly on the distal portion of the nerve in denervated SCs. There is also an increased transport of all neurotrophins dependent on binding to p75NTR and TrK in sensory neurons, but only to p75NTR which is upregulated in motoneurons. (Curtis, 1998; Webber, 2008).

The role of **BDNF** in regeneration is controversial, although the presence of its receptor seems crucial for axonal regeneration (**Fig14.**). In intact PNS normal conditions, BDNF protein and mRNA will decrease only after myelination has already been initiated. However, deprivation of endogenous BDNF impairs axonal growth and myelination, whereas local infusion improved nerve regeneration. It was demonstrated that elevated levels of BDNF in the SCs during the early stages of myelination increase the speed and extent of the final process, but after peripheral injury, the positive effects of BDNF are only detected in the more severe protocols (Zhang, 2000; Boyd, 2003; Vögelin, 2006). As a consequence, expression of BDNF could be a diagnostic value and predict the prognosis and severity, of the injury as functional electrophysiological examinations are not distinguishable from different types of injuries. Sensory neurons are the major contributing source of the increased traffic level in the sciatic nerve (Grothe, 2000).

Signal transducer and activator of transcription-3 (STAT3) mediate a wide variety of biological functions in the CNS and PNS such as cell growth, regulation, inflammation, and embryological development (**Fig15.**) (Dziennis, 2008). Injury-induced ligand binding to cell-surface receptors activates STAT3 by phosphorylation, being identified as an acute phase response factor (Akira,1994). This factor is expressed cytoplasmically in both neuronal and glial cells during development and in the adult in axonal regeneration (De-Fraja, 1998; Gautron, 2006). STAT3 activation after sciatic nerve injury occurs in axons within 15 min of lesion, leading to retrograde signaling to the nucleus (Lee, 2004), where it is involved in the program promoting axon growth. STAT3 induces GAP43, a protein found in growth cones, suggesting a role for the JAK/STAT3 pathway in GAP43 expression and neurite outgrowth and regeneration (Wu, 1996).

There is huge number of different studies investigating the complex association between ATF3 and c-Jun expression after injury. ATF3 can also interact with other transcription factors upregulated after peripheral injury, such as, STAT3. In normal conditions after peripheral nerve injury, ATF3 is overexpressed in neurons, blocking the expression of injury and pain markers such as CCL2, and potentiating the transcription of tropic and trophic factors associated to axon growth and regeneration, such as GDNF or NGF (Hunt, 2004; Dubov, 2013; Gey, 2016).

4. Neuroinflammation in PNS injury

Cells communicate with each other by three major categories of intracellular signaling molecules, sometimes overlapping in actions, produced by a variety of cell types and local tissues themselves: peptide hormones, growth factors and cytokines. Whereas growth factors are produced constitutively, cytokines most of cases are inducible in a variety of ways. All of them are involved in regulating inflammatory cells, connective tissues and vascular responses against pathological conditions, including infections or injuries. (Akira, 1990; Ebadi, 1996).

Microglia and peripheral glial cells are able to detect primary damage in nerve (Fig15.). In response to nerve injury, these cells become activated and release prostaglandins and reactive oxygen species (ROS) that excite pain-sensitive neurons. Moreover, microglial cells also release proinflammatory molecules, including IL1beta, IL6 and TNFalpha; generating a positive feedback loop that increase p38 MAPK and release of BDNF, to finally exacerbate the pain response (Munoz-Fernandez, 1998, Tonelli, 2005, Truettner, 2005).

These cytokines in intact nervous system have low expression levels, and their physiological functions are also reduced in comparasion with its role against injury or other pathologies. The induction of proinflammatory cytokines allows the expression CAMs and other cytokines as well a self-regulation, by SCs, macrophages or endothelial cells (Schmidt, 2005; Lucas, 2006). The inflammatory cascade also allows macrophages and lymphocytes to enter into the injury area and increase the expression of IL1beta and other molecules involved at vasodilation process (Romanic, 1998, von Gertten, 2003; Lindberget, 2004; Lucas, 2006).

NO, iNOS and ROS are also produced through different mechanisms by activated SCs or macrophages (Fig16.), due to cell membrane damage, demyelination and apoptosis. All of them are events that cause oxidative stress. (Stewart, 1998; Munoz-Fernandez, 1998; Blocket, 2005; Hendriks, 2005; Lo, 2005). However, during inflammatory response there are also produced trophic factors and neurotrophic factors produced, that they help to resolve the inflammation and promote beneficial actions (Morrison, 2000; Wang, 2002; Correale, 2004).

Macrophages and the phagocytic capacity of other cells such SCs and also neutrophils, during injury, are a beneficial process to the remodeling and regeneration of the lesion site, thanks to WD and trophic factors. (Frautschy, 1991; O'Donnell, 2002; Schwartz, 2003). However, the migration and phagocytic rate of infiltrated macrophages in CNS are reduced versus PNS, explaining the poor and lower regeneration capacity of CNS (Schwartz, 1999; Stoll, 1999; Yamagami, 1999; Nygardas, 2000; Charo, 2006; Rebenko-Moll, 2006; McColl, 2007).

A cytokine, from greek: cyto-cell and kinesi-movement, is defined as a molecule that is produced by a cell but exerts its effect in another different cell. Cytokines are secreted as small polypeptides and/or glycoproteins (5-20 kDa) that are secreted de novo to react against an immune stimulus in a short period of time and are important in autocrine, paracrine and endocrine immunomodulating agents. Normally, cytokines are characterized by considerable pleiotropism, and also antagonistic effects between pairs of them (Kushner, 1998; Munoz-Fernandez, 1998).

The cytokine currency theory suggests that pro- and anti-inflammatory cytokines are constantly available to modulate gene expression in the injured nerve, and to control responses of cells during nerve WD and regeneration. Thus, after inflammatory lesions, they could change the neuropeptides expression pattern and might be important in regulating the responses associated with defense and repair of both, neuronal and non-neuronal tissues.

Cytokines act through 5 major families of tyrosine kinase membrane receptors that allow the cytokine classification due to their structural similarity. The cytokine-receptor complex, initiates intracellular signaling pathways and stimulates the release of intracellular calcium to lead downstream activation of MAP kinases that modulate a broad spectrum of cellular responses (Abbas, 2000;

Hehlgans, 2002; Boulayet, 2003; Langer, 2004, Adler, 2005). Following nerve injury, cytokines and their receptors are upregulated being considered key components in WD (Wahl, 1989; Chung, 1990). “**The cytokine network of WD**” (Fig15.) was a term given to refer to the orchestrated production of cytokines during these injury-induced inflammatory responses. TNFalpha and IL10 seem to be the most relevant cytokines involved in the WD process. Although other factors act on nerve degeneration and regeneration, it is considered that TNF plays a beneficial role in the breakdown and recovery of BNB (blood nerve barrier), and IL-10 is the key to these changes. Other pro-inflammatory cytokines such as IL6, IL-1 alpha and IL1 beta, that are also released by macrophage after TNFalpha production, may also be responsible as they are upregulated immediately after nerve injury (Rotshenker, 1997; Be'eri, 1998).

The classical view of inflammation suggests a network of cytokine production after PNS injury, in which inflammatory cytokines TNFalpha, IL1 alpha and the posterior IL1 beta induction, first upregulate the production of additional pro-inflammatory cytokines in SCs and, thereafter, the production of anti-inflammatory cytokines, such as IL10 to downregulate production altogether and, consequently, turn off the inflammation.

4.1 Proinflammatory cytokines

IL1, IL6 and TNFalpha are essential **proinflammatory cytokines** to start the immune system response. However, IL6 and TNFalpha also have anti-inflammatory roles (Munoz-Fernandez, 1998; Borish, 2003; Lucas, 2006). These pro-inflammatory cytokines contribute to macrophage recruitment to inflammatory sites, developing macrophage-dependent functions such as myelin removal by phagocytosis. Moreover, macrophages also regulate, indirectly, the survival of PNS cells and the neuropathic pain through the regulation of neurotrophic factors production, such BDNF (Bouhy, 2006; Scholz, 2007).

The cytokines produced by SCs, TNFalpha, IL-1 alpha and IL-1beta, together can further induce recruited macrophages to produce mostly IL-6 but also TNFalpha, IL-1 alpha and IL-1beta in a feed-back loop (Fig.15.). Almost immediately after injury, SCs also begin to express CCL2/MCP-1, and CCL3/MIP-1, with proinflammatory actions. Both of them play an important role in the influx of macrophages into the damaged nerve and reach a maximum 1

day after injury (Toews, 1998).

The IL1 family includes three types of proteins, product of different genes: IL1alpha (a membrane form), beta (secreted form) and IL1ra, being IL1 alpha and beta agonists in functions. All of them act through the Ig superfamily receptor IL1RI, and the NFκB signalling pathway. In normal conditions the levels of this receptor are low, but they are increase after injury or nerve damage due to the glial and macrophage activation to increased the synthesis and secretion of proinflammatory mediators. (West, 1999; Penkowa, 2000b, Basuet, 2002; Rothwell, 2003; Li, 2005). IL1ra is an antagonist receptor and the main mechanism to regulate the IL1 signalling pathway (Masada, 2001).

IL-1alpha mRNA is constitutively expressed but protein is not synthesized in intact PNS of mice (Vitkovic, 2000; Shamash, 2002; Gaudet, 2011; Fregnan, 2012). Injury induces the rapid upregulation of IL-1alpha mRNA within the first 5 hr after injury, and thereafter protein in SCs.

TNFalpha and IL-1alpha are most likely the first inflammatory cytokines to be produced rapidly in WD by SCs. The TNF immunopositive cells increased significantly in all segments distal to the crush site 3 dpl to diminish significantly 7-14 dpl, when nerve starts to regenerate and the BNB is restored.

Then, it follows the production of IL-6, within 2 hr after injury, and GM-CSF, within 4 hr after injury, cytokines that are only expressed after injury, probably induced by diffusible TNFalpha and IL1alpha by SCs. Moreover, IL-6, which inhibits TNFalpha, is responsible for the reduction in TNFalpha production after the first day of WD.

IL-6 is known for its multiple roles in development, repair, and inflammatory events, having context-dependent effects. For example, if IL6 is injected into healthy adult nerves, through the BDNF production, increases neuroinflammation and a demyelination pathological process (Lisak, 1994; Zhong, 1999; Inserra, 2000; Wyss-Coray, 2002; Leibinger, 2013; Wolf, 2014). Moreover, IL-6 knock-out mice, after nerve crush injury, have a delay in recovery of motor function, suggesting the role of IL6 in promoting axonal regrowth and SC proliferation being involved in a secondary neuroprotected response. (Ishihara, 2002, Munoz-Fernandez, 1998, Raivich, 1999). It was also demonstrated that IL-6, by activating

STAT3, can enhance synthesis of myelin proteins in Schwann cells (Haggiag, 2001; Ikeda, 2010).

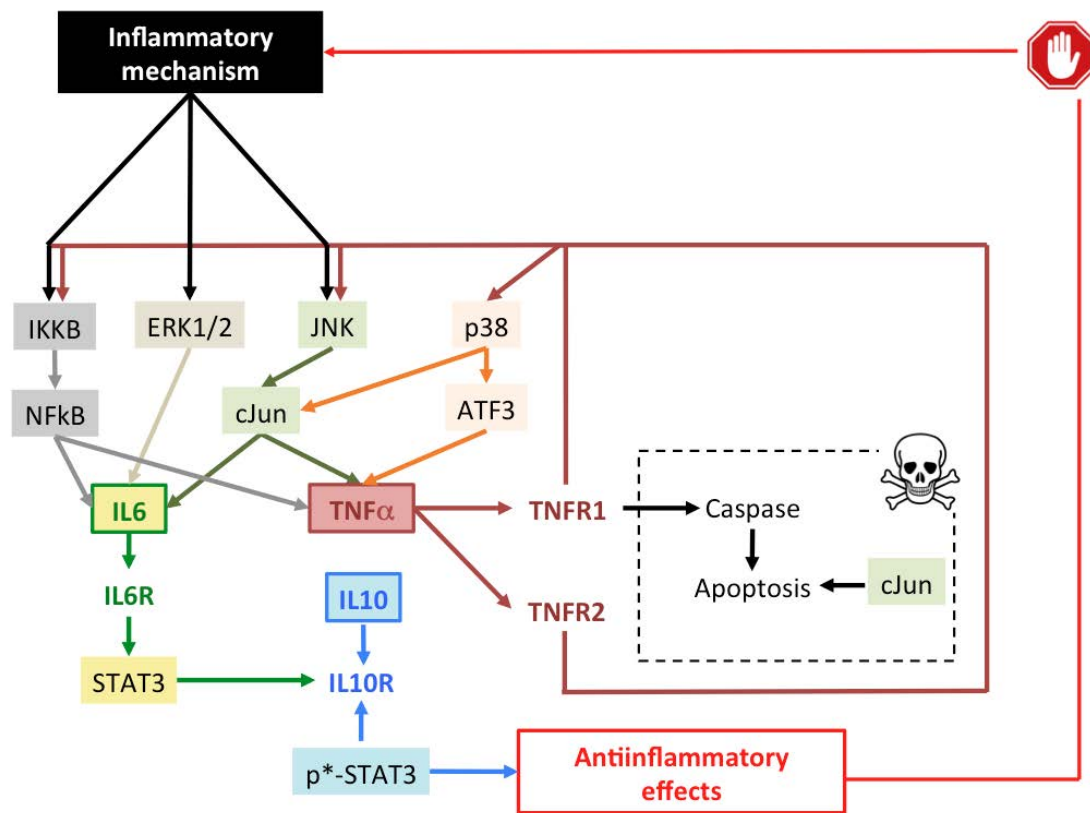


Figure 15. Schematic representation of the principal signalling pathways involved in the inflammatory process followed to peripheral nerve damage.

On the other hand, IL6 can be used as a therapy to reduce inflammation and demyelination (Deretzi, 1999a; Deretzi, 1999b). The beneficial outcomes using anti-IL6 treatments in vivo may be responsible for the reduced iNOS expression observed. It is known that an overage of iNOS levels contribute to neurotoxicity and axon damage (Levy, 2001; Zochodne, 2005).

Finally, the **IL1beta** activation is able to induce the expression of TNFalpha and IL6. (Norris, 1994; Basu, 2002b). Injury also induces the rapid expression of IL-1beta mRNA and protein by SCs, but the onset of IL-1beta production is delayed.

4.1.1 Tumor Necrosis Factor alpha (TNFalpha)

TNFalpha is almost ubiquitous and pleiotropic. In the PNS, TNFalpha is constitutively expressed and synthesized at low levels in SCs in intact peripheral nerves. Injury induces the rapid upregulation of TNF in wild type

mice, being detected within the first 5 hr after PNS injury, suggesting that SCs may be the first among the non-neuronal cells to respond to axonal injury. In addition, after injury and inflammation, this cytokine also activates and is produced by macrophages, peripheral blood monocytes, T cells, endothelial cells and microglia.

TNF is considered a prototypic proinflammatory cytokine that defines the fundamental biological network of the neuroimmune system axis, due to its principal role in initiating the cascade of activation to amplify the inflammatory response and blocking the axonal regeneration. Furthermore, TNF α does main actions during WD, needed to start the regeneration such as the induction of macrophage recruitment from the periphery and phagocytosis of myelin debris in injured nerves (Fig15.).

TNF α itself has not myelinotoxic properties, although it is associated to inflammatory demyelination and cell death, as well as is upregulated in a variety of neuropathological diseases, not only peripheral injury (Griffin and George, 1993, Stoll et al., 1993, Munoz-Fernandez, 1998; Liefner, 2000, Schafers, 2002a, Shamash, 2002, Van Herreweghe, 2002; Wright, 2004; Kamata, 2005; George, 2005; Shubayev, 2006; Schwabe; 2006).

The concentration of TNF α is important to determine its effects on the organism. At low concentrations TNF α stimulates pathophysiological modifications are relevant to exert a direct chemotactic effect and promote migration and invasion of circulating cells to facilitate WD in PNS (Shubayev, 2000; Shubayev, 2006; Zhang, 2009; Yadav, 2010). In addition, the administration of large amounts of TNF α causes cardiorespiratory death by inhibiting myocardial and vascular smooth muscle contractility through iNOS production. TNF α also causes hyperglycemia metabolic shock due to TNF production in adipocytes is related to insulin resistance, DM and obesity (Abbs, 1994; Burger, 2002; Masson, 2004; Bastard, 2006, Dyck, 2006).

TNF α is produced as a 26KDa membrane precursor and through ADAM17 or TACE (TNF α converting enzyme) is processed to a 17KDa soluble form that binds to TNFR1 or TNFR2 (Fig16.). Transmembrane TNF α also binds to both receptors but its biological activities are supposed to be mediated mainly through TNFR2 and mediated neuroprotection., whereas soluble TNF α preferentially binds to TNFR1. Both, transmembrane precursors and the soluble

form are expressed on activated macrophages and lymphocytes as well as in other cell types involved in the inflammatory response (Fontaine, 2002).

After releasing soluble TNF- α by TACE cleavage, the residual cytoplasmic domain of transmembrane TNF- α , cleaved by other proteolytic enzyme (SPPL2b) is translocated into the nucleus to possibly modulate gene expression. There is another molecular form of TNF α , a 14-kDa, present exclusively in lesioned axonal preparations, suggesting that this form may be specific for injury-induced axonal transport and may function as a supply for the active 17-kDa form (Fig.16.) (Shubayev, 2001; Shimoda, 2010).

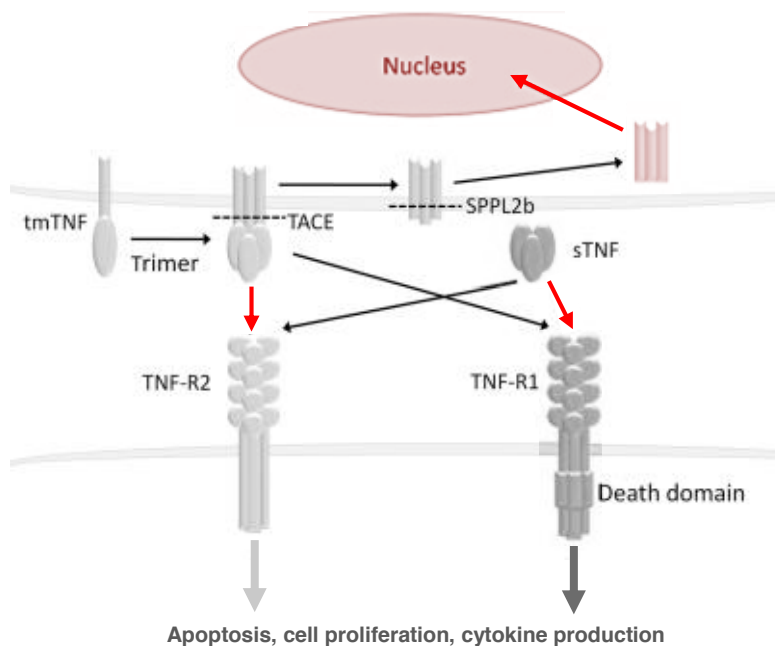


Figure 16. TNF α and the TNF α receptors (TNFR1 and TNFR2). Adapted from Shimoda et al., 2010.

Recently, it was seen that this transmembrane TNF could be a receptor by itself in a positive feed back loop also called an “outside-to-inside signal” or “reverse signal” (Baud, 2001; Ruulset, 2001; Hallenbeck, 2002; MacEwan, 2002; Eissner, 2004; Chan, 2007; Shimoda, 2010).

4.1.1.1 The TNF α receptor (TNFR) family

The TNF α receptor (TNFR) family consist of 12 homologous receptors distributed on T cells, B cells, macrophages and some also expressed in the glial cells. However, cellular signaling is mainly mediated through TNFR1 (also

known as p55 in mice or p60 in humans) and TNFR2 (also known as p75 in mice and p80 in humans). TNFR1 and 2 receptors only share a 28% homology in the extracellular portion, and the homology does not exist in the cytoplasmic domain.

The main action of TNF α is through the TNFR1 receptor to activate MAPK/JNK/p38 pathways to finally induce NF κ B and express proinflammatory and proapoptotic genes (**Fig15.**) (Abbas, 2000; Baud, 2001; Hallenbeck, 2002). TNFR1 is usually expressed at low levels but is higher in immune cells and increases one week after injury to modulate most pro-inflammatory responses. The TNF-TNFR1 complex regulates biological activities, including nerve degeneration (**Fig15.**) (Barbara, 1996; Malek, 1998).

Specifically for pain, it has been shown that thermal hyperalgesia requires TNFR1 while mechanical and cold allodynia depend on both receptors (Vogel, 2006; Woolf, 2007; Shubayev, 2010; Myers, 2011; Yamacita-Borin, 2015). In DRG, TNF α , TNFR1, and TNFR2 are greatly increased between 3-5 dpl. It is important to note that initial and acute local increase of TNF α at the site of nerve injury by activated SCs might give rise to the sequence of inflammatory events that can culminate in neuropathic pain. (George, 2005; Vogel, 2006).

4.2 Antinflammatory cytokines

Anti-inflammatory cytokines, such as **IL10**, are potent inhibitors of macrophage activity that plays a timely role in the early proinflammatory response and resolution of inflammation and axon regeneration (**Fig15.**). The role was demonstrated in IL10 null mice, showing an enhanced and prolonged inflammation with detrimental effects on regeneration. In addition, IL10 has been shown to prevent mechanical hyperalgesia resulting from intradermal injection of TNF α by functionally inhibiting TNF α action. In mouse sciatic nerve, the endoneurial IL-10 protein decreases after crush or chronic nerve injury.

In addition, TNF α , IL-1 α and IL-1 β also rapidly induce, IL-10 production by fibroblasts but levels are low. The timing of high levels of IL-10 on the fourth WD day, is determined by the timing of macrophage recruitment, which produces large amounts of IL-10. Then, IL-10 downregulates the

production of inflammatory cytokines, particularly TNF α , and itself, to finish WD.

On the other hand, at 1dpl IL10 decreases significantly except for the distal segments to the crush site. Decline of IL-10 triggers up-regulation of TNF α , being the transient decrease of IL-10 the key to promote TNF production and BNB permeability on 3 dpl. IL-10-immunopositive cells increased on 3-7 dpl. Beyond 14dpl, the BNB starts to recovery and the axon regeneration occurs from proximal to distal. The number of IL-10-immunopositive cells normalized but remained significantly higher in the distal segments. At this time, IL-10 may suppress the inflammatory response and promote axonal regeneration by inhibiting TNF α production in the same direction: from proximal to distal. BNB full recovery finishing 3 wpl in the more distal segment, and TNF α cells also decreased in the same segments. In rodents the regeneration process is usually completed within 1 month, a time course corresponding to the associated hyperalgesic pain. (Zhou, 2009; Thompson, 2013). Moreover, IL10 indirectly inhibits iNOS release, and thus, after a nerve crush, a significant increase in the iNOS mRNA at 1dpl and in the iNOS protein at 10 and 28 dpl is seen (Peluffo, 2015).

4.3 The activation of macrophages activation in the PNS

Macrophages are commonly distributed in the normal peripheral nerves of rodents and humans. **In PNS injury**, they have at least two basic functions: phagocytosis of degenerating myelin, where SCs also have a minor role, and production of cytokines and neurotrophic factors responsible for the anti-inflammatory environment after nerve damage. This relevant role of macrophages was proposed by Ramon y Cajal at 1928 where the decomposition of axons and myelin liberates positive chemotactic substances capable of attracting macrophages. (Oldfors, 1980; Esiri, 1989; White, 1989; Perry, 1990; Monaco, 1992; Griffin, 1993; Farah, 2011; Farah, 2012).

The protective role of macrophages in WD might also be explained by the **alternative activation of macrophages** (Fig17.) to a M1 proinflammatory phenotype and the transient M2 antiinflammatory phenotype. This modulation of M1-M2 phenotype may represent a strategy to promote regeneration (Martinez, 2014).

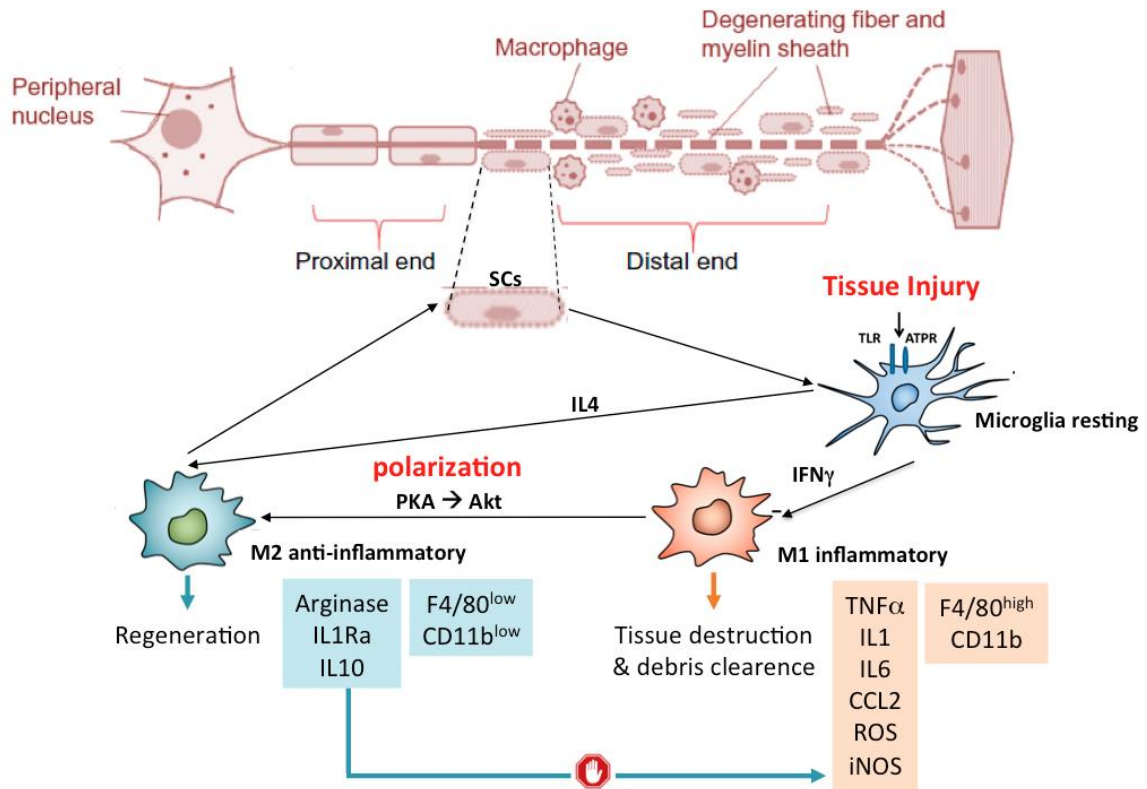


Figure 17. Schematic diagram summarizing the working model for macrophages in peripheral nerve degeneration and regeneration. Peripheral nerve injury induces the disruption of axons/SCs and then upregulates a variety of chemokines, cytokines and other factors to recruit macrophages into the injured nerves. The infiltrated macrophages on one hand contributes to WD by removing the cellular debris; on the other hand they are educated by the local injured environmental and polarized to an anti-inflammatory phenotype M2, thus promoting peripheral nerve regeneration. The polarization seems to occur through the AKT and PKA signalling pathway (Adapted from Johnson, 2012; Nakagawa, 2012; Martinez, 2014).

Normally the **M1 microglial** (Fig17.) responses are cytotoxic to neuronal cell cultures and are “classically” activated macrophages. M1 macrophages, produce high levels of oxidative metabolites like iNOS and ROS, as well as pro-inflammatory cytokines (Peluffo, 2015).

On the other hand, a **M2 or “alternatively activated”** (Fig17.) macrophages can be activated by IL-4 and IL-10 by producing anti-inflammatory cytokines. This response promotes axon outgrowth and it is considered as neuroprotective in vitro. After nerve transection, mice show a rapid M2 polarization of

macrophages due to a rapid induction of mRNA for IL-1beta and IL-10 at 1 dpi and the upregulation of other M2 markers like Arg1 and the mannose receptor (CD206) (Fairweather, 2009; Lawrence, 2011; Cherry, 2014).

In degenerating sciatic nerve IL-10-null mice, macrophages showed increased expression of M1 markers and decreased expression of M2 markers, compared with wild types. Moreover, it was accompanied by increased numbers of macrophages at the early (3dpi) and later (14-21dpi) stages after crush injury, demonstrating the control of IL-10 in the recruitment and efflux of macrophages (Liefner, 2000; Siebert, 2000).

4.4 Neuropathic pain after peripheral injury

Normally, peripheral nerve injury can result in **neuropathic pain**, by definition an incompletely understood pain state caused by injury to components of the nervous system, and typically manifested days or weeks after, involving the entire sensory neuroaxis with components of extreme sensitivity to mechanical and thermal stimuli. In addition, it is suspected to be implicated in neuropathologic process involving neuroinflammation.

Due to pathogenic role of neuroinflammation in neuropathy, it is clear that proinflammatory cytokines are key modulators in the cross-talk between immune cells/neurons/glia and the environment during the processes of degeneration, regeneration, and pain development. The question remains how these events and pro-nociceptive events are linked. Specially TNF alpha seems to be painful itself. It was shown that TNFalpha produced a similar form of hyperalgesia after acute injection into nerve. (Myers, 1993; Sommer, 1993; Myers, 2006).

The induction of hyperalgesia apparently involves the release of TNFalpha at an early stage and has immediate effects on aberrant spontaneous electrophysiologic activity in normally quiescent polymodal C-nociceptor fibers. This is thought to be an important mechanism in chronic pain development. (Sorkin, 1997).

Nevertheless, it is difficult to know the absolute initial event that begins the self-upregulation of TNFalpha, but the release of calcium and chloride by damaged axons may cause glial and other cell activation via ion channels such as the Nav1.3 and Nav1.6 voltage-gated sodium channels in DRG neurons. However,

these ion channels and electrophysiologic changes alone can facilitate a neuronal tendency toward sensitization. The effect is potentiated by a direct action of TNF alpha on sensory neurons, as well as the inhibition of TNFalpha activity is associated with the reduction of pain during WD. (Waxman, 1994; Schäfers, 2003; Xu, 2006; Skaper, 2011).

The retrogradely axonal transport from the site of injury to neurons and glia in the sensory pathway (within 5 hrs to 96 hrs post-nerve damage) causes glial activation with a strong positive signal of GFAP observed and the astroglial and spinal glia activation in neuropathic pain development (Milligan, 2009; Gao, 2010). Thus, the retrograde TNFalpha transport is a key factor in sensitizing the nervous system and facilitating neuropathic pain. Strategies to interfere with this transport may be effective as new therapy for pain reduction (Wagner, 1996a; Sommer, 1998; Shubayev, 2002; Wagner, 1998; Üçeyler, 2007; 2009).

5. Animal models for peripheral neuropathies

Despite the capacity of axonal regeneration in the PNS, functional recovery is slow and peripheral nerve injuries cause a decline in patient quality of life, motivating further investigation to optimize recovery. At these days, greater attention has been paid to develop animal models that mimic the human condition more reliably to better understand the pathogenesis of neuropathies, neuropathic pain and demyelination/regeneration injuries; and to develop new strategies based on effective therapies. Experimental animal models, spontaneous or induced by chemical compounds, physical injury or genetic engineering, exist for many of the human peripheral neuropathies.

Transgenic/knockout animals to different important genes important for have been generated nowadays focus on SCs, which are key actors in the degenerative/regenerative process seen in peripheral neuropathies. Thus, knockout heterozygous mice to NRG1typeIII show a high proportion of unmyelinated axons, while transgenic animals overexpressing this isoform are hypermyelinated (French-Constant, 2004), demonstrating the main role of NRGs family in myelination.

Moreover, BACE1 knockout mice show a decreased expression of MBP and PLP proteins but a normal level of MAG, as well as an increased in full length

NRG1 and a reduction of PI3K-AKT. The level of hypomyelination was similar than knockout heterozygous mice to NRG1 type III or ErbB2. (Hu, 2006; Ohno, 2009; Hu, 2015).

Animal models associated to myelin proteins mutations, are, mainly, related also to inherited NP diseases. Most of these mutations are found in genes encoding for proteins implicated in SC and neuron physiology, such as myelin-related proteins PMP22, P0 and Krox20; as well as genes essential for axonal transport and regeneration.

In humans, duplication of PMP22 gene is associated with the most common form of inherited peripheral demyelinating neuropathy CMT1A, as well as transgenic mice for PMP22 show CMT-like phenotypes. Several animal models of inherited neuropathies exist, such as CMT1A and DSS related to PMP22 gene mutations, and overexpressing (ubiquitously or conditionally) or knockout of these genes (Sereda, 2006; Fricker, 2007; Fledrich 2012).

Furthermore, significant deviation in gene dosage for PMP-22, or point mutations, has severe functional consequences and demyelinating phenotypes in mouse models, for example in the *trembler* mice (Young, 2010).

Another example is the *mpz* knockout mouse, which produces poorly compacted myelin sheaths. Young heterozygous and knockout mice appear normal but develop progressive demyelination with age and may involve inflammatory mechanisms. This knockout is a model to study CMT1B disease (Martini, 1995b). Interestingly, overexpression of MPZ disrupts myelination demonstrating the precise stoichiometry needed between myelin proteins (Shy, 2001).

P0 missense mutations cause a variety of clinically defined human peripheral neuropathies (Warner, 1996). In humans, there are described more than 50 point mutations in different *mpz* regions, some of them responsible for human neuropathies, such as CMT1B and also DSS (Mandich, 1999; Wrabetz, 2000, 2006; Magot, 2008; Marchini, 2009).

In the MBP-deficient *Shiverer* mice, PNS myelin is unaltered, while there is a great reduced amount of CNS myelin (Martini, 1997). This CNS/PNS difference in the role of MBP is probably because the cytoplasmic domain of P0 has an important role in stabilizing PNS myelin, and the MBP proportion in both

nervous systems is quantitatively different. In PNS myelin, MBP varies from approximately 5% to 18% of total protein, in contrast to the CNS it is close to 30%. For example, animals doubly deficient for P0 and MBP have a more severe defect in compaction than P0-null mice, which indicates that both proteins contribute to compaction of the cytoplasmic surfaces in PNS myelin (Martini, 1995a).

There is no may point mutations in the MAG genes. MAG-null aged mice develop a peripheral neuropathy characterized by degeneration of myelinated axons (Bjartmar, 1999; Schachner, 2000; Pan, 2005; Dashiell, 2002; Kumar, 2002). These findings demonstrate an essential role for MAG in signaling from SCs–axon interactions. In this regard, MAG is one of several neural proteins that inhibit neurite outgrowth in tissue culture and axonal regeneration *in vivo* after peripheral nerve injury (Yiu, 2006; Tomita, 2007).

In contrast, models of chemically or drug-induced neuropathy are sometimes more distant to the phenotype seen in humans, and these models reproduce only partly limited aspects. Unfortunately, nowadays the preclinical data using these animals may not have been the most optimal models to clearly allow the underlying of peripheral neuropathy pathologies. There are many discrepancies as a consequence of the genetic background of the animal used, route of administration (intravenous vs intraperitoneal), dose and duration of drug administration.

Leprosy, leads to a NP acquired by infection. This is an old but still poorly understood disease, despite is one the most common diseases worldwide. The causative pathogen of this chronic disease (*Mycobacterium leprae*), binds direct to SCs in dermal nerves of the superficial skin. It was hypothesized that *M. leprae* has a preference for non-myelinated SC, offering a safe niche protected from the immune response that allows proliferation and later myelinating SCs infection. However, none of the existing models account for a real leprosy neuropathy (Pineiro, 2011).

On the other hand, because there is no direct infection of rodents with HIV, it has been difficult to develop a reliable small animal model for HIV derived neuropathy (Höke, 2015). Moreover, the pathogenesis is still unclear, as neurotoxicity due to antiretroviral drugs was also postulated, both of a direct

toxicity of secreted viral protein gp120 in SCs and the capacity of this antigen to activate macrophages, pro-inflammatory cytokines and lymphocyte infiltration in peripheral nerves and DRG sensory neurons.

5.1 Diabetic Peripheral Neuropathy (DPN)

Multiple animal models of DPN have been developed in the context of modeling both types 1 and 2 diabetes, in addition to the naturally occurring animal, from chemically induced diabetes and genetically engineered diabetic mice. It is necessary to note that, nerve structural changes in DPN varies, specially according to the type of diabetes, the strain, the age of the animals and the duration of diabetes. Compared to rats, mouse models of diabetes offer a big advantage due to gene knockouts or overexpression effect can be studied.

Rodent models of diabetes used streptozotocin (STZ), a toxin to partial kill pancreatic beta cells from Langerhans islets. Injection of a single or multiple doses of STZ caused rapid induction of hyperglycemia, and it mimics **type I DM**. The pathological changes in the peripheral nerves of these STZ-induced rodents exhibited mild axonal atrophy, degeneration and demyelination little resembling to human DPN. Changes in the electrophysiological parameters, such as a decrease in MNCV and SNCV also occurs at early stages. These electrophysiological modifications do not correlate with the few structural nerve abnormalities. In later stages of the pathology starting 2 months after STZ injection, morphometric studies show a mild decrease in myelinated axon area, abnormal appearance of myelin and WD.

Several animal models of **type II DM** are available. The most commonly used are the natural occurring BKS-db/db, B6-db/db and B6-ob/ob mice, with disruption of the leptin-signaling pathway; in which hyperglycemia develops impaired glucose tolerance and mild peripheral neuropathy has increased. Structural studies also show slight axonal atrophy, important segmental demyelination and WD (Dobrestov, 2007; Jaggi, 2009; Pasnoor, 2013).

Currently, there is a model of prediabetes, which mice are fed a high-fat diet and develop features that mimic alimentary obesity, including high insulin and free fatty acids levels, as well as hyperglycemia. The advantage is that studies are carried out in a normal genetic background. Behavioral characteristics

displayed by these mice include light mechanical allodynia and thermal hyperalgesia, but, however, do not display any significant changes in nerve pathology, being necessary to use another type of animal models to deeper and focus in regeneration studies (Stewart, 2010; Höke, 2012, Kumar, 2013).

Animal models are widely used to investigate the cellular and molecular mechanism in degeneration/regeneration processes of peripheral nerve following trauma (nerve crush or axotomy). However, the spatiotemporal evolution of axonal degeneration varies with the experimental procedure (axotomy, crush, chronic ligature) and depends on factors including the laboratory animals, age, site of lesion and assessment method. Referent to chronic constriction models, although axotomy is considered a most suitable model to study degeneration, a weak of knowledge about peripheral nerve biology and SCs myelination has been obtained from studies in acute nerve injury paradigm (Beirowsky, 2013; Stratton, 2017).

Various models of nerve injury are used to develop viable treatments. For example, in vitro models including 3D organotypic and glial cell cultures. The two general and widely used models of nerve injury in rodents are the transient crush and the axotomy of the sciatic nerve at mid-thigh level; due to the inexpensive housing cost and similar anatomic location and distribution of nerve trunks to humans, and easier accesibility. In other hand, femoral nerve injuries are relevant in the study of particular nerve types because it has one exclusively motor branch and another exclusively sensorial (Menorca, 2013).

However, most of the animals models do not developed neurophatic pain after nerve injury, being necessary to generate other strategies or animal models. Two types of painful behaviours are often associated with transient nerve crush, a spontaneous pain-related behaviour, like postural abnormalites, that are absent or moderate; and a chronic constriction injury with an inappropriate response to stimulus-evoked pain. On the other hand, acute crush injury of peripheral nerves induces moderate and transient hyperalgesia and allodynia in response to mechanical and thermal stimulation (Magill, 2007).

5.2 Animal model for cytokines

As stated before, cytokines are recognized to play important roles during health and diseases. The molecular therapeutic insights into cytokine mechanisms of degeneration can hopefully be exploited to help control the balance between degeneration and regeneration and mitigate the consequences of painful neuropathies.

Generation of transgenic animals is a good tool to elucidate and prove the roles of the different cytokines and neurotrophic factors released in the nervous system, deep in the knowledge about cytokine and pain and also generate appropriate animal models to study neuropathic pain.

A transgenic mouse model for IL6 (constitutively expressed), which increased production is associated with upregulated IL1 alpha and beta, TNFalpha and other acute-phase proteins, caused angiogenesis and reactive microgliosis, a characteristic pathologic state that correlated closely with the progression of neuropathy (Brett, 1995; Campbell, 1995). Genetic deficiencies in IL6 and IL1b have been shown to result in delayed recovery after nerve injury (Nadeau, 2011).

Using null mice for IL10 was provided, its role in the inflammatory response in macrophages after peripheral nerve crush injury with an increased influx and prolonged retention of macrophage was provided. These effects induced a more proinflammatory environment and were accompanied by reduced axonal regeneration and impaired recovery of motor and sensory function.

However, opposing effects of TNF signaling on axonal regeneration are reported, possibly reflecting the pleiotropic effects of TNF (Schneider-Schaulies, 1991; Tartaglia, 1992, Vandenabeele, 1995, Ledgerwood, 1999, Larsson, 2005; Gerbod-Giannone, 2006, Myers, 2006). For example, TNF inhibits neurite outgrowth in vitro whereas a TNF antagonist enhances initial outgrowth of axons in the injured sciatic nerves.

In TNF KO mice, macrophage infiltration into degenerated nerves is impaired and myelin debris clearance is delayed in the distal stump (Louis, 1993; Liefner, 2000; Shamash, 2002; Bradley, 2008; Kato, 2010). Moreover, it is not clear if a compensation in IL1 and IL6 cytokine activity results in TNF knockout animals, or if acutely TNFalpha inhibited animals would have the same response.

Additionally, axonal regeneration is also impaired in TNFR1 KO injured nerves by blocking the recruitment of macrophages (Schaefers, 2002b). Another evidence is that, mice with a limitation in macrophage recruitment to the injured nerves (WLDS) have delayed WD, reduced pain and the expression of TNFalpha is delayed (Perry, 1990; Myers, 1996; Sommer, 1998).

We hypothesized that a model that overexpress TNFalpha in PNS could possible develop peripheral neuropathy, indeed the injection of recombinant TNF into the sciatic nerve of rats also resulted in damage to the BNB and an inflammatory infiltration of vessel walls (Sawada, 2007). At present, experimental therapeutic interventions playing with TNFalpha activity and availability, have being used in humans, such as anti-TNF agents, to control of sciatic and low back pain. In addition, similar clinical therapies based on the blockage of TNF alpha are currently being used to some demyelinated CNS pathology, such as MS treatments (Arnett, 2001).

Furthermore, mice overexpressing TNFalpha constitutively under the control of its own promoter, specifically revealed also an important role for controlling apoptosis and develop a chronic inflammatory demyelinating disease following by an incomplete remyelination in adult CNS after damage (Probet, 1995; Pasparakis, 1996) and they have been used as a model for MS.

TNFalpha transgenic models, present severe cardiac and respiratory failures, and are good models for autoimmune disease and inflammatory arthritis, all of them by activating both, pro and anti-apoptotic pathways (Galkina, 2009; Horiuchi, 2010; Sedger, 2014; Fisher, 2015). According to these results, working with animal models for TNFalpha, as well as other cytokines, could have unspecific and undesirable downstream negative effects which are necessities to evaluate and characterize properly.

Nowadays, selective strategies have been developed to confine transgene expression in target tissues. Using appropriate tissue-specific promoter, time-inducible expression controlled by exogenous agents, or miRNA techniques; should be prevent the tissue-toxicities associated to cytokine overexpression and to achieve and spatial and temporal control of transgene expression, improving the in vivo study of cytokines in the near future (Robson, 2003; Walther, 2015).

II. OBJECTIVES

The general objective of this thesis is to generate a suitable animal model for peripheral neuropathy and chronic pain and to be used latter on to develop new therapeutic approaches.

With this aim, we established the following specific objectives:

1. To generate a transgenic mouse model overexpressing TNF- α in Schwann cells under the control of the peripheral myelin protein P0 promoter (P0TNF- α mice).
2. To characterize the effects of overexpression of TNF- α in myelinated Schwann cells in P0TNF- α mice at different periods of myelination (postnatal days 5, 21 and 65)
3. To analyse the pro-inflammatory role of TNF- α in the regenerative capabilities after peripheral nerve injury in P0TNF- α mice.
4. To determine the role of local inflammation driven by chronic overexpression TNF- α in the development of neuropathic pain in P0TNF- α mice.

III. RESULTS

1. Generating a transgenic P0TNFalpha mice line

Genetically manipulated mouse models are very helpful for studying gene functions in whole animals. Transgenic mice represent the approach for defining molecular and cellular functions of a gene of interest. This approach can be also used to analyse tissue-specific or developmental stage-specific gene expression under the control to specific gene promoters. The main objective of this thesis was focus on the generation of an animal model overexpressing TNF alpha in the PNS as a model of chronic peripheral neuropathy.

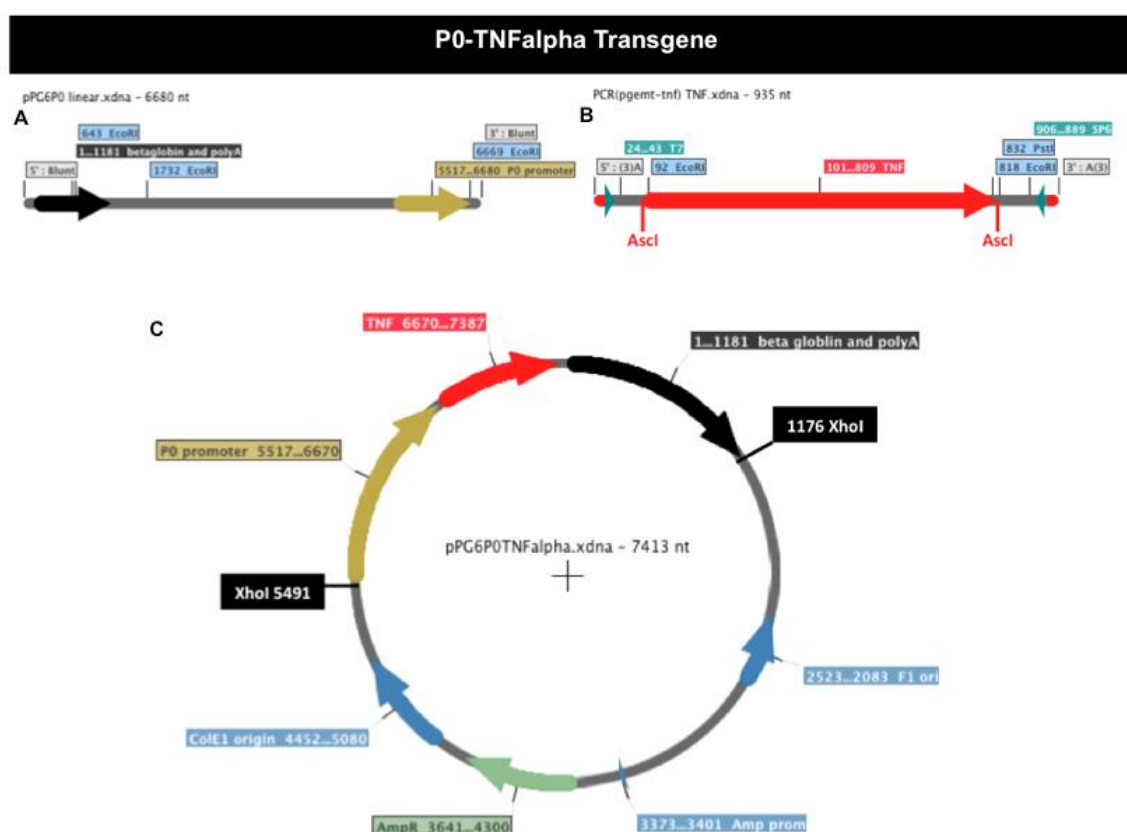


Figure 18. (A) The pPG6 vector contains the intron of rabbit beta-globin and the complete P0 myelin glycoprotein gene, including 6 kb of the 5' upstream region, all exons and introns, the natural polyadenylation signal and 400 nucleotides of the 3' flanking sequence. (B) The murine cDNA of TNFalpha was cloned in a pGemt-T vector and the sequence was flanked by two *Ascl* sequences, allowing the subsequent detection of the transgene after a DNA genomic extraction. (C) The final construct was digested with *XhoI* to linearize and remove the prokaryotic sequences. The final fragment has a size of 3.1 kb.

With the aim to overexpress TNFalpha in Schwann cells (SCs), a transgene construct was made containing the rat P0 promoter, driving myelin P0 protein in PNS, with the cDNA for murine TNFalpha. The inclusion of an intron such as

rabbit beta-globin (Fig18.A) in the transgene construct leads to significantly greater transgene expression due to mRNA stabilization and the efficient translocation from nucleus to cytoplasm (Brinster , 1988, Huang, 1990).

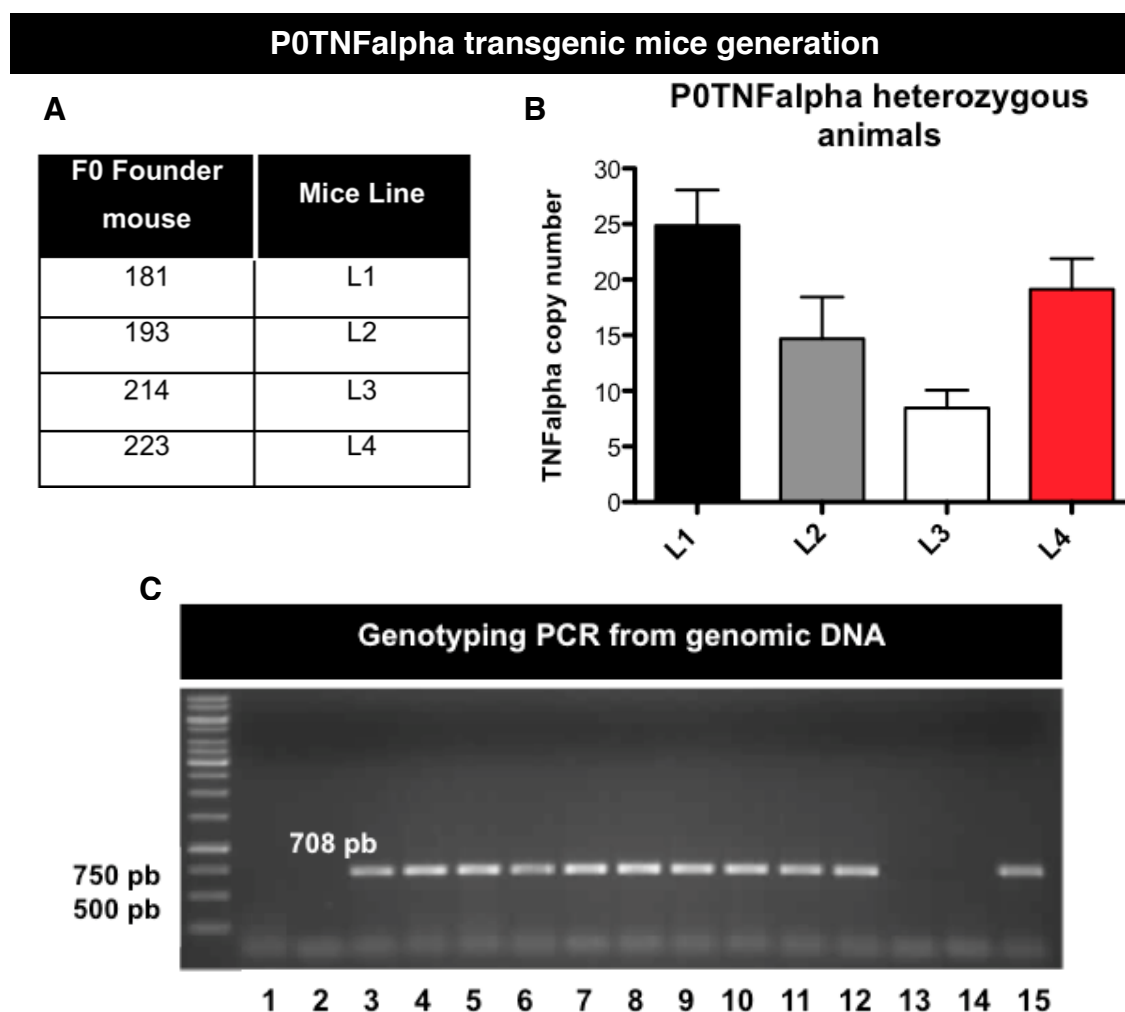


Figure 19. (A) Identification of the F0 founder mice, heterozygous for P0TNFalpha transgene. These four animals showed a positive band by Southern-blot. (B) Copy number of the transgene in animals for each specific founder's line, n=8 for each group, determined by qPCR in DNA genomic extracts of tail clips. (C) Electrophoresis gel to check the positive (heterozygous and homozygous) or negative (wild type) animals for the transgene P0TNFalpha, after conventional PCR reaction. Positive band is expected in 708 pb size. In this gel, sample 14 is a negative wild type control and sample 15 a positive heterozygous control.

TNFalpha was detected by Southern-blot in four animals from F0 (Fig19.A). Higher intensity detection bands are related to a major copy number of tandem TNFalpha sequence (not shown).

Once the founders reach sexual maturity, they can be crossed with wild-type mice to establish separate transgenic (Tg) lines. After verifying transmission from F0 founder mice to next offspring, heterozygous animals were crossed to establish a colony, being a 25% of homozygous and wild type animals, and 50% of heterozygous genotype animals (Fig19).

The copy number of the transgene was determined from DNA extracts of tail clips by subsequent analysis with qPCR (Mat&Meths). It was performed for all the transgenic mouse lines, although line 3 was rapidly excluded because of low DNA copies of TNFalpha (Fig19.B). mRNA expression, correlated with DNA copy number, shows the highest values for line 1 and line 4, while line 2 showed about half of the expression (data not shown).

The offspring of the founders was analysed by conventional PCR to exclude wild type animals, and the results were validated with Southern-blot at least once. A specific pair of primers was designed to recognize the Ascl sequence that was included in the transgene construct (Fig18.B). Products allow to distinguish between wild type and TNFalpha transgenic animals, which have an expected band of 708 bp (Fig19.C).

After the genotyping PCR, a qPCR from genomic DNA was performed to distinguish between homozygous or heterozygous animals (Mat&Meths.). Mice zygosity was determined using as reference the average Cq obtained for Cyclophilin B, a housekeeping one copy/genome gene, as well as TNFalpha of a set of known F1 heterozygous mice. The zygosity of the experimental mice was calculated based on Pfaffl, 2001. Expected zygosity values were about 0 for wild-type mice, 1 for heterozygous mice and above 2 for homozygous transgenic mice (Fig20.).

Animals from the L2 line were excluded for the next experimental steps, according to the relative low TNF alpha copies and lower mRNA levels (not shown), the difficulty to obtain progeny and the lower percentage relative to homozygous transgenic animals (Fig20.).

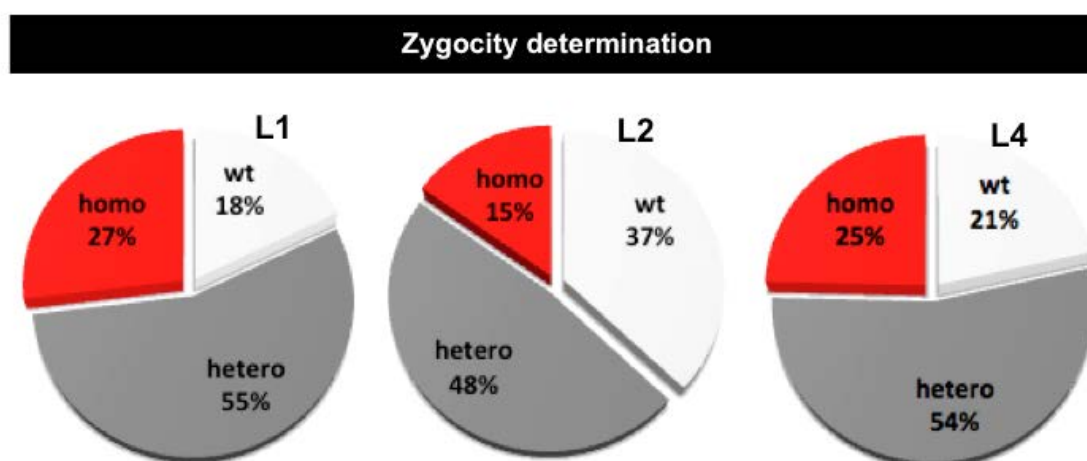


Figure 20. Representation of the percentage of zygosity to each transgenic line. The expected values, if animals do not show mosaicism effects, progeny will be around 25% homozygous, 25% wild type and 50% heterozygous.

1.1 Molecular characterization of L1 & L4 lines

Results of qPCR show no difference in the expression of TNF alpha between homozygous animals from L1 and L4, although L4 seemed to have more consistent results along different mouse ages (Fig21.A.,C.,& D.).

Once the mRNA levels of the TNFalpha transgene were quantified, the next step was evaluate the level of TNFalpha protein in sciatic nerves in a longitudinal study at different ages (P05, P21 and P65) by ELISA (Mats&Meths.).

Furthermore blood samples were analysed, but no secretion of TNFalpha into the blood was detected within the sensibility of the ELISA (Fig21.D.).

According to the copy number of the transgene, the expression of mRNA and protein in both germlines, as well as the lack of mosaicism phenomena, we decided to maintain and perform the following steps of the experimental design using only L4 homozygous transgenic P0TNFalpha animals.

mRNA & protein characterization in transgenic sciatic nerves

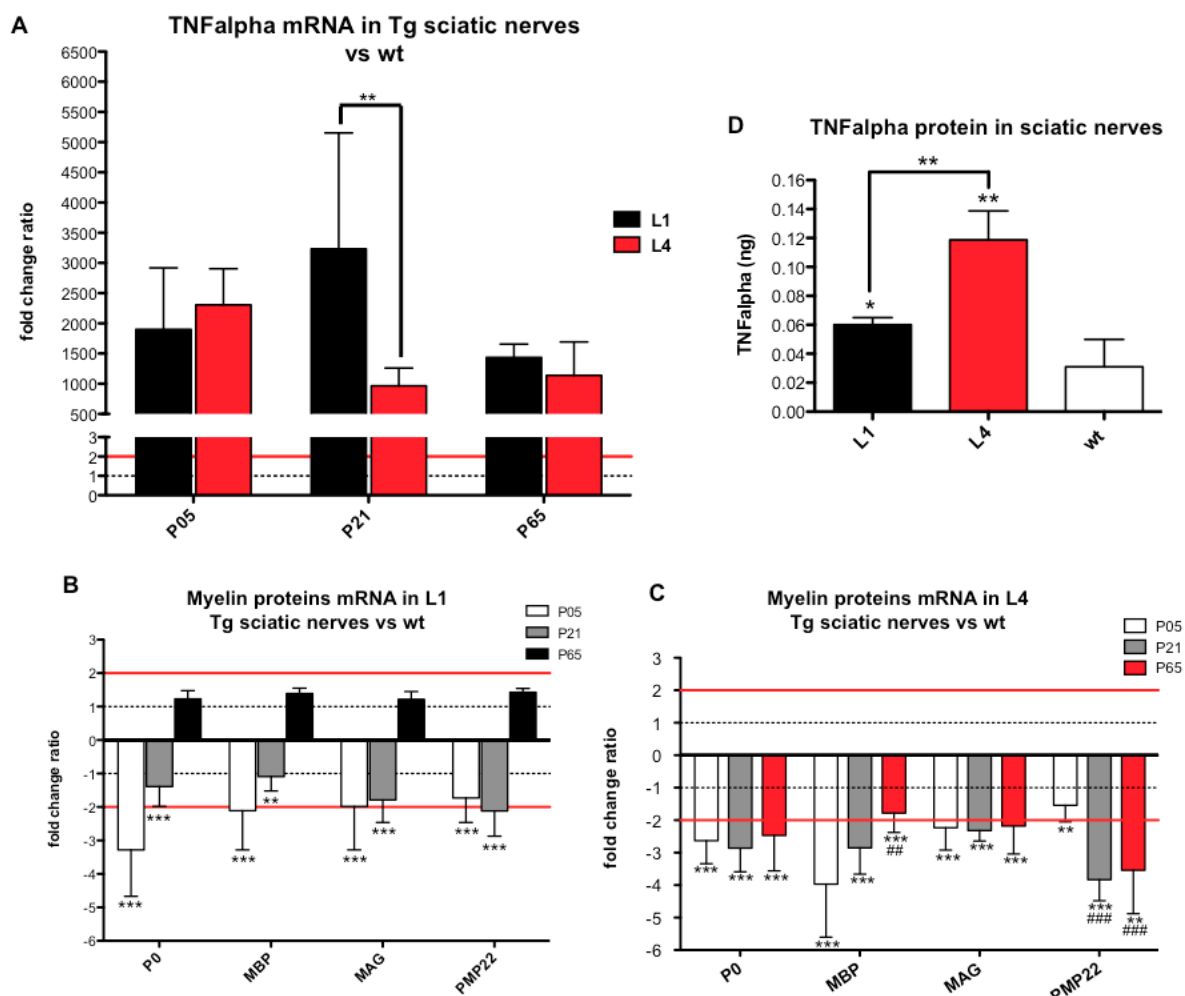


Figure 21. (A) TNFalpha expression levels determined by qPCR after mRNA extraction for sciatic nerves at three different age-points: P05, P21 and P65 in the L1 and L4 lines. The gene expression is relative to wild type animals at the same ages (dotted line represents $y=1$, the value normalized for wild types. Red line $y=2$ represents a difference of one gene copy expression. Both lines are statistical significant (** $p < 0.001$ compared to wild type animals). However, only at P21 L1 and L4 show significant differences. **(B)** Myelin protein gene expression in animals of both transgenic lines, L1 and L4, at the three different ages, relative to wild types. L1 animals only show statistical differences (** $p < 0.001$ and ** $p < 0.01$) at P05 and P21, and the expression is restored to wild type levels at P65. **(C)** L4 animals myelin protein genes expression have significant differences (** $p < 0.001$ and ** $p < 0.01$) in all genes and for all the time-points. Moreover L4 animals also have difference between aged in PMP22 gene (### $p < 0.001$ compare to P05 P0TNFalpha mice) and in MBP (## $p < 0.01$ at P65 compare to P05 homozygous animals). **(D)** TNFalpha protein levels (ng) relative to total protein concentration obtained from sciatic nerve homogenates of adult (P65) animals. The protein levels were detected by ELISA. Both lines have higher expression of TNFalpha compare to wild type animals (* $p < 0.05$ and ** $p < 0.01$). In addition, L4 animals exhibit more TNFalpha protein than L1 mice (** $p < 0.01$). $n=3$ for each group.

NOTE:

Hereinafter, we will use the terms of Transgenic (Tg), homozygous (Homo) and P0TNFalpha as synonymous to refer the L4 transgenic animal model.

2. Crush protocol: inducing peripheral injury

Electrophysiological studies at different ages were performed in L4 P0TNFalpha mice without finding significant differences between transgenic and wild type mice. Thus, a stressful protocol would be desirable to maximize the amount of information and visualize better the effects that are derived from the P0TNFalpha transgenic model. For example, streptozotocin Diabetes Mellitus (DM) type1 induced model, or injury at sciatic nerve are two possible methods that are being evaluated in our lab (Homs, 2014).

Crush surgery is a useful type of injury to identify the regeneration capacity of PNS (Menorca, 2013; Sulaiman, 2013). It was performed in 1.5 months-old male and female animals and sham operation was done as surgery control. We used both P0TNF homozygous and wild type mice of both sexes. Recovery was evaluated by Sciatic Functional Index (SFI) (Inserra, 1998).

We found no evidence of differences in SFI values among male or female animals. Thus, we decided pool both sexes to increase the numbers and improve the statistical analysis (Fig22.).

	wt			P0TNFalpha		
	Male	Female	n	Male	Female	n
Crush	13	19	32	15	28	43
Sham	4	4	8	7	5	12

Figure 22. Total number of 1.5 month-old (P65) animals that were used to crush surgery.

2.1 Sciatic Functional Index (SFI) calculation

The SFI index was measured initially by walking tracks 24h before and 48h after surgery. SFI was calculated with the average measure of the Toe Spread (Ts) and Print length (Pl) of pawprints. The average pre-operative and post-operative SFI for the animals are in agreement with the SFI values described for a sham operation or a non-transected nerve (SFI = 0) and for a transected nerve lesion (SFI = -100) (Inserra, 1998).

		wt			P0TNFalpha		
		Mean	SD	n	Mean	SD	n
Crush	Pre-crush	-7,7	1,2	32	-2,3	1,4	43
	Post-crush	-161,3	6,4	32	-129,3	6,6	43
Sham	Pre-crush	-8,3	3,1	8	11,7	1,9	12
	Post-crush	-9,8	2,3	8	-14,3	4,3	12

Figure 23. The average of values obtain after SFI determination pre-surgery and 48h post-crush.

The recovery was monitored by measurements made every a week after sciatic nerve injury. Moreover a more accurate timing was performed among one and two weeks to determine the restoration rate changes of both genotypes after the crush protocol (Fig24 .& 25.). The non-injured Sham animals of both genotypes have the same expected behavior pattern, obtaining SFI values between 0 and -25, along the study (Fig23.).

Forty-eighth hours after crush both genotypes achieved a SFI index lower than -100 and these values were maintained until 7 days later, when the remyelination process starts. However, it is possible to observe a delayed progression in P0TNFalpha crushed mice (Fig23., Fig.24 & 25.). While the wild type crushed animals achieved a minimum SFI value one week after injury, as it is expected due to Wallerian Degeneration (WD), transgenic animals reached this situation at 9 days post injury (dpi), which is the time point as which this genotype starts to regenerate (Fig25.).

On the other hand, although the transgenic model seems to start the remyelination process two days later than wild type mice, the speed rate of recovery is quite similar until the thirteenth day.

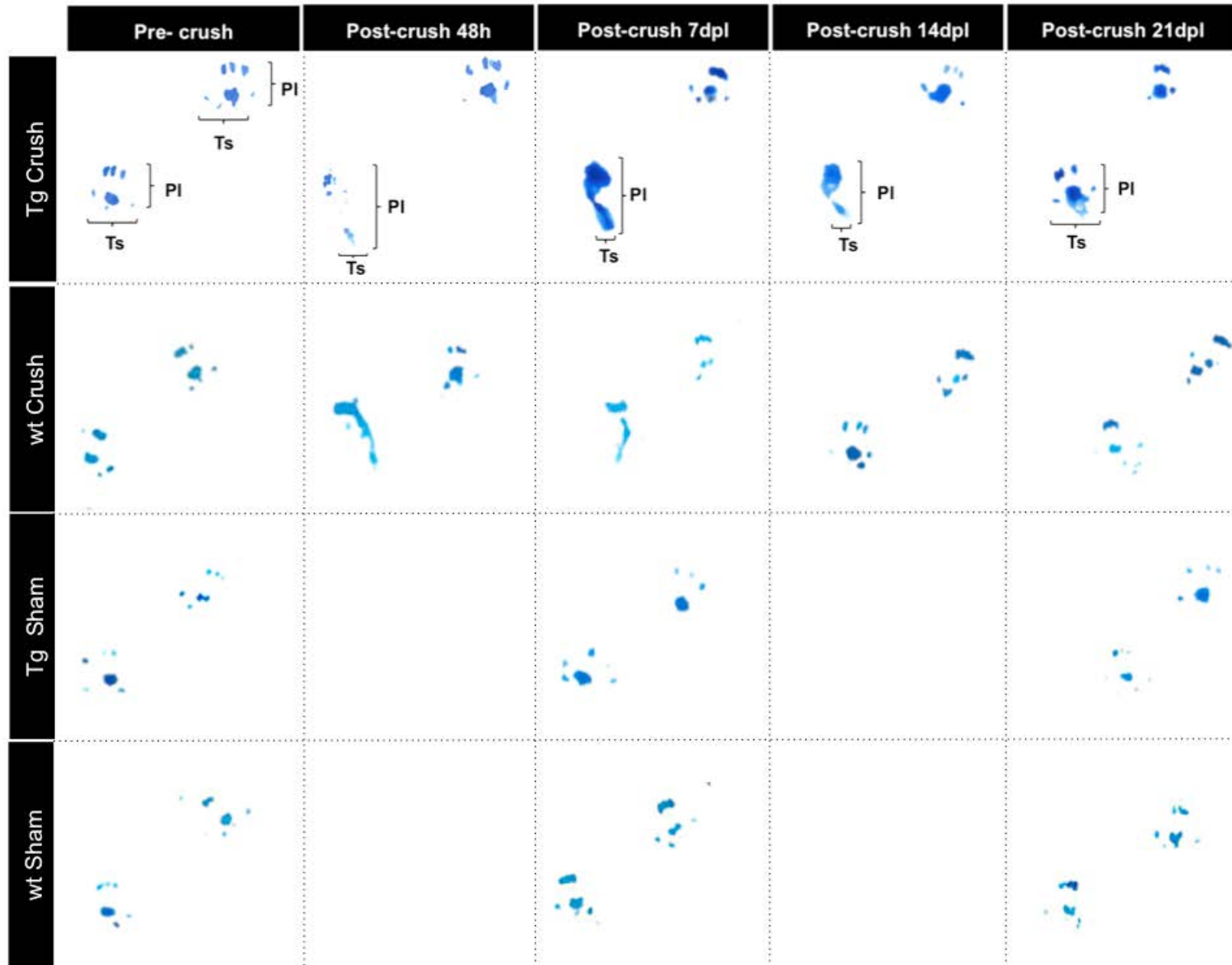


Figure 24. Representation of the pawprints measured at 24h before and 48h after surgery. SFI was calculated with the average measure of the Toe Spread (Ts) and Print length (PI) of pawprints (Inserra, 1998).

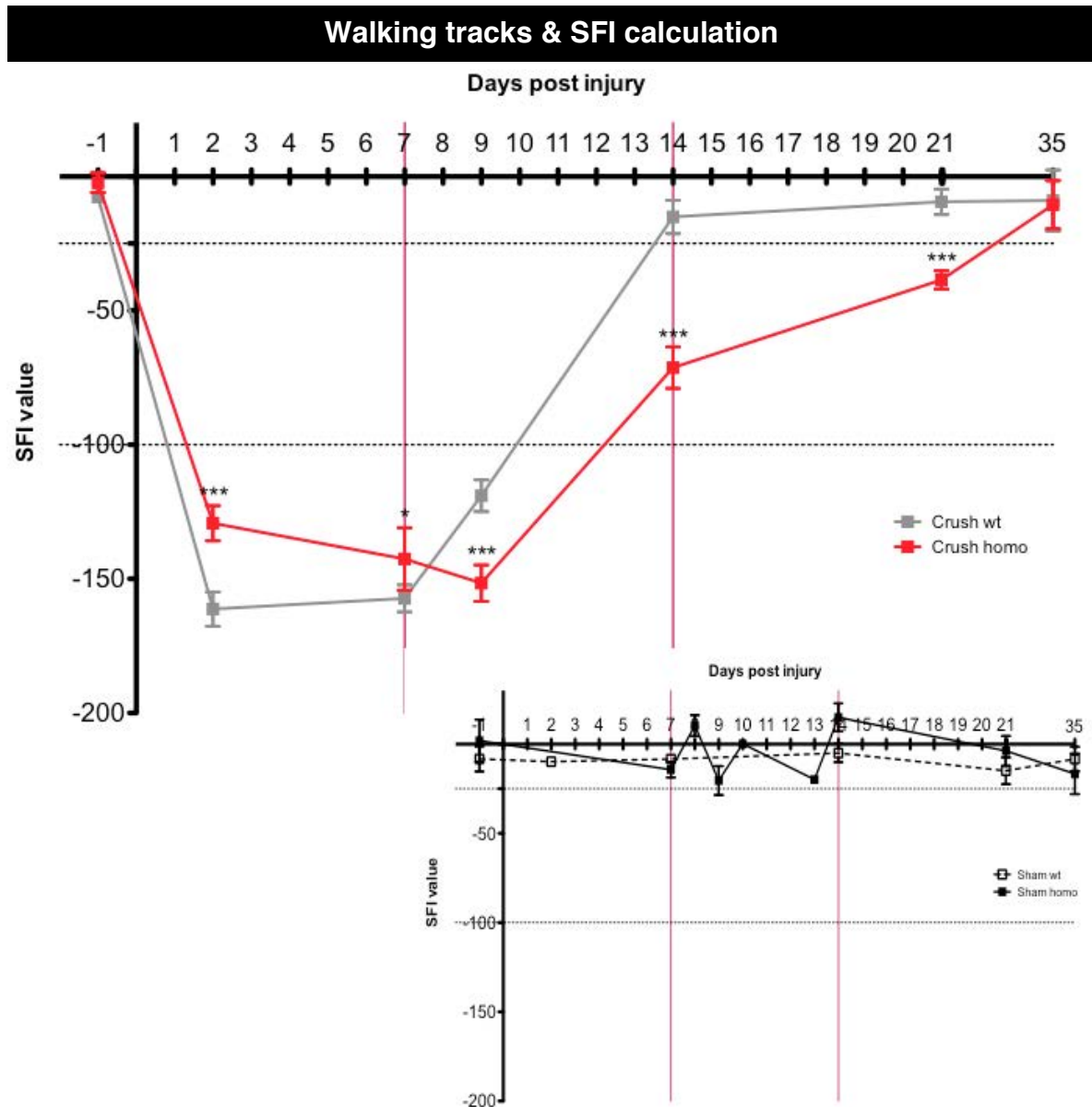


Figure 9. The pre-surgery SFI for the animals and also for a sham operation or a non-transected nerve is SFI = 0; and for a transected nerve post-surgery SFI = -100 (Inserra, 1998). Red vertical line represent each week after crush injury, the checkpoints of the regeneration process. Dotted horizontal black lines represent the normal/Sham values, localized between SFI=5 and SFI=-10; and the SFI values typical for injury animals: SFI<-100. (* $p < 0.05$ at 7dpl and *** $p < 0,001$ versus wild type, about 25-fold change at 9dpl, 30% at 48hpl)

We conclude that, while Sham intact animals of both genotypes have not differences in the theoretical SFI pattern, injured P0TNFalpha animals exhibit a delayed recovery, probably as a consequence of retardation in initiation and progression of WD, as well as in the posterior regeneration. There were not behavioural differences among female or male sexes.

3. Molecular characterization of P0TNFalpha mice

3.1 TNFalpha detection in intact animals

We quantified levels of TNF mRNA in the L4 of P0TNF animals by qPCR analysis in different tissues (Fig26.A.&.B.). In all cases, values were relative to the cDNA of reference genes (Mat&Meth).

It is possible to observe a highly significant increase (Fig.10A) in the mRNA level of TNFalpha at all ages, especially at P05, compared to control animals. However, there is a tendency to decrease TNFalpha expression with age. Thus, differences between TNFalpha mRNA levels at P21 and P65 are statistically significant compared to young P05 animals, but the expression is similar versus P21 and P65 animals. Similar results of mRNA expression were obtained by ELISA protein detection (Fig26.C.).

TNFalpha and other cytokines are biomarkers of inflammatory processes. Many cytokines are undetectable in serum by ELISA because they are produced locally or/and have a very short half-life. In order to circumvent these limitations, cytokines are often optimally measured in affected tissues, here directly in sciatic nerves.

However, it was not possible to detect TNFalpha protein in of sciatic nerves extracts from control wild type animals at different ages, neither from peripheral organs and tissues, such as liver or brain, from any wild type or P0TNFalpha mice.

On the other hand, high concentrations TNFalpha protein were detected in sciatic nerve extracts from homozygous transgenic animals compared to adult transgenic mice at P65 (Fig26.c.). It is possible to perceive a negative tendency in the amount of TNFalpha within days, mainly at first stages. These results are according to the P0 promoter expression peak, around the post natal fourth-fifth day (Fig. 8.), and correlates with TNFalpha expression (Fig26.A.).

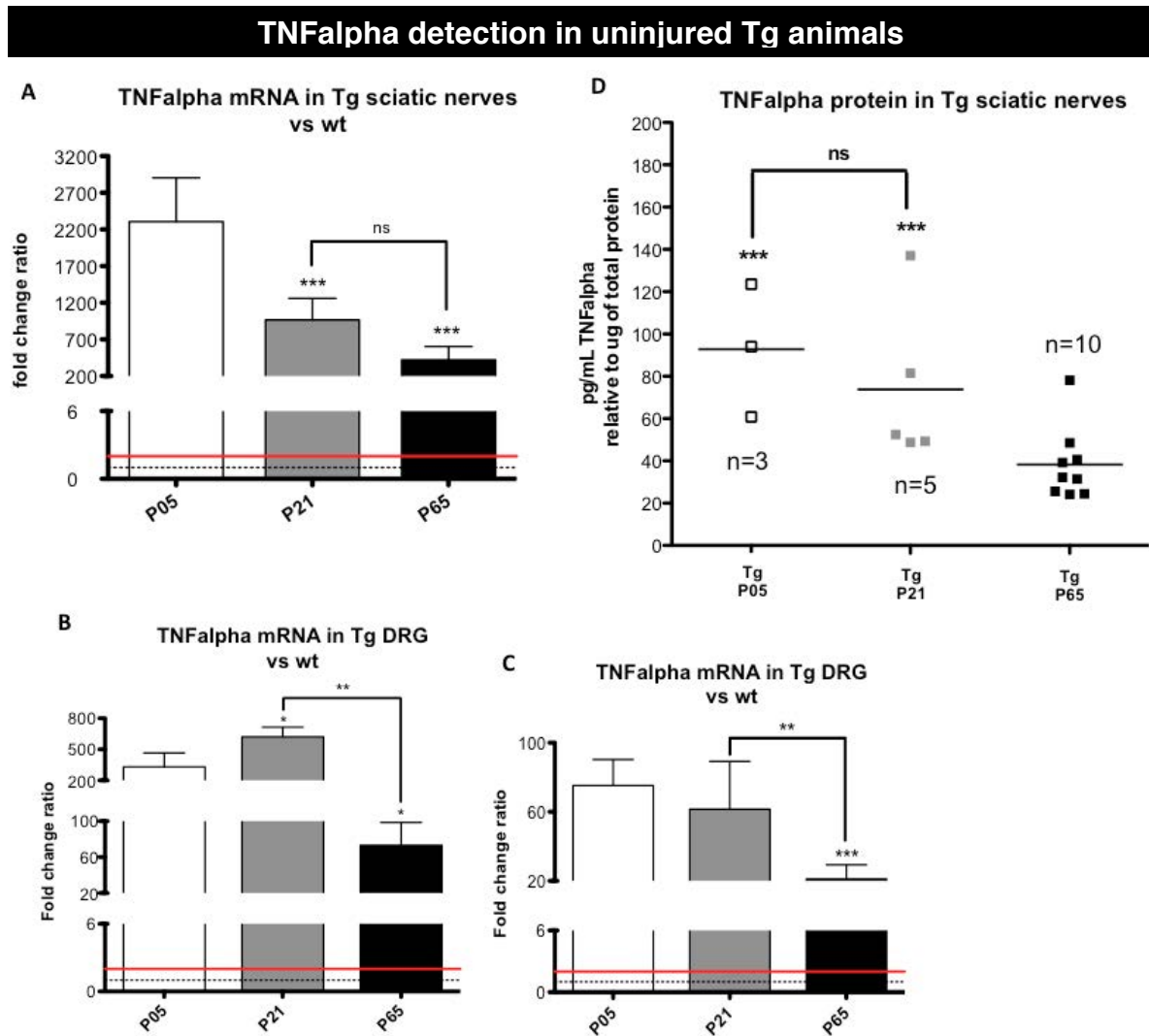


Figure 26. (A), (B) & (C) TNF α mRNA levels in the PNS tissues: Sciatic nerves, DRG and Spinal cord. are relative to the cDNA of m36B4 reference genes. Dotted line, situated at $y=1$ represent the normal value to control wild type animals, and red line at $y=2$, means significant differences higher than 1 genes copies, compared to wild type. (***) $p < 0.001$, ** $p < 0.01$, * $p < 0.05$ ANOVA and Bonferroni post-test. Sciatic nerves at P21 about 58 fold change versus P05, and 83-fold P65 versus P05. (C) TNF α protein concentration relative to total protein of sciatic nerve tissue homogenates (***) $p < 0.001$ compared to adult transgenic animals).

TNF α protein overexpression is up to 75-fold compared to adult transgenic mice at early ages (P05 to P21) in homozygous transgenic animals. Moreover, adult transgenic animals have only about 35-fold being statistically different from younger ages.

Although TNF α expression is regulated by a SCs specific promoter it is possible to detect TNF α increased expression also in other related tissues, as DRG and spinal cord (Fig26.B.). We observed again, an age-dependent reduction.

In DRGs, TNFalpha expression is higher than at the spinal cord, but lower than sciatic nerve. Probably the values could be an artifact due to cross-contamination with root node nerve tissue and not to the DRG-TNFalpha expression per se. It is also possible to observe the same age-reduction seen in sciatic nerves, particularly for older animals.

We also detected TNFalpha mRNA in spinal cord but it was considerably lower, about more than one order of magnitude lower than in sciatic nerves. Moreover, the age-dependent decrease it was also confirmed.

We observed a highly increased in the TNFalpha mRNA and protein at all ages in P0TNFalpha mice correlating to P0 expression, but we also perceived an age-dependent tendency to reduce TNFalpha. Although TNFalpha expression is regulated by a specific promoter to SCs, we also detected TNFalpha increased expression in other related tissues, as DRG and spinal cord. On the other hand, we were not able to detect TNFalpha protein in wild type animal tissues.

3.2 TNFalpha detection in injured animals

Crushed sciatic nerves were divided into two segments: distal or proximal related to the injury site. In addition, right contralateral nerves from the same animals were collected and used as inner control. We demonstrated that there are no differences between intact or sham nerves from wild type or transgenic animals (Fig27.). Thus, it is possible to pool them as a normal phenotype condition.

P0TNFalpha and wild type animals had surgery at 1.5 month old and sacrificed 21 dpl, being P65 old animals. We also detected changes in the expression of TNFalpha mRNA by qPCR at sciatic nerve 3 weeks post injury.

P0TNFalpha transgenic animals show higher TNF alpha mRNA than wild types (Fig27.A.&B.)

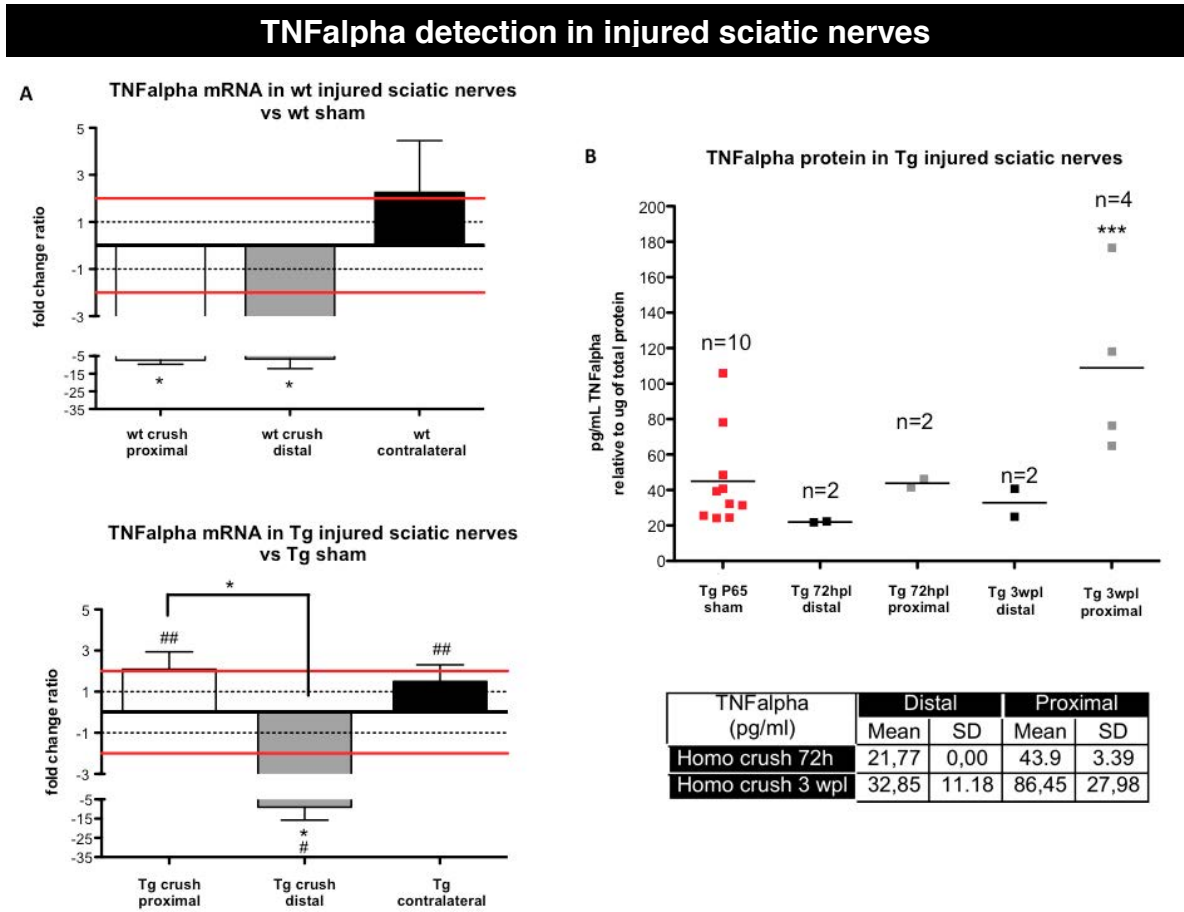


Figure 27. (A) Values are compared to wild type control animals with the same surgery protocol: sham or crush (* p<0.05 versus sham animals. # p<0.05 and ## p<0.01 Tg versus wt. ANOVA and Bonferroni post test. **(B)** TNFalpha protein concentration relative to total protein of sciatic nerves tissue homogenates. Average of TNFalpha concentration in animals without injury or after different times post crush are represented in the table (***) p<0.001 versus sham Tg mice).

There is a significant decrease in mRNA TNFalpha in distal stump from injured sciatic nerve, compared to uninjured nerves. However, changes are not detected at the sciatic proximal section although TNFalpha expression is also reduced versus uninjured transgenic animals. TNFalpha concentration is so elevated in transgenic animals that, effectively, differences would possibly only be noticed if they are dramatic. Thus, in the distal section of injured transgenic nerves, we also see an important decrease in TNFalpha (Fig27.A.), indicating a decline in myelinating SCs expressing the transgene, due to the regenerative process fulfilled in this nerve section.

In wild type animals, both nerves sections show diminished TNFalpha. As a consequence, although they seem to be completely regenerated by SFI, at the molecular level demonstrate to have lower proinflammatory TNF, thus being at the final regeneration phase of WD. TNFalpha reduction seems necessary to initiate WD events and the consecutive regeneration process. The lack of this depletion in the proximal section of transgenic injured mice could be the reason for the delayed recovery from transgenic animals.

TNFalpha expression was also checked in DRGs and spinal cord after crush, but no changes were detected (**not shown**).

To study the degenerative/regenerative process, we also analyzed the injured animals at 72hpl. Whole left sciatic nerves of crushed animals, compared to uninjured transgenic animals showed similar amount of TNF alpha protein (**not shown**). However, the analysis of proximal sections from crushed transgenic animals at 3wpl, exhibits statistical significant differences (**Fig27.B.**) versus sham animals. Distal end had similar levels than sham and these values were about 35-fold higher than wild type animals.

These different patterns between whole, distal and proximal stumps of injured sciatic nerves, show the probable role of TNF alpha in the peripheral regeneration which takes place, first, in the proximal part while at that time WD occurs in the distal parts.

The TNF alpha protein concentration obtained 3 wpl from the proximal part of homozygous transgenic animals it is close to the protein levels present in new born (P05) and young (P21) control sham transgenic mice. The study was also done in the control genotype (wild type animals), in same conditions (sham, 72 hpl and 3 wpl), but TNFalpha protein was below the sensitivity of ELISA (**data not shown**).

Peripheral myelination process starts around P05, corresponding to a peak of P0 expression, the main protein in PNS myelin (**Fig27.B.**). These ELISA results, could demonstrated regeneration and myelination active phase in proximal sections of transgenic animals at 3wpl, while in wild type is almost finished.

Increased levels of TNF alpha are related to the P0 expression in this model, due to the transgene is under the control of the P0 promoter and regulated equally by the same transcriptional elements. Moreover, in the regeneration events P0, as the main PNS myelin component, is rapidly over-regulated but TNF alpha expression could be deleterious to the proper myelination and regeneration.

TNFalpha mRNA was also detected in other peripheral organs (data not shown), such as brain or liver at P65 adult uninjured animals, and it is lower but similar to spinal cord values and statistically significant from wild type animals. Probably, the results may indicate a global compensatory inflammatory mechanism, although TNFalpha expression was specifically confined in peripheral nerves.

The final number of animals for control condition, in both genotypes, are a pool of intact and sham nerves, due to there are no differences between them.

We conclude that TNFalpha concentration is so elevated in transgenic mice that differences would only being noticed if there are dramatic. The lack of the TNFalpha depletion in transgenic mice, necessary for initiate WD, could cause the delayed recovery and consecutive regeneration. The results observed by ELISA confirm a regeneration and myelination active phase in proximal section of transgenic animals at 3wpl, while wild type animals are almost finished. The TNFalpha upregulation associated to P0 overexpression in regeneration, could be deleterious to proper remyelination.

3.3 Compensatory mechanisms: TNFRI/RII detection

Association of TNFalpha with its cell surface receptor triggers intracellular signal transduction cascades that culminate in changes in gene expression. In order to determine whether the increased levels of TNFalpha is related to increase expression of TNFRI and/or RII as a compensatory mechanism and activated the signaling pathway that is implicated, the levels of mRNA for both receptors were examined by qPCR (Fig28.).

Surprisingly, were observed (Fig28.A.) a significant reduction in the mRNA levels of TNFR1 in an age-dependent manner particularly at P21 and P65. P05 mice do not show statistically differences compared to controls. However if they are

compared to wild type animals, they showed significant differences as for other ages.

TNF Receptors mRNA quantification

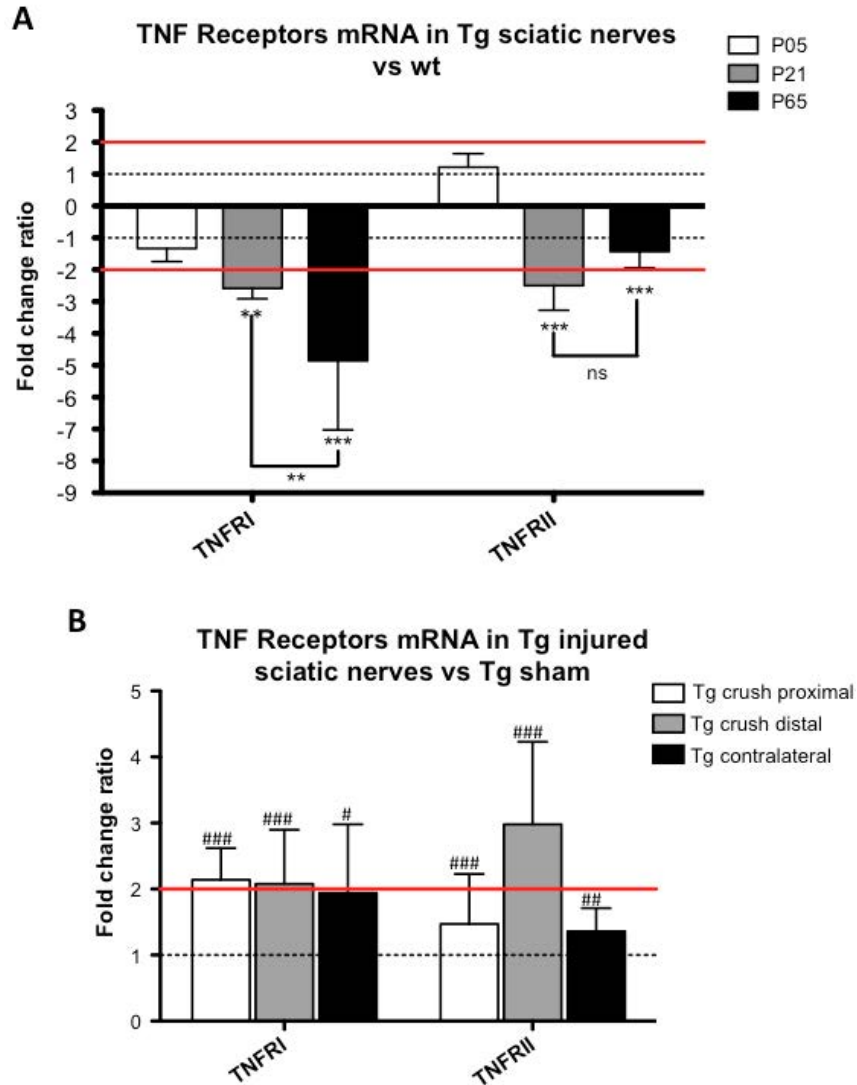


Figure 28. (A) Values are relative to the cDNA of m36B4 reference genes, and compared to wild type control animals (** p<0.01 and *** p<0.001) P65 animals show a reduction about 75-fold change versus wt and young Tg mice, and 50% versus P21 Tg animals **(B)** (# p<0.05, ## p<0.01 and ### p<0.001 Tg injured versus wt injured nerves).

No changes are detected for TNFR2 (Fig28.A.), although a tendency to reduce the expression, is seen. If two receptors genes, TNFR1 and R2, are compared between them at P21, the expression is similar. In addition, TNF receptors have not significant changes in DRG or spinal cord compared to wild types.

We did not observe significant alterations in the mRNA levels of both TNF receptor TNFR1 and TNFR2 after crush both in wild type and transgenic mice (Fig28.B.), although we confirmed a significant reduction in both receptors in transgenic animals compared to crushed wild types.

We observed a decrease expression in both TNF receptors, probably as a compensatory mechanism against the effects of TNF α in PNS.

3.4 Antiinflammatory responses: IL10 detection

Another possible mechanism of compensation to decrease the effects of TNF α expression, could be through the regulation of anti-inflammatory cytokines, such as IL10.

Both, TNF α and IL10 cytokines are implicated in the events of the WD: TNF α in the first proinflammatory steps, and IL10 later to resolve the process. Thus, IL10 has the function to inhibit the synthesis of high number of cytokines, including TNF α and GM-CSF, produced by activated macrophages. As a consequence, we postulated a possible overexpression IL10 in P0TNF α transgenic animals to modulate the effects of high levels of TNF α as a compensatory response.

The results (Fig29.A.) show a negative correlation between both cytokines, as expected. Although there are not significant differences due to variability, P65 adult animals have lower levels of TNF α protein and mRNA, probably due to the action of the high protein concentration of IL10, both to the decreased activity of P0 driving TNF α expression and indeed, its receptor TNFR1 and Egr2, the transcription factor which regulate the transgenic TNF α and P0 expression.

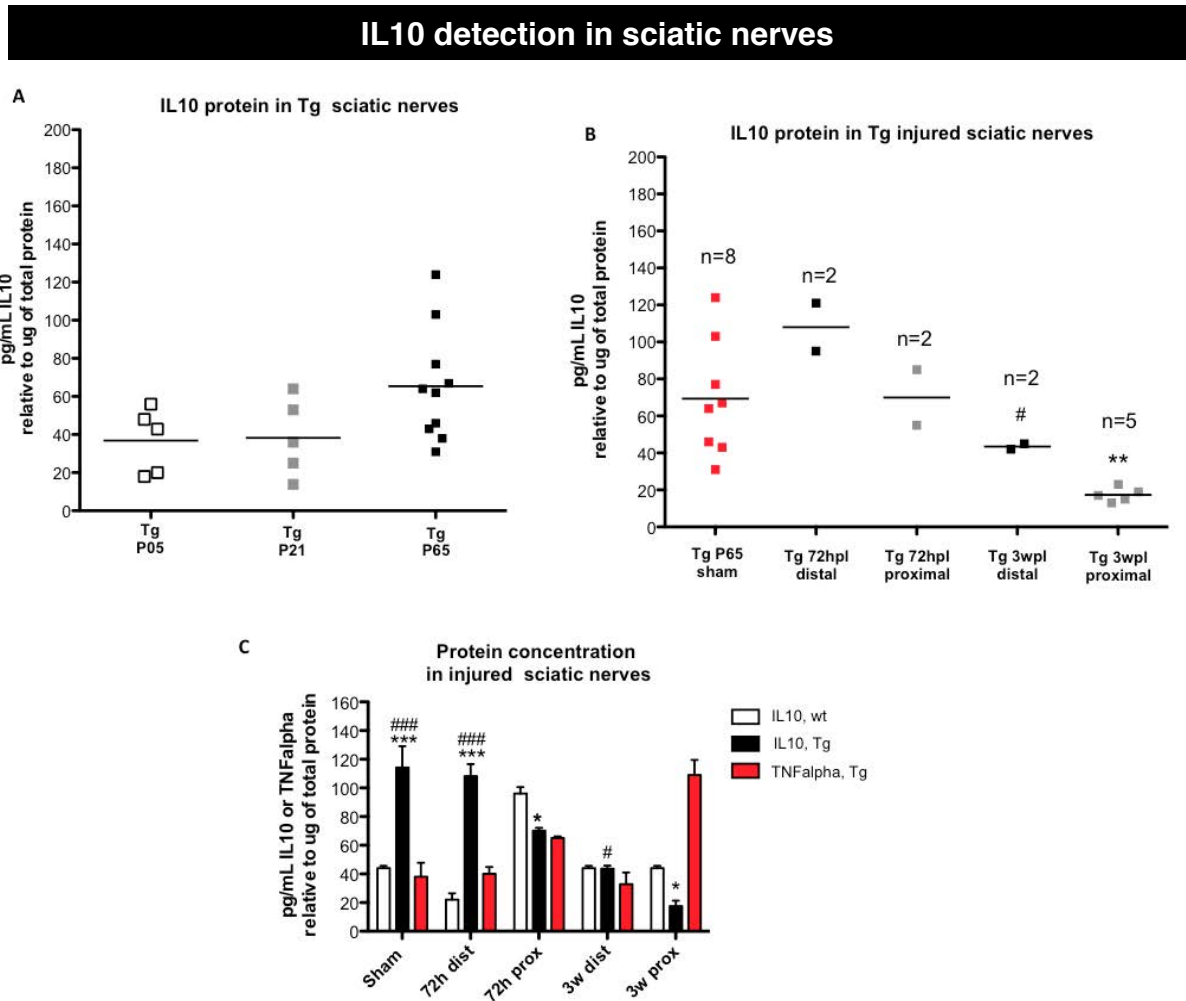


Figure 29. IL10 protein relative to total protein in intact transgenic sciatic nerves **(A)** or injured transgenic nerves **(B)** ** $p < 0.01$ compared to sham animals and # $p < 0.05$ compared to distal section at 72hpl and 21dpl. ANOVA and Bonferroni post-test. **(C)** Correlation between IL10 and TNFalpha in sciatic nerves. *** $p < 0.001$ and * $p < 0.05$ compared to wild type and ### $p < 0.001$ compared to the transgenic proximal section at 72hpl.

There was not possible to detect IL10 protein in wild type animals at P05 and P21 and it was 3 times lower in adult wild type animals than P0TNFalpha mice. Neither IL10 mRNA was detected in wild type animals (Fig29.c.).

After crush, we found again a negative correlation between TNFalpha and IL10 (Fig29.c.) both at 3 dpl and 21dpl.

It was possible to detect IL10 in wild type animals at 72hpl, being higher in proximal than in distal segments. However, at 3wpl there are not differences between wild type intact animals (Fig29.c.).

The results, after peripheral injury, represent a typical and almost successful finished process of WD in wild type animals. However the distal segment of P0TNFalpha mice at 72hpi, IL10 is very high, indicating that the WD was not started in this part, at this time. However, the proximal transgenic sections show lower IL10 concentration than wild type and the TNFalpha start to increase, necessary to the initial pro-inflammatory events of WD, culminating at 3wpi with a higher concentration of this cytokine (Fig29.B.).

All together, the results show a negative correlation between both cytokines (IL10 and TNFalpha) in transgenic mice without or with peripheral injury, confirming the delay in the WD process of P0TNFalpha mice necessary to restore and complete the regeneration of peripheral nerves.

3.5 Myelination process characterization

The regulation of expression and production of different cytokines depends on different factors that act, mostly, at transcriptional, message turnover and protein degradation levels. Thus, the TNFalpha specific expression in PNS could alter the myelin protein gene expression (Fig21.C.) as well as the process of remyelination after regeneration from injury.

The four main myelin proteins (P0, MBP, MAG and PMP22) were analyzed and showed a significant reduction compared to wild type animals (Fig21.C.). P0 expression shows a reduction about 25 fold. However, MAG expression has not statistical changes, although it shows a decrease about 10%.

We found no differences when comparing animals between different ages for P0 and MAG genes. However, we detected an age-dependent increase for MBP statistically significant comparing p65 to P05 and P21 about 30% (Fig21.C.) P65 transgenic animals have not different expression levels than wild types ones. On the other hand, a statistically significant age-dependent decrease is detected for the expression PMP22.

Protein production for two of the main structural myelin proteins of PNS (P0, MBP) was studied at sciatic nerves by western blot (Fig30.). Both of them show a protein reduction, mainly at P05 animals but also at P21. At P65 proteins were normalized, probably due to the long half life of P0.

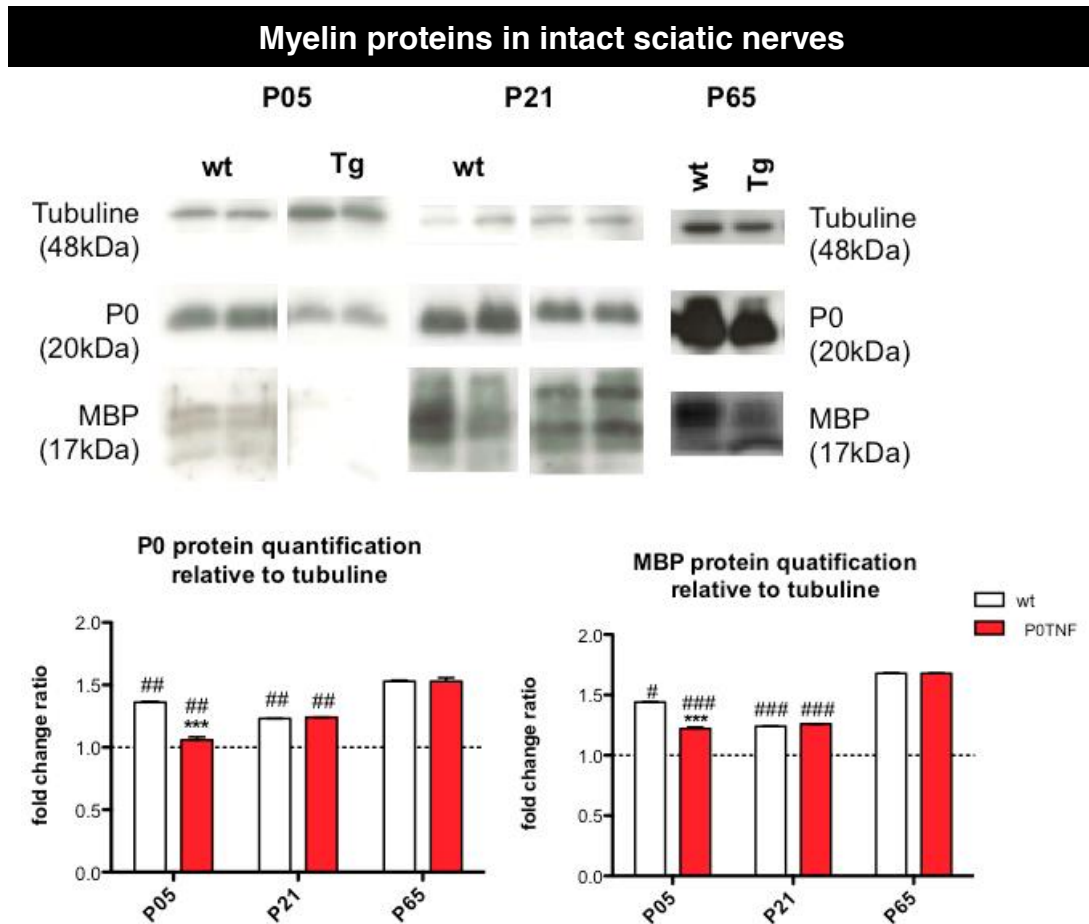


Figure 30. Protein levels detected by western blot in wild type and P0TNFalpha animals at the three different ages of the development. (***) $p < 0.001$ versus wild type intact animals, and ### $p < 0.001$, ## $p < 0.01$ and # $p < 0.05$ compared to adult transgenic mice at P65).

Moreover, the immunohistochemical analysis of longitudinal slides from tibialis nerves confirm the reduction of MBP levels, being more dramatic at P05 and P21 than P65 homozygous transgenic animals; as well as the recovery if P65 animals are compared between genotypes (Fig49.A.,C.&D.).

Egr2/Krox20 and Sox10, altogether with Oct6, are some of the most important transcription factors implicated in peripheral myelination by directly activating SCs and myelin genes, such as P0 (Ghislain, 2006; Svaren, 2008; Heinen, 2010). Furthermore, the transcription factor Sox10 is believed to influence myelination by inducing Krox20 as a pivotal regulator of peripheral myelination. However, although changes are observed in myelin genes correlating with TNFalpha levels, there are not differences in Egr2/Krox20, Sox10 or Oct6 in intact transgenic animals compared to wild type mice.

As a general conclusion, the TNFalpha specific expression in PNS altered myelin gene expression and protein at the three different ages tested. These results show an initial delay in myelin expression and translation, which normalizes in adulthood, probably due to the long half life of myelin proteins. However there are not changes observed in the transcription factors Egr2, Oct6 or Sox10 in intact transgenic mice compared to wild type mice.

3.6 Demyelination & remyelination characterization

3.6.1 Egr2 detection

Following 3 wpl, we observed a significant reduction in both sciatic sections of wild type animals compared to intact nerves (**Fig31.**) Moreover, there are also statistically significant differences if distal and proximal sections are compared among them.

In transgenic mice we found a decrease in Egr2 in the distal sciatic segment (**Fig31.**) is correlated to a significant decrease expression of Egr2 (** $p < 0,01$ compared to intact animals but similar to wt injured sciatic nerves. However, no differences were found between proximal and intact nerves in P0TNFalpha animals. Results indicate that at 3wpl transgenic mice start the remyelination in the proximal segment while wild type mice have probably finished this process at that time in distal and proximal stumps.

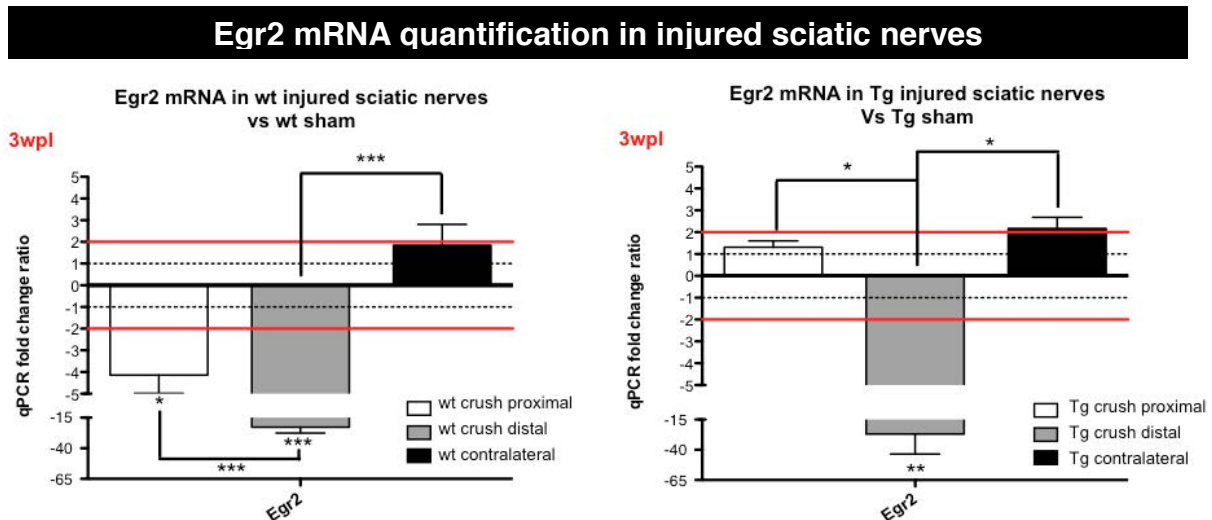


Figure 31. Egr2 expression analyzed by qPCR 3wpi in wild type and transgenic P0TNFalpha animals compared to the intact sciatic nerves (* $p < 0.05$, ** $p < 0.01$ and *** $p < 0.001$).

In transgenic mice we found a decrease in Egr2 in distal segments but not in proximal where remyelination is starting, While wild type mice have probably finished. As a consequence, Egr2 specific changes will affect the myelin protein gene regulation after peripheral nerve injury, necessary to a successful regeneration.

3.6.2 Myelin protein detection

Expression of the four main myelin proteins (Fig32.) (P0, MBP, MAG and PMP22) is significantly reduced in the distal segment referent from both genotype compared to intact nerves, being higher in transgenic mice. However, the proximal sections of wild type animals also show a myelin reduced expression while the proximal stumps of P0TNFalpha mice have similar values than intact transgenic nerves (Fig32.). Only the distal part of transgenic injured sciatic nerves have a diminished expression of myelin genes.

The results are according to Egr2 (Fig31.) and TNFalpha (Fig27). changes after crush injury.

Myelin proteins mRNA quantification in injured sciatic nerves

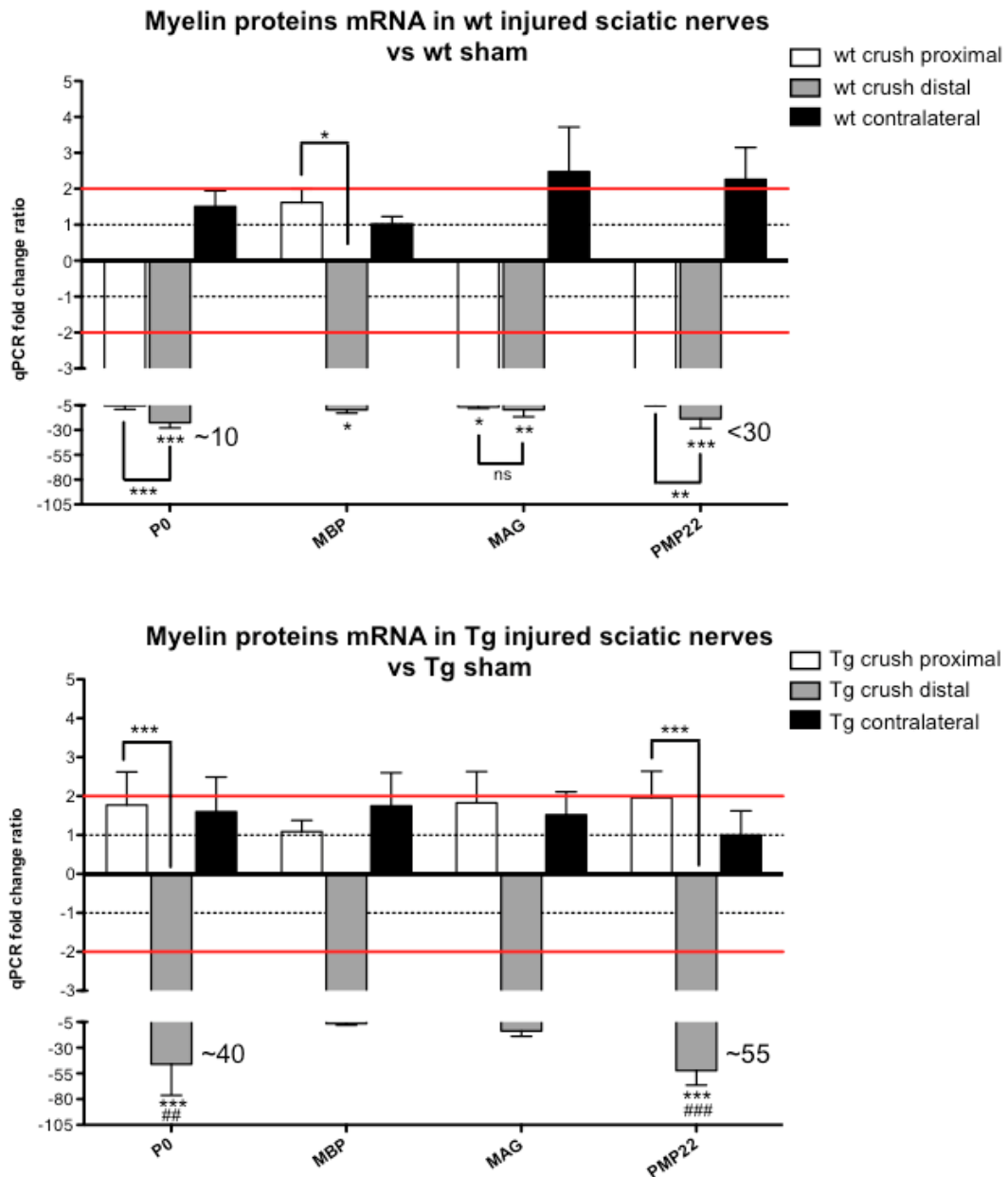


Figure 32. Myelin protein gene expression analyzed by qPCR 3wpl in wild type and transgenic P0TNFalpha animals. Injured wild type mice were compared to wild type sham animals (*** p<0.001 to P0 and PMP22, * p<0.05 to MBP and ** p<0.01 to MAG). Transgenic animals after injury were correlated to intact transgenic nerves (*** p<0.001) and versus wild type (### p<0.001, ## p<0.01)

The reduction in MBP levels was confirmed by immunohistochemistry of sciatic nerves. Sciatic nerves of wild type animals have the lowest MBP signal at 14dpl, in both distal and proximal sections. However, these animals show a partial recovery in MBP at 21dpl, mainly in the proximal segments, relative to wild type control sham animals and in according to the regeneration process (Fig33. & 34.).

Transgenic animals have similar levels of MBP in the proximal segments at both times 14dpl or 21 although the MBP reduction is more evident in proximal sections at 21dpl, compared to homozygous sham animals. MBP quantification of P0TNFalpha animals, compared to wild types, show also a significant reduction in both, time point and sciatic section that have been studied (Fig33.).

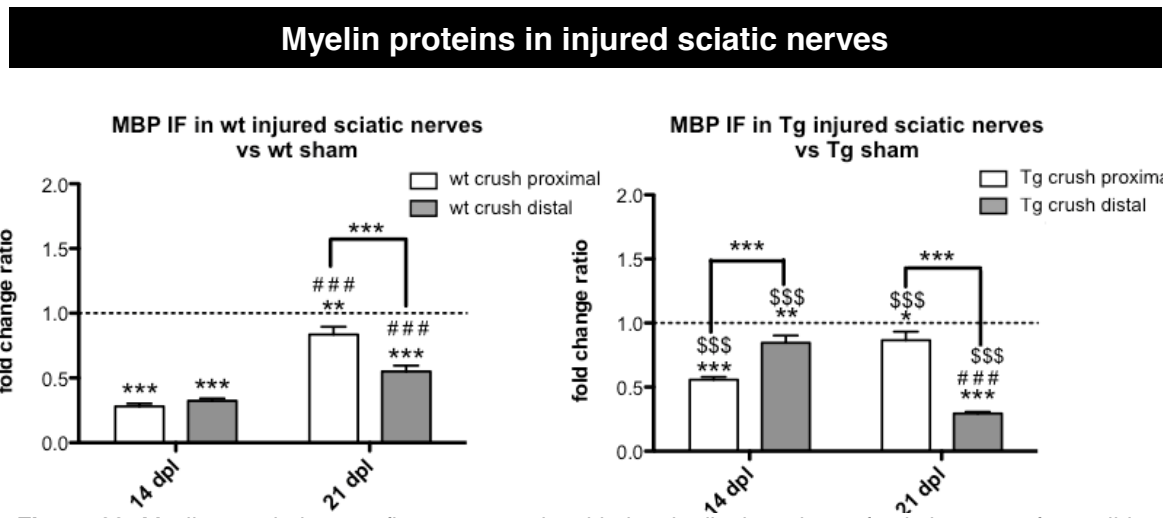


Figure 33. Myelin protein immunofluorescence signal in longitudinal sections of sciatic nerves from wild type and transgenic animals after crush injury compared to intact animals, wild type or transgenic mice respectively (*p<0.05, ** p<0.01, *** p<0.001). Animals at 21dpl are also compared to animals at 14 dpl (### p<0.001). Moreover, injured transgenic animals were compared to wild type (\$\$\$ p<0.001). ANOVA and Bonferroni post-test.

These results show MBP signal have not differences compared to intact nerves at 14dpl in distal sections. Moreover MBP is still low at 21dpl in transgenic proximal section (Fig33.).

The results of IF quantification and mRNA expression for myelin proteins, show a delay in the regenerative process in transgenic animals. WD is not started yet at 14dpl in distal sections, and myelination has not finished so far at 21dpl in transgenic proximal section.

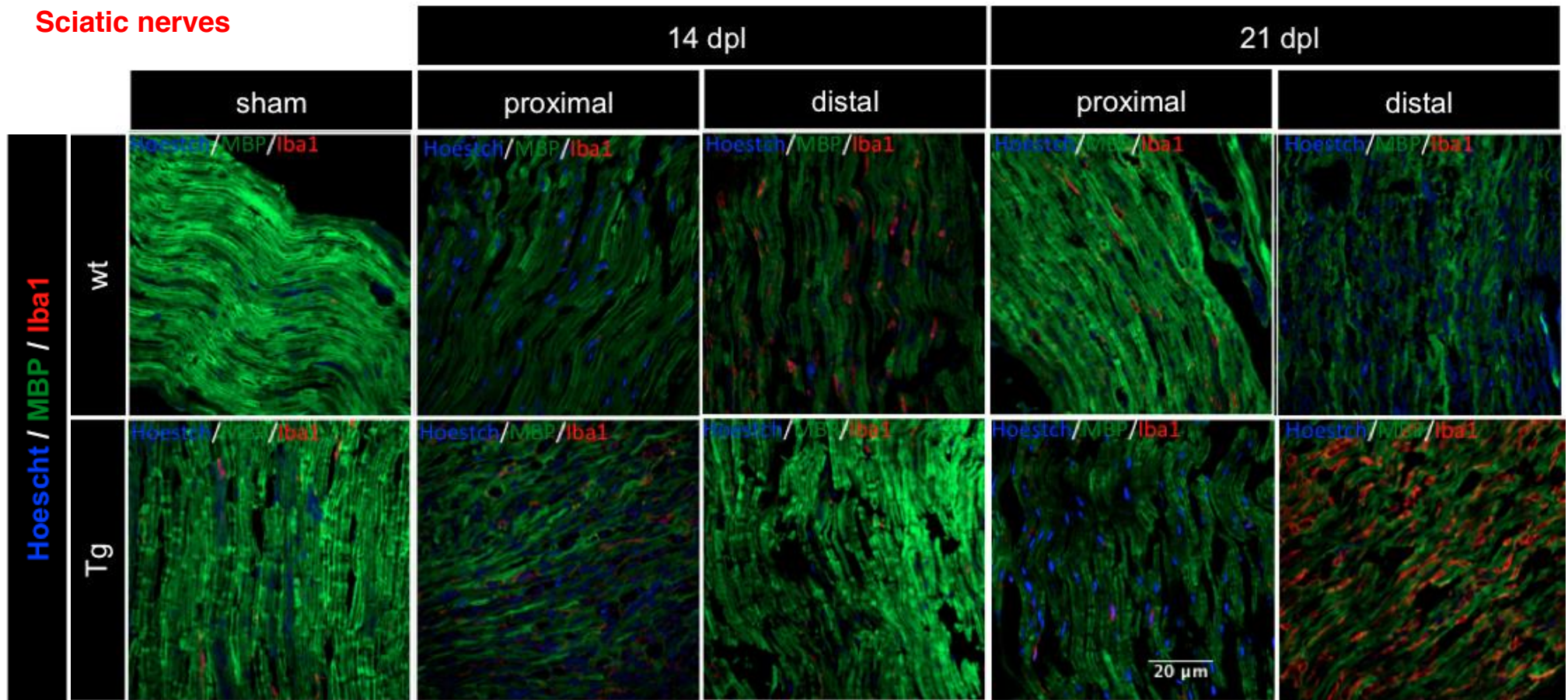


Figure 34. Myelin protein immunofluorescence signal in longitudinal sections of sciatic nerves from wild type and transgenic animals after crush injury.

3.6.3 Short timing study

When we studied shorter times after crush we detected an acute decline in Egr2 expression at 1dpl and 3dpl, only in distal segments of sciatic nerve and in both genotypes relate to intact nerves. This reduction triggers a negative transcriptional control for genes regulated by Egr2, such as the myelin protein P0 and also TNFalpha in transgenic animals (Fig35.).

However, although proximal stumps showed similar Egr2 (Fig35.A.) expression in wild type and transgenic animals, Egr2 and P0 (Fig35.B.) were reduced in both genotypes at 3dpl, compared to sham animals and to 1dpl injured animals), in the distal section. P0TNFalpha animals showed a more dramatic decreased in P0 than wild types, probably as a consequence of high concentrations of TNFalpha in the organism, allowing a reduction in the expression of myelin gene proteins, as well as it was observed (Fig35.B.).

We expected a similar transcriptional regulation of transgenic TNFalpha produced by SCs and P0 protein. However, infiltrated macrophages during WD could change the pattern of cytokines expressed in the microenvironment of the nerve to promote degeneration and regeneration (Fig35.C.).

We observed a rapidly TNFalpha expression peak at 1dpl, in both sciatic segments of wild type animals, as a consequence of initiation of WD (Fig35.C.). Furthermore, correlating with the Egr2 pattern (Fig35.A.), it was observed a decline in TNFalpha to achieve basal levels at 3dpl in wild type animals. On the other hand, injured P0TNFalpha animals show no differences with sham transgenic mice.

Short time study in injured sciatic nerves

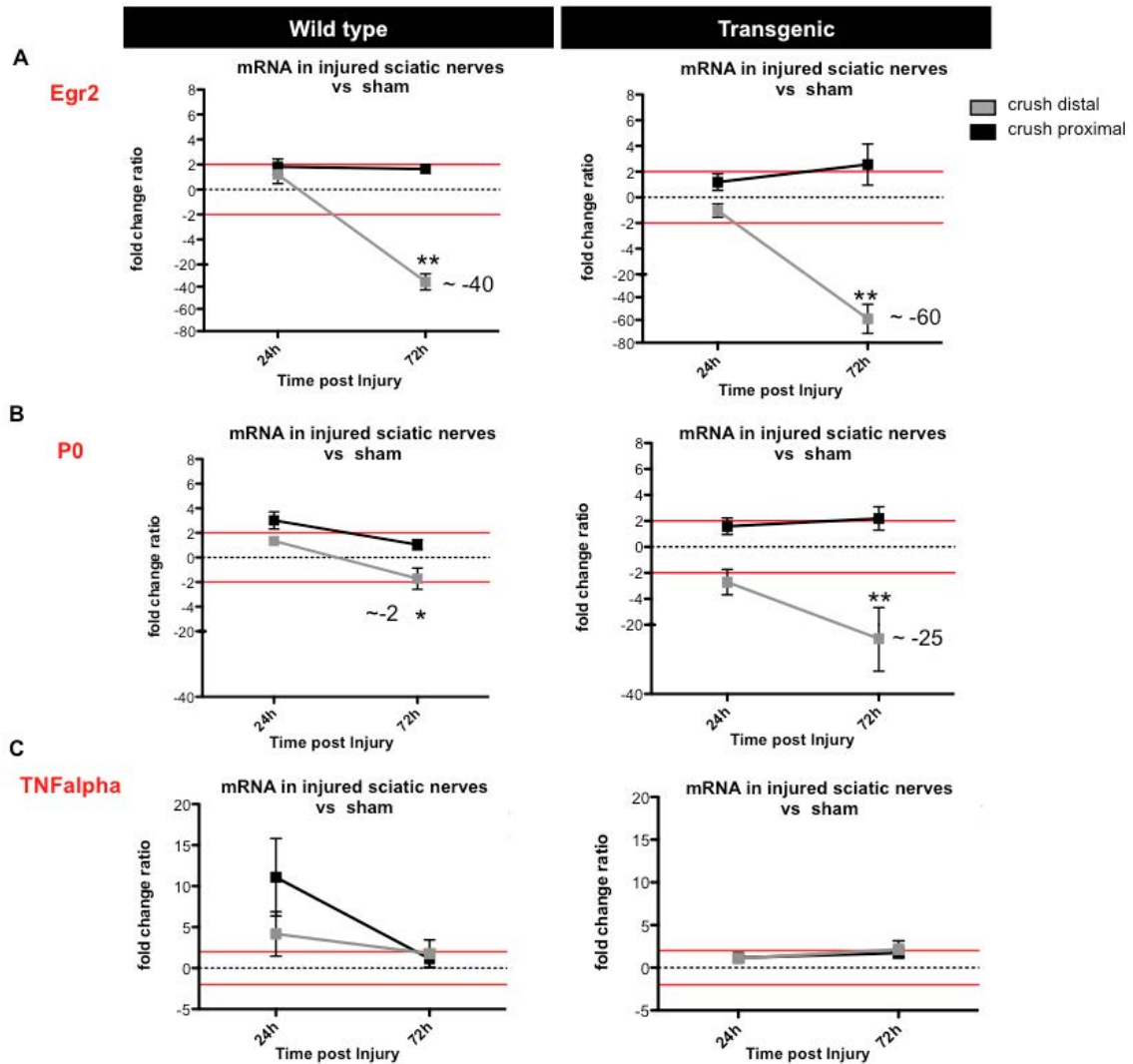


Figure 35. mRNA from distal and proximal segments of injured sciatic nerves from wild type and transgenic mice, compared to sham (intact) mice qPCR analysis of **(A)** Egr2 **(B)** P0 and **(C)** TNFalpha, at 1dpl and 3dpl. (**p<0.01 and * p<0.05 compared to their respective sham control animals).

Probably, the high expression of TNFalpha in transgenic animals masks smaller changes in this cytokine were not visualized. In addition, probably a delay in WD process was occurring which also delay the infiltration of phagocytic cells and the release of TNFalpha by activated macrophages.

4. Morphometric characterization of P0TNFalpha mice

Morphometric analysis allows to quantify the myelination, size and number of axons and the overall regenerative process. We analyzed tibialis nerve from animals with or without sciatic crush at P65. We found that the total surface of tibialis nerve was not different between genotypes (Fig36). In the same way, number and density of myelinated axons do not show important differences, and the number of total axons was maintained in intact nerves for both genotypes.

Clearly, wild type mice exhibit bigger axons than the other experimental groups (Fig37.).

The more abundant axon size range in uninjured wild type animals ranged from 4 to 8.99 μm , and from 4 to 6.99 μm after crush injury. However, the axon size in P0TNFalpha mice ranged from 4 to 7.99 μm in intact nerves and from 3 to 6.99 μm for damaged nerve. Thus showing a small reduction in the nerve diameter compared to wild type mice (Fig37&38.).

The distribution of the axon size was adapted to a theoretical normal distribution in both genotypes with and without nerve damage. Wild type sham animals group (Fig38.A.) were considered as control to superimpose the distributions of the other groups. Although both of them are quite similar, transgenic animals (Fig38.B.) moved to the left side of x axes, as smallest axons are more common.

After crush surgery, wild type mice (Fig38.C.) show similar behaviour as sham P0TNFalpha mice (Fig38.B.). Data from P0TNFalpha animals at 21dpi (Fig38.D.) were also shifted to the left x side. However, although axon size average is smaller than uninjured P0TNFalpha animals, no significant differences were observed between them.

Morphometric characterization in tibialis nerves

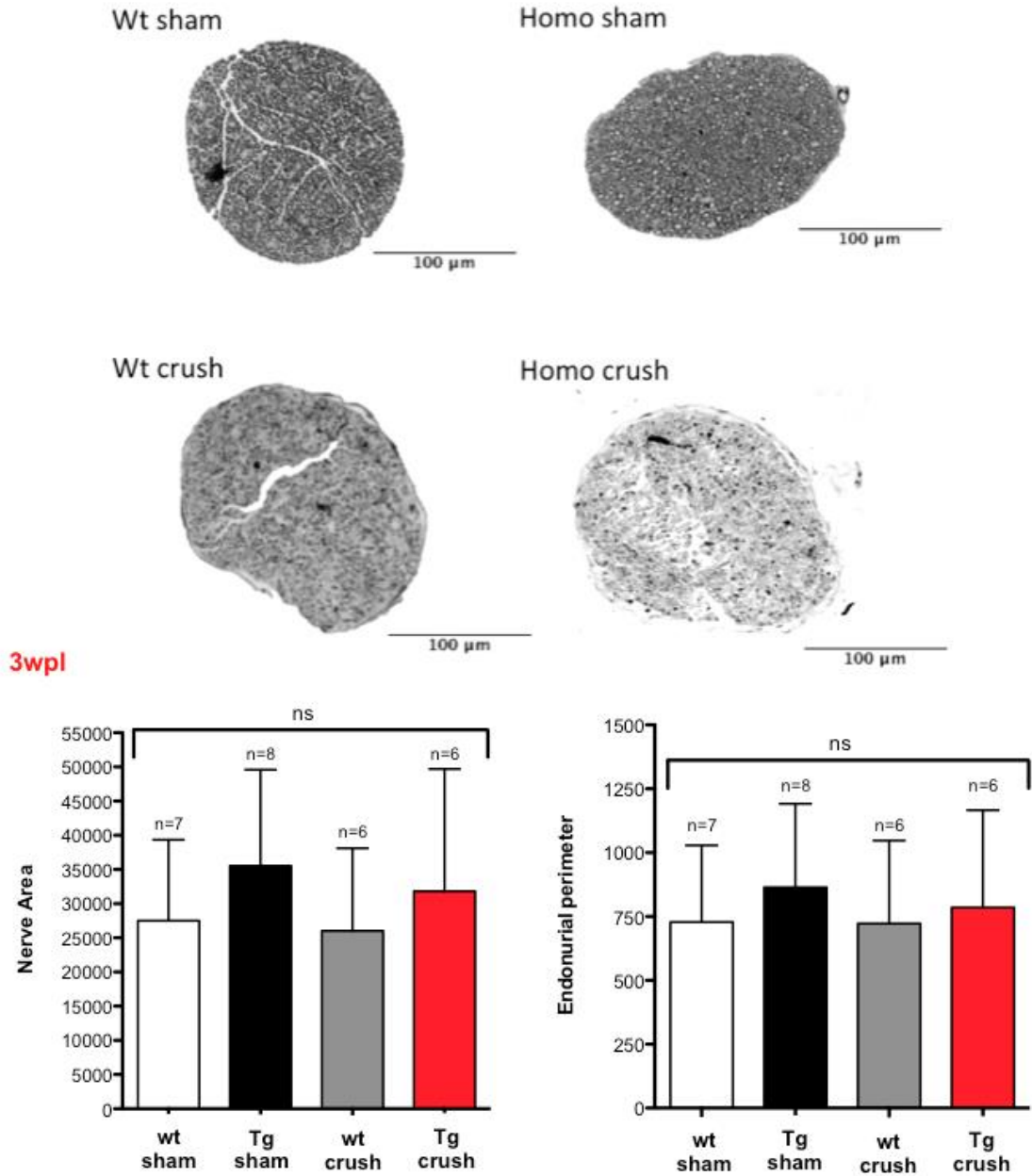


Figure 36. Representative morphological slides from tibialis nerves of the different animals group analyzed at P65: sham wild type, transgenic sham animals and wild type and P0TNFalpha transgenic animal at 3wpl. Neither nerve area (μm²) or endonurial perimeter (μm) show any significant difference between groups.

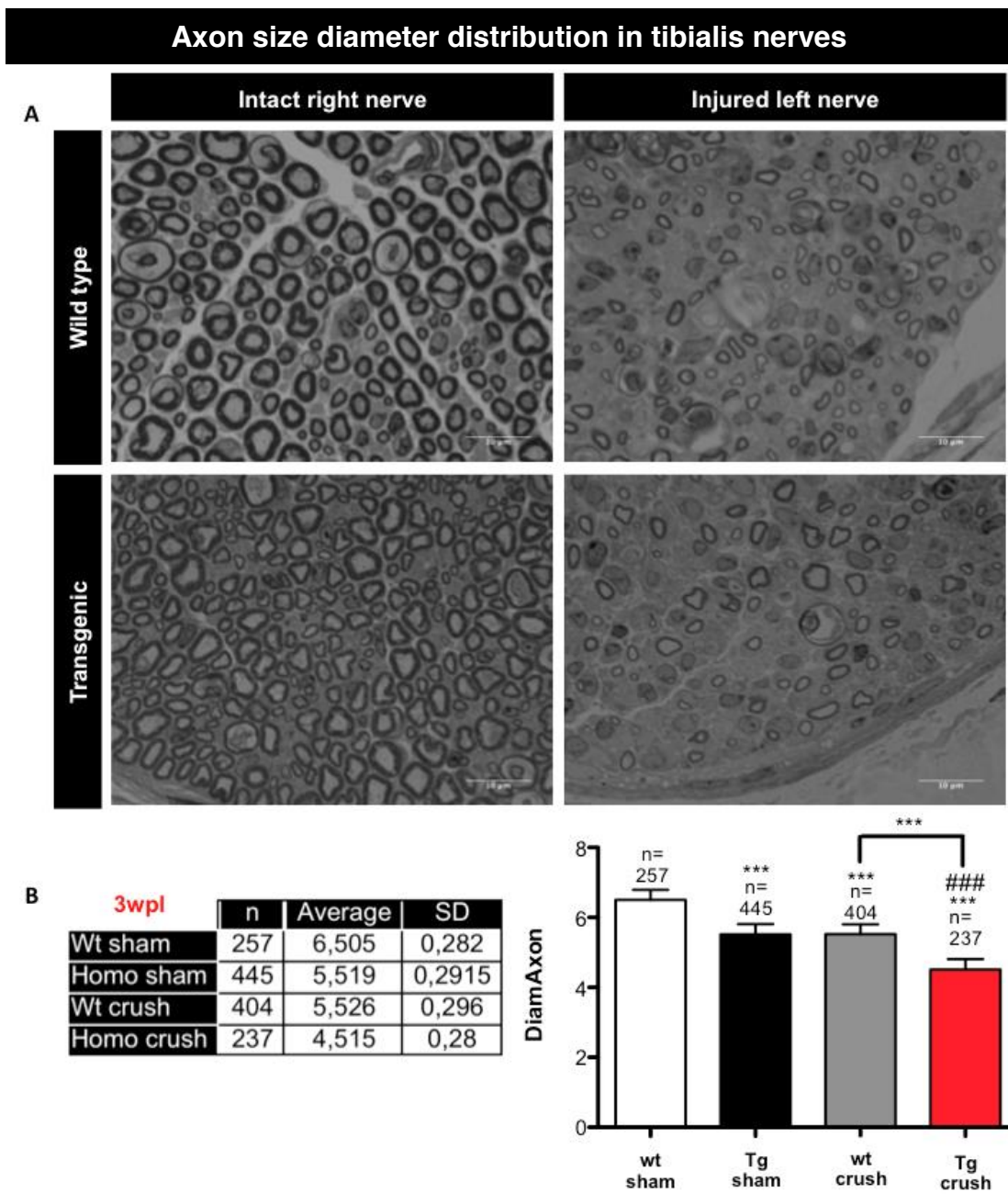


Figure 37. A detailed representation of the axons size and myelin thickness in the four animal groups, and the average values of axon diameter for each genotype and injured or intact animals.

Axon size diameter frequency in tibialis nerves

3wpl

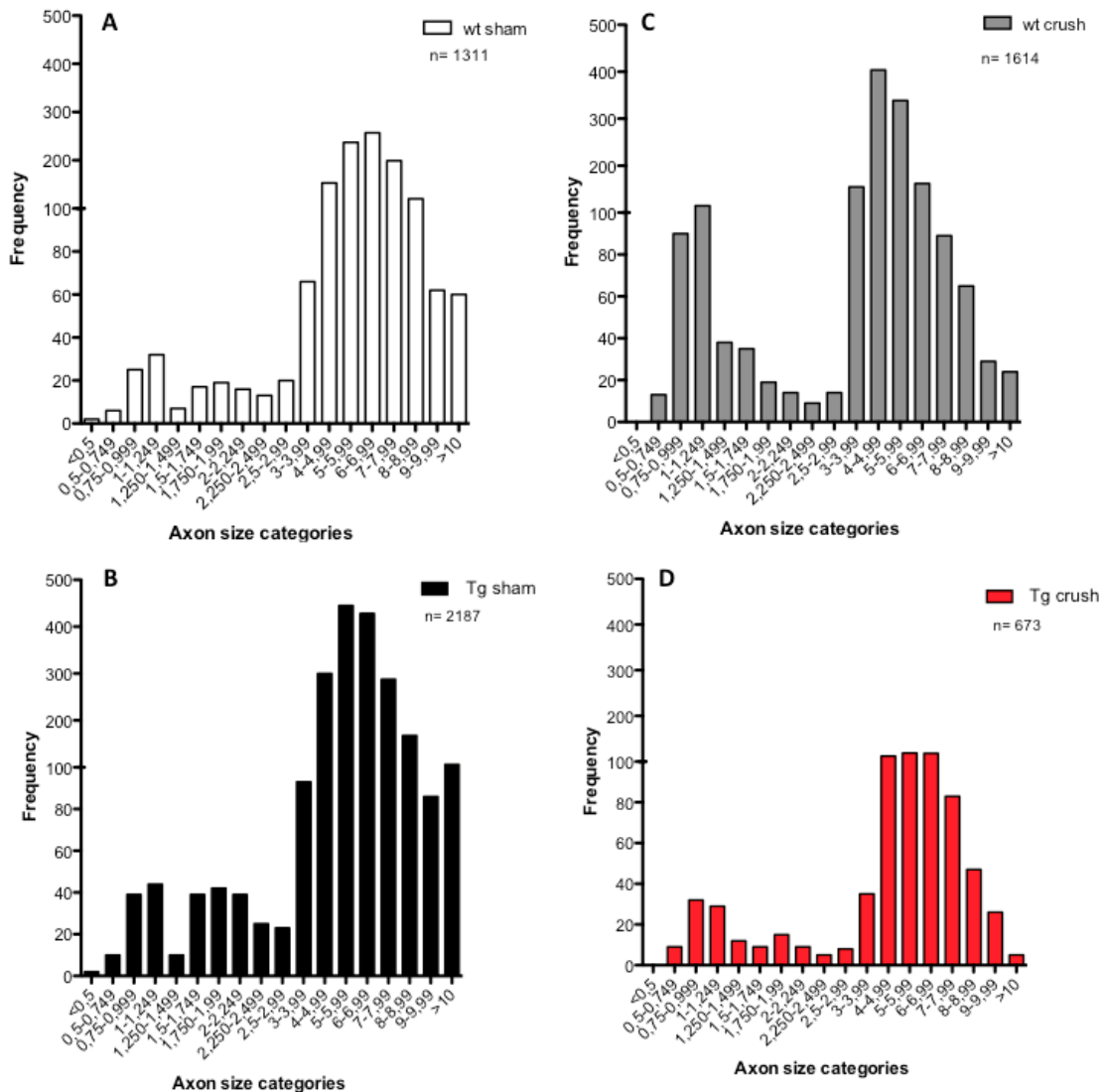


Figure 38. Axon size diameter frequency to each animal group: genotype and intact (A) & (B) /injured (C) & (D) nerves. The frequency was adapted to a normal distribution. (0.75-2.25 μm range, statistically significance of *** $p < 0.001$ between sham P0TNFalpha animals compared to wild types. *** $p < 0.001$ compared injured transgenic animals to wild type intact animals).

These morphometric studies demonstrated that P0TNFalpha animals, both intact and injured, contain a significant thinner myelin sheath than wild type animals (Fig39.). As expected, both genotypes at 21dpl displayed a significant reduction of myelin thickness.

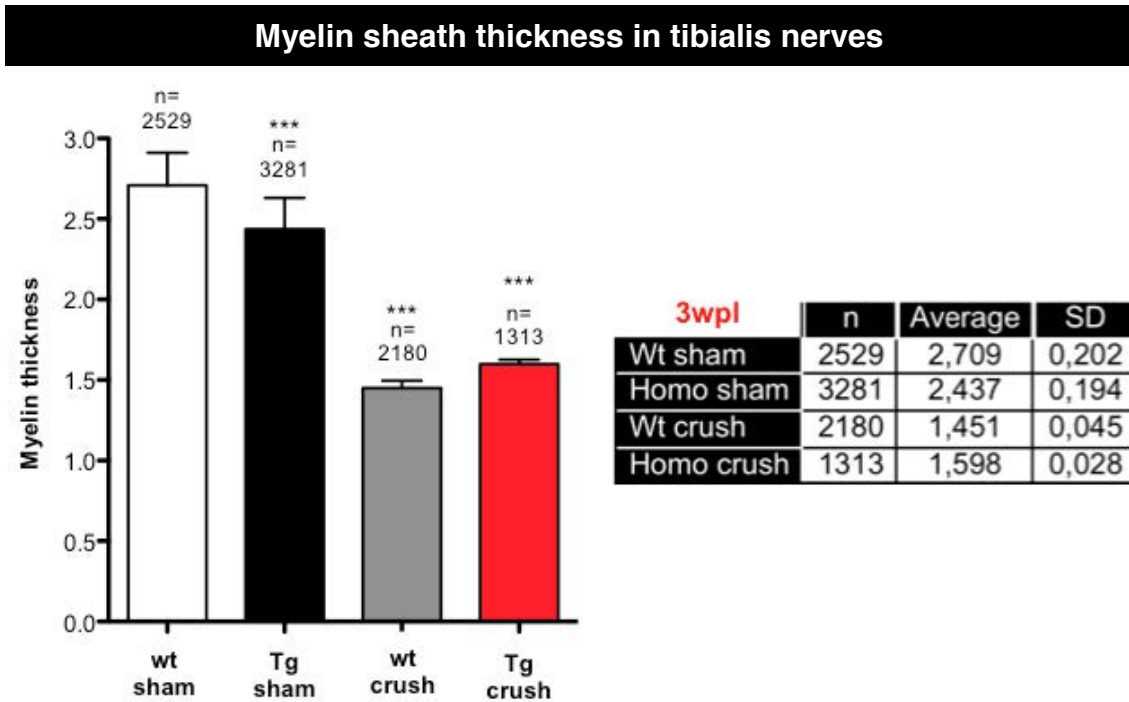


Figure 39. Myelin sheaths thickness average to each experimental group.

If each group data were individually analyzed to focus on the myelin sheath thickness range frequency, the normal distribution generated from transgenic control animals shifted to the left side of x axes as for axon size, demonstrating that myelin sheaths thicknesses were lower than wild types (**Fig40.**). This bias is more notorious after crush (**Fig40.B.&D.**), especially if they are compared to wild type mice.

When we quantified axons from the same size range, myelin thickness frequency suggested a clear myelin sheath reduction in the transgenic model, which was maintained after nerve injury (**Fig39.**). Particularly from 1 to 4 μm thickness (**Fig40.**), the differences between genotypes were more evident; while from 4 μm to biggest axons, the ratio of thickness were maintained between genotypes and surgery.

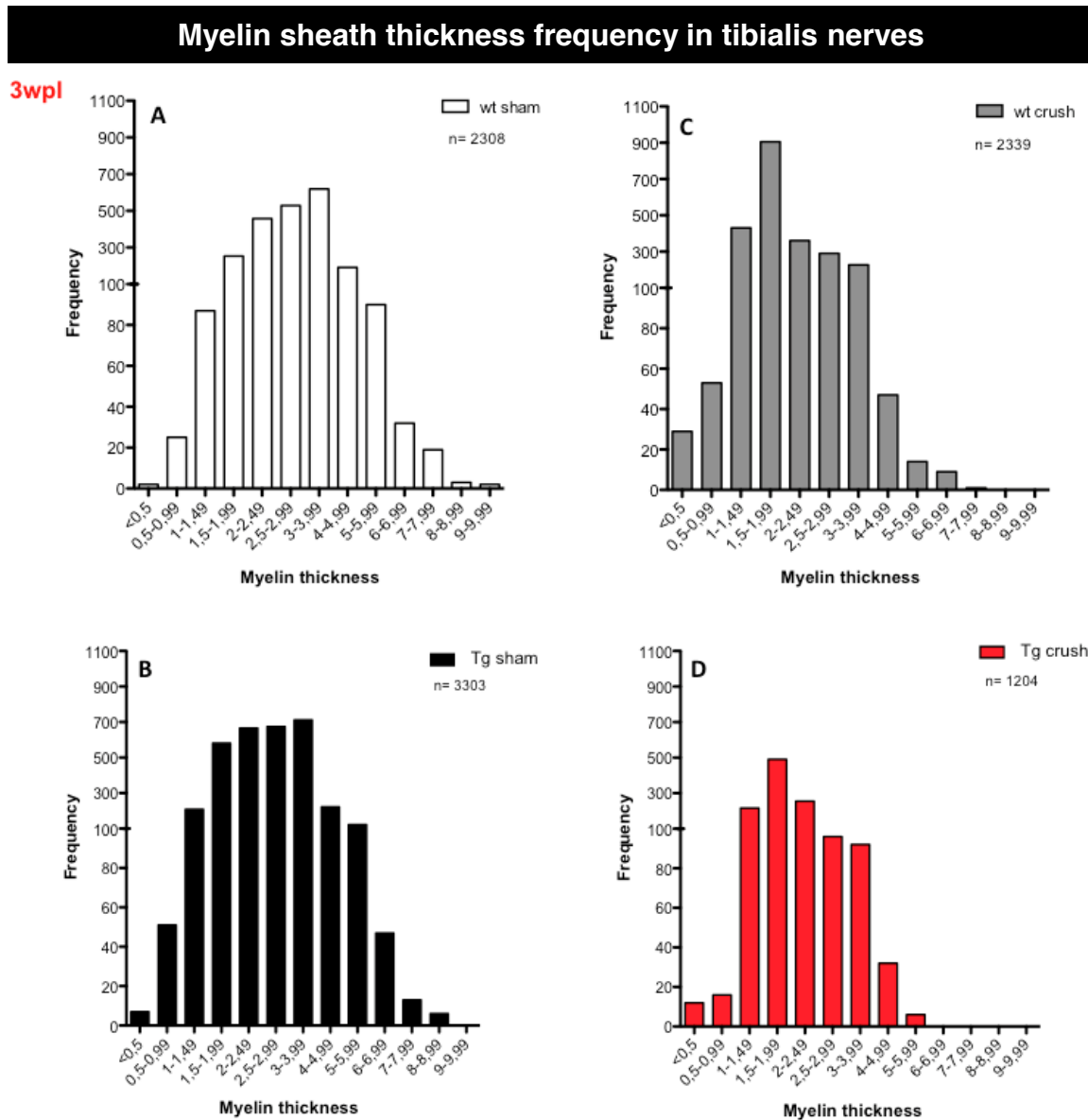


Figure 40. Myelin thickness range frequency to each animal group: genotype and injury surgery. The frequency was adapted to a normal distribution.

The dramatic reduction in myelin proteins of transgenic animals after crush, was more evident focused on axons sizes from 8 μ m. Uninjured P0TNFalpha animals or wild type animals showed myelinated bigger axons than injured transgenic mice (Fig40).

Thus, we demonstrated that myelin thickness range frequencies achieved by transgenic animals after crush are lower than for other groups, mainly for biggest axons, being obtained similar results by g-ratio calculation.

Results from myelin thickness were corroborated by g ratio calculation. The g ratio index is widely used as a functional and structural parameter to determine an optimal axonal myelination. G-ratio values have a negative correlation with myelin thickness. Usually, the theoretic estimated value of the optimal g-ratio to reached rapid nerve conduction in rodents is 0.6 (Rushton, 1951).

In both cases, the g-ratio value is equivalent between different groups of animals and conditions (Fig41.). Wild type sham mice achieved standard values, near to 0.6, while the transgenic model has more axons with higher g-ratio than wild type, confirming the lower myelin thickness of these transgenic fibers. Moreover, if we considered only axons for the same size range, the g-ratio values achieved by P0TNFalpha animals are higher.

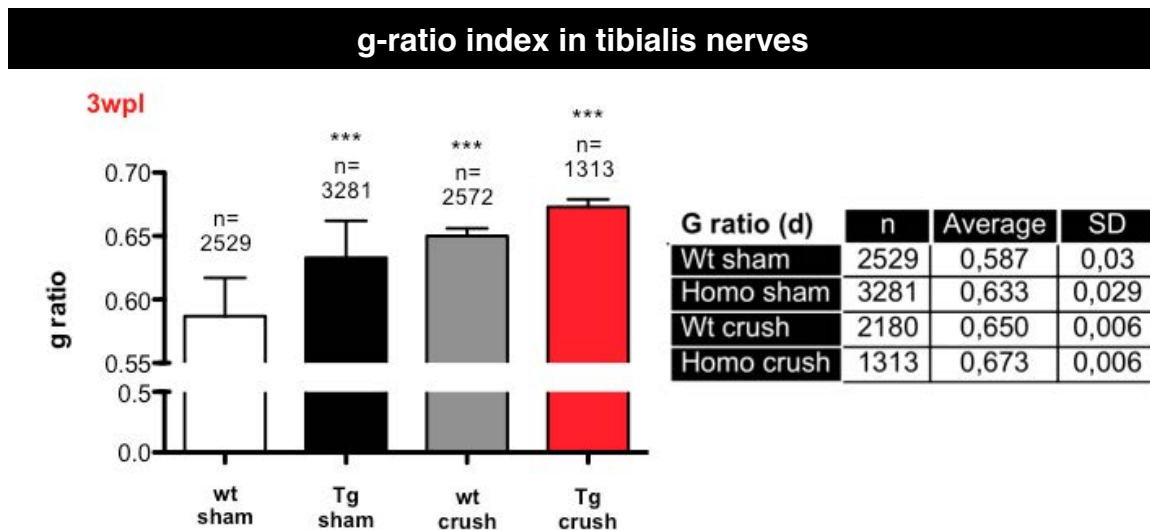


Figure 41. g-ratio average calculation to each animal group analyzed

Transgenic sciatic nerves at 21dpl showed an impairment in the remyelination process, although wild type nerves ones are also poorly myelinated than intact nerves. After crush, wild type animals have similar g-ratios than intact transgenic mice (Fig41.). As expected, when P0TNFalpha animals were injured the most abundant interval of g-ratio ranged from 0.6 to 0.7; corresponding also to thinner myelin thickness, confirming that the transgenic model had thinner axons than wild type (Fig42.).

Indeed, it is clear that injured P0TNFalpha model has smaller axons than sham or wild type animals after crush. However, the axonal diameter was maintained in wild type animals, although g-ratio increased and myelin thickness diminished, after injury (Fig42.)

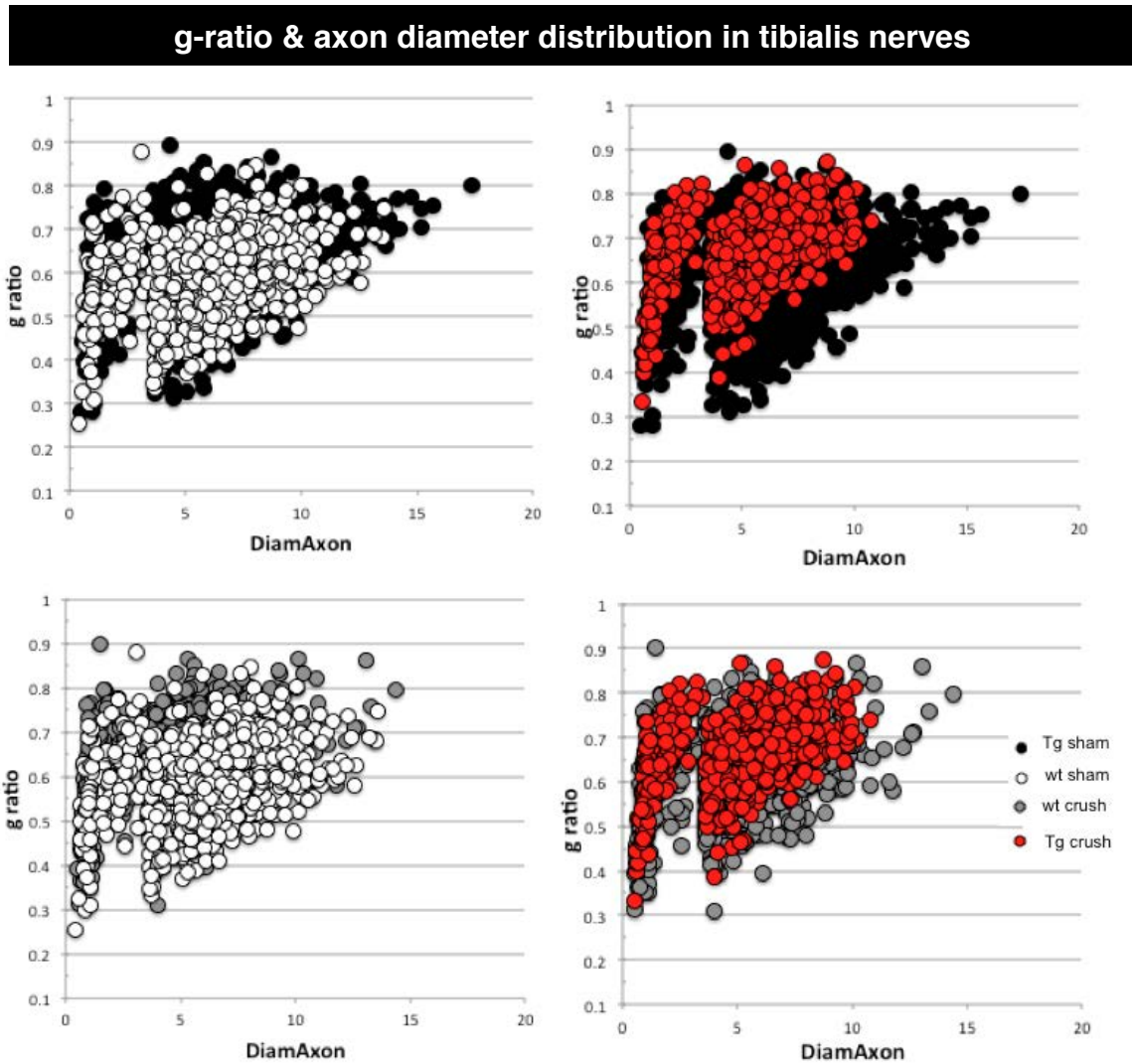


Figure 42. Distribution of axonal diameter according to g-ratio values, comparing the animal groups between them by superposition.

Although total nerve surface are maintained between genotypes and injury, clearly wild type exhibit bigger axons than other experimental groups. Transgenic mice show a slight reduction in the nerve diameter and the smallest axons and thinnest myelin are the more common axons. Moreover, P0TNFalpha mice, intact and injured, show a significant thinner myelin sheath than wild types, and thus higher g-ratio values.

5. Phenotype of SCs in P0TNFalpha mice

In the process of WD and regeneration of PNS, SCs dedifferentiate and proliferate having specific cell markers of immature cells.

5.1 Immature SCs: p75NTR detection

Thus, SCs in developing and regenerating peripheral nerves also express elevated levels of the p75NTR receptor as neurotrophins are key mediators of PNS myelination. Moreover, myelin formation and/or remyelination is inhibited in the absence of functional p75NTR. As a consequence, p75NTR expression can be used as a marker for immature or non myelinating SCs (Cosgaya, 2002).

In wild type animals, injury led to decrease p75NTR mRNA (Fig43.), suggesting that SCs of wild type animals at 21dpi dedifferentiated and have started the regenerative process. These wild type SCs are in a pro-myelination phenotype both in proximal and distal segments.

On the other hand, transgenic animals do not show lower p75NTR mRNA in the proximal segment (only in distal stump) (Fig43.), which result combined with decrease in myelin protein expression and reduction in the myelinating transcription factor Egr2, indicative of an immature phenotype of SCs, typical of WD (Fig43.).

The p75NTR expression was analyzed accurately at short time after crush (data not shown). The lower p75NTR expression detected in wild type sciatic nerves at 21dpi (Fig43.) seems to decrease immediately after crush, while injured P0TNFalpha animals do not show changes versus sham animals at early times after crush, again reinforcing the evidence of a delayed regeneration.

Both, p75NTR and S100 (Fig44., 45. &46.), a marker of myelinated and non-myelinated SCs, were also analysed in sciatic nerves by immunohistochemistry, showing that total number of SCs in transgenic animals are maintained compared to wild type, although most of these SCs are in an immature or non-myelinating state.

P75NTR mRNA quantification in injured sciatic nerves

3wpl

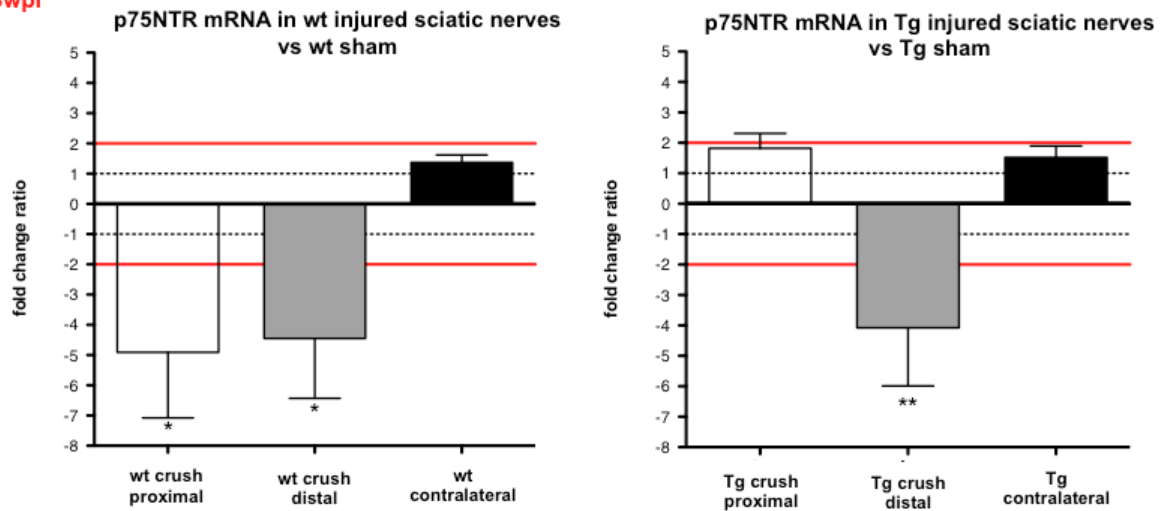


Figure 43. p75NTR expression in wild type and P0TNFalpha animals 21dpl. Injured wild type animals compared to intact nerves (* $p < 0.05$). Relative to P0TNFalpha mice, lower expression levels of TNFalpha, Egr2, myelin protein and p75NTR, were observed in distal section from injured P0TNFalpha mice compared to contralateral nerves or uninjured transgenic animals (** $p < 0,01$).

In transgenic animals immunofluorescence for p75NTR (Fig44.) perfectly correlated with mRNA data, indicating a high number of immature SCs, particularly in the proximal section. In wild type animals, the proximal section contains fewer immature SCs, thus this results is indicative of faster regeneration process in these mice (Fig44.).

Total number of SC was evaluated by S100 immunofluorescence after injury, correlating with p75NTR. The reduction in the total number of SCs could explain the decreased MBP expression in transgenic animals (Fig45.&46.). While wild type animals seemed to recovery most SCs at 21 dpl in both proximal and distal segments; transgenic animals exhibited a dramatic reduction in the proximal segment at 14dpl, which is almost recovered at 21dpl.

However, in the distal segment the number of S100 positive SCs was reduced at 21dpl, indicating a delay in the proliferation of SCs (Fig. 46)

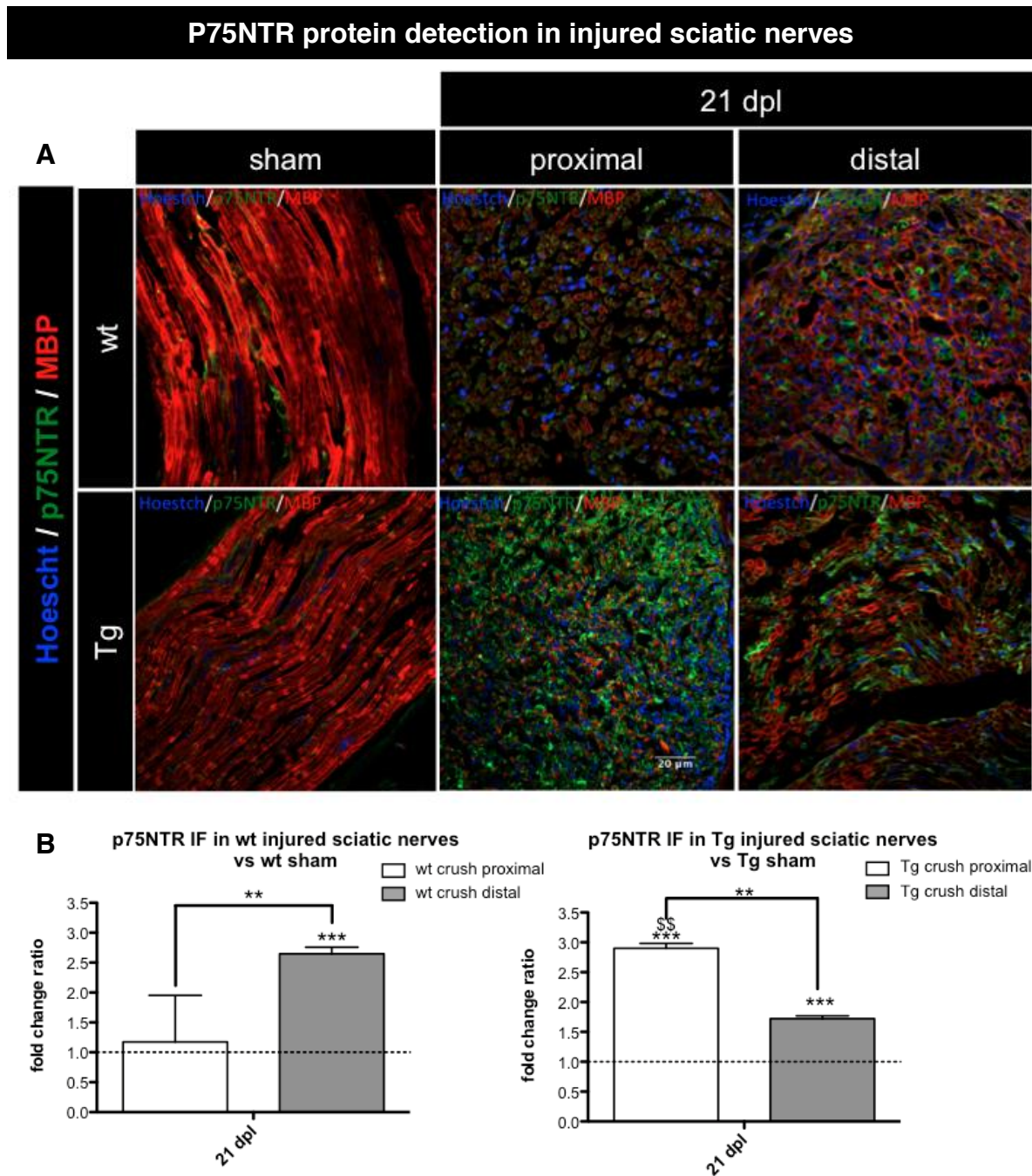


Figure 44. (A) p75NTR expression in intact longitudinal slices of sciatic nerves, from wild type and P0TNFalpha animals sham animals and transversal sections of injured sciatic nerves at 21dpl. **(B)** Injured animals were compared to control intact animals to each genotype (*** $p < 0.001$) and wild type or transgenic injured animals were also compared proximal versus distal segments (** $p < 0.01$). Injured transgenic nerves were compared to injured wild type nerves (\$\$ $p < 0.01$ in the distal segment). ANOVA and Bonferroni post tests.

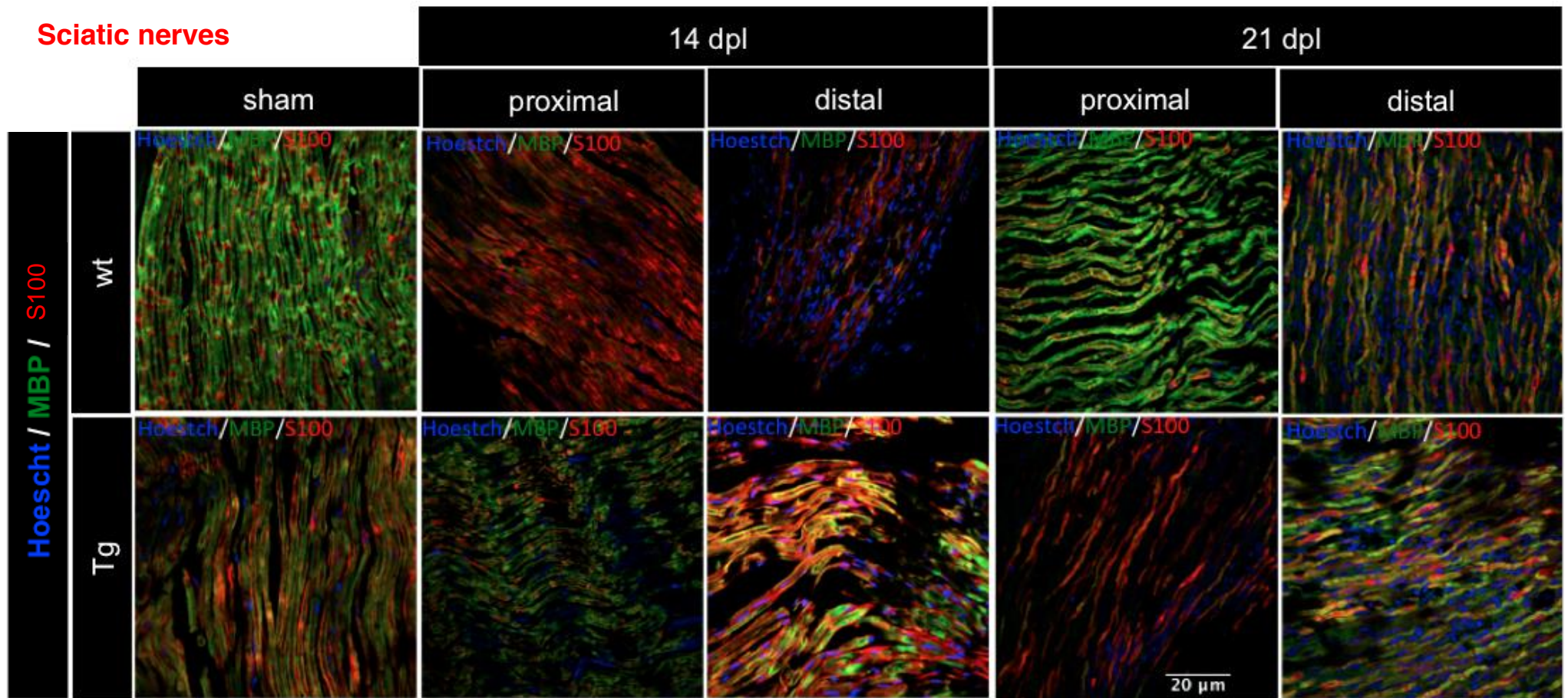


Figure 45. S100 expression in injured sciatic nerves of wild type and P0TNFalpha animals at 14dpl and 21dpl.

S100 protein detection in injured sciatic nerves

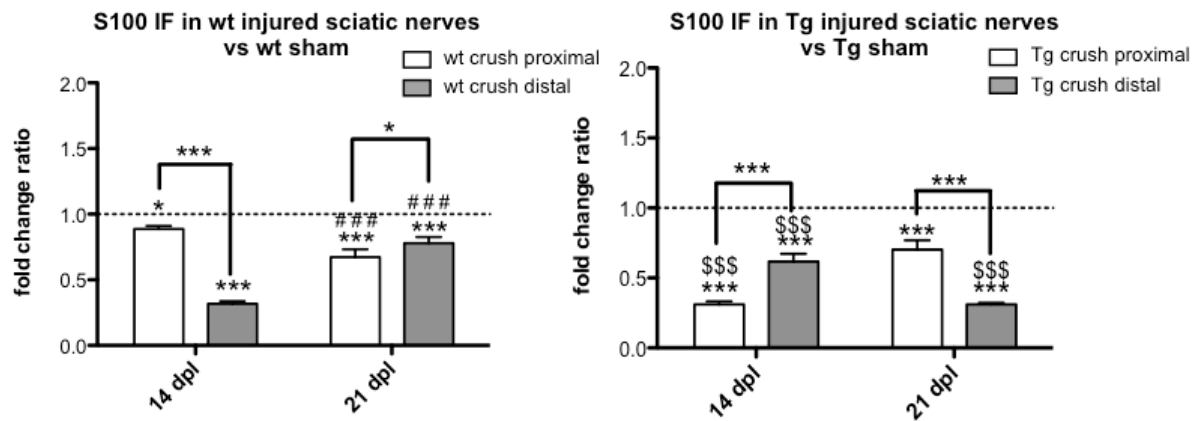


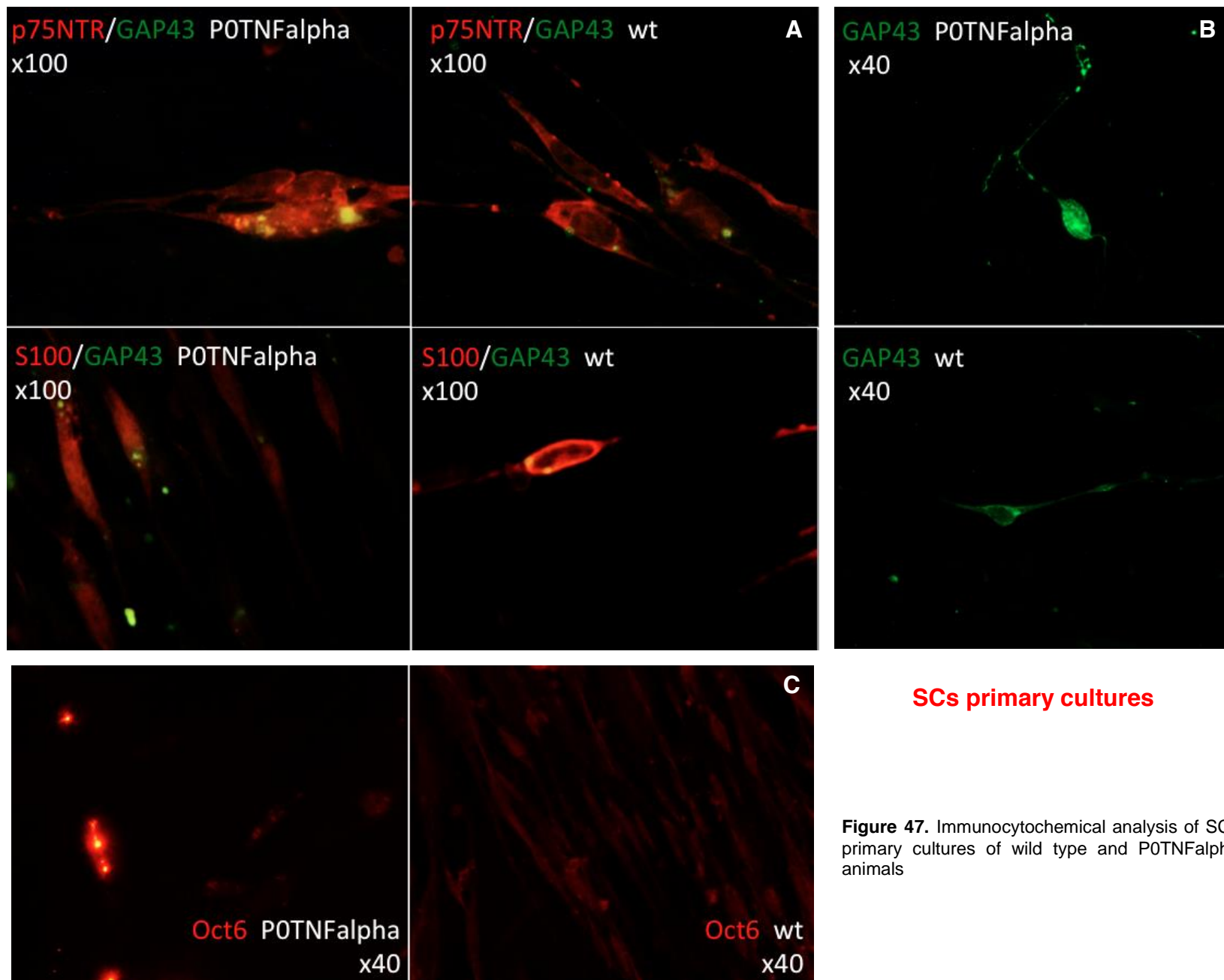
Figure 46. S100 expression in injured sciatic nerves of wild type and P0TNFalpha animals at 14dpl and 21dpl. Wild type and transgenic injured animals were compared to control intact nerves, wild type or transgenic, respectively (* $p < 0.05$, *** $p < 0.001$). Injured wild type animals at 21dpl were also compared to wild type injured nerves at 14 dpl (### $p < 0.001$). Injured transgenic animals were compared to wild type injured animals (\$\$\$ $p < 0.001$). ANOVA and Bonferroni post-test.

mRNA and IF protein results for p75NTR confirm that the wild type SCs at 21dpl are in a pro-myelination phenotype, both in proximal and distal segments, while transgenic SCs remain in an immature phenotype, typical of WD.

5.1.1 SCs primary cultures

For better elucidate the profile of transgenic SCs, we performed primary cultures of SCs from P05 sciatic nerves. Preliminary results from primary cultures of SCs show no significant differences in p75NTR immunofluorescence, between wild type or P0TNFalpha primary cells, although we observed a small tendency to increase p75NTR in transgenic cells (Fig47.A). Moreover, a small tendency to decrease the S100 detection was also observed in transgenic primary SCs (Fig47.A). In addition, Oct6, a transcription factor necessary to induce the myelin expression in SCs show a different pattern of expression among primary SCs cultures in both genotypes. Although it is not expected Oct6 in primary cultures of SCs due to the lack of myelination factors in the media, as well was observed in wild type cultures (Fig47.C); Oct6 immunofluorescence signal was detected, several times in several experiments, in nucleos of P0TNFalpha primary SCs (Fig47.c). Probably, as Egr2 is necessary to express transgenic TNFalpha, and Oct6 is necessary to express also Egr2, the unexpected detection of Oct6 in transgenic SCs is a consequence of a positive loop of expression.

Preliminary results from primary cultures of SCs show no significant differences in p75NTR immunofluorescence, between wild type or P0TNFalpha primary cells, although we observed a small tendency to increase p75NTR in transgenic cells, related to a more immature phenotype than wild type cells.



SCs primary cultures

Figure 47. Immunocytochemical analysis of SCs primary cultures of wild type and POTNFalpha animals

6. Macrophages & inflammation in P0TNFalpha mice

6.1 Chemoattractive environment: CCL2 detection

CCL2 is a secreted cytokine involved in immunoregulatory and inflammatory processes. This cytokine displays a chemotactic activity and it has been implicated, together with both its receptor CCR2, in nerve macrophage infiltration and as mediator of macrophage-related neural damage and demyelination in many diseases (MS or ALS and also in inherited demyelinated neuropathies, CMT1A and 1B) In addition, it is a therapeutic target linking adipose tissue inflammation, obesity and DM type 2 (Guilherme, 2008; Ota, 2013; Agrawal, 2014).

The upregulation of CCL2 during neuropathologic or neuroinflammatory conditions, leads to recruitment of activated monocytes that are differentiated into macrophages producing inflammatory molecules and, through the PIK3 cascade pathway and MEK and ERK1/2 activation, it usually causes apoptosis and axon damage. In DRG of P0TNFalpha mice we found a significant CCL2 mRNA upregulation coincident with the peak of TNFalpha expression. However, no changes were detected in CNS-spinal cord (Fig48.)

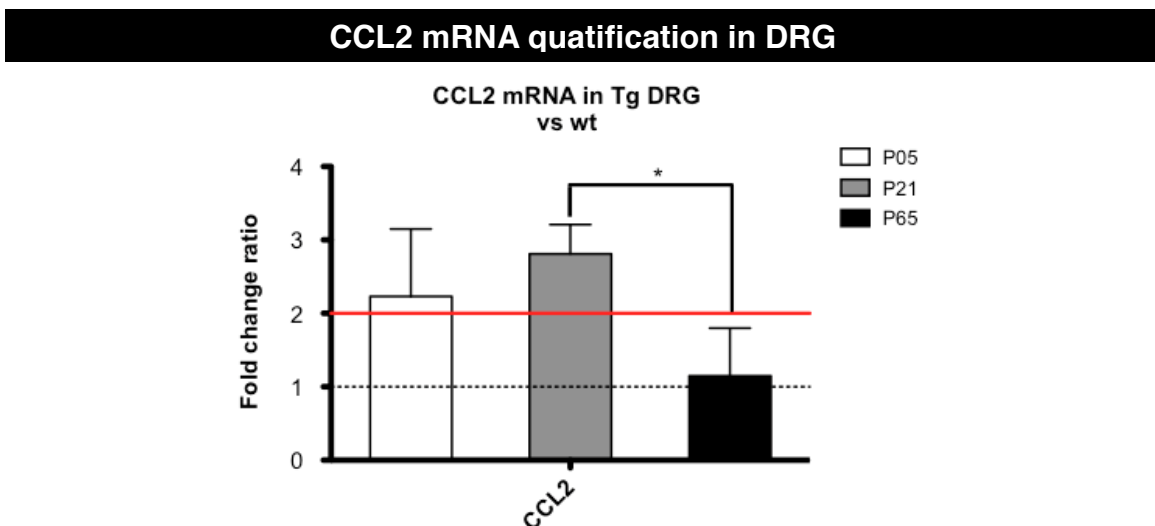


Figure 48. CCL2 expression in DRG of P0TNFalpha animals intact animals (* $p < 0,05$ at P05 versus wild type and ** $p < 0,01$ at P21; but not at P65 old animals). ANOVA and Bonferroni post-test.

In DRG of P0TNFalpha mice we found a significant CCL2 mRNA up regulation coincident with the peak of TNFalpha expression. However, no changes were detected in CNS-spinal cord. Sciatic nerves were not analysed.

6.2 Macrophages markers: Iba1 & GFAP detection

6.2.1 Detection in peripheral nerves

In agreement with the increased expression of monocyte chemoattractant protein CCL2 (Fig48.) we also detected an increase in Iba1, a specific marker for microglia/macrophage in tibialis (Fig49.A&B), and sciatic nerves (Fig49.D). We found an age-dependent decreased of Iba1 in P0TNFalpha animals, while Iba1 positive cells were not detected in wild type animals. We also observed a direct correlation with TNFalpha at these ages.

In the spinal cord only small variations in Iba1 and p75NTR were observed in P0TNFalpha mice versus wild type. While, no changes were observed for GFAP a marker for astrocyte activation (Fig53. & 54.).

Longitudinal slices from tibialis and sciatic nerves after crush surgery were also analyzed at 21dpl (Fig50.A.&C.). The results showed a clear increase in Iba1 immunofluorescence (about 70%) which indicates a higher infiltration of macrophage and microglia in PNS of P0TNFalpha mice after crush.

This is also consistent with a delay in the regeneration process of transgenic mice, as it was detected by SFI, morphological studies, hystological and mRNA and protein molecular analysis.

Iba1 positive cells were not detected in wild type animals. However, the increase detection of the infiltration of Iba1 positive cells in peripheral nerves, with and without injury, but not in spinal cord, are consistent with a delay in the regeneration process of transgenic mice, as it was detected by SFI, morphological studies, histology and mRNA and protein molecular analysis.

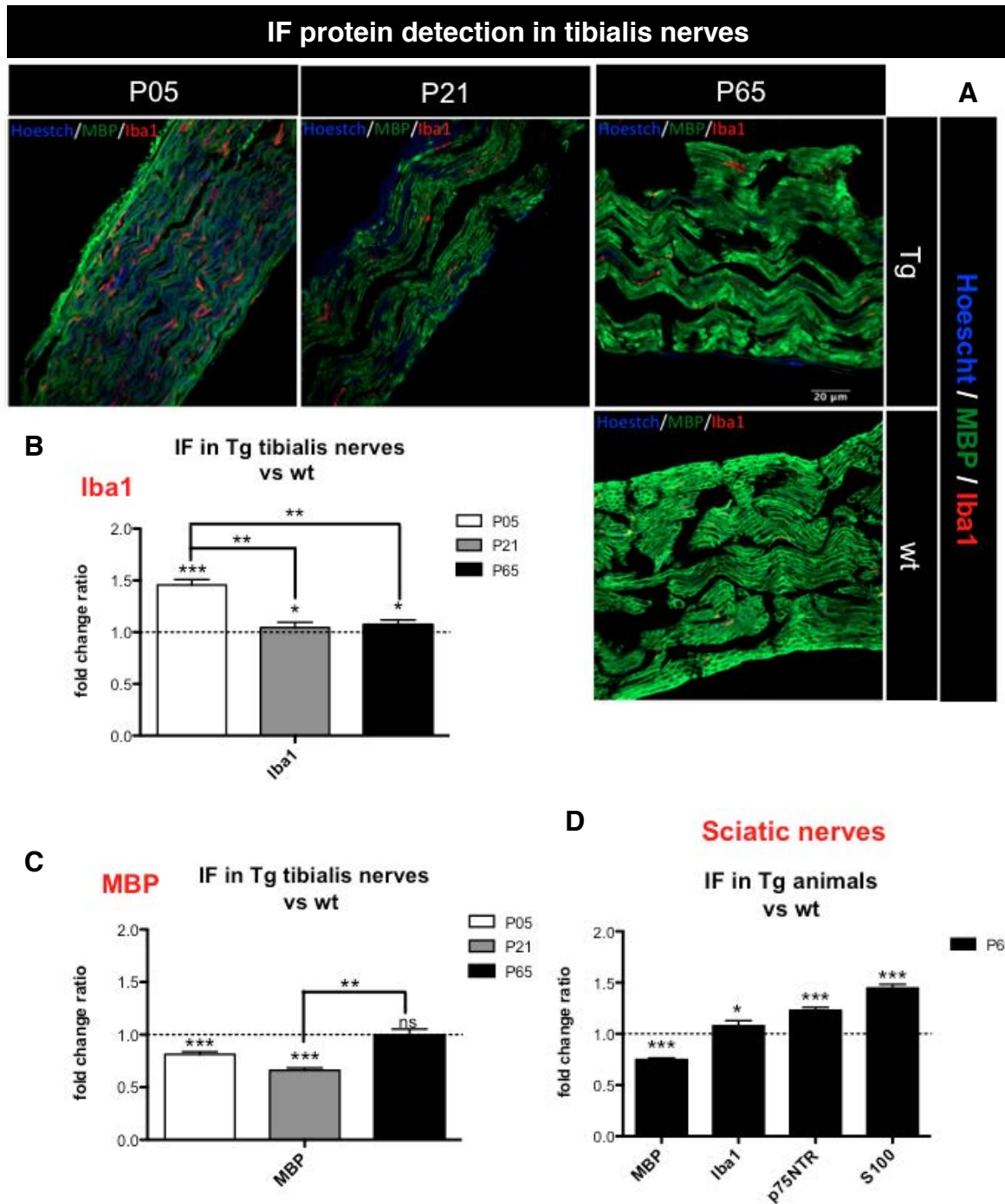


Figure 49. Immunofluorescence detection in peripheral nerves: tibialis **(A)** **(B)** and **(C)** and sciatic **(D)** for specific markers of activated macrophages (Iba1), PNS myelin protein (MBP), SCs (S100) and immature SCs (p75NTR). **(B)** Higher detection levels at P05 (about 45%) than at P21 (around 15%), and at P21 higher than at P65 (5%). Wild type control at P65 showed 1% of Iba1 positive cells. (* $p < 0.05$, ** $p < 0.01$ and *** $p < 0.001$ ANOVA and Bonferroni post test).

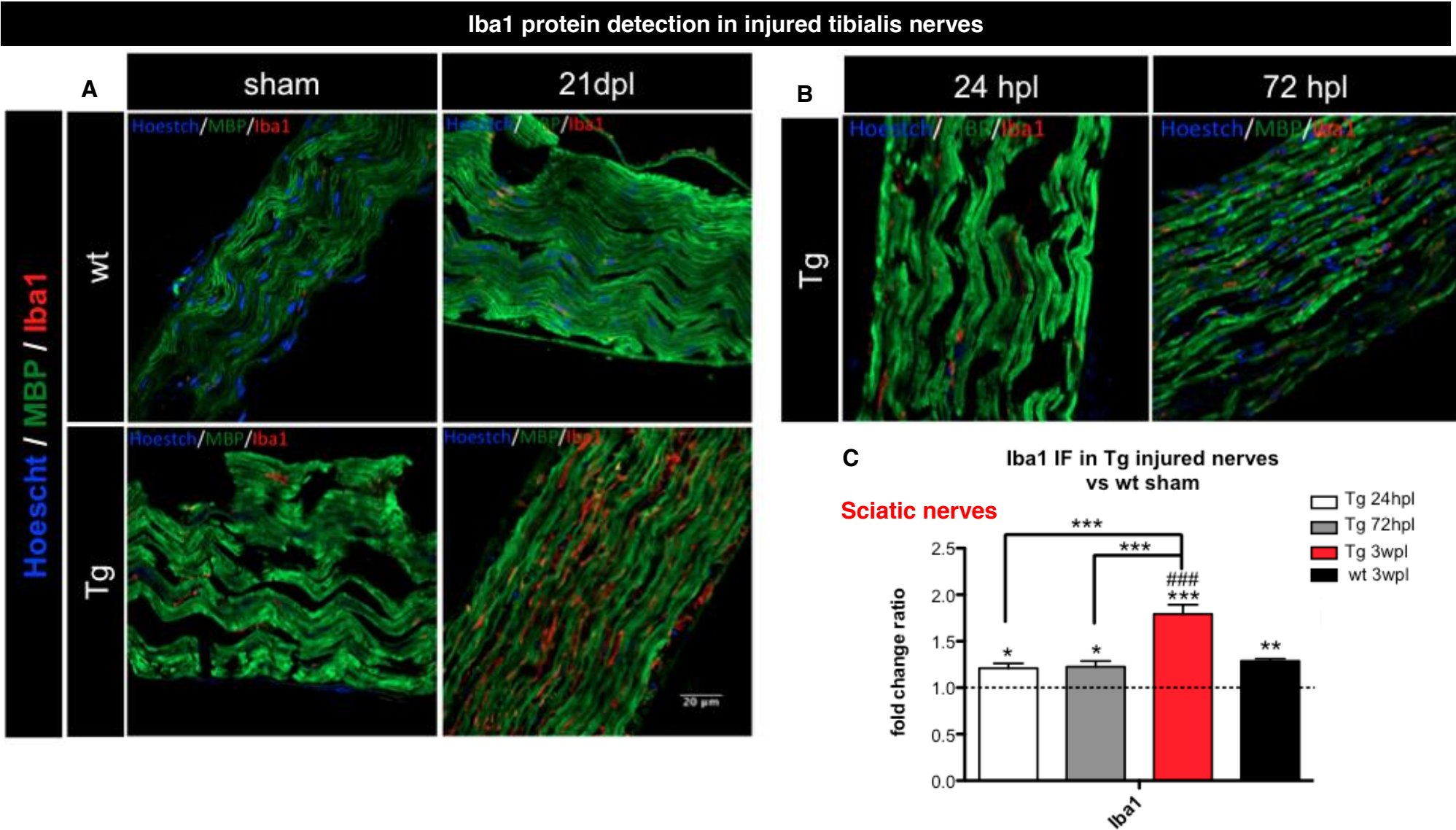


Figure 50. Immunofluorescence detection in peripheral nerves: tibialis nerves at 21dpl (**A**), tibialis nerves at 24hpl and 72hpl (**B**) and quantification of injured sciatic nerve at shorter times after crush (**C**) for specific markers of activated macrophages (Iba1), PNS myelin protein (MBP), ### p<0,001 Transgenic mice compared to wild type crushed animals and homozygous sham. * p<0.05, ** p<0.01 and *** p<0.001 compared to homozygous sham animals, about 20-fold change).

6.2.2 Short-time study of macrophage infiltration

In order to better analyse the regeneration process and the possible early infiltration of macrophages, Iba1 was studied in tibialis nerves of transgenic animals at acute phases after crush: 24hpl and 72hpl (Fig50.B.&C.). The results showed that infiltration starts at 24 hpl and it is maintained to 3dpl (about 20fold change). This infiltration is still very active at 21dpl.

Similar results were obtained in the distal section of sciatic nerves, and tibialis, at 21dpl although overexpression of Iba1 is also evident at 14dpl, similar in both transgenic sciatic segments (Fig51.).

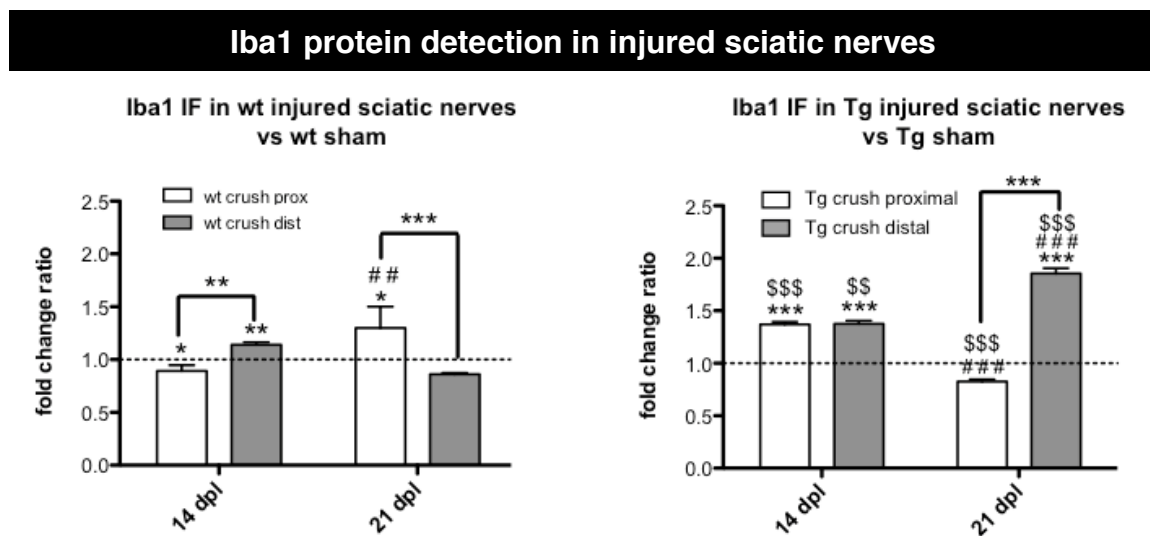


Figure 51. Immunofluorescence detection (related to Fig.22.) and quantification of Iba1 immunofluorescence markers in sciatic nerves of wild type and P0TNFalpha animals. (*p<0.05, **p<0.01 and *** p<0,001 compare to transgenic/wild type sham control animals; ### p<0,001 compared to animals at 14dpl, and \$\$\$ p<0.001 compare to wild type animals)

The infiltration of macrophages in transgenic sciatic nerves start at 24hpl and it is maintained to 3dpl. This infiltration is still very active at 21dpl.

6.2.3 Detection in spinal cord

Iba1 immunofluorescence was also checked in spinal cords (Fig52.&53.). Wild type animals showed Iba1 immunofluorescence overexpression in the lumbar region of the spinal cord at 14dpl, innervating the sciatic nerve. Normal levels are almost restored one week later. On the other hand no Iba1 was detected in the thoracic segments of the spinal cord (Fig52.).

On the other hand, transgenic animals exhibited increased immunofluorescence for the microglial marker at 14dpl, without any differences between lumbar or thoracic regions. In addition, the levels increased at 21 dpl in both regions (Fig52.&53..)

Similar to Iba1, GFAP immunofluorescence detection, was not increased in wild type animals after peripheral injury. Nevertheless, P0TNFalpha model clearly show higher GFAP levels at 21dpl in the spinal cord than uninjured animals (Fig52. & 53.) .

Some studies hypothesize that glial cells may also play a role in the pathogenesis of pain, due to the secretion of several cytokines that induce pain hypersensitivity (Meller et al., 1994; Fu et al., 1999; Sweitzer et al., 1999; DeLeo and Yeziarski, 2001; Winkelstein et al., 2001; Watkins et al., 2001a,b; Ji et al., 2002b Mantyh et al., 2002). In this case both, microglia and astrocytes (Fig52.&53.), were activated in the spinal cord after inflammation and nerve injury. The signalling pathway implicated in the activation of these events is the MAPKs-ERK-p38-JNK. p38 and its active form phospo-p38, are usually activated in DRG nociceptor neurons by peripheral inflammation and participate in the maintenance of inflammatory hyperalgesia (Jin, 2003).

Both, microglial and astrocytes were activated in the spinal cord after inflammation and nerve injury

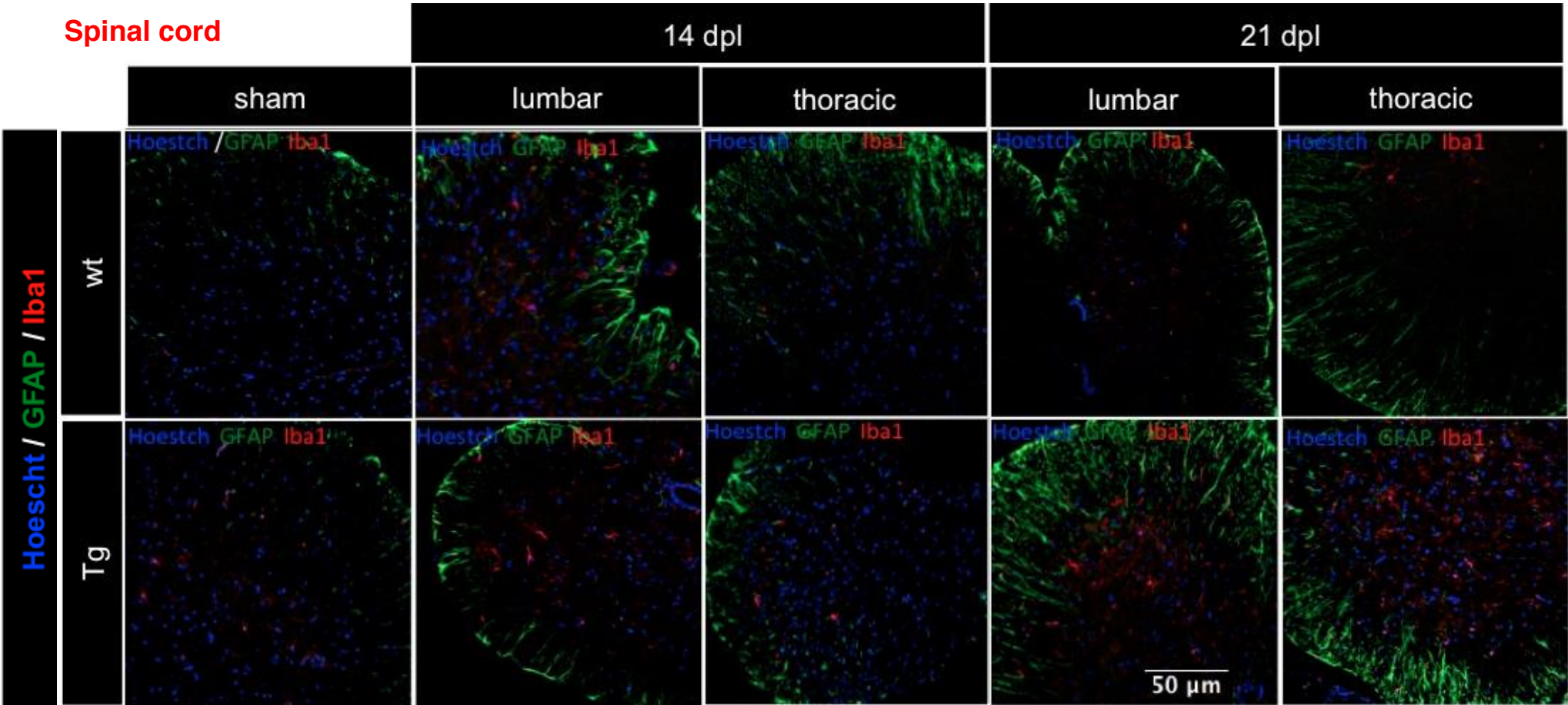


Figure 52. Immunofluorescence detection and quantification of GFAP and Iba1 immunofluorescence markers in spinal cord sections of wild type and P0TNFalpha animals at 14dpl and 21dpl. (Lumbar section=proximal, and thoracic section=distal).

Macrophage infiltration in spinal cord

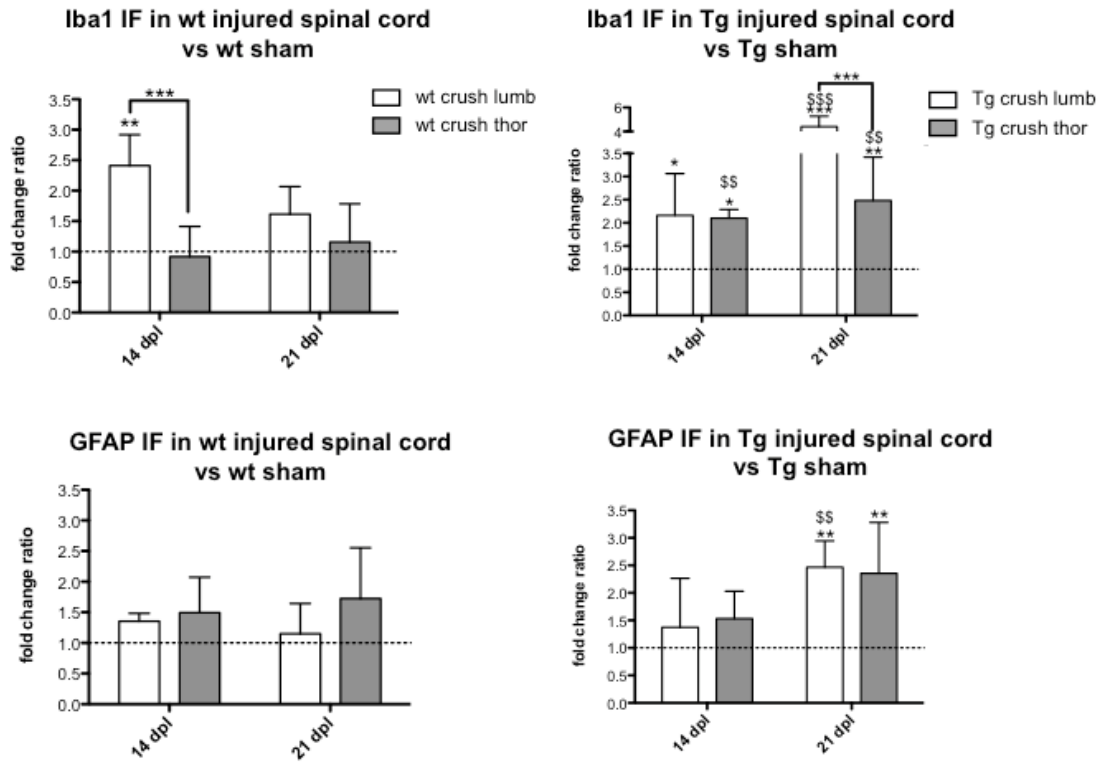


Figure 53. Immunofluorescence quantification of GFAP and Iba1 immunofluorescence markers in spinal cord sections of wild type and P0TNFalpha animals at 14dpi and 21dpi. (Lumbar section=proximal, and thoracic section=distal). * p<0.05, **p<0.001 and *** p<0.001 transgenic mice compared to sham wild type animals, and \$\$ p<0.01 and \$\$\$ p<0.001 if lumbar region is compared to thoracic distal section).

7. WD delay & pain initiation in P0TNFalpha mice

7.1 Molecular pathways

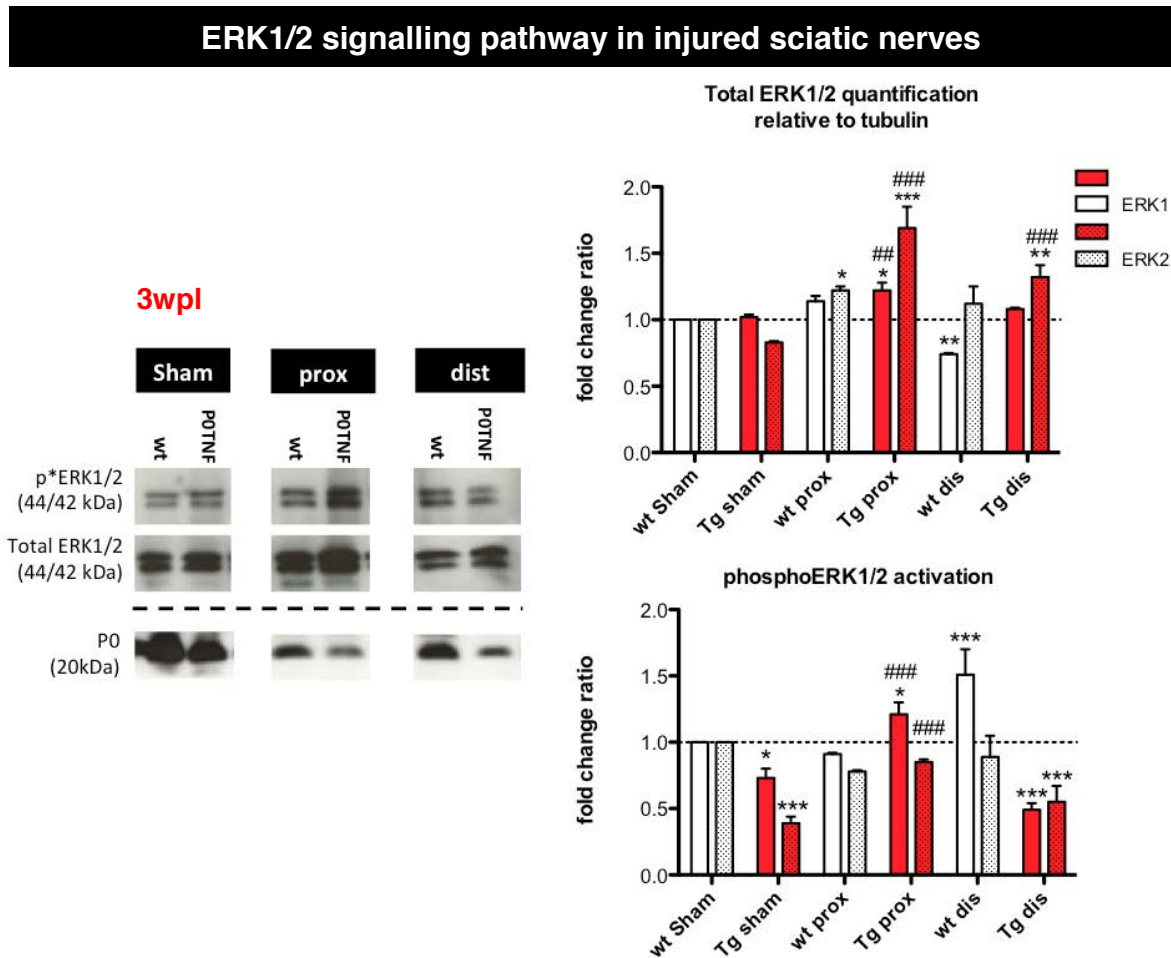


Figure 54. Western Blot detection of ERK1/2 activation in wild type and P0TNFalpha 3wpl (* $p < 0.05$, ** $p < 0.01$ and *** $p < 0.001$ compared to intact wild type nerves. ## $p < 0.01$ and ### $p < 0.001$ compared to intact transgenic nerves).

Although the ERK pathway is involved, as well as Akt pathway, in the regulation of myelin thickness and promoting myelination after damage, the increased activation of this pathway has negative effects. Thus, the inflammatory molecules produced by macrophages after injury, through the early ERK1/2 activation, cause apoptosis and axon damage. Moreover, the MAPKs-ERK-p38-JNK signalling pathway seems to be also implicated in the activation of microglia and astrocytes in the spinal cord after inflammation and nerve injury and participates in the maintenance of inflammatory heat hyperalgesia in DRG (Jin, 2003). Furthermore, through this pathway TNFalpha can directly modulate its own production (Song, 2003).

Uninjured P0TNFalpha animals did not show any differences in the activation of ERK1/2 (also called p42/44) (Fig54.). As was expected, after sciatic nerve injury there was observed a significant increase in ERK activation, according to the high number of macrophage and microglia infiltration in nerves and spinal cord. These results suggest and confirm axonal damage in transgenic mice, still evident at 3wpl while wild type animals were almost molecular and functionally recovered. A neuropathic pain states associated to a delayed remyelination and regeneration, will be expected in P0TNFalpha animals, at least after injury stress.

This pathway exhibits an overregulation after injury in transgenic animals, being the total levels of ERK1/2 higher than intact nerves. It is known that ERK1/2 also can exert functions without phosphorylation (Wortzel, 2011; Ishii, 2014, 2016). Moreover, the increased activation in injured P0TNFalpha mice is only significant in the proximal stump. Wild type mice show ERK1/2 overactivated in distal segment, versus intact nerves at 21dpl. Altogether these results suggested, again, the delayed regeneration in transgenic animals compared to wild types.

The ERK1/2 signalling pathway is up regulated after injury sciatic nerves of transgenic mice according to the high number of macrophage and microglia infiltrated. These results confirm axonal damage in transgenic mice and, the delay in regeneration compared to the ERK1/2 activation levels in wild type animals.

7.2 p75NTR & WD: spinal cord detection

Induction of p75NTR in spinal cord could be one of the first steps that initiate the apoptotic cascade after peripheral injury to eliminate damaged cells after activating the apoptotic machinery. Moreover, p75NTR immunofluorescence detection in P0TNFalpha animals at 14dpl and 21dpl (Fig55.) but not in wild type mice, could indicate regeneration responses by the injured system, possibly in collaboration with the Trk receptors. Nevertheless, these results could be also related to pain stages.

Moreover, TNFalpha overexpression peak correlated with the decreased of both, myelin genes and the main transcription factors implicated in the myelin process, as well as a high expression of CCL2 in DRG.

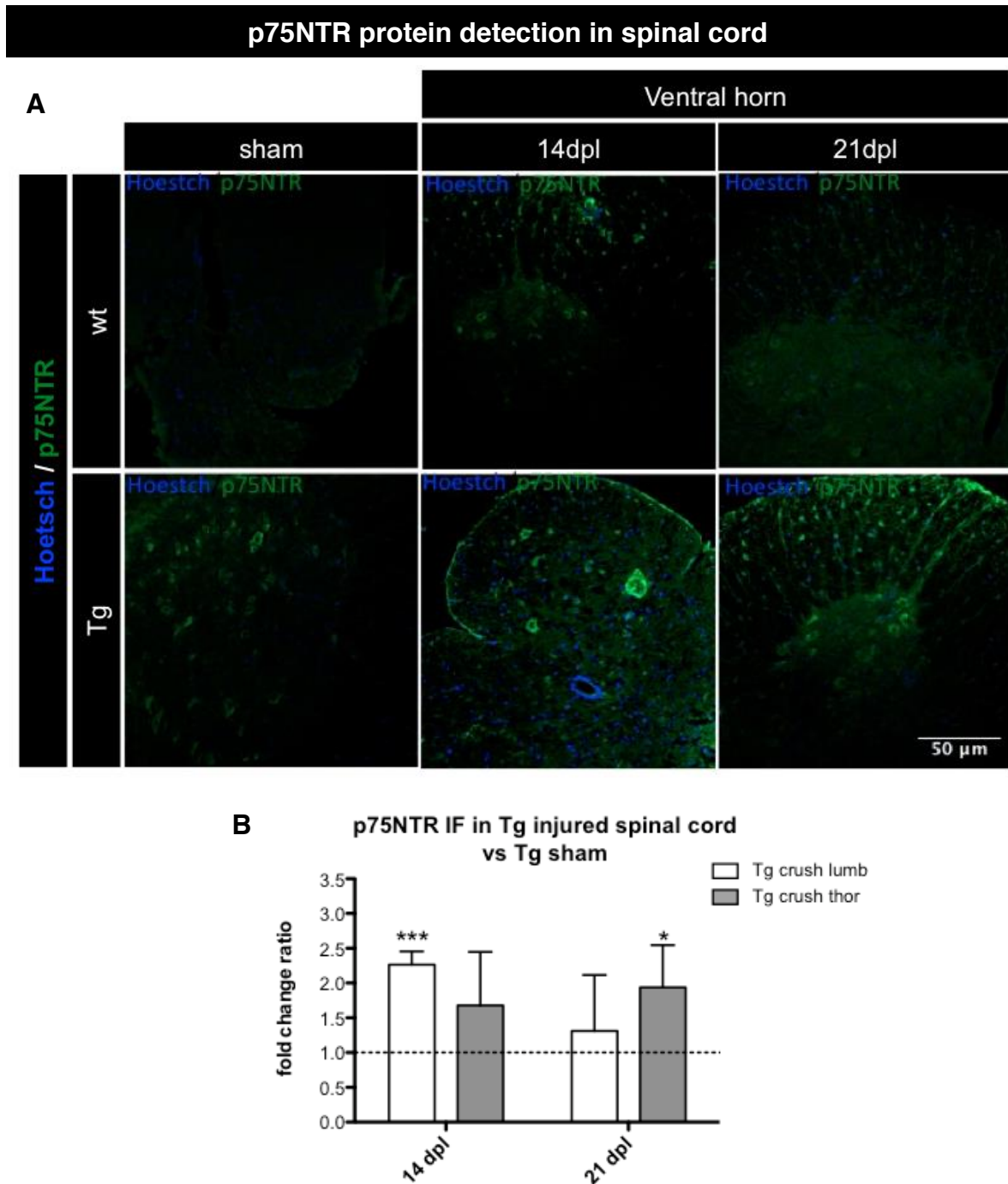


Figure 55. (A) Immunofluorescence detection and **(B)** quantification of p75NTR in spinal cord sections of wild type and POTNFalpha animals at 14 and 21 dpl. (* $p < 0.05$ and *** $p < 0.0101$ transgenic injured spinal cord compared to transgenic intact).

Moreover, p75NTR immunofluorescence detection in P0TNFalpha animals at 14dpl and 21dpl but not in wild type mice could indicate regeneration responses by the injured system, possibly in collaboration with the Trk receptors. Nevertheless, these results could be also related to pain stages.

7.3 Ion channels & pain: Nav1.7 & Nav1.8 detection

These results could point out at the neuroinflammation process leading to the neuropathic pain, in the transgenic mice. On the other hand, there are two peripheral nerve voltage-gated sodium channels: Nav1.7 and Nav1.8, that are expressed selectively in DRG neurons and have been suggested to play an essential role in regulating the excitability of nociceptive primary afferent neurons. We detected overexpression of both voltage-gated sodium channel in DRG of P0TNFalpha model at P65. The values remain unaltered in neonates and young P0TNFalpha mice (Fig56.).

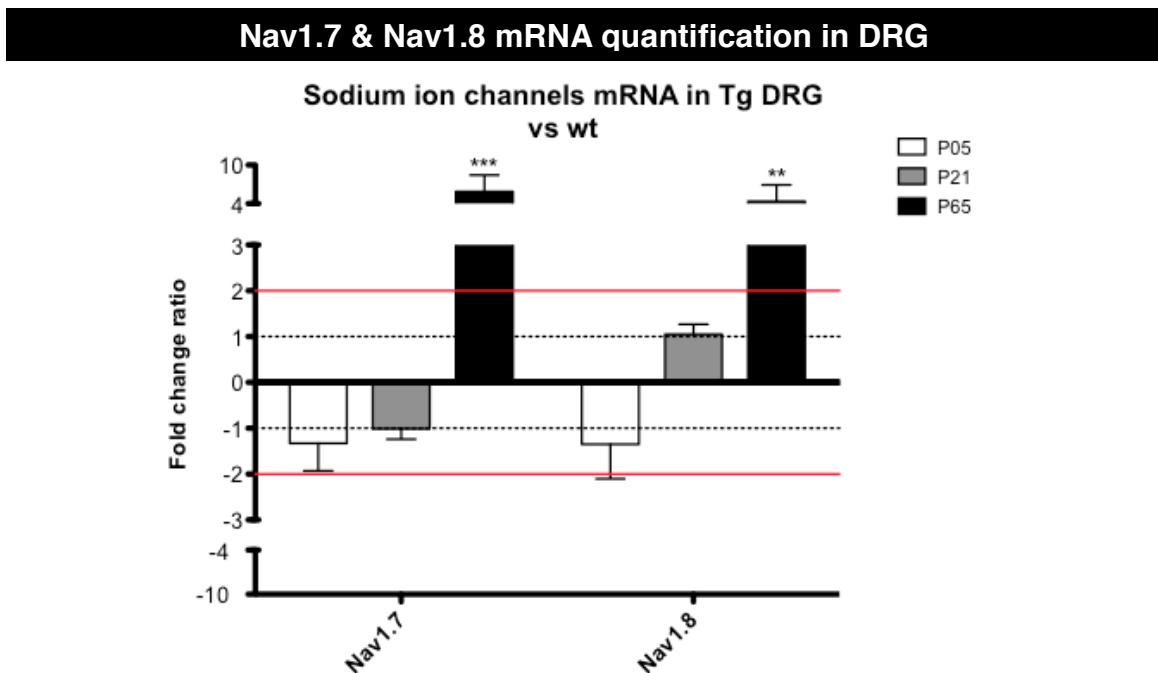


Figure 56. Nav1.7 and NAV1.8 ion channels detection by qPCR mRNA in P0TNFalpha animals at the three differentes ages of development, relative to the reference gene m36B4 and compared to wild type animals at the same ages. (***) $p < 0,001$ at Nav1.7 and ** $p < 0,01$ at Nav1.8 compared to wild types).

Increased correlation of Nav1.7 and Nav1.8 channels in DRG suggests, at least in part, their function in the maintenance of chronic inflammatory pain, several weeks after the initial insult, as the TNFalpha overexpression peaks at P05, being necessary a long-time expression of TNFalpha to induce a pain state.

7.4 Molecular factors related to injury

Other markers of PNS regeneration, also involved in myelin recovery but also in pain development are ATF3, BDNF or GAP43. In DRG and spinal cord of wild type animals we did not detect differences neither ATF3, BDNF nor GAP43 mRNA comparing intact and injured animals.

7.4.1 ATF3 detection

The activating transcription factor ATF3 is a general injury-inducible factor affected after injury and is used as a marker of neuronal and SCs injury. Although the level of ATF3 mRNA is undetectable in normal unstressed mice, it is greatly induced upon stimulation by physiological injury stress (Hai, 2006; Hai, 1999). In addition, ATF3 could be important to enhance peripheral nerve regeneration with the implication of neurons and non-neuronal cells in the spinal cord, DRGs and injured SCs (Smith, 1997). Moreover, it is suggested that ATF3 expression increases mitochondrial transport and protects demyelinated axons from oxidative damage (ROS and iNOS production) (Herdegen, 1991; Costigan, 2002; Raivich, 2004; Bontioti, 2006a; Pannucci, 2007; Seiffers, 2007; Kiryu-Seo, 2010; T.V. Damodaran, 2014).

P65 P0TNFalpha transgenic mice showed not changes in ATF3 expression in DRG compared to wild types, although the expression was significantly increased in spinal cord. Probably these results could indicate a pathological stress of the central level as a consequence of the activation of pathways related to oxidative damage pathways (Fig57.A).

Probably the ATF3 high expression in spinal cord of transgenic mice could indicate a pathological stress of the central level as a consequence of the activation of pathways related to oxidative damage pathways.

7.4.2 BDNF

However, we detected increased expression of BDNF in DRGs of transgenic animals, but not in spinal cord (Fig57.A). The brain-derived neurotrophic factor BDNF, as well as p75NTR, are upregulated in SCs and DRGs in WD, being necessary for the enhancement of myelination of regenerating axons after injury. This BDNF factor also contributes to neuropathic pain, and higher BDNF in DRG were related to thermal hyperalgesia and mechanical allodynia. BDNF is also synthesized by neurons, astrocytes, macrophages and microglia in the spinal cord; and maximum levels are reached in a more acute injury phase, between one and seven days after injury (Xin-Fu, 2000; Ikeda, 2001; Garraway,2016).

The high BDNF detected in DRG of transgenic animals may contribute to thermal and mechanical hypersensitivity.

7.4.3 GAP43

We did not observed changes in GAP43 expression in the transgenic animals (Fig.57.A). The growth-associated protein GAP43 is associated with neuronal development and plasticity. Peripheral nerve injury and the disconnection from peripheral target tissue, results in the increased synthesis of this factor in DRGs, coincident with the regenerative growth- cone. However, elevated GAP43 levels may contribute to an inappropriate reorganization that could play a role in sensory disorders that follow nerve injury (Woolf, 1990).

In SCs primary cultures, we detected GAP43 by immunofluorescence in the cytoplasm of both, P0TNFalpha and wild type cells (Fig47.A.&B.). Moreover, the detection was higher in transgenic cells than in wild types, probably associated to a phenotype of injury as a consequence of high levels of TNFalpha.

On the other hand (Fig57.B), ATF3 and GAP43 mRNA were significant increased significant in the ipsilateral intact DRG from transgenic injured animals. BDNF was maintained to non-injured levels.

Elevated GAP43 levels in P0TNFalpha mice may contribute to an inappropriate reorganization that could be implicated in sensory disorders that follow nerve injury.

7.4.4 Short-time study after peripheral injury

GAP43 and ATF3 are injury markers implicating ER and/or oxidative stress. We also analyzed them accurately at short timepoints trying to correlate early changes in the expression of these factors with an increase in the macrophage infiltration, as well as it was detected at 14dpl and 21dpl.

While GAP43 did not experience any changes in wild type animals, we confirmed increased levels in ipsilateral DRGs and spinal cord of transgenic animals, but in distal section we only detected a tendency. Again, altogether these results indicate a possible delay in the injury process.

On the other hand, we found a clear raise of ATF3 in both genotypes, particularly at 3dpl in the distal segment of wild type animals, indicative of injury (Fig57.D.). However, the expression was restored to normal values at 14dpl. P0TNFalpha animals, show a tendency to increase the values in sciatic nerve, indicative of tissue damage, but the delay in ATF3 expression in these animals is clear compared to wild type mice.

We confirmed the possible delay in WD in transgenic animals, contributing to a long-term injury state that could generate, finally, a pain phenotype in P0TNFalpha animals.

Injury related factors mRNA quantification

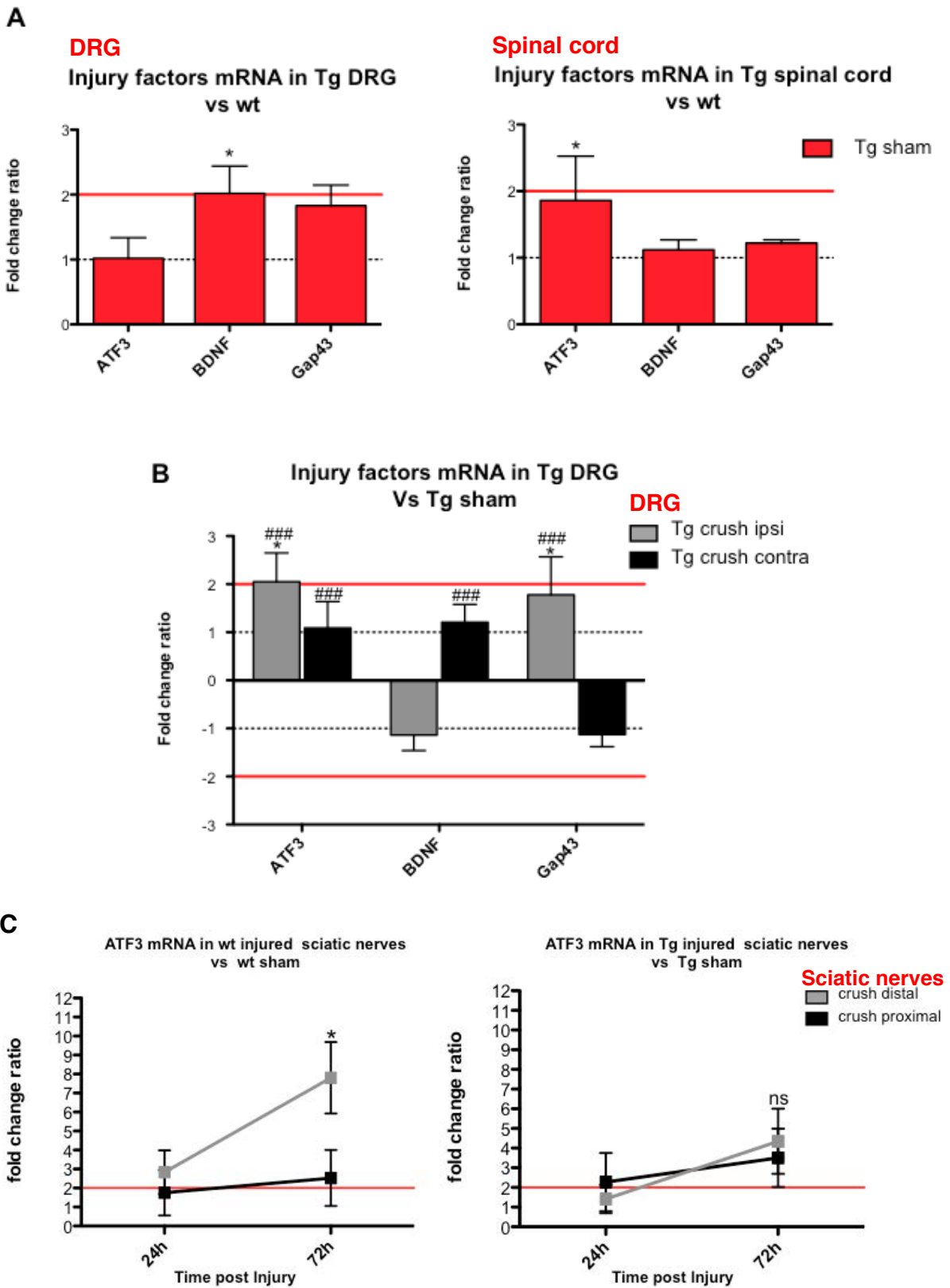


Figure 57. ATF3, BDNF and GAP43 injury related factors expression (A) in P0TNFalpha animals at P65 in DRGs and spinal cord. (* $p < 0.05$ relative to wild type intact animals) (B) mRNA expression detected in injured transgenic spinal cord (* $p < 0.05$ compared to intact transgenic animals, ### $p < 0.001$ compared to wild type uninjured animals). (C) mRNA qPCR analysis of injury related factor (ATF3) in wild type and P0TNFalpha animals in sciatic nerves at 1dpl and 3dpl (* $p < 0.05$ compared to intact animals).

8. Cytokines pattern after injury: WD & pain implications

The complex and synergistic action of inflammatory cytokines is necessary to finally promote axonal regeneration. While pro-inflammatory cytokines are expressed in the first phase of WD and promote the recruitment of macrophages; anti-inflammatory cytokines, expressed later, downregulate the production of all cytokines and determine the end of the degenerative process.

For this reason, we performed a kinetic study to determine the individual peak of cytokine production during the first 24 hpl and before the arrival of blood-derived macrophages, to control WD and demyelination. Thus, we tried to confirm the results obtained by others that have found cytokine mRNA production to peak at 4 to 8h and also protein production at 24 to 48 h (Kleinschinitz, 2005; Rothman, 2009; Fregnan, 2012).

We selected a pool of several cytokines (Fig59.) to characterize the local inflammatory environment of transgenic animals after injury in the context of high local TNFalpha. Moreover, an incorrect response of these cytokines could be related to the induction of painful signaling pathways, and infiltrated macrophages also contribute to cytokine production. Thus, we hypothesized that the higher number of macrophages in peripheral nerve of P0TNFalpha animals might also change the pattern of expression of some cytokines and, together with both the injury factors (ATF3 or GAP43 and BDNF) may activate the neurophatic pain pathways in this model.

8.1 Macrophages role: F4/80 detection

However, we could not detect some of cytokines, such as Caspase 6 or IL1a. We analyzed expression of F4/80 (Fig58.), a well-characterized mouse mature macrophage marker. Immediately after nerve injury, macrophage recruitment is promoted to eliminate cellular debris and tissue remodeling. The rapid clearance of degenerated myelin activated by SCs and macrophages is a crucial step for successful nerve regeneration. However, we observed an initial reduction in transgenic animals at 24hpl, followed by a positive slope at seventy-two hours post-crush (Fig58.). Moreover, the induction in the number of mature macrophages in wild type animals was detected early in both, proximal and distal sections, at 6hpl and the maximum peak was achieved at 1dpl.

Again, a delay in the WD and later regeneration was demonstrated in P0TNFalpha animals after crush.

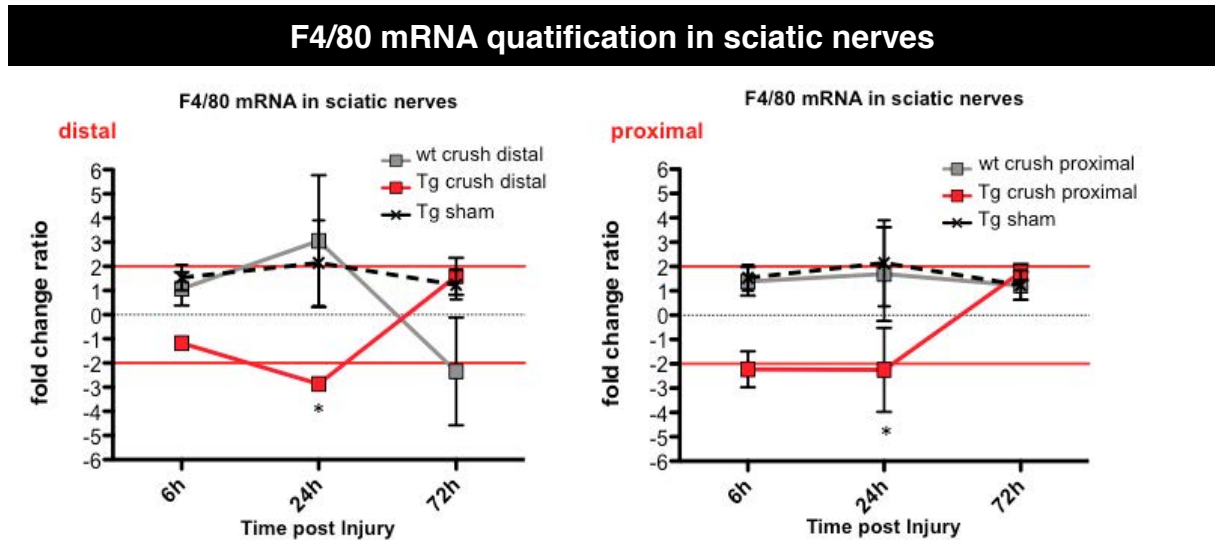


Figure 58. mRNA qPCR analysis of mature macrophages (F4/80) in wild type and P0TNFalpha animals in sciatic nerves at 6hpl, 1dpl and 3dpl (* $p < 0.05$ compared to intact transgenic nerve).

Again, a delay in the WD and later regeneration was demonstrated in P0TNFalpha animals after crush as a consequence of no positive cells to F4/80 in sciatic nerves of transgenic animals immediately after injury.

8.2 Pro-inflammatory cytokines

8.2.1 IL1b detection

Some of the pro-inflammatory cytokines involved in peripheral nerve injury are the IL-1 family, which activates T and B lymphocytes. The IL-1 family consists of two agonists, IL-1alpha and IL-1beta, two receptors, biologically active IL-1RI and inert IL-1RII, and a specific receptor antagonist, IL-1Ra, which is a highly specific, competitive endogenous antagonist. In the intact peripheral nervous system, IL-1 α mRNA is constitutively expressed, but IL-1 α protein is not synthesized (Kang, 1996). Due to nerve injury, IL-1 α is rapidly upregulated by SCs, both at mRNA and protein after 5 to 6 hours following, when they lost their close contact with interrupted axons (Nadeau, 2011; Fregnan, 2012).

We observed that, in transgenic mice IL-1 β expression during WD was detected 5–10 hpl and the delayed expression might be due to SC-derived TNF α . Interestingly, the highest levels of TNF α and IL-1 β protein secretion were detected 1 dpl before macrophage recruitment (Fig59.A)

IL1b is increased at 6hpl in distal sections of both genotypes and the levels are maintained to 3dpl in wild type animals. The IL1b overexpression declined in transgenic animals, although the levels remained higher than intact wild type animals. In the proximal segment, we observed a peak at 1dpl, being higher in P0TNF α than wild type mice compared to their intact controls. However, both genotypes achieved similar levels at 3dpl. (Fig59. A)

The down regulation of IL1b in transgenic mice after injury evidence the delay in WD.

8.2.2 IL6 detection

The fundamental role of IL-1 α after injury is to induce IL-6 production. This cytokine plays a role in neuroprotection and modulation of pain, in axon regeneration after peripheral nerve injury, and also makes an important contribution in the overall cellular response.

IL6 cytokine showed the most different pattern among genotypes (Fig59. B). While the distal segment of wild type animals exhibited an increase at 6hpl, the levels are normal in the proximal section. Conversely, transgenic animals showed an expression peak at 6hpl in both, distal and proximal segment, which was maintained at 1dpl. Then, the expression decreases to sham values.

The up regulation in IL6 cytokine rapidly in transgenic mice could play a role in the modulation of pain.

8.2.3 IL1RA detection

Binding IL alpha and beta to IL-1RA receptor prevents the generation of a normal intracellular signal. The balance between IL-1 and IL-1RA plays an important role in the susceptibility and severity of many diseases. IL-1RA also serves to limit the inflammatory response in WD in peripheral nerves by exerting inhibitory control over IL-1/IL-1R activation. IL1RA levels are overexpressed after crush in both genotypes, the distal part of sciatic nerves keeps a regular growth and achieved higher values in wild type than transgenic animals. The proximal sections of crushed nerves showed an expression peak 1dpl, higher in transgenic than in wild types, to decrease later (Fig59. C).

The low expression of IL1RA in distal stumps of transgenic animals are related to an active WD, due to IL1RA expression are necessary to inhibit degeneration process, starting regeneration.

8.2.4 Caspase3 detection

Finally, the Caspase3 pattern was similar among genotypes. It is important to remark the induction at 6hpl in P0TNFalpha animals, being rapidly restored at 3dpl (Fig59.D). Caspase3 is used as a measure of SCs apoptosis. After injury, Caspase3 significantly increased at the site of lesion 1dpl. Caspase 3 was seen in DRG on the injured side, but no motor or sensory neurons were observed at any time-point. Delayed nerve repair is associated with more pronounced Schwann cell apoptosis which may explain impaired nerve regeneration after nerve injury and delayed repair.

Delayed nerve repair is associated with more pronounced Schwann cell apoptosis which may explain impaired nerve regeneration after nerve injury and delayed repair, due to caspase 3 was induced rapidly after injury in SCs.

Cytokines mRNA quantification in sciatic nerves

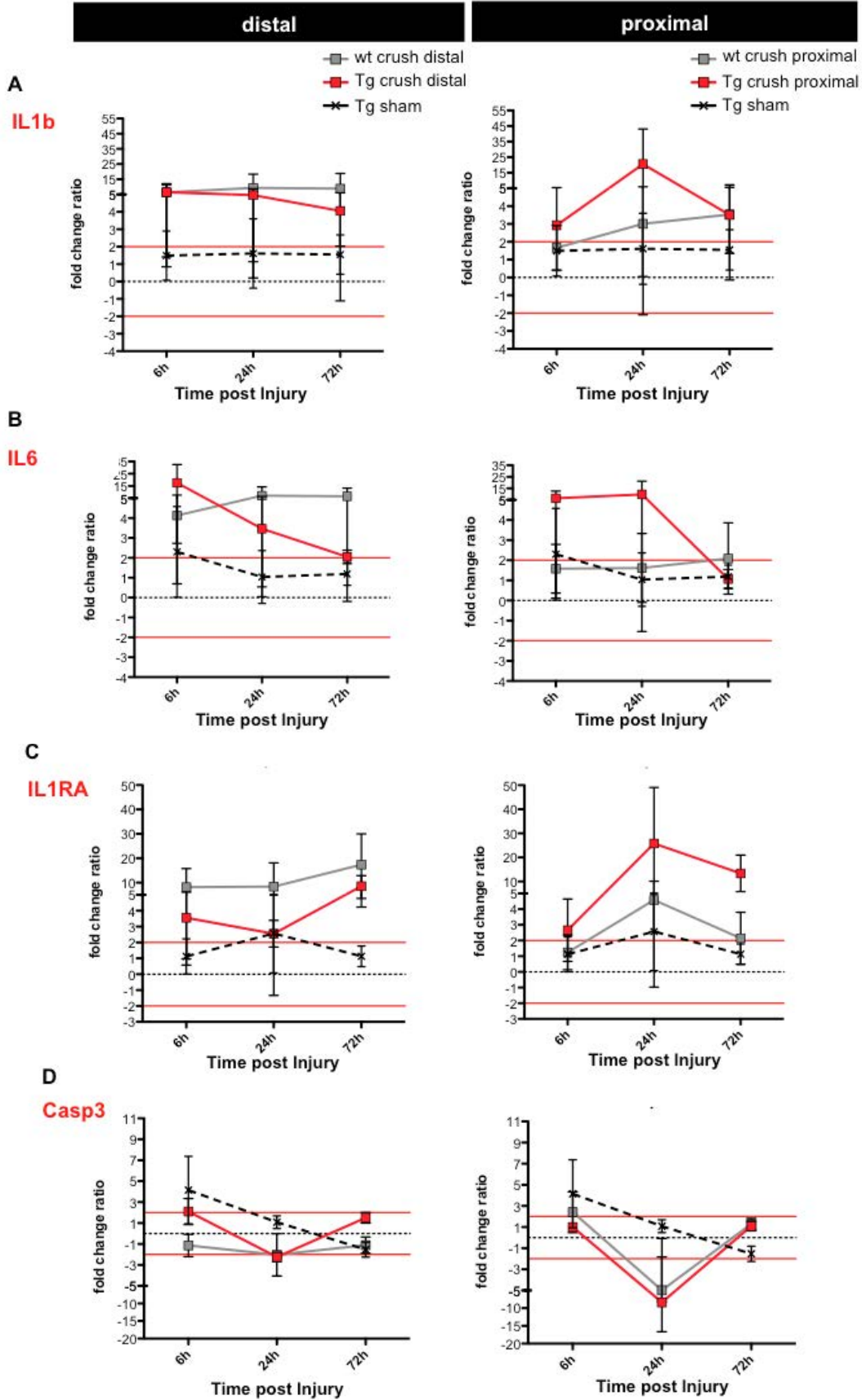


Figure 59. mRNA qPCR analysis of cytokine (IL1b, IL6, IL1RA and Caspase3) expression pattern in wild type and P0TNFalpha animals in sciatic nerves at 6hpi, 1dpi and 3dpi

9. Algesimetry tests characterization in P0TNFalpha mice

Inflammatory pain, caused by immune system activation in response to tissue injury have a protective role. In contrast, neuropathic pain emanating from disease or damage to the somatosensory system, is deleteruos. Moreover, dysregulation of cytokines has been implicated in a variety of neuropathic pain conditions in both humans and animals (Woolf, 2010; Lees, 2013).

To evaluate pain changes in P0TNFalpha animals with or without damage, we tested thermal and mechanical hypersensitivity (Fig60.). After crush, higher neuropathic pain responses, related to hypersensitivity to stimuli (hyperalgesia) were seen in P0TNFalpha transgenic animals compared to wild type injured animal at both time points: 14dpl and 21dpl. These animals showed lower sensory thersholds, more remarkable to thermal than mechanical stimulus. P0TNFalpha crushed animals display not significant differences versus wild types at 21dpl.

Moreover, there are not changes when contralateral paws of crushed animals were compared to sham control mice and neither among contralateral and ipsilateral legs of these uninjured animals.

Sham transgenic animals also exhibited remarkable differences of thermal responses compared to wild types, at both 14 and 21 dpl (Fig60.). These results were according to bibliographic reviews that implicated TNFalpha as a pain inducer, as animals with TNFalpha overexpression have faster responses to thermal stimulation (Zhang, 2007; Miller, 2009; Shubayev, 2010). In addition, differences widen after damage, suggesting the role of TNF alpha in a delay in the peripheral regeneration process, as showing by electrophysiological study.

Thermal and mechanical algometry tests

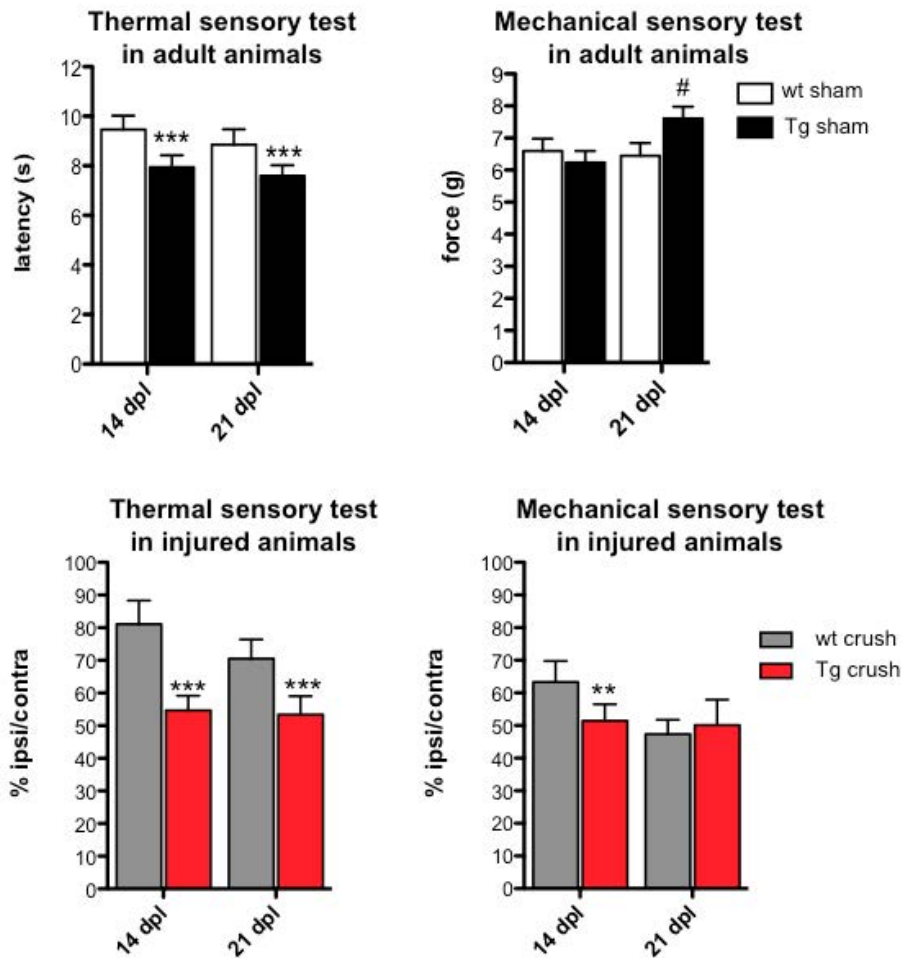


Figure 60. Algometrical analysis to thermal and mechanical stimulus in adult animals with and without crush (** $p < 0.01$ and *** $p < 0.001$ compared to wild type animals. # $p < 0.05$ 21 dpl versus 14 dpl).

Thermal and mechanical hypersensitivity was tested to characterize the pain responses in P0TNF α animals. We do not observed changes when contralateral paws of crushed animals were compared to sham control mice and neither among contralateral and ipsilateral legs of these uninjured animals. Differences in sciatic nerves are widening after peripheral injury, suggesting the role of TNF α in a delay in the peripheral regeneration process, as showing by electrophysiological study.

10. Electrophysiology study in P0TNFalpha mice

Electrophysiological tests, which were performed at 14dpl and 21dpl, are another useful tool for investigating the functional integrity of peripheral nerves. Results show a poor regeneration in transgenic mice after peripheral injury as low values for amplitude in transgenic injured animals at 21dpl. The compound motor action potential (CMAP) amplitude correlated with the number of functional axons and is an indicator for axonal damage when it is significantly reduced (Fig61.).

Moreover, high values for latency, that represents the time delay between stimulation and CMAP onset, were significant to plantar muscles although there was also a tendency in tibialis anterior and digital nerve. This data showed a possible reduction in conduction velocities after nerve damage related to a demyelinated state. It is known that the nerve conduction velocity (SNCV) is highly dependent on rapid signal propagation enabled by myelination and therefore, demyelinating processes generally showed decreased conduction velocities.

Reduction in CMAP and increased latencies in P0TNFalpha mice confirm the impairment in myelination in P0TNFalpha animals, as well as the impairment in regeneration after peripheral damage.

Electrophysiological characterization

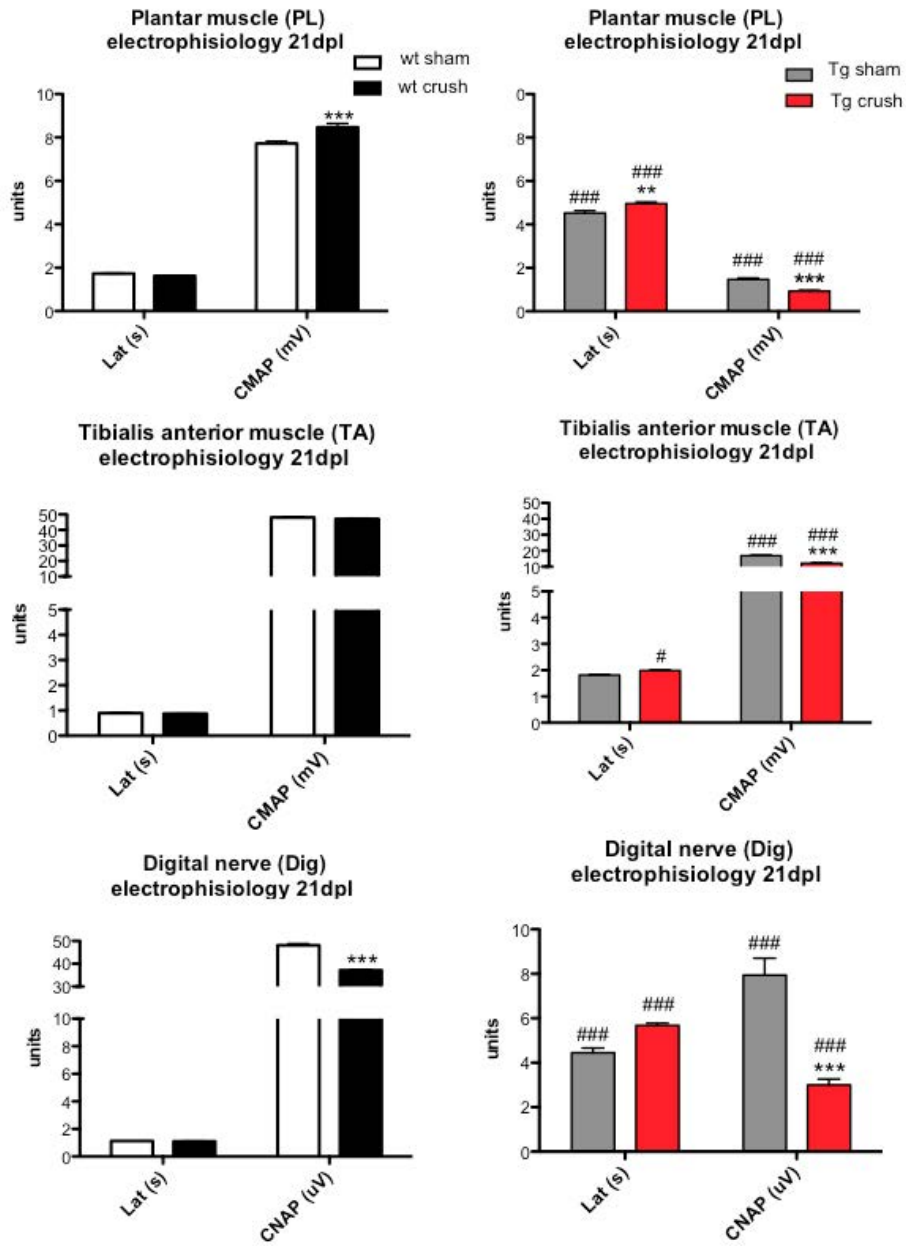


Figure 61. Electrophysiology analysis in adult animals, wild type and P0TNFalpha mice, with or without crush at 21dpl (***) p<0.001 compared to wild type and # p<0.05, ## p<0.01 and ### p<0.001 14dpl versus 21dpl).

IV. DISCUSSION

1. A Transgenic P0TNFalpha mouse model

With the aim to develop an useful animal model to study peripheral neuropathy and chronic pain to apply possible treatments, we generated a transgenic mice overexpressing murine TNFalpha cDNA under control of the P0 promoter, specific to SCs.

Macrophages stimulated by bacterial lipopolysaccharide (LPS) released TNFalpha, a potent proinflammatory mediator. The ubiquitous production of TNFalpha, through NF- κ B and other transcription factors, could cause undesired deleterious effects in other systemic tissue such as a heart failure (Stoelckin, 2013). On the other hand, the mRNA of this cytokine has a short half-life (Yoshizumi, 1998; Mijatovic, 2000). For these reasons it was necessary to restrict the expression of P0TNFalpha to the PNS.

Initially, four founders integrated the P0TNFalpha transgene. Most of the F0 animals could be mosaic animals, which means the presence of two populations of cells with wild type and/or transgenic genotype due to the integration of the transgene would have been developed after the first mitotic division of embryonic development (Wilkie, 1986; Whitelaw, 1993). Suggesting a mendelian inheritance, we expected a progeny proportion of 50% heterozygous and 25% of homozygous and wild types animals if heterozygous animals were crossed themselves to generate homozygous transgenic P0TNFalpha mice. Lower percentages will be related to mosaicism events. L1 and L4 animals keep the expected theoretical results (55% in L1 and 54% in L4 heterozygous mice and 27% in L1 and 25% in L4 homozygous offspring). However, we excluded L2 line (37% of wild type animals).

Finally, we choose L4 germline to evaluate the effects of TNFalpha in the development, WD and regeneration as it showed consistent high TNFalpha expression based on mRNA and protein in sciatic nerves of P0TNFalpha at P65, although L1 was also consistent. It was observed high overexpression of mRNA and 0.11 ng of TNFalpha, while it was not detected in adult wild type animals. The expression of other important genes, such as the main myelin proteins were reduced of myelin protein compared to wild type mice.

The different stages of the myelination process are coordinated to the postnatal expression patterns of several proteins, lipids and transcription factors needed for PNS nerve development. According with myelin development we decided to study 3 different ages to complete the characterization of the P0TNFalpha transgenic mouse model: P05, P21 and P65 mice (Figure 53.).

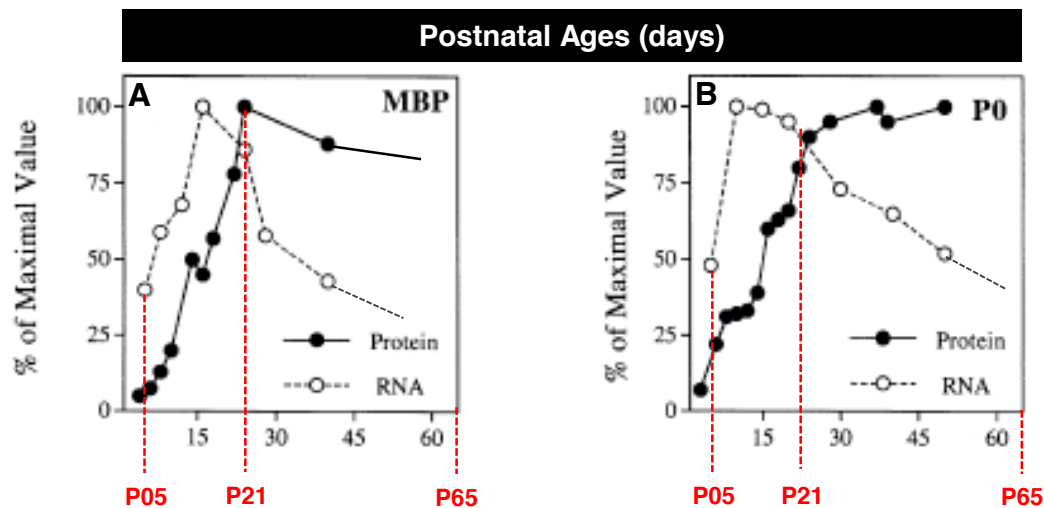


Figure 62. Myelination of the mouse sciatic nerve. **(A)** Evolution of MBP and **(B)** P0 protein levels and mRNA levels during sciatic nerve development. Data are expressed as % of the maximal value (adapted from Garbay, 1988, 1989 and 2000).

After birth, murine sciatic nerves contain low proportion of promyelin and myelinated fibers. The transition to the promyelin stage is accompanied by a strong SCs proliferation, culminating with the one to one SCs-axonal relationship, necessary to start the myelination process. Thus, the number of myelinated fibers increases progressively at P04-P05 newborn mice, corresponding with the peak of expression of P0, the major myelin protein in PNS. The most active phase of myelination is around P08-P10 (Maier M., 2002). MBP mRNA expression peak is delayed over P14, and only a few promyelin fibers remain at this timepoint. Moreover, young mice have both, P0 and MBP, maximum protein concentration at P21, maintained to adulthood (Garbay B et al 2000).

In the initial phases of myelination, SCs express GAP43 constitutively (Curtis et al 1992; Scherer et al 1994a). GAP43 expression is downregulated when SCs establish the axonal contact to start myelination. Whereas, MAG expression is also

induced at this early stage of the myelination process, preceding the P0 and MBP expression (Stahl et al., 1990; Notterpek et al., 1999).

We observed, clearly, a delay in the myelination process in P0TNFalpha animals. However, GAP43 is not detected in intact P0TNFalpha mice, suggesting a correct axon-SCs contact and normal myelin process in the P0TNFalpha mouse model. However, MAG mRNA was downregulated compared to wild types. This result could be associated to a delay in the early induction of the myelination process in P0TNFalpha mice.

On the other hand, peripheral nerves of MAG KO mice revealed no abnormalities in nerve conduction, histology or ultrastructure compared to wild type animals. However, old mice mutant for MAG exhibited axonal atrophy and myelin degenerative abnormalities (Montag et al., 1994; Li et al., 1994). In accordance, it was suggested a crucial role for MAG in the prolonged maintenance of normal SCs-axon interactions, as well as in the axonal maturation and viability. Moreover, the function of MAG supporting the SCs-axon interaction in adult organism was confirmed with morphological and ultrastructural studies. Thus, consistant with MAG downregulation, P0TNFalpha animals showed significant thinner myelin sheaths, especially in bigger axons, as well as higher g-ratio index.

By the end of the promyelin phase, SCs start the active myelination period characterized by a massive synthesis of membrane compounds, not only myelin proteins, but also phospholipids, just leading the formation of mature myelin sheaths. This period is extended through the fourth weeks after birth (Garbay B., et al.; 2000).

The accumulation of the P0 protein and mRNA during peripheral myelination in mice increases during the first days after birth, and although mRNA expression decreased, P0 protein reaches a plateau at P30 (Trapp, 1981; Martini, 1988; Baron, 1994). P0TNFalpha mice show a marked downregulation of P0 gene expression in P05 animals. The decline in expression is sustained over lifespan compare to control animals, although the expression levels are almost normalized at P65.

P0 protein is essential for normal compaction and maintenance of peripheral myelin sheaths and axonal integrity. Although heterozygous P0 KO mice are apparently normal, homozygous P0 knockout mice started to exhibit an abnormal phenotype at P21, related to the maximal P0 expression. Deficiencies in motor coordination, tremors and convulsions are some of the clinical symptoms observed. However, the lack of P0 did not affect the initiation of myelination but the subsequent differentiation shows unusually thin and poorly compacted myelin. Morphological and ultrastructural studies revealed severe hypomyelinated axons and degeneration events (Jessen, 1990; Giese, 1992 and Martini, 1995a). We observed similar results in P0TNF α transgenic animals.

Although MBP expression starts later, the pattern of MBP is quite similar to P0 in mouse sciatic nerves. TNF α P0 mice have also a down-regulation of MBP expression. Moreover, although wild type animals have a reduction of MBP at P65, P0TNF α mice show higher values. These results are consistent with the hypothesis of the myelination process retardation in the transgenic model.

On the other hand, P0 KO mice show low MBP expression than control animals (Martini, 1995a). As a consequence, the reduction in MBP expression at early stages of myelin process (P05) could be due to the initial downregulation of P0, suggesting the role of P0 as a regulator element of MBP and other myelin genes. In addition, the MBP absence but normal myelin observed in shiverer mutant mice, could be compensated by changes in the proportions of some lipids as well as other myelin protein, such as P0 (Martini, 1995b).

The down-regulation of P0 and MBP expression in P0TNF α mice were confirmed by western blot and immunohistochemistry of peripheral nerves. Both myelin proteins increased at P21, corresponding with the maximal concentration of P0 and MBP protein, and achieved wild type levels at P65 (Garbay, 2000).

Myelin proteins are very stable, thus even if their expression is delayed or diminished in the myelination process, they may accumulate achieving normal levels in adult animals.

PMP22 is one of the minor peripheral nerve myelin proteins but necessary to correct myelin formation (Hahn et al., 1987). Mutations in the PMP22 gene were

identified in the trembler-J mutant mice, showing a dysmyelination phenotype comparable to the P0 KO mice. Moreover the total disruption of PMP22 gene leads only a focal hypomyelination and demyelination probably due compensatory mechanism; as well as minor changes in PMP22 gene dosage cause Charcot-Marie-Thooth type 1A disease, which present strong effects on the development and maintenance of peripheral nerves (Suter, 1992a, 1992b, Adlkofer, 1995 and Garbay, 1999, Maier, 2002). Thus, P0 and PMP22 play similar roles during PNS myelination and normal expression of both proteins are required.

Surprisingly, although small changes in PMP22 expression were observed at P05 P0TNFalpha mice, a strong dowregulation occurs at P21 and P65. This pattern for PMP22 is different compared to the other specific myelin genes.

PMP22 is a structural myelin protein mainly found in compact myelin, being implicated in adhesive processes and forming communication channels and pores between the membrane layers of SCs. PMP22 was also involved in the maintenance of the homeostasis of SCs as well as SCs defective to PMP22, would not be able to maintain the integrity of a normal myelin sheath (Welcher, 1991; Spreyer, 1991; Snipes, 1992, 1995; Hammer, 1993; Kuhn, 1993). These findings are consistent with the high expression of PMP22 necessary in adult peripheral nerves.

In a longitudinal expression study, PMP22 was detected in sciatic nerve lysates, during late fetal and early postnatal development, after MAG but before MBP expression. A dramatic upregulation of the transgene is induced at the most active phase of myelination; and the highest levels of PMP22 were associated to late stages of myelination process. Moreover the induction of this gene depend of axonal contact, like MAG (Kuhn, 1993). However, the protein was also present in nonmyelinating SCs, supporting multiple roles in peripheral nerve biology (Notterpek, 1999).

As it was hypothesized, the dual function of PMP22, as an integral structural component and as a regulatory element to cell proliferation and differentiation, is supported by the idea that PMP22 expression involves two alternatively tissue specific promoters. Both transcripts are highly expressed in peripheral nerves. While the more distal promoter, CD25 transcript, is mainly activated in myelinating SCs to control the expression patterns of other myelin genes during

development and nerve regeneration; the proximal promoter, SR13 transcript, is expressed ubiquitously in non-neural tissues (Kuhn, 1993; Bosse, 1994; Suter, 1994; Suter, 1995a,b). Moreover, in degenerating and regenerating segments of peripheral nerve, SR13 expression is inversely regulated compared to SCs proliferation, being associated to cell growth arrest. In addition, proliferating SCs expressed low amounts of PMP22 mRNA SR13 transcript, as well as genetically modified SCs that overexpress both PMP22 isoforms, showed a diminished rate of proliferation (Spreyer, 1991; Bosse, 1994; Zoidl, 1997).

Substantial amounts of CD25-PMP22 mRNA are expressed in developing sciatic nerves, during the major postnatal proliferation phase of SCs. Whereas a dramatic reduction of SR13-growth arrest transcript was observed. P0TNFalpha transgenic mouse show downregulation of PMP22 mRNA levels even at P05-P14. It would be necessary to determine the specific expression pattern for each PMP22 transcript. We hypothesize about the specific downregulation of CD25 mRNA and/or an upregulation of SR13 mRNA expression. However, P0TNFalpha animals show a defective expression of PMP22 in adulthood, but not earlier, due to the expression peak of PMP22 is located at P08-P10.

Morphometric results demonstrate that P0TNFalpha mice achieve a higher g-ratio index. Altogether with the decrease expression of MAG, P0, and other myelin proteins, this suggests the possible peripheral myelination retardation in P0TNFalpha mice. Furthermore, if the specific overexpression of SR13-PMP22 transcript would be confirmed, the results could explain a possible growth arrest of SCs, staying in a nonproliferative/immature states, and the inaccurate myelin phenotype observed in ultrastructural studies of P0TNFalpha animals.

p75NTR, a specific marker of non-myelinated SCs, is also related to axonal degeneration. Significant changes in p75NTR expression were not observed in adult P0TNFalpha mice relative to wild type. The results could be consistent with the hypothesis about the specific decreased expression of PMP22 mRNA for CD25 transcript. Thus, SCs might have a correct, but delayed, proliferative phenotype. We can observed similar results obtained from primary cultures for SCs, wild type and transgenic. We think that could be important check the TNFalpha levels in the supernatant of cell culture media and analyse the proliferative phenotype of primary SCs.

However, immunohistochemistry showed high levels of p75^{NTR} in P0TNF α animals at P65 compared to control mice, related to an immature, non-myelinating state of SCs. The immunohistochemical results also manifest high expression of S100 in P0TNF α than wild type mice. S100 is a marker expressed specifically by SCs independently of their myelination fate. This result also rejects the idea of a upregulation of growth arrest isoform of PMP22 and confirm that the increased number of SCs is also a consequence of the downregulation of the PMP22 arrest-growth transcript in transgenic animals.

Axonal degeneration and nerve injury change SCs metabolism, increase the proliferation of SCs, as it was observed by immunofluorescence detection of S100 marker, and decrease myelination, that was also observed in g-ratio index and in the reduction of myelin-specific proteins in the transgenic animals (Salzer, 1980; Poduslo, 1985; LeBlanc, 1987; Trapp, 1988; LeBlanc, 1990).

Oct6/SCIP, Krox20/Egr2 and Sox10 are the transcription factors, induced after axonal contact, essential for the correct temporal expression of myelin specific genes in SCs. However, we did not observed significant differences in P0TNF α animals.

The absence of Oct6 causes a normal myelin phenotype, although a marked delay in the myelination process and sporadic abnormalities in the myelin sheaths organization were observed, as it was showed in P0TNF α mice (Nickols, 2003). After the postnatal reduction in Oct6, we observed an upregulation of Egr2/Krox20, another essential regulator of myelin and molecules related to myelination, such as Cell Adhesion Molecules (CAMs). Egr2 was also identified as initiator of lipid and cholesterol synthesis pathway during myelin membrane formation (LeBlanc, 2005). Thus, Egr2 KO animals show a complete absence of myelin, arresting SCs in a promyelinating stage (Topilko, 1994).

Other genes such as MAG and PMP22 are also target for Egr2 (Nagaranja, 2001). P0TNF α animals have the transgene codifying to TNF α under the control of the P0 promoter, directly regulated Egr2. Nevertheless, Egr2 is not altered in P0TNF α mice. Moreover, the myelination process occurs in P0TNF α model. This might indicated a properly activation of the axonal signals to induce the differentiation program in SCs, although the process is delayed. The retardation could be a consequence of small changes in the Oct6

dose, more evident if adult transgenic animals are stressed by a peripheral nerve injury. After damage, nerves are infiltrated by macrophages and together with SCs, regulate the inflammatory response by the secretion of cytokines such as IL1, IL6 and TNF α ; and the activation of NF κ B (Betz, 1998; Topilko, 1994). Thus, P0TNF α mice may provide a dynamic equilibrium between demyelination signals from proinflammatory cytokines and remyelination events through activation NF κ B.

The cooperative functions of both, Egr2 and Sox10, transcription factors are required for proper P0 expression (Topilko, 1994; Zorick, 1999; Peirano, 2000; Le, 2005), and myelin formation (Jones, 2007). Sox10 is also expressed in mature SCs (Feltri, 1999; Britsch, 2001; Aquino, 2006; LeBlanc, 2006; Schreiner, 2007; Finzsch, 2010) although is not essential for SCs proliferation, is required to preserve the differentiated state and functions of SCs in adult PNS (Bremer, 2011). Mutations in Sox10 are also associated with peripheral demyelinating neuropathies (Inoue, 2004) and the deletion of Sox10 in adult mice causes the degeneration of myelin sheaths axonal death and nerve conduction alterations (Bremer, 2011).

The myelination process begins in the embryonic state, such as Oct6 detected at E16. P0TNF α transgenic animal overexpress TNF α under the control of the P0 promoter, specially regulated by Egr2. Egr2 is expressed at P05. Therefore, TNF α , as well as the expression of Oct6 and Egr2, should not be very different from wild type animals in later embryonic days. Differences relative to control animals were expected to be observed on post natal days.

The myelination process happens in a normal way, although it was delayed. Overexpression of TNF α starts to be significant different to wild type mice at P05, being implicated in the destruction of myelin sheaths. The downregulation of Egr2 was expected to reduce, slightly, TNF α expression. However, changes in Egr2 will not be observed due to the strong accumulation of TNF α in transgenic animals.

TNF α have not myelinotoxic properties by itself, although it is associated to inflammatory demyelination and cell death through the balance of ROS and iNOS that could inhibit MPK anti apoptotic pathways, and activate apoptotic

signals (Griffin, 1993, Stoll, 1993, Munoz-Fernandez, 1998; Liefner, 2000; Schafers, 2002a; Shamash, 2002; Van Herreweghe, 2002; Wright, 2004; Kamata, 2005; George, 2005, Shubayev, 2006; Schwabe, 2006).

The concentration of TNF α is also important to determine the effects on the organism. The endothelial cell surface becomes adhesive for leukocytes through the expression of CAMs and other cell membrane molecules, such as monocyte chemoattractant protein (MCP1) or matrix metalloproteinases (MMPs), at low concentrations of TNF α . These pathophysiological modifications exert a direct chemotactic effect and promote the migration and invasion of circulating macrophages and microglial cells, leading the MBP degradation (Shubayev, 2000, 2006; Zhang, 2009; Yadav, 2010).

TNF potentiates the cytolytic T cell lysis in moderate quantities. Finally, the administration of large quantities of TNF α causes cardiorespiratory death by inhibiting myocardial contractility and vascular smooth muscle through iNOs production. TNF α also causes hypoglycemic metabolic shock due to TNF α production in adipocytes is related to insulin resistance, DM and obesity (Abbs, 1994; Burger, 2002; Masson, 2004; Bastard, 2006, Dyck, 2006).

Large overregulation of TNF α expression is achieved in peripheral nerves of P0TNF α mice. Although there are no changes in the expression of the transcription factors associated to the P0 expression, we observed a downregulation of TNF α mRNA and protein in adult transgenic mice.

However, TNF α protein concentration was maintained up to P21 mice, as a possible consequence of the large mRNA accumulation as well as the long half life (15-30 min) and low bioavailability of the TNF α protein (Mijatovic, 2000; Stoecklin, 2003; Ma, 2015). However, we did not detect TNF α in serum of transgenic mice, neither in other peripheral tissues such as liver, heart or brain. Moreover, although no TNF α protein was present in DRG or spinal cord tissue, mRNA was detected in a minor quantity. Probably the TNF α values in DRG could be a cross-contamination effect with root node of nerve tissue, as it is not described that motorneuron from ventral horn of the spinal cord, either sensory neurons express P0 (Brunden, 1992).

Transgenic mice often develop molecular strategies to compensate the overexpressed transgene. In the P0TNF α mouse, there is probably a

compensatory mechanism related to TNF α receptors RI and RII. Although we expected the upregulation of the TNF α receptor against the high amount of TNF α , sciatic nerve of P0TNF α animals show a reduction of the TNFR1. The tendency to decline TNFR1 starts at P21 and it is more evident in adult transgenic animals.

P0TNF α mice through the reduction of TNFR1 try to counteract the deleterious effects of TNF in the organism and maintain the proper homeostasis in transgenic P0TNF α animals. As a consequence the myelin gene expression deficits are not so obvious and similar to control wild type animals. Unfortunately we could not properly detect the protein levels of both TNF α receptors to confirm the results of mRNA expression. Soluble TNF preferentially binds to TNFR1, whereas membrane-bound TNF preferentially binds to TNFR2 to mediated neuroprotection (Fontaine, 2002).

Physiologically, TNF α has the capacity to maintain axonal synapsis, neuroprotection and learning. Overexpression of TNF α affects the behavior pattern in mice and also acts as a negative regulator of hippocampal neurogenesis in adult mice through TNFR1. In addition, deficient animals for TNFR1 and TNFR2 show higher locomotor activity and a global behavior alteration. We did not evaluate P0TNF α animals for behavior. It could be relevant despite TNF receptors are not extremely reduced in P0TNF α mice.

The TNF-TNFR1 complex regulates biological functions by inducing NF κ B and express proinflammatory and proapoptotic genes (Abbas, 2000; Baud, 2001; Hallenbeck, 2002). These biological activities include nerve degeneration (Barbara, 1996; Malek, 1998). KO mice for TNFR1 has a reduced number of infiltrated glia and macrophages after injury, a reduction of proinflammatory cytokines, CAMs, MMPs and genes involved in the apoptotic pathways; and also a decreased in the transcription factor associated to antiinflammation process, such as cJun or cFos (Fioreet, 1998; Hallenbeck, 2002; Nakajima, 2004; Stellwagen, 2006; Iosif, 2006).

Thermal hyperalgesia requires TNFR1 signaling while mechanical and cold allodynia depend on both receptors. Accordingly, adult P0TNF α animals exhibit a light phenotype of hyperalgesia, characterized by faster responses to thermal stimulus as well as sensory nerve conduction velocities were higher

than wild type animals. In the transgenic P0TNFalpha model, TNFalpha peak correlates with the myelin gene expression reduction, and also the expression of CCL2 in DRGs. These results are linked with the neuroinflammation process that goes before the NP state.

CCL2/MCP1 gene is a secreted cytokine which displays a chemotactic activity as an important mediator of macrophage-related neural damage and demyelination. These actions have been described in many models, like multiple sclerosis and EAE models, or ALS, and also in two inherited demyelinated neuropathies: CMT1A and CMT1B syndromes. In addition, CCL2 is a therapeutic target linking adipose tissue inflammation, obesity and type 1 DM.

The upregulation of CCL2 during neuropathologic condition and neuroinflammation, leads the recruitment of activated macrophages, producing inflammatory molecules. Moreover, through the PIK3 cascade pathway and MEK and ERK1/2 activation, overexpression of CCL2 in DRGs usually causes apoptosis and axon damage, promoting regeneration after spinal cord or peripheral nerve injury (Kwon, 2015).

Concordantly, we found significant changes in the intensity of Iba1 immunoreactivity in peripheral nerves of adult P0TNFalpha animals, a specific marker for microglia/macrophage cells. These findings demonstrate the infiltration of circulating macrophages to peripheral tissue, as Iba1 was absent in control animals. Overinfiltration of macrophages and microglial cells in peripheral nerves is associated to the increased levels of CCL2. Consistently, no changes were detected in Iba1 or GFAP in spinal cord of transgenic animals.

Voltage-gated sodium channels play an essential role as regulator elements of the excitability of nociceptive primary afferent neurones. In particular three sodium channels, Nav1.7, Nav1.8, and Nav1.9, are preferentially expressed in peripheral neurons and have been suggested as molecular mediators in inflammatory pain (Waxman, 1999; Goldin, 2000; Black, 2002), contributing to the hyperexcitability of sensory neurons in DRG and regulating the excitability of nociceptive primary afferent neurons (Strickland, 2007). However, the role of these channels in hereditary pain syndromes is less well understood.

Nav1.7 and Nav 1.8 are expressed selectively in DRG sensory neurons and both of them are upregulated after injury (Nassar, 2004; Priest, 2005; Ekberg, 2006). The expression of both channels in particular has been shown to be highly dynamic in models of neuropathic and inflammatory pain. Thus, the modulation of these channels in DRG may present a therapeutic opportunity for the selective manipulation of primary sensory neurons (Amir, 2006; Ekberg, 2006). Neuropathic pain (NP) is a chronic disorder defined as pain initiated or caused by a primary lesion or dysfunction in the nervous system and it affects a high percentage of the population. However, it remains extremely difficult to treat, due to poorly understood etiology and a lack of well-defined molecular targets.

Several peripheral nerve injury-based rat models have been developed and exhibit symptomatology, including hindpaw hypersensitivity to mechanical and thermal stimuli. However, a more appropriated animal model is needed.

P0TNFalpha mouse showed an increased presence of both channels in DRG at P65 suggesting, at least in part, that to induce and maintain chronic inflammatory pain, probably high TNFalpha concentrations are needed for long term at high level.

There are a lot of painful neuropathies which are based on the gain-of-function mutations in sodium ion channels (Dib-Hajj, 2005; Faber, 2012). These mutations increased excitability of small DRG neurons, such as nociceptors Nav1.7 has been genetically linked to human pain, whereas a role for Nav1.8 and Nav1.9 in pain transmission is supported by animal studies. A crucial role for Nav1.8 in pain signaling has been supported by the impairment of thermal hyperalgesia following inflammation and cold-induced pain observed in knockout Nav1.8 and after ablation of Nav1.8-positive neurons (Thakor, 2008).

It is possible that the mutations of Nav channels generate a persistent sodium current and it may trigger injurious intracellular levels of calcium ion by the reverse Na/Ca exchange (Thakor, 2008).

The role of Nav1.9 is less understood (Priest, 2005). Although changes were not observed in Nav1.9 expression in DRGs of a mouse model of acute pain, a potential role in the maintenance of chronic inflammatory pain has been

suggested (Dib-Hajj, 1998; Tate, 1998; Akopian, 1999; Fjell, 1999).

Releated to NP as well as other immune diseases characterized by the overexpression of TNFalpha, several anti-TNFalpha drugs are available to target circulating and transmembrane TNF isoform: soluble receptors able to neutralize TNF (Etanercept) and therapies based on antibodies (monoclonal, chimeric like Infliximab or humanized such Adalimumab). Specifically, Etanercept reduces pain in chronic constriction injured nerves, but axonal degeneration or macrophage infiltration remain unaltered by the therapy. (Smith, 2009; Buchheit, 2012).

The inhibition of TNF through the recombinant human TNFR-antibody fusion protein (rhTNFR:Fc), resulted in a marked improvement of sciatic nerve, as well as DPN rats exhibited a significant increase in electrophisological parametres (SNCV and MNCV values). rhTNFR:Fc has been applied in human-clinical practice to treat rheumatoid arthritis and psoriasis. Moreover it was also used in inflammatory diseases of rat models (Okada, 2004; Mukaino, 2010).

The use of analogous of the TNFalpha receptors, that could be administrated to compite with TNFalpha binding and reduce the molecular pathways implicated, could be a good therapeutic strategy in peripheral nerves of 0TNFalpha mice.

To summary, the characterization of the mouse model overexpressing P0 in peripheral nerves, P0TNFalpha, show no changes in the transcription factors involved in the regulation of the myelin protein expression, although a marked decrease in TNFalpha mRNA and protein was observed. Thus, myelin protein is delayed but normal at the end. Probably a more robust phenotype could be found through another mechanism, perhaps related to WD after nerve damage.

Therefore, a proper process of myelination is expected in the P0TNFalpha model. The ubiquos and regular levels of TNFalpha in the environment would potentiate a little downregulation of myelin proteins, which never will reach the levels of wild type mice. Overtime, transgenic animals show a small reduction of TNFalpha, as well as detected in the sciatic nerves, probably due to the observed upregulation of IL10 protein to compensate the TNFalpha actions.

Long-term studies will need to be performed in older P0TNFalpha animals to check alteration in the molecular pathways associated to NP. Moreover, these

studies will elucidate the implication of TNFalpha overexpression and the development of aging phenotypes in PNS tissue. Recent works have been suggested that inflammation is a common component of age-related diseases (Combs, 2001;Csizer, 2007; Hanish,, 2007; Steinle, 2009), as well as the capabilities for axonal regeneration and reinnervation are delayed and less effective with aging (Verdu, 2000).

2. P0TNFalpha model stressed by sciatic nerve *crush* injury

One of the main difficulties to obtain and/or generate a proper mouse model to study the secondary complications of DM type I and II, such as pain or demyelination, is found in the short lifespan of mice. Moreover, diabetic animals untreated with insulin to control the glucose blood levels, have a shorter life expectancy.

One way to stress the P0TNFalpha mouse model and see more important differences between wild type and transgenic animals, was by inducing a disease or a type of injury and studying the progression/generation capacity of the insult. We hypothesize that, inducing DM by streptozotocin (STZ) administration in adults animals, could be an approach (Deeds, 2011), as well injuring sciatic nerve with crush (Homs, 2011, 2014), could potentiate the NP phenotype.

Accordingly, we evaluated the possibility to stress P0TNFalpha mice through sciatic nerve injury. Sciatic damage by crush is considered one of the best stimulation protocol to maximize the myelin degeneration/regeneration deficits (Mats&Meths). Thus, the role of TNF in peripheral myelin and NP could be better understood.

The sciatic nerve is the most representative nerve in the PNS, in humans and other animals, such rodents. This nerve is the longest and provides connections to skin, muscles of the back, thigh and lower limbs. Sciatic nerve is derived from DRG localized in L4, L5 and S1 in humans, and L3, L4 and L5 in most mouse strains (Rigaud, 2008). Sciatic nerve is divided into two branches at knee joint, and forms tibialis nerve and common peroneal nerve. Most of the peripheral degenerative process, like DPN, start in the foot and the progress to the tibialis, sural and finally, sciatic nerve.

Peripheral nerve injury rodent models often target mouse sciatic nerve due to the big size, anatomical accessibility, similarity to human nerve and the capacity to perform motor and nociceptive tests. Although most of animals models are

focus in compression and/or total section of sciatic nerve; metabolic, infectious and chemical agents are often used to generate animal models (Yalcin, 2014; Challa, 2015) for the study of peripheral degeneration/regeneration, peripheral neuropathies and neuropathic pain (NP) as well as the screening of proregenerative compounds.

The spatiotemporal evolution of axonal degeneration depends on the experimental procedure (axotomy, crush/axotnmesis or chronic ligature) and also other factors such as animal strain, age, site of injury and environmental conditions. However, no significant differences were described among sexes.

The more common peripheral compressions are categorized as neurapraxia or grade I of nerve injuries, which are defined by focal demyelination without axonal and connective tissue damage. These compressions can be acute (external compression) or chronic (as the carpal tunnel syndrome). Both of them show normal nerve morphology and neuromuscular junctions, but thinner myelin sheaths.

Human crush injuries (axonotmesis) typically occur from an acute compression of nerve to a blunt or crushing object, such as a surgical clamp. Complete transection injury is known as neurotmesis or grade V nerve injuries. However, in humans, nerve transection occurs less often. Both of them, crush and transection, are commonly war injuries and cause a decline in patient life-quality. As a consequence, government institutions invest grants and financial support to further investigation to improve recovery and to develop viable treatments.

Transient crush and the axotomy of the sciatic nerve at mid-thigh level are widely used models. However, most of them do not developed neuropathic pain, although they are able to start WD, thus it is necessary to generate other strategies or animal models. Alternatively to mouse models, 3D, organotypic and glial cell cultures have been used, but are less relevant to human disease (Menorca, 2013; Santos, 2016; Cole, 2017). In other hand, femoral nerve injuries are relevant in the study of particular nerve types because it has one exclusively motor branch and another exclusively sensory branch (Menorca, 2013).

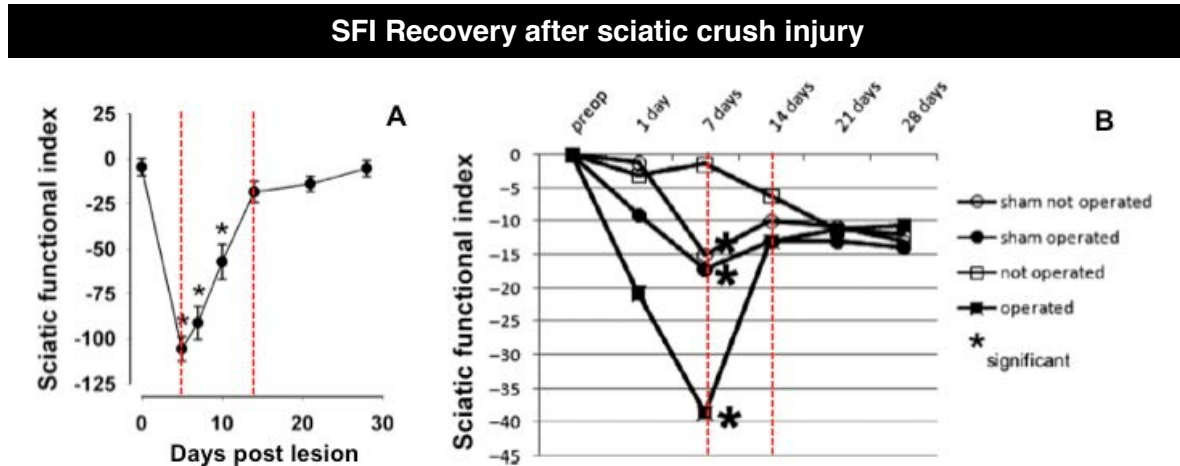


Fig 63. SFI index representation after sciatic nerve crush injury in wild type animals. Dotted red line represent the more representative point time in the recovery process: 7dpl which animals achieve the lower values of SFI, and 14dpl which control animals show a full motor recovery. **(A)** Adapted from Fey et al., 2010. It is represented the motion analysis for sciatic nerve injury in wild type mice. **(B)** Adapted from Pavic R et al., 2008. The graphs represent the side distinct sciatic nerve recovery of mice sham or crush animal. The injured leg is represented compared to the intact contralateral leg. Both sham animals operated and non operated, as well as the contralateral intact leg of crush animals show similar recovery patterns.

Functional recovery can be monitored with the Sciatic Functional Index (SFI), based on walking track analysis (Inserra, 1998). Different studies described the expected pattern of animal recovery. The maximum nerve injury (SFI=-100) was obtained at 7dpl, and the recovery (SFI=0) in wild type animals occurs at 21dpl (Fig 54.), although basal levels are reached at 7wpl. These time lapses are normally in slight injury models as neuropraxia and axonotmesis, but it was also observed there are retardation in the recovery of axotomy models (one month after injury).

In WD are two differentiated segments in injured sciatic nerves. First, the end of the injured neuron which is still attached to the neuron cell body, as known as proximal stump. Second, the end of the injured neuron that is still attached to the end of the axon is the distal stump. The proximal sciatic segment shows better rates of regeneration, while distal stump degenerates and the axonal proximal cone grows toward it (Schlaepfer, 1973; Oaklander, 1988; Kidd, 1991; Wu, 1994; Bruck, 1997).

P0TNF α animals showed a delay in the regeneration process, which was observed even in early phases of WD process. While wild type animals achieved the complete myelin degeneration at 7dpl and start remyelination;

transgenic animals achieved the minimum SFI at 9dpl. In addition to the delay observed in WD, P0TNFalpha animals show slower regeneration velocity rate (over 2-fold compared to wild type mice). Finally, full recovery of transgenic mice was achieved more than one month after nerve damage, while wild type mice are recovered at 21dpl.

These results suggest a retardation in the phagocytosis of myelin debris necessary to complete the WD and the initiation of regeneration. WD was described as a macrophage-driven process (Perry, 1987; Brück, 1997; Myers, 2011). After injury, circulating macrophages enter into the distal stump of the nerve through the damaged blood-nerve barrier (BNB) and phagocytose axonal and myelin debris from degenerated fibers that are digested in cytoplasmic vacuoles by hydrolytic enzymes after lysosomal fusion. The recruitment of resident macrophages starts within hours after injury, while the infiltration of macrophages from blood begins 2-3 dpl and the peak is at 7-14 dpl in wild type animals (Holtzman, 1965; Han, 1989; Hirata, 1999).

Moreover SCs are also rapidly transformed from myelinating cells to myelin phagocytotic cells, before the recruitment of circulating macrophages (Sulaiman, 2010).

The clearance of myelin debris of injured tissues is one of the most important and critical events preceding the regenerative process (Schubert, 1981; Beuche, 1984; Scheidt, 1987).

Although we observed that P0TNFalpha animals have higher amount of macrophages and microglial cells in peripheral nerves, these phagocytic cells could have not a complete activation due to high concentrations of TNFalpha. As a consequence, P0TNFalpha mice show a delay in regeneration. Moreover, the functional role of resident endoneurial macrophages remain undefined, because there are not specific histochemical markers available to discriminate resident from circulating macrophages. Recently an extremely rapid response from resident endoneurial macrophages after nerve injury was described. This activation might be crucial to successful nerve regeneration (Mueller, 2003).

However, although the number of macrophages in P0TNFalpha peripheral nerves is higher than in wild types, the highest infiltration starts at 14dpl in the proximal segment of sciatic nerves and at 21dpl in the distal section and in tibialis nerves, localized distally. It is possible that P0TNFalpha SCs never acquire the phagocytic phenotype in early WD, contributing to the delay of the degenerative process. Although activated microglia exhibit morphological transformation, it was not possible to detect any changes to confirm its activation in transgenic peripheral nerves.

Moreover, the behavior of P0TNFalpha mouse is quite similar to Wlds mutants mice. A slow WD and impairment of axonal regeneration characterizes Wlds animals. Furthermore, while WD in the PNS is fast, taking 14-21 days it is dramatically slow in the CNS. These facts suggest that degeneration is an active process and slow or deficient myelin debris removal could create an inhibitory environment for axonal regeneration (Levy, 2001; Gillingwater, 2002; Barrette, 2010; Peluffo, 2015).

Iba1 is a microglia/macrophage-specific calcium-binding protein which modulates actin reorganization to facilitate cell migration and phagocytosis by microglia (Ohsawa, 2004). We observed, , that Iba1 immunofluorescence correlated inversely with the myelin protein levels, particularly MBP.

On the other hand, F4/80 is a well-characterized marker for macrophages in mice. P0TNFalpha animals show high F4/80 mRNA in distal and proximal sciatic nerves at 6hpl, 1dpl and prolonged to 3dpl. However wild type mice initiated the downregulation of F4/80 expression only at 3dpl. We also observed that uninjured P0TNFalpha have a similar expression pattern that injured wild type, both compared to sham wild type nerves.

Moreover, SCs start proliferating at 1-5dpl and the peak of activation occurs around 3dpl to decrease afterwards. SCs proliferation plays a key role in the first step of WD and, in coordination with macrophages, initiate degradation of myelin debris. A second phase of proliferation occurs later, in the second stage of WD, to create a permissive pathway to regenerating axons (Schroder, 1972; Powers, 2013).

The regular pattern of SCs activation is according to the results observed in the expression of the F4/80 mRNA and Iba1 protein in wild type animals. Contrarily, P0TNFalpha mice show an increase in F4/80 expression at 3dpi and the maximum Iba1 was detected at 14dpi in the proximal sciatic section and at 21dpi in distal segments of injury nerves.

We conclude that, although the levels of F4/80 positive macrophages are higher in transgenic animals, they are not enough to be activated and start the phagocytosis mechanism necessary to resolve degeneration after damage.

Cytokines, neurotrophic factors and ECM and CAMs are released by SCs, macrophages and peripheral microglia to provide a permissive microenvironment for axonal re-growth, after detecting primary damage in nerves (Griffin, 1992; Schmidt, 2005; Lucas, 2006; DeFrancesco-Lisowitz, 2015).

The cytokine currency theory suggests that pro- and anti-inflammatory cytokines are constantly available to modulate gene expression in WD and regeneration. These cytokines have low expression and reduced physiologic functions in normal nervous system (Wahl, 1989; Chung, 1990).

Accordingly, some authors suggest the term of “cytokine network of WD” to the orchestrated production of cytokines that are considered key components during the inflammatory physiopathology of WD. Thus, WD is classified as a two-stage process. First, an inflammatory process which activates resident macrophages and SCs to release pro-inflammatory cytokines such as IL1b and TNFalpha. Followed, by the second stage of WD that concerns the resolution of inflammation through the secretion of anti-inflammatory cytokines such as IL-10 to downregulate the production of proinflammatory molecules and, consequently, turn off the inflammation.

The role of the pro-inflammatory cascade is to increase vascular permeability and allow the infiltration of macrophages into the injured area. The activation of these cells, together with SCs, increases the expression of proinflammatory cytokines like TNFalpha, IL1 and IL6 to develop a strong inflammatory response (Munoz-Fernandez, 1998; Tonelli, 2005; Truettner, 2005). Moreover, macrophages also release ROS, and the combination of these molecules damages the myelin sheath and axons. Finally, the symptoms decrease due to antinflammatory

responses and cellular apoptosis. Nevertheless, neither apoptosis or changes in Caspase 3 expression and activation were observed in P0TNF α animals. TNF α and IL10 seem to be the most relevant cytokines involved in the WD process. TNF α is considered to play a beneficial role in the breakdown and recovery of BNB while IL-10 is the regulatory key of these changes.

In the classical view of inflammation, other pro-inflammatory cytokines such as IL6, IL-1 α and IL1 β , are released by macrophage immediately after injury (Rotshenker, 1997; Be'eri, 1998) and may be also involved in the vasodilation process (Romanic, 1998, von Gertten, 2003; Lindberget, 2004; Lucas, 2006).

TNF α and IL-1 α are the first inflammatory cytokines produced in WD by SCs. IL-1 α mRNA is constitutively expressed but not its protein, in intact PNS of mice. Injury induces the rapid upregulation of IL-1 α mRNA at 5hpl, and thereafter protein in SCs. Moreover, IL1 α mRNA was not possible to detect in wild type or P0TNF α transgenic animals, even 6hpl.

We found that peripheral injury induced the rapid upregulation of TNF α in wild type mice, being detected also at 5hpl. Later on, TNF α immunopositive cells increased significantly distal to the crush site at 3 dpl to diminish when nerve start to regenerate and the BNB was restored at 7-14dpl. Control wild type animals reproduced these theoretical pattern expected and TNF α mRNA expression get normal uninjured levels at 3dpl.

However, TNF α mRNA remains unaltered in P0TNF α at 1-3dpl, compared to sham transgenic mice. In addition, TNF α protein upregulation was only detected in the proximal section of sciatic nerve 21dpl, confirming a delay in the denegeration/regeneration process which has a proximal-distal directionality. Intact wild type animals had almost resolved the regeneration process at 21dpl. Moreover, the expression of TNF α mRNA was downregulated at this time to block the initial upregulation of this cytokine.

We hypothesized that TNF α levels were so high in P0TNF α mice that the peak of expression and the subsequent downregulation, both needed to start the WD process, were failed. However, although we demonstrated the simultaneous overexpression of IL10 to inhibit and control the production of

TNF α , high levels are still maintained and block the antiinflammatory actions of IL10.

Later on, follows the production of IL-6, which inhibits TNF α and is only expressed 2hpi, probably induced by TNF α and IL1 α . Moreover, IL-6 is responsible of the early reduction of TNF α as well as it was observed in the wild type animals after crush: IL6 upregulation was observed at 6hpi, and the peak was achieved for 1dpi to 3dpi, while TNF α is down. Moreover, the IL6 levels were higher in distal sections, being more disconnected from the axonal cell body, and it was described that show better degeneration process.

P0TNF α model showed an early increase in IL6 levels at 6hpi, but were downregulated at the same time (1dpi) as TNF α expression is upregulated.

The expression of the cytokine IL6 does not promote regeneration by itself but it is supposed to play a key role in the early reaction of SCs to peripheral nerve injury (Grothe, 2000). However, IL6 and TNF α have context-dependent antiinflammatory roles (Munoz-Fernandez, 1998; Borish, 2003; Lucas, 2006). For example, IL6 injected in healthy nerves, increases neuroinflammation and demyelinated pathological processes through BDNF production (Lisak, 1994; Zhong, 1999; Inserra, 2000; Wyss-Coray, 2002; Leibinger, 2013; Wolf, 2014). IL-6 KO mice, after nerve crush injury, show a delayed recovery of motor function (Ishihara, 2002, Munoz-Fernandez, 1998; Raivich, 1999). Moreover IL6 can be used as a therapy to reduce inflammation and demyelination through the reduction of iNOS (Deretzi, 1999a; Deretzi, 1999b; Levy, 2001; Zochodne, 2005).

Finally, IL1 β activation is able to induce the expression of TNF α and IL6 (Norris, 1994; Basu, 2002b). Injury also induces the rapid expression of IL-1 β but the onset is delayed compared to the other proinflammatory cytokines.

While IL1 α and IL1 β are agonists in functions, the third type of cytokine from the IL1 family, IL1Ra, is an antagonist receptor which regulates the IL1 signalling pathway (Masada et al. 2001) in wild type and P0TNF α animals. The upregulation of IL1Ra expression was correlated to a decrease in of IL1 β , and viceversa.

The anti-inflammatory second phase of the WD and regeneration was initiated at 3dpi in wild type animals. IL10 overexpression was also detected at this

timepoint to balance the proinflammatory events and start the phagocytosis of cellular and myelin debris. Therefore, IL10 was only reduced in proximal segments at 3dpl in P0TNFalpha, to promote the TNFalpha peak necessary to start WD.

The endoneurial production of IL-10 protein decreases significantly after crush in normal phenotypes. IL-10 is the key to promote TNFalpha production and BNB permeability at 3 dpl. After that, anti-inflammatory cytokines, such as IL10, are also induced at 7dpl, determined by macrophage recruitment, which produces large amounts of IL-10. This anti-inflammatory cytokine is also a potent inhibitor of macrophage activity to resolve inflammation and axon regeneration, by the downregulation of inflammatory cytokines, especially TNFalpha to finish WD. The role was demonstrated in IL10 null mice, showing an enhanced and prolonged inflammation with detrimental effects on regeneration (Zhou, 2009; Thompson, 2013).

Increased IL10 levels could be related to a decrease in the number of macrophages infiltrated in sciatic nerves of transgenic P0TNFalpha, as we observed in F4/80 expression and Iba1 immunofluorescence detection.

Moreover the oscillations in TNFalpha in WD and regeneration correlated with the mRNA expression of Egr2, the transcription factor implicated in the regulation P0 myelin protein. Thus, a decline in TNFalpha mRNA is associated to the downregulation Egr2 in both, wild type and transgenic animals, although more evident in wild type mice.

However, changes in the expression of TNFalpha receptors were not detected after crush in wild type animals, while transgenic mice showed a little increase in TNFR1 mRNA compared to intact P0TNFalpha animals at 21dpl. After injury, the relative contribution between TNFR1 and TNFR2 are complex. Although classically, TNFR1 is implicated in the neurotoxic action and TNFR2 in survival, nowadays is known that the relationship between both receptors is more complex (Suvannavejh, 2000; Eugster, 2001). Different authors hypothesized that blocking the signalling pathways of both receptors could be a beneficial effect in early steps of regeneration after nerve injury. However, these actions could be different in other phases or tissues due to the dual roles of TNFalpha (Shohamiet, 1999).

The TNF-TNFR1 complex regulates nerve degeneration. As a consequence, TNFR1 expression is higher at 7dpl to modulate most pro-inflammatory responses (Barbara, 1996; Malek, 1998). TNFalpha, TNFR1, and TNFR2 are greatly increased at 3-5 dpl in DRG, probably related to NP pathways (George, 2005; Vogel, 2006).

Erg2 regulates the expression of TNFalpha, but the main role of Egr2 is the expression of myelin proteins.

A tight regulation of myelin protein are also necessary to be regulated properly in WD and peripheral regeneration. Interruption of axonal contact following nerve transection leads ta dramatic drop in PMP22 and P0 at 3dpl, due to axonal degeneration and the differentiation SCs to an unmyelinated phenotype (Poduslo, 1985). PMP22 and P0 reinduction correlates with the reexpresion of MBP, as well as it was observed in nerve development (Lemke, 1988; Kunh, 1993). Wild type animals had almost a complete regeneration of the sciatic nerves at 21dpl, and myelin protein levels, like MBP, almost achieved sham concentrations. However, a dowregulation in the myelin protein expression was observed in both, distal and proximal stumps, probably as a compensatory mechanism to stop protein production and to maintain normal levels.

On the other hand, uninjured P0TNFalpha animals showed a slight demyelinated phenotype, as explained earlier. However, the degeneration/regeneration process is still ongoing at 21dpl demonstrating the delay in regeneration concordant with myelin protein and mRNA. The proximal section showed pattern of myelin proteins similar to that of uninjured P0TNFalpha animals at 21dpl. Moreover, distal sections were clearly downregualted, probably due to WD is still ongoing distals from the injury site while at that time proximal sections started the anti-inflammatory response followed by the regeneration events, with the increase in IL10 concentration.

Tropic and trophic cues also play important roles in the guidance of axons regrowing towards target tissues (Navarro, 2003). Neuron-glia interactions through basal lamina, ECM-CAMs, cadherins-integrins, as well as by several trophic factors secreted into the extracellular space, are implicated in the axonal microenvironment crucial for regeneration. The tropic and trophic cues can have

both, chemoattractive and chemorepulsive properties to create this permissive environment for axonal growth or a molecular barrier that impairs axonal elongation (Wen, 2006).

The specific receptors for neurotrophic factors, are the Trks (Tyrosine kinase receptors), like BDNF and TrkB. These receptors, are found in motoneurons and sensory neurons in normal/uninjured conditions (Eser, 2009)., although they are upregulated mainly in the distal portion of the injured nerve (Curtis, 1998; Webber, 2008).

Mature SCs have the remarkable capacity to reverse their phenotype and dedifferentiate when they lose contact with axons. Therefore, after a peripheral nerve injury, the molecular markers characteristic of mature SCs are dramatically downregulated as a consequence of axonal degeneration distal to the injury site, whereas markers of immature and non-myelinating SCs are re-acquired (Jessen, 2008). Thus, denervated SCs express several receptors for neurotrophic factors, such as the rapid over expression of the p75NTR, a low affinity receptor for neurotrophins, which can exert pro-apoptotic functions (Bennet, 1996a; Hoke, 2001, 2006); and release neurotrophic and neurotropic molecules to guide by chemotaxis the distal portion of the nerve. Once SCs regain the contact with axons, SCs return to a quiescent state and the expression of these factors and receptors are suppressed (Mackinnon, 1991). Moreover it was demonstrated that the downregulation of p75NTR helps to achieve a proper and functional sensorial and motor reinnervation (Scott, 2010).

Injury often results in the reactivation of signaling pathways only active in development. p75NTR is one of them and contributes to neuronal and glial cell damage, axonal degeneration and dysfunction during injury and cellular stress (Li, 2008; Ibañez, 2012).

Wild type SCs shows a mature and myelinated phenotype at 21dpi and the number is maintained compared to sham animals, although distal sciatic nerve segments have higher concentrations due to that regeneration is almost finished but still ongoing.

Instead, in injured P0TNF α sciatic nerve p75^{NTR} is higher than wild type mice, but not changes from sham transgenic animals. Thus, indicating an immature phenotype of P0TNF α SCs. Protein quantification is clearly higher than uninjured animals at 21dpi while total SCs (S100 positive cells) were reduced. On the other hand, P0TNF α mice showed lower levels (mRNA and protein) of p75^{NTR} and S100 in distal stump compared to sham transgenic mice at 21dpi. Thus, the downregulation of p75^{NTR} is a consequence of the total reduction of SCs in the distal part of the nerve.

In addition different authors published the association to the activation of the p75^{NTR} and apoptotic pathways, being involved the activation of c-Jun and JNK. Moreover the dramatic alteration in p75^{NTR} expression and the reduction of S100 after injury could be explained through these apoptotic events in SCs (Byers, 1992, Arendt, 1995; Zhou, 1996; Syroid, 2000, King, 2000, Xie, 2003), although Caspase3 seems not to be altered in P0TNF α animals, with or without damage.

There is a growing evidence of the important role that p75^{NTR} plays in the myelination process (Chan, 2001; Cosgaya, 2002; Tolwani, 2004). Recently, p75^{NTR} knockout mice showed impairment of remyelination after sciatic nerve injury (Song et al. (2006). Moreover, p75^{NTR} enhances myelination by BDNF in SCs (Cosgaya et al., 2002).

Most of the signalling pathways activated during the myelination process finally converge on the NF κ B upregulation in pre-myelinated SCs. For example, this transcription factor was found in p75^{NTR} positive premyelinating-SCs. Then, NF κ B expression progressively declined and is almost absent in adult mice. Moreover, the inhibition NF κ B also prevents the activation of Oct6, localized downstream in the induction of SCs (Nickols, 2003). NF- κ B is an inducible nuclear transcription factor involves cellular responses to a variety of stimuli such as stress, cytokines, ROS, for example. In addition, this transcription factor has been also associated to the upregulation of antiapoptotic genes and regulates the proliferative checkpoint of the cell cycle, such as cyclin D1, to increase the neural survival (Chu, 1997; Guttridge, 1999).

After injury, there is an early upregulation of the MAPKs, c-Jun, ERK1/2 and p38 in SCs, driving dedifferentiation and proliferation of SCs. The Nrg-ErbB pathway has also a fundamental role in the myelination process. The specific

inhibition of any of these pathways, alters myelin clearance, regeneration, remyelination and neuromuscular junction reinnervation (Ilim, 2017). It will be necessary to study the relative activation of these signaling pathways in P0TNFalpha animals. Probably, the alteration in the myelin process during the development and in WD and regeneration events after peripheral crush injury could be explained by modifications in these pathways. Moreover, if the problem in P0TNFalpha animals is as a consequence of a lack of activation of microglial and macrophages, probably we expect a reduction in the ERK1/2 activation.

In addition, alterations in NFkB expression and protein activation could be tested. It was observed, at least in cardiac myocytes, that the overexpression of TNFalpha is involved in the induction of ROS and iNOS in a dose-dependent manner, as well as the association between TNFalpha and the TNFR1 triggers intracellular signal transduction to activate NFkB through ROS (Bergmann, 2001; Higuera, 2002). Moreover, NFkB acetylations have been recently associated to Sox10, MBP and MPZ down-regulation (Tsukahara et al 2016)

As a consequence, we hypothesize a downregulation in the NFkB in P0TNFalpha transgenic animals after crush injury as well as an upregulation in uninjured transgenic animals as a consequence of increased concentrations of iNOS and ROS due to TNFalpha overexpression.

The role of BDNF in regeneration is controversial (Cosgaya, 2002). Sensory neurons are the major contributing source of the increased traffic in the sciatic nerve. It was demonstrated that BDNF is transported in the anterograde direction (from peripheral to central neurons) (Zhang, 2000; Boyd, 2003; Vögelin, 2006).

In PNS normal conditions, BDNF decrease after myelination. Moreover, deprivation of endogenous BDNF impairs axonal growth and myelination, whereas local infusion improved nerve regeneration (Zhang, 2000; Boyd, 2003; Vögelin, 2006). Related to these observations, P0TNFalpha animals showed an increased expression of BDNF in sensory neurons but not in spinal cord or sciatic nerve compared to wild type mice. In addition, wild type mice downregulate the expression of BDNF at 21dpi in DRG and spinal cord, while injured P0TNFalpha show no differences with uninjured transgenic animals, but the expression is higher than in wild type. These data could suggest that the

myelin process is not completed in transgenic animals at 21dpl as BDNF deprivation negatively affected the axonal growth and myelination.

Chronic NP is a serious disorder of the nervous system, associated with inflammation and neural damage, characterized by hyperalgesia and allodynia. The description of several pro-inflammatory mediators that play a crucial role in the pathogenesis of NP was reported (Zhang, 2007; Fregnan, 2012; Ramesh, 2013; de Oliveria, 2016). Immune and glial cells after PNS injury, generated a cytokine network leading to chronic inflammation which causes NP by direct activation of nociceptors.

Several studies demonstrated that TNF α produces dose-dependent thermal hyperalgesia by release IL1 β (Wtakins, 1995). This hyperalgesia, that was also observed in P0TNF α transgenic model without injury, is blocked by IL1RA antagonist. There was a significant correlation between the level of IL1RA and TNF- α and IL-6. Moreover, plasma levels of IL1RA were closely correlated with the severity of inflammation (Endo, 1996). In addition, IL10 has been shown to prevent mechanical hyperalgesia, after intradermal injection of TNF α , by inhibiting this cytokine (Toews, 1998).

P0TNF α animals showed high expression of both IL1 β and IL6 in proximal and distal segments after damage, although there is a delay in WD and the inflammatory pattern is different compared to wild type mice. Maybe, in the transgenic model, the pattern of cytokine expression is causing the thermal hyperalgesia observed by functional tests after sciatic crush. Moreover, the levels of IL1RA are also upregulated as a compensatory mechanism to mediate in the pain response.

It was demonstrated recently that peripheral nerve injury triggered the upregulation of IL-1 β which could bind to their receptors and transmit signals by the adaptor MyD88. IL-1 β activates calcium mobilization in DRG neurons and stimulate astrocytes or microglia to produce proinflammatory mediators such as TNF- α by NF κ B, MAPK, or IL1RA activation. These mechanism contribute to hyperalgesia and the establishment of peripheral and central sensitization. It was suggested that MyD88 may act through phosphorylated NF κ B and ERK to regulate the expression of proinflammation cytokines and activate glial cells, playing a role in induced neuroinflammation and NP (Liu F et al., 2017). Thus, a

potential strategy for the treatment of NP is to focus on targeting MyD88. Inhibition of MyD88 suppressed the phospho-NF κ B, phospho-p44/42 MAPK, the production of TNF- α , and the activation of astrocytes and microglial cells (Liu, 2017).

Moreover, macrophages regulate, indirectly, the survival of PNS cells and NP through the production of neurotrophic factors, such as BDNF, in the proinflammatory phase of WD and regeneration (Bouhy, 2006; Scholz, 2007). Thus, an increase in Iba1 and GFAP was detected in spinal cord of P0TNF α animals at 21dpi, related to a higher number of macrophages and microglial cells, while wild type animals have been restored at 14dpi.

SCs also express proinflammatory CCL2/MCP-1 and CCL3/MIP-1, immediately after injury. Both of them play an important role in the influx of macrophages into the damaged nerve, showing a maximum peak at 1 dpi (Toews, 1998; Kiguchi, 2010).

In addition a multiplex assay will be performed to confirm the pattern of cytokine expression after injury in the P0TNF α model, as well as the correct activation of infiltrated macrophage. Molecules such as MCSF, that is considered the main responsible for maintaining the activation of microglia (Imai, 2002) will be checked in the assay, together with IL6, IL1 α and β and CCL2.

Although CCL2 was not analyzed by qPCR after crush injury, significant differences were detected in adult P0TNF α animals compared to wild type mice. It was also described that the neuron-macrophage interactions to create an outgrowth-promoting environment, required CCL2 in neurons and its receptor CCR2 in M2 macrophages. However, CCL2 is dispensable for the initial growth response. CCL2 can polarize macrophages to acquire M2 phenotypes in non-neuron environment such as sciatic nerves, as well as in injured spinal cord (Sierra-Filardi, 2014; Lee, 2015; Gadani, 2015). It has been proposed that M2-polarized macrophages make essential contributions to neural repair processes, such as neurogenesis, angiogenesis, remyelination, and axon regeneration (Kigerl, 2009; Hu, 2015).

Upregulation of CCL2 expression is usually limited to several days after injury (Ma, 2002; Perrin, 2005). This result suggests that the acute upregulation CCL2

mobilizes macrophages capable of remove myelin debris at the injury site.

ATF3, an injury neuronal marker, is induced in DRG neurons and SCs after peripheral, but not central, axonal damage. ATF3 promotes regeneration when contact with the target tissue was lost and the expression of ATF3 is down-regulated as a result of reinnervation (Katoka, 2007). The peak of ATF3 is at 3dpl in motor and sensory neurons and is normalized at 12 wpl (Seijffers, 2007).

Accordingly, P0TNFalpha mice show an overexpression of ATF3 in motor neurons of the spinal cord. After crush injury, only the ipsilateral DRGs of the transgenic animals exhibit upregulation of ATF3 at 21dpl, while wild type animals show no differences with or without injury, probably due to the regeneration is almost finished at this time. However, if the ATF3 expression was studied in sciatic nerve at short timepoints after injury, both wild type and transgenic animals have overexpressed this transcription factor at 3dpl by SCs (Hunt, 2004).

Gap43 is also called growth or plasticity protein, because high levels of this protein are expressed in neuronal growth cones during development and axonal regeneration. This protein is considered a crucial component for an effective regenerative response in the nervous system. Although no differences were detected in sciatic nerve of P0TNFalpha animals, Gap43 mRNA was upregulated in DRG of transgenic animals at 21dpl compare to wild type mice, as a consequence, again, of a delay in the regeneration process.

The protective role of macrophages in WD might also be explained by “the alternative activation” of these cells. Macrophages can be polarized in 2 different functional phenotypes in response to different environmental cues (Murray et al., 2014; Wang et al., 2014). The multiplicity of the phenotypes may provide a huge range of tools in addition to their original role as phagocytic cell. Macrophages involved in WD might be polarized to the prolonged M1 phenotype on the first stage (proinflammatory) and to the transient M2 phenotype for the resolution of inflammation (anti-inflammatory). This modulation of M1-M2 phenotype may represent a strategy to promote regeneration (Martinez and Gordon, 2014).

In addition it was demonstrated that soluble TNF α expression, dominated by M1 pro inflammatory macrophages, increases in SCs and in nonneural cells at 1dpl in the distal stump. Normally M1 macrophages, also produce high levels of the oxidative metabolites iNos and ROS as well as pro-inflammatory cytokines.

The second wave of TNF expression occurs at 5dpl to recruit M2 anti-inflammatory macrophages and accelerated the clearance of myelin debris and axonal regeneration by activation of TNFR1 (Shamash, 2002; Siqueira, 2015). These M2 or “alternatively activated” macrophage can be activated also by IL-4 and IL-10. IL-10-null mice showed increased expression of M1 and decreased expression of M2 markers compared with wild types. After nerve transection mice showed a rapid M2 polarization due to a rapid induction of IL-1 β and IL-10 mRNA at 1 dpl.

These studies suggested the ‘double-edged’ characteristics of macrophages and the immune system. Macrophage phenotypes can be dynamically regulated by release of biological cues to the tissue microenvironment, allowing the SC migration and microglial infiltration. Nowadays a new term of “regenerative bias”, based on the ratio of M2/M1 macrophage phenotypes is used to find a direct correlation between macrophage phenotype and the regenerative rate. The SCs proliferation and migration can be affected in a different way by M1/M2 phenotype. Thus, M2 macrophages increased the migration rate of SCs 2-fold compared to M1 (Liefner, 2000; Siebert, 2000).

As a future perspective, it will be also interesting to study the phenotype of macrophages activated and infiltrated in intact and injured peripheral nerves of P0TNF α mice compared to wild type mice. Normally M1 macrophages produce high levels of oxidative metabolites iNOS and ROS as well as pro-inflammatory cytokines. This intracellular signaling pathway stimulates the release of calcium to activate, downstream, MAP kinases and modulate a broad spectrum of cellular responses (Abbas, 2000; Hehlgans, 2002; Boulayet, 2003; Langer, 2004, Adler, 2005, Ydens, 2012).

In order to determine the phenotype of the macrophages it will be necessary to study mRNA expression by qPCR as well as a flow-cytometry detection of the macrophages population. In addition, the analysis of iNOS by western blot, a

marker typically associated with M1 macrophages, in sciatic nerves and spinal cord will be necessary. Local activation of the iNOS-NO system may play an important role in the pathogenesis of peripheral nerve injury and NP (Levy, 1999 and 2001).

Moreover, an important correlation among nitric oxide, WD, NP, and axon regeneration were confirmed (Levy, 1999 and 2001; Keilhoff, 2002) Neuronal NOS (nNOS) seems to be the primary source of NO released after injury, and it is detrimental to the survival of injured motoneurons. Endothelial NOS (eNOS) appears to be the major source of NO that interferes with axonal regrowth, after injury (Keilhoff, 2002 and 2003; Moreno-Lopez, 2010). Finally, several authors demonstrated that iNOS could be a critical factor in the repair of injured tissues. Mice lacking iNOS showed evidence of a regenerative delay, preceded by slow WD, after different types of sciatic nerve injury. These knockout mice also showed fewer and smaller regenerating myelinated fibers, being associated to NP. On the other hand, wild type mice show iNOS mRNA and protein upregulation in both macrophage and SCs, distal to injury site, at 5dpl and 14dpl, when the macrophages infiltration reach their maximum peak in peripheral nerves (Levy, 1999 and 2001). Moreover, IL10 indirectly inhibits iNOs.

Actually, specific inhibitors of NO isoforms can be used to protect injured neurons from degeneration and promote axonal regeneration (Moreno-Lopez, 2010).

Acute crush injury of peripheral nerves induces moderate and transient hyperalgesia and allodynia in response to mechanical or thermal stimulation, as well as pain-related secondary modification are often observed in the controlateral paw. P0TNFalpha animals show only a thermal hyperalgesia at 14dpl and 21dpl. Wild type animals have not differences in pain behavior after sciatic nerve injury.

The remyelination mechanism seems to be initiated first in motor roots than sensorial axons, and knowing that the sciatic nerve is a specific motor branch nerve, probably no changes in mechanical algesimetric test was expected (Abe, 2008). Functional analysis offers the most unequivocal way to demonstrate the nerve regeneration and establish the appropriated end organ connection and functional integrity of peripheral nerves (Nichols, 2005; Vleggeert-Lankamp, 2007). In vivo electrophysiological studies after a nerve crush reported different timelines

in the regeneration process according to the fibre diameter, and the type of peripheral nerve injury protocol (Krarup, 1988; Navarro, 1994; Verdu, 1997).

The compound motor action potential (CMAP) amplitude correlates with the number of functional axons, being an indicator for axonal damage when it is significantly reduced. In a normal situation, sciatic nerve crushed induces a marked decrease in CMAP amplitude at 3dpl. Muscle progressively reinnervates and CMAP amplitude increases, although the amplitude values stay low until 14-21dpl and remains below the basal level up to 5 wpl in gastrocnemius and plantar muscles. Electrophysiological recovery of distal muscles takes more time and is still abnormal 100 days after injury, as well as it is observed in digital nerve (Navarro, 2003). Injured P0TNFalpha mouse model showed clear differences in the amplitude values for sensory responses of digital nerve compared to wild type. As a consequence, times of latency were higher but no differences were observed in sensory velocities. Results confirmed the poor regeneration in the transgenic animals and a possible reduction in conduction velocities after nerve damage related to a delayed demyelinated state (Santos-Nogueira, 2012; Dias, 2013; Conianchi, 2015; Van der Wal, 2015).

Morphometric analyses indicated that in the first period of WD fibre density and myelin thickness decreased. Later, the total number of fibres increased but a significant deficit in large myelinated fibres was described (Fernandez, 1993; Rasband, 1997,2011; Branner, 2004). Thus, wild type animals showed a reduction in axon size diameter at 21dpl compared to uninjured wild type nerves, and the same pattern was observed in P0TNFalpha mice, although the reduction was even higher. In addition, both phenotypes showed also lower myelin thickness than intact nerves, and the results were confirmed by g-ratio calculations.

3. TNFalpha and DM

Nowadays there is not an effective therapy to stop and reverse the axonal degeneration and painful symptoms that characterized peripheral neuropathies. An appropriate animal model is needed to develop effective strategies and replicate the essential features of peripheral neuropathies. Unfortunately, the preclinical data using animal models demonstrated the lack of optimum models and outcome measures to underly the pathogenesis of the disease. In vivo models are critical for understanding DPN pathophysiology and elucidating treatment strategies.

The increasing worldwide prevalence of diabetes has fueled the development of several diabetic mouse models (O'Brien et al., 2014).

DM is one of the main diseases in industrialized countries and the most common metabolic disorder associated with both genetic and environmental factors. Based on the increasing trends toward sedentary lifestyles and the lack of effective treatments, it was estimated that over 360 million of people worldwide will be diagnosed as DM in 2025. Most of these patients will show progressive diabetes-related complications.

The term of metabolic neuropathy includes peripheral nerve disorders associated with systemic dysfunction of metabolic origin, such as DM, nutritional deficiencies and alcoholism. In accordance with their high frequency and severity, diabetic polyneuropathies (DPN) are the most common chronic and severe longterm complication of DM, showing similar prevalence in type I or type II DM, and one of the best studied diseases of PNS pathologies. Hyperglycemia, insulin resistance, and dyslipidemia had been provide as the major factors underlying this disease.

DPN is characterized by painful neuropathic symptoms due to demyelination and motor/sensory axonal loss. Patients at early states of DPN, show no changes in nerve velocities, being necessary the obtention of skin biopsy to evaluate intraepidermal nerve fibers. On the other hand, late stages of DPN show a decrease in sensory nerve action potential amplitude (SNAP) and

SNCV, but an increase in MNCV; associated to axonal degeneration and demyelination related to WD (Misra, 2008; Chung, 2014; Zhang, 2014).

DPN is the result of neuronal stress and abnormal insulin signaling. Although the mechanism of the development of DPN has not yet been fully elucidated, glucose control is the only established effective method. Recently, it was reported the localization of insulin receptors (IRs) on SCs, demonstrating the neurotrophic role of insulin in DPN and PNS.

Several theories have been established to describe the etiology of DPN. It was demonstrated that hyperglycaemia triggers the accumulation of sorbitol and fructose in SCs, according with the role of sugar substitutes and artificial sweeteners in the increase rate of DM prevalence, nowadays (Nseir, 2010; Chattopadhyay, 2014). Moreover the auto-oxidation of glucose produces the induction of reactive oxygen species (ROS) and iNOS (Mittal, 2014; Fakhruddin, 2017). Both of them are related to nerve damage, cellular stress and the production of advanced glycation end products (AGEs). Axons and myelin sheaths become vulnerable to phagocytic attack of circulating macrophages and glia cells as a consequence of AGEs deposition, which are recognized as external antigens (Shi, 2013; Bisht, 2016; Becher, 2017). As a consequence, the BNB (blood-nerve-barrier), necessary to keep the immune tolerance in peripheral nerves, is damaged, which allows immune cells infiltration.

An important observation about different peripheral neuropathies is the increased levels of TNF α in plasma, being implicated in the onset and/or malignant progression of peripheral diseases. For example, elevated levels of TNF α and TNFR1 and TNFR2 receptors, have been reported in the serum of patients with DPN (Nieto-Vazques, 2008; Fernandez-Real, 2010; Leung, 2010; Liu, 2014; Olmos, 2014; Putki, 2014; Sonoda, 2015; Andrade, 2016). Thus, TNF α could be implicated in the BNB vulnerability, promoting T cell proliferation and other inflammatory markers.

A metanalysis study demonstrated that serum TNF α and IL6 could be biomarkers to screen DPN risk and pain. TNF α stimulates the production of IL6 promoting the pathological process of DPN. Anti-TNF α therapies, such as antibodies or soluble fusion proteins acting as competitors of TNF receptors, seem to be a good option for treatments of DPN by reducing serum TNF α

(Okada et al., 2004; Gupta et al., 2005; Mukaino et al., 2010; Tristano, 2010; Singh et al., 2013; Stovicek et al., 2014).

However, the main discrepancies related to the proper generation of a mouse model for the study of peripheral neuropathies, and secondary complications of DM, are consequence of the anatomical differences and the incomparable life expectancies between humans and rodents. Thus, although mouse models for DM type I or DM type II (induced by STZ or genetically modified, such as db/db or ob/ob mice) can develop hyperglycemia and insulin resistance, the life span is shorter to detect severe long-term secondary complications of DM, such as peripheral neuropathy, retinopathies or kidney and heart diseases. These complications generally occur after years of non-controlled high blood glucose, at least in humans (Aaberg, 2008; Kountz, 2012).

Several animal models are described to study DM diseases. For example, NOD animals and STZ-induced mouse model, which is one of the most common DM type1 model, based on the pharmacologic toxicity of STZ to induce β cell destruction.

DM type2, model based on leptin signaling pathways are good models of diabetes due to the early onset of the disease. Moreover, these animals exhibit a clear phenotype of DPN. However, we should consider the systemic consequences of disrupted leptin signaling. Contrary, these mice show a fast decline in hyperglycemia at 4 weeks of age (Clee et al. 2005, O'Brien et al. 2014). High-Fat-Diet mouse models may provide a better model of the human condition, but the variability in diet composition complicates interstudy data comparisons versus laboratories and animal care facilities.

Overall, there is a critical need to explore and characterize novel mouse models that provide clinical relevant representations of human DPN. Moreover, a complete characterization of diabetes, neuropathic phenotype, and metabolic and physiologic profile are essential to understand the implications of DPN (O'Brien et al., 2014).

Nowadays the relation found between DPN and the activation of the TNF-alpha system could be explained by two alternative hypotheses. The first one hypothesized that the generation of oxidative stress factors (ROS and iNOS) and the exposure of macrophage to Advanced Glycosilated Species (AGEs)

both of them induced by hyperglycaemia and insulin resistance, can stimulate the production of the TNF α . Thus, although type I and type II DM show different pathogenesis, it is traditionally assumed that neuropathy is the consequence of hyperglycemia.

A second hypothesis attributes to TNF α the direct pathogenic role in the development of neuropathy. Several studies reported the role of TNF α in the resistance to insulin in type 2 DM by the inhibition of the insulin receptor insulin receptor substrate 1 (IRS1). Thus, the oxidative stress pathway is activated through TNF α -TNFR1 binding (Shi 2013).

Moreover, a positive loop of regulation exists between TNF and DM. NF κ B has been identified as a master piece in the pathogenesis and complications of diabetes. A well-regulated activation of NF κ B in the inflammatory processes is beneficial due to the overexpression of this transcription factor contribute to the progression of diabetic complications. ROS, AGEs, polyol pathways, as well the overexpression of proinflammatory cytokines such as TNF α , IL6, and IL1 β ; are induced by hyperglycemia. All of these factors also induce overexpression of NF κ B, which contributes to further increase proinflammatory cytokine concentrations and oxidative stress, promoting programmed cell death and apoptosis.

On the other hand, several inflammatory microRNAs participate in the regulation of NF κ B activation. microRNA-155 (miR-155) has been recently identified as NF κ B-dependent and a negative correlation, between expression of miRNA-155 in DM and sustained activation of NF κ B was postulated, as a consequence of the remarkable reduction in miR-155 expression levels that was observed in blood and other tissues of diabetic rats (Devier, 2015; Hu, 2015; Li, 2016).

Thus, as well as TNF α is involved in NF κ B pathway, this transcription factor is also involved in the TNF α expression. Moreover, TNF α stimulates the production of ROS to, directly or indirectly, activate even more NF κ B leading to nerve and vascular dysfunctions. p38 MAPK signaling pathways seem to be also implicated in the reduction of TNF α signaling (Sommer, 2001; Myers, 2003; Kato, 2009; 2010).

As a consequence, the generation of an adequate mouse model to DM type1 that exhibits robust peripheral neuropathy is necessary. Accordingly to preliminary results we will need to develop and characterized the neuropathic phenotype of P0TNFalpha-STZ mice, as well as it was done in cruh-injury P0TNFalpha transgenic mice.

In addition, other strategy could be the generation of a double transgenic mice by crossbreeding P0TNFalpha animals and a leptin-based mouse model, for example db/db animals. The advantage is that leptin-based a model show a robust phenotype of DPN (O'Brien et al. 2014) which could be potenciated in P0TNFalpha/dbdb mice.

However, despite the discrepancies between murine models of peripheral neuropathy and human pathology, we think that the P0TNFalpha mouse model generated could be used to allow a better knowledge of the molecular and cellular mechanisms implicated in the neurodegenerative processes of peripheral neuropathy, as well as to help in knowloding the human symptomatology, to test potential neuroprotective compounds and new therapeutic strategies to modulate such pathological conditions. Moreover, P0TNFalpha animal model could be useful in the characterization of chronic pain development and injury, as well as in testing new therapeutic strategies

V. CONCLUSIONS

1. Two transgenic mouse germlines overexpressing TNF- α in myelinating Schwann cells, were successfully generated and named L1 and L4 P0TNF- α , containing a homozygous genotype for the transgene.
2. No statistically significant differences were observed among female or male animals during the experimental procedures. Both sexes were pooled to increase the total animal numbers and improve the statistical analysis.
3. The strong overexpression of TNF- α was confirmed specifically in peripheral nerves.
4. A compensatory mechanism against the effects of TNF- α in peripheral nervous system was observed by means of increased expression of IL10 in P0TNF- α mice, as well as a downregulation of both TNF- α receptors. TNFR1 was altered in the transgenic animal, while TNFR2 did not change.
5. A delay in the process of myelination was detected at the peak expression of myelin proteins (P05), which continued up to P21, coincident with the stabilization of myelin proteins and is maintained to adulthood (P65).
6. Most of the Schwann cells in P0TNF- α exhibit an immature non-myelinated phenotype while wild type animals did not.
7. Morphometrical studies revealed that P0TNF- α transgenic animals show loss of structured myelin, correlating to a slight reduction in the nerve diameter and a significant thinner myelin sheath than wild types. Injury exacerbated the morphometric differences between genotypes.
8. Central nervous system mild inflammation was exhibited in the slight up-regulation of TNF- α mRNA, but not protein, detected in spinal cord and brain of P0TNF- α transgenic animals.

9. Infiltration of macrophages and microglial cells was detected in uninjured sciatic nerves and spinal cord of P0TNF- α animals and it was highly increased after injury and maintained while wild type mice were already fully regenerated,

10. A high expression of molecular factors related to injury (like ATF3, BDNF) as well as sodium ion channels were detected in uninjured adult P0TNF- α animals and these factors were increased after peripheral injury, indicating the development of chronic inflammatory pain.

11. Long-term overexpression of TNF- α in P0TNF- α mice allow for the maintenance of chronic inflammatory pain. Thermal, but no mechanical, nociception are altered in the P0TNF- α mouse, most importantly after peripheral injury.

12. P0TNF- α animals exhibit a delayed recovery in SFI motor functions correlating with slower peripheral myelin regeneration.

13. Electrophysiological studies confirm the delay in peripheral nerve regeneration and the deleterious role of TNF- α for successful initiation and progression of Wallerian degeneration.

14. TNF- α also affects the activation of signalling pathways involved in Wallerian degeneration, like ERK1/2.

15. This model could be useful for the characterization of peripheral neuropathies and chronic pain development and injury, as well as in testing new therapeutic strategies to modulate such pathological conditions.

VI. MATERIALS & METHODS

1. Materials

1.1 Plasmidic vectors

The TNF α cDNA sequence was generously provided by Dr Arthur Feldman from Cardiovascular Institute of the UPMC Health System, Pittsburgh, Pennsylvania. Feldmans's lab used RAW 264.7 cells treated with lipopolysaccharide for 6 hours to generate cDNA of murine TNF α sequence, that was called TNF1.6.

The TNF1.6 sequence was cloned in a pGem-T commercial expression plasmid (**Figure 1.B**).

The construct for P0 promoter, named as pPG6 vector, was provided by Dr. Maria Laura Feltri from San Raffaele Scientific Institute, Milano, Italy.

1.2 Mice

All the transgenic mice used were accomplished in the UAT-CBATEG, in the Universidad Autonoma de Barcelona and supervised by Dr. Anna Pujol.

The genetic background of transgenic mice generated are c57Bl/6J in a 99%. Homozygous animals were selected to perform the experimental procedures.

Mice were bred in the SPF animal facility of the CBATEG which were bred in the Servei d'Estabulari of the Universitat Autònoma de Barcelona. Mice were fed ad libitum with a standard diet (2018S Teklad Global; Harlan Laboratories Inc., Indianapolis, IN, USA) and kept under temperature and light controlled conditions (12 h light and 12 h dark).

1.3 Primer pair sequences

1.3.1 DNA Primers sequences

Primers pairs were used to amplifying specifically DNA sequences

1.3.2 mRNA primers sequences

Specific sequences of primers were used in mRNA expression studies

1.4 Antibodies & counterstaining reagents

Antibodies were used as specific detection reagents in different experiments as western blots, immunofluorescence staining a ELISA.

1.5 Buffer solutions

The standard buffer solutions were used in different experimental techniques. All buffer reagents from Panreac, Castellar del Vallès, Barcelona, Spain.

Phosphate buffer: 0.1 M phosphate buffer pH 7.4, prepared by equilibration of NaH_2PO_4 and Na_2HPO_4 . For 100 ml of phosphate buffer we used 2.565 g of $\text{NaH}_2\text{PO}_4 \cdot 1 \text{ H}_2\text{O}$ and 13.502 g of $\text{Na}_2\text{HPO}_4 \cdot 2 \text{ H}_2\text{O}$.

Carbonate buffer: 0.1 M carbonate buffer pH 9.2, prepared by mixing 1 volume of Na_2CO_3 0.1 M and 9 volumes of NaHCO_3 0.1 M.

D-PBS, Dulbecco's Phosphate Buffer Saline, pH 7.4: 137 mM NaCl, 3 mM KCl, 10 mM Na_2HPO_4 and 1.7 mM KH_2PO_4 . Adjust pH using HCl 37%.

1.6 Imaging equipment

The magnified images of this work were taken using the following devices and software located in the INc-UAB.

Bright-field and epifluorescence microscopy: Nikon Eclipse E-800 microscope with Nikon Digital Camera DXM 1200F and ACT-1 software package (Nikon Corp., Tokyo, Japan).

Confocal microscopy: Leica TCS-SP2 AOBS (Leica Microsystems GmbH, Heidelberg, Germany).

WESTERN BLOT			
PRIMARY ANTIBODIES	name	comercial	dilution
Actina (42kDa)	Polyclonal rabbit anti-actin A2066	Sigma-Aldrich	1:1000
Tubulin (48KDa)	Monoclonal mouse anti-gamma tubiline T6557	Sigma-Aldrich	1:5000
MBP	SMI94R	Calbiochem	1:5000
P0	ab31851	abcam	1:1000
p44/42 MAPK	9102	cell-signaling	1:1000
phospho p44/42 MAPK	9101S	cell-signaling	1:1000
SECONDARY ANTIBODIES	name	comercial	dilution
antirabbit-HRP	swine anti rabbit P0399	Dako	1:10000
antimouse-HRP	sheep anti mouse NA931	GEHealthcare	1.10000
IMMUNOHISTOCHEMISTRY			
PRIMARY ANTIBODIES	name	comercial	dilution
GAP43	antirabbit Ab5220	Millipore	1:500
GFAP	Monoclona mouse anti-GFAP G3893	Sigma-Aldrich	1:500
Iba1	019-19741	Wako	1:500
MBP	SMI94R	Calbiochem	1:500
Oct6		D meijer	1:200
p75NTR	Ab1554	chemicon	1:500
S100	Z0311	Dako	1:500
PGP9.5	RA95101	Ultraclone	1:800
SECONDARY ANTIBODIES	name	comercial	dilution
antimouse-588	alexa fluor 568 goat anti mouse A11004	Molecular probes	1:200
antirabbit-568	alexa fluor 568 goat anti rabbit A11011	Molecular probes	1:200
antirabbit-488	alexa fluor 488 donkey anti rabbit	Molecular probes	1:200
antimouse-488	alexa fluor 488 goat anti mouse A11001	Molecular probes	1:200
antirat-488	alexa fluor 488 goat anti rat A11006	Molecular probes	1:200
antirat-568	alexa fluor 568 goat anti rat A11078	Molecular probes	1:200
cy-3	affini pure donkey anti rabbit 711-165-152	Jackson immunology	1:200
COUNTERSTAINNING REAGENTS	name	comercial	dilution
Hoechst	Hoechst Stain solution	Sigma-Aldrich	1:1

Figure 64. Table to summarize the antibodies and counterstaining reagents used in this work.

PRIMERS DNA GENOMIC		
PCR	Fwd (5' - 3')	Rv (5' - 3')
Ascl-TNFa	GGCGCGCCATGAGCACAGAA	GGCGCGCCCTTCACAGAGCA
Cyclophilin B	CATGCCTATGGTCTAGCTT	GGTTTCTCCACTTCGATCTTGC
qPCR	Fwd (5' - 3')	Rv (5' - 3')
TNFa	TGCCTATGTCTCAGCCTCTT	TTTGAGAAGATGATCTGAGTGTG
Cyclophilin B	TCAACCTCTCCTCTCCTGCC	GGTTTCTCCACTTCGATCTTGC
PRIMERS cDNA		
qPCR	Fwd (5' - 3')	Rv (5' - 3')
m36B4	ATGGGTACAAGCGCGTCTCTG	AGCCGCAAATGCAGATGGATC
18S	GGGAGGTAGTGACGAAAAATAACAAT	TTGCCCTCCAATGGATCCT
TNFa	ACCACGCTCTTCTGTCTTACTG	TTTGAGAAGATGATCTGAGTGTG
P0	TCTCAGGTCACGCTCTATGTC	CAGGTAGAAGAGCAACAGCAG
PMP22	CTCTTGTTGGGGATCCTGTTC	AAGGCGGATGTGGTACAGTTC
MAG	AGCACAGCGTCTGGACATC	GGCCAGCCAGCTCAGCTC
MBP	GGTGCGCCCAAGCGGGGC	ACTTCTGGGGCAGGGAGCC
Egr2	GAAGTGGGAGGCCCTTTG	CAGAGATGGGAGCGAAGCTAC
OCT6	GCGAGCACTCGGACGAGGATGC	GGGGTCATGCGATTCTCCTTCTGA
TNFR1	CTTCTTTGGTGACCGGAG	GACAGTCACTACCAAGTAGG
TNFR2	ACTGCAGCTGTGGGGCACC	CTTAGCACAGCACATCTGAGC
GAP43	AGCCTAAACAAGCCGATGTGCC	TTCGTCTACAGCGTCTTCTCCTCC
ATF3	TGCCAAGTGTGAAACAAGA	TCAGCTCAGCATTCACTC
BDNF	AGTAAACGTCCACGGACAAG	AACCTTCTGGTCTCATCCA
Caspase 3	TCTTCATCATTGAGGCTGCC	GTAGAGTAAGCATAACAGGAAGTC
IL1b	GCAACTGTTCTGAACTCAACT	ATCTTTTGGGGTCCGTCAACT
IL1a	CCCATGATCTGGAAGAGACCA	CAAATTCTGCCTGACGAGC
IL6	TAGTCCTTCTACCCCAATTTCC	TTGGTCCTTAGCCACTCCTTC
IL1RA	GCTCATTGCTGGTACTTACAA	CCAGACTTGGCACAAGACAGG
F4/80	ATGGACAAACCACTTCAAGGC	GCAGACTGAGTTAGGACCACAA
CCL2	ACTCACCTGCTGCTACTCAT	TGGTTCCGATCCAGGTTTTT
Nav1.7	GCCATGGATCCCTATGAATA	CAATCTAAAGGACCGCAGGA
Nav1.8	GATGAGCTCGAGGAAGATGTGG	GCCTGGTGATCTTCACACTTTTGG

Figure 65. Sequence of the pair primers used in this work to perform the mRNA expression analysis (cDNA primers) and to genotype de transgenic animals generated by PCR (DNA genomic) and qPCR (DNA genomic primers).

2. Methods

2.1 Mouse handling

All the experimental procedures with mice were approved by the Comitè d'Ètica en Experimentació Animal i Humana of the Universitat Autònoma de Barcelona.

2.1.1 Surgical procedures

2.1.1.1 *Sciatic nerve injury: crush protocol*

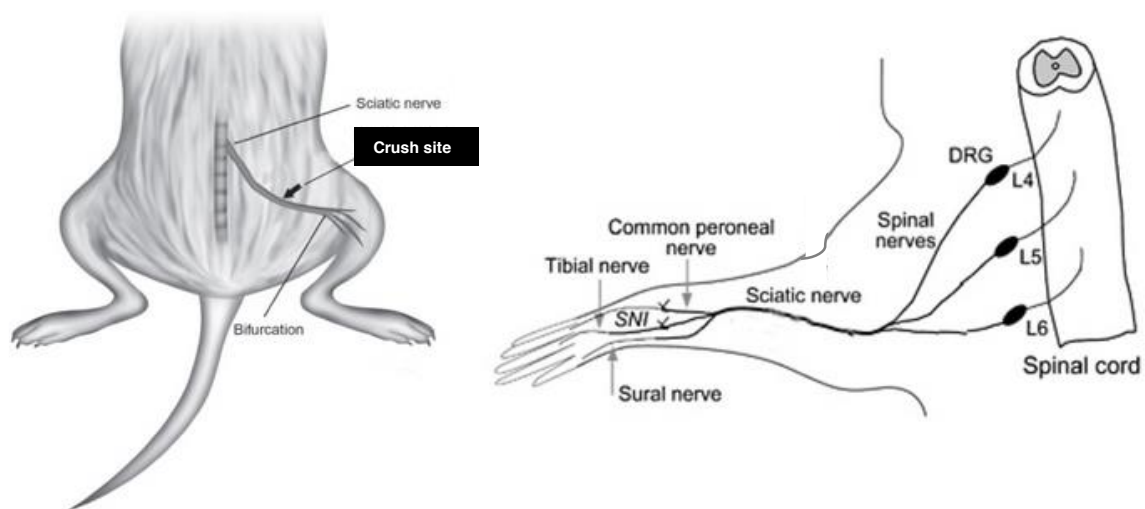


Figure 66. Scheme and site where crush protocol was performed in mouse sciatic nerve-

We used 6-8 week homozygous P0TNFalpha and littermate control wild type mice. Left hindquarters are carefully shaved using a surgical clippers and depilation is completed with a removal surgical blade. Skin is cleansed using sterile cotton tipped applicators and betadine surgical scrub. Ophthalmic ointment is applied to the eyes using sterile cotton tipped applicators. The mouse is placed on a clean stainless steel plate, under which has been placed a pre-heated homeothermic blanket system trying to maintain animal temperature at 37°C. All limbs are taped down, with care taken to position the hind limbs symmetrically so that the knee joint makes an anatomical normal angle with the body. All instruments are sterilized by autoclave.

After preparation, a semi-circular incision across midline is made in the skin. The skin is gently dissected from the underlying musculature, and folded over to remain out of the way during the procedure. Opening the fascial plane between the gluteus maximus and the anterior head of the biceps femoris reveals the sciatic nerve. For a surgical control, the contralateral right sciatic nerve are not exposed. Sham animals were used as control, and their left sciatic nerve should be exposed. The gluteal musculature is then re-opposed and sutured using a 6-0 braided silk, non-absorbable sutures.

The experimental sciatic nerve is then exposed using inexpensive hardware supplies and insect pins. The sciatic nerve is then gently freed from the surrounding connective tissue using iridectomy scissors. Using a fine 5/45 forceps, the nerve is placed on the bottom jaw of a hemostatic forceps. The crush is made perpendicular to the nerve at 45 mm from the third toe, as measured by a thread that approximates the path of the sciatic nerve. The nerve is crushed once for 30 seconds at 3 clicks of the hemostatic forceps. Care is taken not to stretch the nerve. When the hemostats are re-opened, the entire nerve should be translucent at the crush site. The nerve is crushed at the same crush site is marker wit a medical steril marker. This is particularly important if precise marking of the crush site is required. The gluteal musculature is re-opposed and sutured in the same way as the sham animals. Finally, the skin incision is closed using 9 mm reflex clips (Homs, 2010; Bauder, 2012).

Following the procedure, animals are placed on a heating pad at 37°C until they show signs of movement. They are then moved back to their home cage, where water and food are readily accessible on the floor.

2.1.1.2 SCs *primary cultures*

This protocol assumes that the sciatic nerve will be used as the source of Schwann cells because of its large size and easy accessibility. However, any peripheral nerve, or combination of nerves, can be used as a starting source. This protocol is designed for processing an entire litter or more, but can be carried out with as little as a single nerve.

Neonatal mice from postnatal day 0 (P0) to P5 are decapitated and pinned on a dissecting board, ventral-side down, and the dorsal skin is removed from the legs and lower torso. The sciatic nerve is isolated away from the surrounding muscle and connective tissue, cut at the knee and the lower back, and transferred to a collection tube filled with ice-cold buffer. The collected nerves are then enzymatically and mechanically dissociated. The Schwann cell enriched population is plated, and then freed of contaminating fibroblasts.

2.1.1.3 *Anesthesia and euthanasia*

For surgery procedures and before perfusion, mice were anesthetized by intraperitoneal injection of a mix of ketamine (Imalgene 50 mg/ml; Merial Laboratorios, Tarragona, Spain) and xylazine (Rompun; Bayer AG, Leverkusen, Germany) diluted in 0.9% saline solution (B.Braun Medical S.A., Rubí, Barcelona, Spain). The dosage for C57BL/6 mice was 120 mg/kg of ketamine and 12 mg/kg of xylazine.

For electrophysiology studies, animals were anesthetized by pentobarbital.

Euthanasia of the mice was performed by different means, depending on the subsequent use of the mouse samples. In order to obtain fresh tissue samples, mice were first anesthetized by inhalation of isoflurane (Isoflo; ESTEVE, Barcelona, Spain) in a closed chamber, and decapitation was performed using scissors. When required, blood samples were taken at the moment of euthanasia. Then, organs and tissue samples were taken and put into 1.5 ml eppendorf tubes, which were flash frozen into liquid nitrogen and preserved at -80°C until they were required.

In order to obtain fixed tissue samples, mice were perfused with 4% paraformaldehyde (PFA). First, the mouse was anesthetized with ketamine/xylazine. Then we performed an incision to the abdominal wall and the torax, in order to expose the liver and the heart. Some cuts were done to the liver, so that the blood could be drained. Using a 27 G needle, 15 ml of phosphate buffer were injected to the left ventricle of the heart, leading to clearance of the blood from organs and tissues. Then, 20 ml of 4% PFA were delivered to the left ventricle of the heart, achieving proper fixation of the organs

and tissues of the mouse. Organs and tissues were dissected and kept in 4% PFA at 4°C until processing.

4% PFA: PFA in powder (Sigma-Aldrich, St. Louis, MO, USA) diluted in phosphate buffer 0.1 M pH 7.4. Overnight stirring at 60°C was required for proper dilution, followed by filtration.

2.1.2 SFI determination

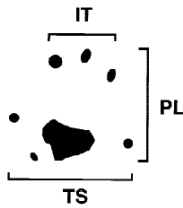
Sciatic Functional Index (SFI) on walking tracks described by Inserra et al. was used to assess the locomotor recovery of the animals after sciatic crush injury (Inserra, 1998)

2.1.2.1 *Walking tracks*

All animals underwent preoperative and postoperative walking track analysis in a fashion similar to that described for rats by de Medinaceli et al. Pawprints were recorded by moistening the hindpaws of each animal with blue inkstick and having them walk unassisted along a 6×44cm corridor lined with white paper. Postoperative tracks were obtained 48 hours following surgical intervention. All tracks were obtained and analyzed in a blinded fashion. Prints for measurement were chosen for clarity and consistency at a point when the mouse was walking at a moderate pace. If necessary, the animals were walked multiple times in order to obtain measurable prints.

The tracks were evaluated for four different parameters: toe spread (TS), the distance between first and fifth toes; intermediate toe spread (IT), the distance between the second and fourth toes; print length (PL), the distance between the third toe and the hind pad. Measurements of all the parameters were made for the right (normal) and the left (experimental) pawprints. This analysis was whether or not a nerve was transected, where a transected nerve lesion was defined as -100 and a sham operation was defined as 0.

$$SFI = 118.9 \left(\frac{ETS - NTS}{NTS} \right) - 51.2 \left(\frac{EPL - NPL}{NPL} \right) - 7.5$$



E = experimental
 N = normal
 TS = toe spread
 PL = print length

Figure 67. SFI equation by Inserra et al.
 Adpated from Medinaceli et al.

2.1.3 Functional tests

2.1.3.1 *Electrophysiology & nerve conduction tests*

Motor nerve conduction test were performed at 14 dpl and 3 weeks after cursh surgery (9 weeks of age) when animals were finally sacrificed to collect the tissue samples. The sciatic nerve was stimulated percutaneously by means of single pulses of 0,02 ms duration (Grass S88) delivered through a pair of needle electrodes placed at the sciatic notch. The compound muscle action potential (cAMP, M wave) was recorded from tibialis anterior (TA) and the plantar (interossei) muscles with microneedle electrodes. For evaluation of the motor central pathways, motor evoked potentials (MEP) were recorded from the TA and plantar muscles in response to transcranial electrical stimulation of the motor cortex by single rectangular pulses of 0.1 ms duration, delivered through needle electrodes inserted subcutaneously, the cathode over the skull overlaying the sensorimotor cortex and the anode at the nose. All potentials were amplified and displayed on a digital oscilloscope (Tektronix 450S) at settings appropriate to measure the amplitude from baseline to the maximal negative peak. During the tests, the mice body temperature was kept constant by means of a thermostated heating pad.

2.1.3.2 *Algesimetry & sensory threshold measurement*

14 or 21 days before surgery, all of the injured animals were habituated to the experimental devices, by allowing them to explore the apparatus for 20 minutes and then starting the test for baseline nociceptive thresholds recording. The nociceptive behavior tests for mechanical and thermal stimuli were performed

on both hind paws before and at different days after injury. In postoperative sensory tests, the experimenter was blind to the assignment of rats to the different groups. Because in this injury model responses in the sciatic territory are completely lost until its regeneration, a medial and a lateral test sites were used to differentiate changes in sensory thresholds produced by saphenous nerve sprouting from those because of sciatic denervation/ regeneration. Sensitivity to mechanical stimuli was measured by means of an electronic Von Frey algesimeter (Bioseb, Chaville, France). Mice were placed on a wire net platform in plastic chambers 10 minutes before the experiment for habituation. A nonnoxious pointed probe was gently applied to each test site, and then the pressure was slowly increased. The threshold was expressed as the force (in grams) at which rats withdrew the paw in response to the stimulus. A cutoff force was set at 40 g, when the stimulus lifted the paw without response. The mechanical nociceptive threshold was calculated as the mean of 3 measurements per test site, with a 3-minute interval between each measurement. Thermal sensitivity was assessed by means of a Plantar test algesimeter (Ugo Basile, Comerio, Italy). Mice were placed into a plastic box with an elevated plexiglass floor. The beam of a lamp was pointed at the same test sites as above in the hind paw plantar surface. Intensity was set to low power (40 mW/cm) with a heating rate of 1 °C/s to elicit activation of unmyelinated fibers. A cutoff time for the stimuli was set at 20 seconds to prevent tissue damage. Heat pain threshold was calculated as the mean of 3 trials per test site, with a 5-minute resting period between each trial, and expressed as the latency (in seconds) of paw withdrawal response.

2.1.4 Sample extraction & collection

Animals anesthetized were dissected immediately after decapitation. Tail tips, sciatic nerves, dorsal root ganglia and spinal cord were extracted, quickly frozen in liquid nitrogen and kept at -80°C until be used.

Sciatic nerve and DRG pools where used for protein and RNA extraction. Of young P05 animals to increase the concentration.

2.2 Biochemical techniques: DNA obtaining & manipulation

2.2.1 Genomic DNA extraction & quantification

Till usage the mouse tails were kept at -20 °C. They were weighted, cut and incubated in digestion buffer (12 ul/mg tail) at 50 °C between 12 h and 18 h at 160 rpm. Same amount of Phenol/Chloroform (Panreac) was added, vortexed and centrifuged (Eppendorf Centrifuge 580412) at 1700 rpm for 10 min. The aqueous (upper) phase, which contained the DNA, was transferred into a new tube. To precipitate the DNA, 3M sodium acetate (1/2 of the volume of used digestion buffer, Panreac) and absolute ethanol (double of the volume, Panreac) was added gently and mixed. The observed “jelly-fish” was centrifuged at maximum speed for 10 min, the supernatant removed and cleaned with 70 % ethanol. After a centrifugation for 5 min at maximum speed, the supernatant was discarded and the pellet dried and resuspended in 75 ul TE buffer.

To quantify the DNA, the NanoDrop ND-1000 (NanoDrop Technologies) was used.

Digestion Buffer: 100 mM NaCl (Panreac); 10 mM Tris pH 8 (Sigma); 25 mM EDTA pH8 (USB); 0,5 % SDS (Amresco); 0,2 mg/ml Proteinase K (Roche) added before use.

TE Buffer: 10 mM Tris pH 8 (Sigma); 1 mM EDTA (USB).

2.2.2 Genotyping by Genomic DNA PCR

The following PCR program was used (Eppendorf Mastercycler gradient).

Heating: 90°C for 5 min. Denaturing DNA strands: 95°C for 10 sec. Primer annealing: 60°C (Ascl-TNF- α) or 58°C (Cyclophilin B) for 30 sec. Elongation: 72 °C for 30 sec. 95 °C for 10 sec. Repetition of step 2. – 4. for 35 times.

In each PCR tube or well of 96 plate, the master mix and 2.0 ul 10 ug/ul DNA was added. The products were mixed with xylene cyanol loading buffer and checked in a 1% agarose (Lonza) / TAE gel with the GeneRuler™ 1 kb DNA ladder (Fermentas).

Master mix: 500 u, 5 u/ul, DreamTaq™ Polymerase (Fermentas); 25 mM dNTPs (Fermentas); 10x Taq buffer incl. MgCl₂ (Fermentas); 10 pmol/ul forward primer (Invitrogen); 10 pmol/ul reverse primer (Invitrogen); Sterile H₂O (Braun). Total volume: 23,0 ul.

Xylene cyanol loading buffer: 50 % Glycerol (Panreac); 100 mM EDTA pH8 (USB); 1% SDS (Amresco); 0,1 % Xylene cyanol (Sigma) in ddH₂O

50x TAE Buffer: 242 g Tris (Sigma); 57,1 ml Glacial acid (Panreac); 0,5 M EDTA pH 8 (USB) in ddH₂O, autoclaved.

2.2.3 Genotyping by Genomic DNA qPCR

2.2.3.1 *qPCR from genomic DNA*

The Real Time PCRs were performed with the BioRad CFX96™ or CFX384™. The following master mix was prepared and 2 ul of 20 ug/ul DNA. A three step Real Time PCR program was designed: Heating: 95 °C for 3 min, Denaturing DNA strands: 95° C for 10 sec. Annealing primers: 58 °C (All primer pairs except TNFalpha) or 60 °C (TNFalpha) for 30 sec. Elongation: 72 °C for 30 sec 5. 95 °C for 10 sec. Repetition of step 2. – 4. for 40 times.

A melting curve between 55 °C and 95 °C was created to obtain information about primer dimers.

qPCR Master mix: 2x SybrGreen (BioRad); Sterile H₂O (Braun); 10 pmol/ul forward primer (Invitrogen); 10 pmol/ul reverse primer (Invitrogen). Total volume: 8,0 ul/well.

2.2.3.2 *Transgene copy number determination*

To evaluate the transgene copy number, two standard curves were done, with a scale from 20 to 0,002 pg of CAG-TNFalpha (produced in our laboratory) or the purified PCR product of cyclophilin B, diluted with salmon sperm (Sigma). The equations of the standard curves were used, to determine the concentration in pg, according to the obtained Cqs of the Real Time PCRs.

Cyclophilin B product: 133 bp

TNF α product: 171 b

Calculations:

molecular weight dsDNA: bp x 660 Da = bp x 660 g/mol

ng dsDNA x (1 nmol dsDNA)/ (bp x 660 g/mol) x (1 mol dsDNA)/ (10⁹ nmol dsDNA) x (6,02 x 10²³) copies/ (1 mol)

ng dsDNA = 9,12 x 10¹¹ copies per genome/bp

2.2.3.3 *Zygoty of transgenic animals*

After a regular PCR to exclude wild type animals, qPCRs were performed to distinguish between homozygous or heterozygous animals. Therefore cyclophilin B (housekeeping gene, one copy/genome) as well as TNF α was analyzed. For homozygous animals of the F1, the means of the Cq's were calculated for each line. For the animals of the F2, the following calculation was done (based on Pfaffl, 2001):

$$\frac{2^{(Ct(TNF-\alpha)_{mean_line} - Ct(TNF-\alpha)_{sample})}}{2^{(Ct(Cyclophilin B)_{mean_line} - Ct(Cyclophilin B)_{sample})}}$$

Figure 68. Equation for zygosity determination and differentiated between homozygous and heterozygous transgenic animals.

Expected values were about 1 for heterozygous animals and 2 for homozygous ones and minor than 0 for controls wild types animals.

2.3 Biochemical techniques: RNA obtaining & manipulation

2.3.1 RNA extraction & quantification

During all the procedure gloves were worn and all the materials cleaned with 70 % ethanol (Panreac) and RNaseZap (Ambion) to ensure an RNase free environment. Filter tips and RNase free solutions were used and the samples were kept on ice. Before the samples were thawed, the QIAzol (QIAGEN) was added: 400 ul per 2 sciatic nerves and they were manipulated with a micropestle (Eppendorf) to break the cells. The samples were centrifuged

(Eppendorf centrifuge 5415R) at 12000 g for 10 min at 4°C. The supernatant was transferred into a new tube and the samples kept on RT for 5 min. Eighty µl of chloroform (Panreac) were added to the samples and incubated on RT for 3 min. A centrifugation for 15 min at 12000 g and 4°C was performed. The upper phase was transferred to a new eppendorf tube and 200 µl of isopropanol (Panreac) added to precipitate the RNA. The tube was inverted to mix the solutions and they were incubated for 10 min at RT, a centrifugation followed. The pellet was washed with 400 µl 70 % ethanol (Panreac) and centrifugated for 7500 g, 4°C and 5 min. The supernatant was aspirated again and the pellet dried and resuspended in 20 µl DEPC water. The quantification was done with the NanoDrop ND-1000(NanoDrop Technologies).

DEPC water: 0,1 % Diethylpyrocarbonate (Sigma) in H₂O at 37°C (o/n). Two times autoclaved.

2.3.1.1 *Automated electrophoresis – Experion™*

To check if the RNA degraded during the process of extraction, the samples were loaded on a Experion™ (BioRad) chip and a automated electrophoresis was performed. With this technique the ratio between the 18S and 28S RNA was calculated and the samples were listed with the corresponding color: Green (extraction of the RNA was successful) or Red (degraded RNA).

2.3.2 Retrotranscription

Therefore 1 µg of RNA was prepared and mixed with DEPC water till the final volume of 7,5 µl was reached. The samples were incubated at 65°C for 20 min and the following master mix (7,5 µl sample) was prepared with the components of the Omniscript RT.

2.3.4 qPCR procedure

Quantitative PCR (qPCR) was performed using 384-well plates and the thermocycler Bio-Rad CFX284 (Bio-Rad, Hercules, CA, USA). Each sample or standard was analyzed in triplicate, in a total volume of 10 µl, which included 5 µl of iTaq Universal SYBR Green Supermix (Bio-Rad) and 0.4 µl of each primer. The PCR program included the following steps: Hot start at 95°C for 3 min; 40 PCR cycles of 3-step amplification (10" denaturing at 95°C, 20" annealing at

58°C and 20" extension at 72°C); denaturing 10" at 95°C; melting analysis (stepwise temperature increase from 65 to 95°C, in 0.5°C steps and 5" periods). Fluorescence was measured in the extension step of the PCR and during the melting process. For each well, obtained an amplification curve from the PCR procedure, from which a Cq value was extracted using Bio-Rad CFX Manager software (Bio-Rad, Hercules, CA, USA) and used for vector genome copies calculation. We also obtained a melting curve from the melting analysis, which was used for quality control of specific amplification.

2.3.4.1 *qPCR data analysis*

Data obtained with the qPCR were a Cq value for each reaction, and replicates were checked for homogeneity and reliability with Bio-Rad CFX Manager software (Bio-Rad, Hercules, CA, USA) and finally analyzed by kPCR software, development by Dr Miguel Chillón and of iner use in our lab after being checked by biostattisc experts and compared versus other programs and available commercial softwares.

2.4 Biochemical techniques: Protein obtaining & manipulation

2.4.1 Protein extraction and quantification

2.4.1.1 *Protein extraction*

Fresh tissue samples were flash frozen in liquid nitrogen immediately after dissection and kept at -80°C until processing.

To homogenize the samples, 60 to 1000 µl of RIPA lysis buffer were used, depending on the approximate weight of the sample (400 µl for sciatic nerves or soinal cord, and 200 µl for DRG). Samples were kept on ice and underwent sonication at 40 Hz with an ultrasonic processor (Vibra-cell™; Sonics & Materials Inc, Newtown, CT, USA) until they were completely homogenized, followed by centrifugation to eliminate cellular membranes and debris (10-15 min, 12000 rcf, 4°C using Eppendorf 5415R; Eppendorf AG, Hamburg, Germany). Protein homogenates were kept at -20°C.

RIPA lysis buffer: 50 mM Tris-HCl pH 7.4 (Sigma-Aldrich), 150 mM NaCl (Panreac), 1 mM EDTA (USB, Affymetrix, Santa Clara, CA, USA), 1% NP-40

(Sigma-Aldrich), 0,25% sodium deoxycholate (Sigma-Aldrich), 50 mM sodium fluoride (Sigma-Aldrich), 1 mM sodium ortovanadate (Sigma-Aldrich), 10 mM β -glycerophosphate disodium salt hydrate (Sigma-Aldrich), 5 mM sodium pirophosphate decahydrate (Sigma-Aldrich) and a protease inhibitor cocktail (concentration following manufacturer's instructions; Calbiochem, Merck-Millipore, Merck KGaA, Darmstadt, Germany).

2.4.1.2 *Protein quantification*

Protein quantification was performed by Pierce BCA Protein Assay Kit (Thermo Fisher Scientific, Waltham, MA, USA) following manufacturer's instructions. Briefly, 10 μ l of a 1:10 dilution of each protein sample were placed in a non-sterile 96-well microtiter plate (note that some samples required 1:5 or 1:20 dilution to fit in the standard curve). To start de reaction, 200 μ l of the protein assay reagents mix were dispensed per well, and the reaction was conducted at 37°C for 30 min. Absorbance reading at 520 nm was carried out with a microplate reader (Power Wave HT; Bio-Tek, Winooski, VT, USA) and the associated software (KC4 v3.3; Bio-Tek, Winooski, VT, USA). All samples were analyzed in duplicate.

2.4.2 Western blot

The analysis of protein samples by western blot allows the identification of specific proteins, and also a relative quantification by subsequent image analysis software. First, a denaturing polyacrylamide gel electrophoresis (SDS-PAGE) separates the proteins by their molecular weight. Then, proteins are transferred to a PVDF membrane, on which the immunodetection of the desired proteins is performed using specific antibodies and a chemiluminescent reagent. The images of the immunodetection can be quantified by specific image analysis software, allowing the comparison of the amount of protein between different samples. Before comparing between different samples, they are normalized by the total amount of protein by a loading control. The loading controls used in this work were tubulin and actin, two proteins of the cytoskeleton.

2.4.2.1 *Sample preparation*

Tissue samples previously homogenized and quantified were used for western blot analysis. For each sample, 20 µg of protein were diluted in deionized water to an adequate volume before the addition of the appropriate volume of 6X loading buffer. Samples were denatured for 10 min at 98°C before loading to the electrophoresis gel. With this process, proteins are denatured and get a negative charge relative to their molecular weight that allows the separation by electrophoresis. To identify the molecular weight of the proteins, standards are required in each western blot (PageRuler Prestained Protein Ladder, Thermo Fisher Scientific, Waltham, MA, USA).

6X Loading buffer: 0.35 M Tris-Cl pH 6.8 (Sigma-Aldrich), 3.3% glycerol (Sigma-Aldrich), 10% SDS (Amresco, Solon, OH, USA), 0.015% bromophenol blue (Sigma-Aldrich), 0.6 M DL-dithiothreitol (Sigma-Aldrich).

2.4.2.2 *Denaturing gel electrophoresis*

Homemade discontinuous denaturing polyacrylamide gels were used for electrophoresis. The stacking part of gel allows the loading of the samples into wells and their concentration before entering the resolving gel, where they get separated depending on their molecular weight. Stacking gel contains 3.9% acrylamide while the percentage of acrylamide of the resolving gel depends on the molecular weight of the proteins to be resolved (i.e. 10% for P0, actin or tubulina, ERK1/2; and 12% for MBP, in this work).

Electrophoresis was run using an electrophoresis chamber (Mini-Protean® Tetra Cell, Bio-Rad, Hercules, CA, USA) filled with electrophoresis buffer and connected to a voltage source (Bio-Rad, Hercules, CA, USA). After loading the samples and the molecular weight marker into the wells of the gel, electrophoresis was run at low voltage (80-100 V) for 10-15 min until proteins reached the resolving gel. Then it was raised to 130-150 V until the end of the run, which was defined checking the prestained protein standards mobility.

Tris SDS: 0,5 M Tris Base (Panreac); 4 % SDS (Amresco). Adjust to pH 8.8 or 6.8.

Preparation of the stacking gel: 3.9% Acryl/Bis 29:1 40% w/v solution (Amresco, Solon, OH, USA), 0.5 M Tris-HCl pH 8.8 (Sigma-Aldrich), 0.4% SDS ().

Preparation of the resolving gel: 10-12% Acryl/Bis 29:1, 1.5 M Tris-HCl pH 6.8, 0.4% SDS. For polymerization, add 25-50 μ l of ammonium persulfate (Amresco) and 5-10 μ l of TEMED (N, N, N', N', tetrametil-etilen-diamine, Sigma-Aldrich).

1x Electrophoresis buffer: 25 mM Tris (Sigma-Aldrich), 192 mM Glycine (Serva Electrophoresis GmbH, Heidelberg, Germany), 1% SDS (Amresco).

2.4.2.3 *Transfer and blocking*

After electrophoresis, proteins were transferred to a PVDF membrane (Amersham Hybond P 0.2 PVDF, GE Healthcare, Waukesha, WI, USA.) using a semidry electrotransfer system (Trans-Blot[®] SD Semi-Dry Transfer Cell, Bio-Rad, Hercules, CA, USA) connected to a voltage source (Bio-Rad, Hercules, CA, USA). Before, transfer, PVDF membrane required activation in methanol for 10 seconds, followed by a 5-min wash in deionized water and a 10-min equilibration in transfer buffer. Polyacrylamide gel required 10-min equilibration in transfer buffer as well. The transfer sandwich was formed with the gel and the membrane stacked together within two thick filter papers (extra-thick blot paper) previously soaked in transfer buffer. Transfer was performed at 25 V during 45 min. Then it was checked by staining the membrane with Ponceau solution during 5 min shaking, followed by destaining with deionized water.

1x Transfer buffer: 25 mM Tris (Sigma-Aldrich), 192 mM Glycine (Serva), 20% methanol (Panreac)

Ponceau solution: 0.5% Ponceau S (Sigma-Aldrich), 1% acetic acid (Panreac).

2.4.2.4 *Immunoblotting*

For the detection of the desired proteins, specific primary and secondary antibodies are used. The antibodies used in this work are specified in table MM1, together with the dilution used for each one. Secondary antibodies are conjugated to horseradish peroxidase (HRP), which cleaves a chemiluminescent agent and the reaction produces luminescence in proportion to the amount of protein. This luminescence is detected and can be quantified.

In order to avoid non-specific binding of the antibodies to the membrane, it was blocked with the blocking solution for 1 hour shaking at RT prior to immunodetection. Membrane was incubated with the primary antibody diluted in blocking solution overnight shaking at 4°C. Three 10-min washes with TBS-T were performed before incubation with the secondary antibody. This was diluted in blocking solution and incubated shaking at RT for 1 hour. Three 10-min washes with TBS-TWEEN were used to remove the excess of secondary antibodies prior to immunodetection.

1x TBS: 50 mM Tris (Sigma-Aldrich), 136 mM NaCl (Panreac), 40 mM KCl (Panreac); pH 7.3

TBS-T: 0.1% TWEEN-20 (Sigma-Aldrich) in TBS

Blocking solution: 5% non-fat dry milk in TBS-T. To phosphorylated antibodies use 0,5% BSA (Bovine serum albumin) or check the commercial specifications.

2.4.2.5 *Chemiluminescent detection and quantification*

Immunodetection was performed by 5 min incubation at RT with a chemiluminescent substrate (EMD Millipore Immobilon™ Western Chemiluminescent HRP Substrate, Thermo Fisher Scientific, Waltham, MA, USA) using ChemiDoc™ MP System (Bio-Rad, Hercules, CA, USA) for luminescence detection. Luminescence data were acquired at different exposition times, and the best acquisition file was considered to be the one that displayed higher signal without image saturation. The best acquisition file was used for density quantification using Quantity One® software (Bio-Rad, Hercules, CA, USA).

2.4.2.6 *Membrane stripping*

The following two ways of stripping were performed at two different stringencies. To remove totally the antibodies and probably also membrane bound proteins, the stripping buffer was used. This was done if an incubation with a “total”-antibody after the “phosphorylated”-antibody was performed (for example: (p) ERK1/2 and ERK1/2). Therefore the membrane was put into a bag with 50 ml stripping buffer at 55 °C for 1 h, shaking. Afterwards the membrane was washed shortly with H₂O, then 3 times 10 min with TBST and blocked with 5 %

milk (Asturiana)/TBST for 1 hour.

Stripping buffer: 2103 μ l β -Mercaptoethanol (Sigma); 20 ml SDS 10 % (Amresco)

31,25 ml 200 mM Tris pH 6,7 (Sigma); 46,65 ml ddH₂O

2.4.3 ELISA

The ELISA of protein extracts of the sciatic nerves homogenates were performed with comercila kit especific for mouse TNFalpha detection and mose IL10, following the manufacturer's instructions.

Microplate reader: PowerWave HT (BIO-TEK®)

Software reader: KC4™ v3.3 (BIO-TEK®)

2.4.3.1 *mouse TNFalpha ELISA*

Comercial ELISA kit for Mouse TNFalpha (KMC3011, 96 tests) supplied by Invitrogen™

The kit is a solid phase sándwich ELISA with a monoclonal antibody specific for Mouse TNFalpha. During the first incubation (90min at RT) the antigen (50 μ L) binds simultaneously to the immobilized antibody to be capture don one site, and to the solution phase biotinylated antibody (50 μ L) on a second site. After removal of excess second antibody, streptavidin-peroxidase (100 μ L) is added to bind to the biotinylated antibody to complete the four-member sandwich. After a second incubation (30 min RT) and washing to remove all the unbound enzyme, a substrate solution (100 μ L) is added, which is acted upon by the bound enzyme to produce color (30 min RT). The intensity of this colored product is directly propotional to the concentration of mouse TNFalpha present in the original specimen. A stop solution (100 μ L) is added and read the plate at 450 nm. The total time invert 2.5 h.

The minimun detectable dose of mouse TNFalpa is <3pg/mL.

2.4.3.1 *mouse IL10 ELISA*

Comercial ELISA kit for IL10-mouse (ab108870) supplied by abcam® for the quantitative measurement of mouse IL10 in tissue extracts.

The minimum detectable dose of IL10 is typically 20pg/mL.

The assay is performed at RT. The sample (50uL) is added to each well used and incubated 2h. Wash 4-5 times and add biotin antibody (50uL) and incubate 2h. Wash again and add streptavidin-peroxidase conjugate for 30 min. Wash and add chromogen substrate (50ul) and incubate 10 min until the optimal color density develops. Add stop solution (50uL) and the color will change from blue to yellow. Read the absorbance on a microplate reader at 450nm immediately and if wavelength correction is available, subtract readings at 570 nm from those at 450 nm to correct optical imperfections.

2.5 Histological analysis

2.5.1 Morphometrical analysis

2.5.1.1 *Sample preparation*

After sample obtention, the manipulation and preparation of tibialis nerves were done by the Servei de Morfologia from Centro de Biotecnologia Animal y Teràpia Gènica (CBATEG-UAB). The tibial nerves of the mice were kept in fixing solution (Glut-PFA, 2,5% : 2%), embedded in epon/spurr and cut into 0.5 um slices and stained with toluidine blue to visualise the myelin.

2.5.1.2 *Morphometric procedure*

Pictures at 100x magnification (microscope: Olympus BX- 40, camera: DP-10) were taken, 300 axons and myelin sheets selected and digitalised with the Intous3 Pen Tablet (Wacom). The diameter of the axon and the fiber was calculated with the program ImageJ (<http://rsbweb.nih.gov>).

2.5.2 Immunohistochemistry

The immunofluorescence technique consists in the labeling of antigens on fixed tissue by specific antibodies and fluorophores. Primary antibodies are used

specific for the antigens and secondary antibodies conjugated to fluorescent molecules to final detection.

2.5.2.1 Sample processing

Fixed tissues were kept in 4% PFA at 4°C from dissection until processing. During the day, several 1-2 hour washes with PBS shaking were performed to remove the excess of PFA of the samples. Then, samples were submerged in a solution of saccharose 30% (Panreac, Castellar del Vallès, Barcelona, Spain), in D-PBS and left at 4°C shaking during 24-48 hours, until the saccharose had penetrated into the sample and the sample did not float on the solution anymore. Each sample was placed into a Cryomold® and embedded in Tissue-Tek® O.C.T™ Compound (Sakura Finetechnical Co, Tokyo, Japan). Then the mold was deposited on dry ice until the low temperature froze the O.C.T compound with the sample embedded in it. Samples were kept at -20°C until they were sectioned.

2.5.2.2 Peripheral nerves, spinal cord and DRG

10-20 um sections were obtained using a cryostat (Leica CM1900; Leica Microsystems, Wetzlar, Germany). Sections were placed on glass slides (Menzel-Gläser Super Frost Plus; Thermo Fisher Scientific, Waltham, MA, USA) and kept at -20°C until required for analysis.

The immunofluorescence protocol started with hydration of the samples by a 5-10 min wash in 0.05 M Tris pH 7.4 followed by two 5-10 min washes with wash buffer to permeabilize the cells. Then the samples were blocked, in order to avoid subsequent non-specific antibody binding, by incubation with blocking buffer 1 hour at RT. Then the primary antibody, or antibodies in case of multiple immunofluorescence, were diluted in blocking buffer to the adequate dilution. Samples were incubated with primary antibodies overnight at 4°C. Then, four 10-min washes with wash buffer were performed, before incubation with secondary antibodies. The secondary antibodies, which were conjugated with fluorophores, were diluted in blocking buffer, added to the samples and incubated in the dark for 1 hour at RT. Incubation was followed by four 10-min washes with wash buffer. At this point, unless some counterstaining was required, samples were ready to mount, for which we used Fluoromount

(Sigma-Aldrich, St. Louis, MO, USA) and glass cover slips (Menzel-Gläser, Thermo Fisher Scientific, Waltham, MA, USA).

Some samples were counterstained with a fluorescent hoechst stain in order to visualize the cell nuclei. The staining procedure was performed following manufacturer's instructions: for 10 min at RT without subsequent wash.

0.05 M Tris pH 7.4: 0.05 M Trizma[®] base (Sigma-Aldrich, St. Louis, MO, USA) in deionized water. Adjust pH with HCl 37% (Panreac, Castellar del Vallès, Barcelona, Spain).

Wash buffer: 0.05 M Tris pH 7.4, 0.01% TWEEN[®] 20 (Sigma-Aldrich)

Blocking buffer: 0.05 M Tris pH 7.4, 0.01% TWEEN[®] 20, 0.05% BSA (Sigma-Aldrich)

Images of the immunofluorescence analysis were taken using the epifluorescence microscope and the confocal microscope previously described.

2.5.2.3 mouse hind paw skin

50-60 um sections were obtained using a cryostat (Leica CM1900; Leica Microsystems, Wetzlar, Germany). Sections were placed on PBS in 96-well plate (Nunc; Thermo Fisher Scientific, Waltham, MA, USA) and kept at 4°C until required for analysis.

The immunofluorescence protocol started with two 5-10 min washes with wash buffer and then permeabilize the cells with PBS-Triton 0.3% 10 min. Then the samples were blocked (PBS-Triton0.3% and NDS 1.5%), in order to avoid subsequent non-specific antibody binding, by incubation 45 min at RT. Then the primary antibody PGP9.5, were diluted in blocking buffer to the adequate dilution. Samples were incubated with primary antibodies overnight at 4°C. Then, 1 h at RT and four 10min washes with wash buffer were performed, before incubation with secondary antibodies. The secondary antibodies, which were conjugated with fluorophores, were diluted in blocking buffer, added to the samples and incubated in the dark overnight at 4°C. 1h RT ncubation was followed by four 10min washes with wash buffer and counterstaining was required to visualizae nucleus. Slides were put on gelatinized glass slides and dehydrated in ethanol increased gradient (50°-70°-96°-100°, about 5min in each

one). Dry at RT and samples were ready to mount, for which we used Cytoseal™ and glass cover slips (Menzel-Gläser, Thermo Fisher Scientific, Waltham, MA, USA).

2.6 Cellular cultures techniques

2.6.1 SCs primary cultures

Transgenic P0TNFalpha and control wild type mice between three and five days after birth were sacrificed by cervical dislocation with forceps. They were washed with 70 % ethanol (Panreac) and the sciatic nerves extracted and kept in cold HBSS buffer with ions. The buffer was removed and the sciatic nerves were incubated for 40 min at 37°C (shaking every 10 min) in HBSS without ions, containing the enzymes to digest the nerves. Afterwards they were mechanically processed with up and down pipetting. When the sciatic nerves settled down on the bottom of the tube, the supernatant was transferred to another tube. HBSS without ions was again added to the nerves, pipetted and the supernatant added to the other tube. The digestion was inhibited by DF-10 medium and the cells 10 min centrifuged at 900 rpm. Afterwards they were counted, resuspended in DF-10 medium and about 500000 cells/well in a 6 well plate seeded, which were previously treated with polylysine (Sigma). After 24 h the medium of the cells was aspirated and centrifuged. Half of it was mixed with fresh DF-10 medium, containing 0,01 mM of the antimitotic substance cytosine arabinoside (Sigma) to inhibit fibroblast proliferation. After 48 h the medium was again aspirated, centrifuged and mixed with fresh DF-10 medium, containing 20 ug/ml pituitary extract (Sigma) and 0,5 uM forskolin (Sigma) to enhance the Schwann cell proliferation. This procedure was repeated every 48 h.

Some time considerations are necessary to know. To achieve a pure culture, a minimum of 5 days is required. The dissections are done on day 1, followed by 2 days of culture in the presence of the mitotic poison AraC. On day 5 or 6, the purity of the cells can be assessed. At this point, if no additional cells are required, they can be used immediately. If a greater number of Schwann cells are needed, the cultures can be expanded as needed.

Hank's Buffered Salt Solution: (HBSS buffer) with ions: Ca²⁺ and Mg²⁺; or without ions (Ca²⁺ and Mg²⁺): containing 2 % collagenase A (Sigma), 1%

trypsin (Sigma), 1% DNase (Sigma).

DF-10 medium: 250 ml DMEM (PAA) with 4,5 mg/ml glucose and L-glutamine, 100 ml MEM (PAA) containing 10 % fetal bovine serum (PAA), 1 % penicillin with streptomycin (PAA), 1 % vitamins (PAA), 1 % non essential amino acids (PAA), 2,5 % gentamicin (PAA)

2.7 Statistical analysis

All the statistics presented in this work were performed using Prims Graphpad. We used some general statistical tests and also other specific tests for some groups of data. In general we used two-tailed *t*-tests to analyze a dependent variable between two independent variables (groups). We used one-way ANOVA to analyze one dependent variable among three or more independent variables (groups). In these cases, we used Bonferroni *post hoc* tests for pairwise comparisons between groups. Finally, we performed two-way ANOVA to compare the data of a dependent variable and check for the effects and interaction of two independent variables. In most of the data analyzed, we did compare the data between the two different ages. Data are represented as mean \pm SEM. The statistical signification depicted on the graphs and tables corresponds to * $p < 0.05$, ** $p < 0.01$ and *** $p < 0.001$. The different pairwise comparisons are depicted using different symbols, which are specified in each graph or table.

VII. BIBLIOGRAPHY

1. Ariza, L. *et al.* Experimental diabetes in neonatal mice induces early peripheral sensorimotor neuropathy. *Neuroscience* **274**, (2014).
2. Ariza, L. *et al.* Central Nervous System Delivery of Helper-Dependent Canine Adenovirus Corrects Neuropathology and Behavior in Mucopolysaccharidosis Type VII Mice. *Hum. Gene Ther.* **25**, 199–211 (2014).
3. Arnett, M. G., Ryals, J. M. & Wright, D. E. NIH Public Access. *Brain* 32–42 (2008).
4. Arslantunali, D. Peripheral nerve conduits: technology update | MDER. *Med. Devices Evid. Res.* **7**, 405–424 (2014).
5. Baechner, D. *et al.* Widespread expression of the peripheral myelin protein??22 gene (pmp22) in neural and non??neural tissues during murine development. *J. Neurosci. Res.* **42**, 733–741 (1995).
6. Baron, P. *et al.* Developmental expression of P0 mRNA and P0 protein in the sciatic nerve and the spinal nerve roots of the rat. *J. Neurocytol.* **23**, 249–257 (1994).
7. Barrette, B., Calvo, E., Valli?res, N. & Lacroix, S. Transcriptional profiling of the injured sciatic nerve of mice carrying the Wld(S) mutant gene: Identification of genes involved in neuroprotection, neuroinflammation, and nerve regeneration. *Brain. Behav. Immun.* **24**, 1254–1267 (2010).
8. Bauder, A. R. & Ferguson, T. A. Reproducible Mouse Sciatic Nerve Crush and Subsequent Assessment of Regeneration by Whole Mount Muscle Analysis. *J. Vis. Exp.* (2012). doi:10.3791/3606
9. Beirowski, B. Concepts for regulation of axon integrity by enwrapping glia. *Front. Cell. Neurosci.* **7**, 1–22 (2013).
10. Biotechnologie, D. & Svinka, J. Characterization of a Transgenic Mouse Model Overexpressing TNF- α in Schwann Cells. (2010).
11. Bisht, K. *et al.* Dark microglia: A new phenotype predominantly associated with pathological states. *Glia* **64**, 826–839 (2016).
12. Boerboom, A., Dion, V., Chariot, A. & Franzen, R. Molecular Mechanisms Involved in Schwann Cell Plasticity. *Front. Mol. Neurosci.* **10**, 1–18 (2017).
13. Bosse, F., Brodbeck, J. & M??ller, H. W. Post-transcriptional regulation of the peripheral myelin protein gene PMP22/Gas3. *J. Neurosci. Res.* **55**, 164–177 (1999).
14. Bouhy, D. *et al.* Delayed GM-CSF treatment stimulates axonal regeneration and functional recovery in paraplegic rats via an increased BDNF expression by endogenous macrophages. *FASEB J.* **20**, 1239–1241 (2006).
15. Bremer, M. *et al.* Sox10 is required for Schwann-cell homeostasis and myelin maintenance in the adult peripheral nerve. *Glia* **59**, 1022–1032 (2011).
16. Brunden, K. R., Ding, Y. & Hennington, B. S. Myelin Protein Expression in Dissociated Superior Cervical-Ganglia and Dorsal-Root Ganglia Cultures. *J. Neurosci. Res.* **32**, 507–515 ST-Myelin Protein Expression in Dissoci (1992).
17. Buchheit, T., Van de Ven, T. & Shaw, A. Epigenetics and the transition from acute to chronic pain. *Pain Med.* **13**, 1474–90 (2012).
18. Chattopadhyay, S., Raychaudhuri, U. & Chakraborty, R. Artificial sweeteners - a review. *J. Food Sci. Technol.* **51**, 611–21 (2014).
19. Chen, L. *et al.* Spatiotemporal Expression of SSeCKS in Injured Rat Sciatic Nerve. *Anat. Rec. Adv. Integr. Anat. Evol. Biol.* **291**, 527–537 (2008).

20. Chen, P., Piao, X. & Bonaldo, P. Role of macrophages in Wallerian degeneration and axonal regeneration after peripheral nerve injury. *Acta Neuropathol.* **130**, 605–618 (2015).
21. Chen, P., Piao, X. & Bonaldo, P. Role of macrophages in Wallerian degeneration and axonal regeneration after peripheral nerve injury. *Acta Neuropathol.* **130**, 605–618 (2015).
22. Chin, Y. E., Kitagawa, M., Kuida, K., Flavell, R. A. & Fu, X. Y. Activation of the STAT signaling pathway can cause expression of caspase 1 and apoptosis. *Mol. Cell. Biol.* **17**, 5328–37 (1997).
23. Chong, M. S. *et al.* GAP-43 expression in primary sensory neurons following central axotomy. *J. Neurosci.* **14**, 4375–84 (1994).
24. Chung, T., Prasad, K. & Lloyd, T. E. Peripheral neuropathy: clinical and electrophysiological considerations. *Neuroimaging Clin. N. Am.* **24**, 49–65 (2014).
25. Clark, A. K., Old, E. A. & Malcangio, M. Neuropathic pain and cytokines: Current perspectives. *J. Pain Res.* **6**, 803–814 (2013).
26. Clin, H. Peripheral Nerve Trauma : Mechanisms of Injury and Recovery. **29**, 317–330 (2015).
27. Cobianchi, S., de Cruz, J. & Navarro, X. Assessment of sensory thresholds and nociceptive fiber growth after sciatic nerve injury reveals the differential contribution of collateral reinnervation and nerve regeneration to neuropathic pain. *Exp. Neurol.* **255**, 1–11 (2014).
28. Cole, K. L. H., Early, J. J. & Lyons, D. A. Drug discovery for remyelination and treatment of MS. *Glia* (2017). doi:10.1002/glia.23166
29. Combs, C. K., Karlo, J. C., Kao, S. C. & Landreth, G. E. beta-Amyloid stimulation of microglia and monocytes results in TNFalpha-dependent expression of inducible nitric oxide synthase and neuronal apoptosis. *J. Neurosci.* **21**, 1179–1188 (2001).
30. Cosgaya, J. M. The Neurotrophin Receptor p75NTR as a Positive Modulator of Myelination. *Science (80-.)*. **298**, 1245–1248 (2002).
31. Csiszar, A. *et al.* Vasculoprotective Effects of Anti-Tumor Necrosis Factor- α Treatment in Aging. *Am. J. Pathol.* **170**, 388–398 (2007).
32. Curtis, R. *et al.* GAP-43 is expressed by nonmyelin-forming Schwann cells of the peripheral nervous system. *J. Cell Biol.* **116**, 1455–1464 (1992).
33. Devier, D. J., Lovera, J. F. & Lukiw, W. J. Increase in NF- κ B-sensitive miRNA-146a and miRNA-155 in multiple sclerosis (MS) and pro-inflammatory neurodegeneration. *Front. Mol. Neurosci.* **8**, 5 (2015).
34. Dib-Hajj, S. D. *et al.* Gain-of-function mutation in Nav1.7 in familial erythromelalgia induces bursting of sensory neurons. *Brain* **128**, 1847–1854 (2005).
35. Dobretsov, M., Romanovsky, D. & Stimers, J. R. Early diabetic neuropathy: Triggers and mechanisms. *World J. Gastroenterol.* **13**, 175–191 (2007).
36. Domenech-Estevez, E. *et al.* Akt Regulates Axon Wrapping and Myelin Sheath Thickness in the PNS. *J. Neurosci.* **36**, 4506–4521 (2016).
37. Faber, C. G. *et al.* Gain-of-function Nav1.8 mutations in painful neuropathy. *Proc. Natl. Acad. Sci.* **109**, 19444–19449 (2012).
38. Fakhruddin, S., Alanazi, W. & Jackson, K. E. Diabetes-Induced Reactive Oxygen Species: Mechanism of Their Generation and Role in Renal Injury. *J. Diabetes Res.* **2017**, 1–30 (2017).

39. Fillit, H. *et al.* Elevated circulating tumor necrosis factor levels in Alzheimer's disease. *Neurosci. Lett.* **129**, 318–20 (1991).
40. Firouzi, M. *et al.* Schwann cell apoptosis and p75NTR siRNA. *Iran. J. Allergy, Asthma Immunol.* **10**, 53–59 (2011).
41. Fledrich, R., Stassart, R. M. & Sereda, M. W. Murine therapeutic models for Charcot-Marie-Tooth (CMT) disease. *Br. Med. Bull.* **102**, 89–113 (2012).
42. Frezel, N., Sohet, F., Daneman, R., Basbaum, A. I. & Braz, J. M. Peripheral and central neuronal ATF3 precedes CD4⁺ T-cell infiltration in EAE. *Exp. Neurol.* **283**, 224–234 (2016).
43. Fricker, B., Muller, A. & René, F. Evaluation tools and animal models of peripheral neuropathies. *Neurodegener. Dis.* **5**, 72–108 (2008).
44. Fromont, A., De Seze, J., Fleury, M. C., Maillefert, J. F. & Moreau, T. Inflammatory demyelinating events following treatment with anti-tumor necrosis factor. *Cytokine* **45**, 55–57 (2009).
45. Gaesser, J. M. & Fyffe-Maricich, S. L. Intracellular signaling pathway regulation of myelination and remyelination in the CNS. *Exp. Neurol.* **283**, 501–511 (2016).
46. Garbay, B., Heape, A. M., Sargueil, F. & Cassagne, C. Myelin synthesis in the peripheral nervous system. *Prog. Neurobiol.* **61**, 267–304 (2000).
47. Gaudet, A. D., Popovich, P. G. & Ramer, M. S. Wallerian degeneration: gaining perspective on inflammatory events after peripheral nerve injury. *J. Neuroinflammation* **8**, 110 (2011).
48. Ge, S. *et al.* Associations of serum anti-ganglioside antibodies and inflammatory markers in diabetic peripheral neuropathy. *Diabetes Res. Clin. Pract.* **115**, 68–75 (2016).
49. Gillingwater, T. H. *et al.* Age-dependent synapse withdrawal at axotomised neuromuscular junctions in Wld(s) mutant and Ube4b/Nmnat transgenic mice. *J. Physiol.* **543**, 739–55 (2002).
50. Girolami, E. I. Anti-inflammatory mechanisms in Wallerian degeneration in injured peripheral nerve. *Diss. Abstr. Int. Sect. B Sci. Eng.* **72**, 695 (2011).
51. Goldfarb, W. Wittgenstein's. *I Can* doi:10.1111/j.1467-8330.1974.tb00606.x
52. Goldstein, E. Z., Church, J. S., Hesp, Z. C., Popovich, P. G. & McTigue, D. M. A silver lining of neuroinflammation: Beneficial effects on myelination. *Exp. Neurol.* **283**, 550–559 (2016).
53. González-Clemente, J. M. *et al.* Diabetic neuropathy is associated with activation of the TNF- α system in subjects with type 1 diabetes mellitus. *Clin. Endocrinol. (Oxf)*. **63**, 525–9 (2005).
54. Goodpaster, T. *et al.* An Immunohistochemical Method for Identifying Fibroblasts in Formalin-fixed, Paraffin-embedded Tissue. *J. Histochem. Cytochem.* **56**, 347–358 (2008).
55. Gordon, S. Alternative activation of macrophages. *Nat. Rev. Immunol.* **3**, 23–35 (2003).
56. Griffin, W. S. *et al.* Brain interleukin 1 and S-100 immunoreactivity are elevated in Down syndrome and Alzheimer disease. *Proc. Natl. Acad. Sci. U. S. A.* **86**, 7611–5 (1989).
57. Group, I. A. 2012 Allodi axonal growth capacity. 1–204 (2012).
58. Hall, B. E. *et al.* Conditional TNF- α Overexpression in the Tooth and Alveolar Bone Results in Painful Pulpitis and Osteitis. *J. Dent. Res.* **95**, 188–195 (2016).

59. Harati, Y. Diabetic Neuropathies: Unanswered Questions. *Neurol. Clin.* **25**, 303–317 (2007).
60. He, P. *et al.* Deletion of tumor necrosis factor death receptor inhibits amyloid beta generation and prevents learning and memory deficits in Alzheimer's mice. *J. Cell Biol.* **178**, 829–41 (2007).
61. Hirata, K. & Kawabuchi, M. Myelin phagocytosis by macrophages and nonmacrophages during Wallerian degeneration. *Microsc. Res. Tech.* **57**, 541–547 (2002).
62. Höke, A. Animal Models of Peripheral Neuropathies. *Neurotherapeutics* **9**, 262–269 (2012).
63. Horiuchi, T., Mitoma, H., Harashima, S. I., Tsukamoto, H. & Shimoda, T. Transmembrane TNF- α : Structure, function and interaction with anti-TNF agents. *Rheumatology* **49**, 1215–1228 (2010).
64. Hörste, G. M. Z., Hu, W., Hartung, H. P., Lehmann, H. C. & Kieseier, B. C. The immunocompetence of Schwann cells. *Muscle and Nerve* **37**, 3–13 (2008).
65. Hövelmeyer, N. *et al.* Apoptosis of oligodendrocytes via Fas and TNF-R1 is a key event in the induction of experimental autoimmune encephalomyelitis. *J. Immunol.* **175**, 5875–84 (2005).
66. Hu, X., Hu, J., Dai, L., Trapp, B. & Yan, R. Axonal and Schwann Cell BACE1 Is Equally Required for Remyelination of Peripheral Nerves. *J. Neurosci.* **35**, 3806–3814 (2015).
67. Hu, X., Fan, Q., Hou, H. & Yan, R. Neurological dysfunctions associated with altered BACE1-dependent Neuregulin-1 signaling. *J. Neurochem.* **136**, 234–249 (2016).
68. Hu, X. *et al.* Both MicroRNA-155 and Virus-Encoded MiR-155 Ortholog Regulate TLR3 Expression. *PLoS One* **10**, e0126012 (2015).
69. Hunt, D. *et al.* ATF3 upregulation in glia during Wallerian degeneration: differential expression in peripheral nerves and CNS white matter. *BMC Neurosci.* **5**, 9 (2004).
70. Ibáñez, C. F. & Simi, A. P75 neurotrophin receptor signaling in nervous system injury and degeneration: paradox and opportunity. *Trends Neurosci.* **35**, 431–440 (2012).
71. Imai, Y. & Kohsaka, S. Intracellular signaling in M-CSF-induced microglia activation: Role of Iba1. *Glia* **40**, 164–174 (2002).
72. Ishii, A., Furusho, M. & Bansal, R. Sustained Activation of ERK1/2 MAPK in Oligodendrocytes and Schwann Cells Enhances Myelin Growth and Stimulates Oligodendrocyte Progenitor Expansion. *J. Neurosci.* **33**, 175–186 (2013).
73. Jaggi, A. S., Jain, V. & Singh, N. Animal models of neuropathic pain. *Fundam. Clin. Pharmacol.* **25**, 1–28 (2011).
74. Ji, R.-R. & Strichartz, G. Cell Signaling and the Genesis of Neuropathic Pain. *Sci. Signal.* **2004**, re14-re14 (2004).
75. Kagiava, A. *et al.* Intrathecal gene therapy rescues a model of demyelinating peripheral neuropathy. *Proc. Natl. Acad. Sci.* **113**, E2421–E2429 (2016).
76. Kai, L. *et al.* The immunohistochemical characterization of human fetal olfactory bulb and olfactory ensheathing cells in culture as a source for clinical CNS restoration. *Anat. Rec.* **293**, 359–369 (2010).
77. Kangas, S. M. *et al.* An approach to comprehensive genome and proteome expression analyses in Schwann cells and neurons during peripheral nerve

- myelin formation. *J. Neurochem.* 830–844 (2016). doi:10.1111/jnc.13722
78. Kataoka, K., Kanje, M. & Dahlin, L. B. Induction of activating transcription factor 3 after different sciatic nerve injuries in adult rats. *Scand. J. Plast. Reconstr. Surg. Hand Surg.* **41**, 158–66 (2007).
 79. Khamaneh, A. M., Alipour, M. R., Sheikhzadeh Hesari, F. & Ghadiri Soufi, F. A signature of microRNA-155 in the pathogenesis of diabetic complications. *J. Physiol. Biochem.* **71**, 301–309 (2015).
 80. Kiguchi, N., Maeda, T., Kobayashi, Y., Fukazawa, Y. & Kishioka, S. Macrophage inflammatory protein-1 α mediates the development of neuropathic pain following peripheral nerve injury through interleukin-1 α up-regulation. *Pain* **149**, 305–315 (2010).
 81. Kim, H. A., Mindos, T. & Parkinson, D. B. Plastic Fantastic: Schwann Cells and Repair of the Peripheral Nervous System. *Stem Cells Transl. Med.* **2**, 553–557 (2013).
 82. Kuhn, G., Lie, A., Wilms, S. & Müller, H. W. Coexpression of PMP22 gene with MBP and P0 during de novo myelination and nerve repair. *Glia* **8**, 256–264 (1993).
 83. Kwa, M. S. G. *et al.* Autoimmunoreactivity to Schwann cells in patients with inflammatory neuropathies. *Brain* **126**, 361–375 (2003).
 84. Kwon, M. J. *et al.* CCL2 Mediates Neuron-Macrophage Interactions to Drive Proregenerative Macrophage Activation Following Preconditioning Injury. *J. Neurosci.* **35**, 15934–15947 (2015).
 85. LeBlanc, S. E. *et al.* Regulation of cholesterol/lipid biosynthetic genes by Egr2/Krox20 during peripheral nerve myelination. *J. Neurochem.* **93**, 737–748 (2005).
 86. Lees, J. G., Duffy, S. S. & Moalem-Taylor, G. Immunotherapy targeting cytokines in neuropathic pain. *Front. Pharmacol.* **4 NOV**, 1–4 (2013).
 87. Leung, L. & Cahill, C. M. TNF-alpha and neuropathic pain--a review. *J. Neuroinflammation* **7**, 27 (2010).
 88. Levy, D., Höke, A. & Zochodne, D. W. Local expression of inducible nitric oxide synthase in an animal model of neuropathic pain. *Neurosci. Lett.* **260**, 207–9 (1999).
 89. Liefner, M. *et al.* The role of TNF-alpha during Wallerian degeneration. *J. Neuroimmunol.* **108**, 147–52 (2000).
 90. Lim, E.-M. F. *et al.* AlphaB-crystallin regulates remyelination after peripheral nerve injury. *Proc. Natl. Acad. Sci.* **114**, E1707–E1716 (2017).
 91. Liu, C. & Tang, J. Expression levels of tumor necrosis factor- α and the corresponding receptors are correlated with trauma severity. *Oncol. Lett.* **8**, 2747–2751 (2014).
 92. Liu, F. *et al.* Suppression of MyD88-dependent signaling alleviates neuropathic pain induced by peripheral nerve injury in the rat. *J. Neuroinflammation* **14**, 70 (2017).
 93. Liu, L. *et al.* Increased TNFR1 expression and signaling in injured peripheral nerves of mice with reduced BACE1 activity. *Neurobiol. Dis.* **93**, 21–27 (2016).
 94. Liu, X. *et al.* AMPK Negatively Regulates Peripheral Myelination via Activation of c-Jun. *Mol. Neurobiol.* 1–11 (2016). doi:10.1007/s12035-016-9913-3
 95. Liu, Z. *et al.* Specific Marker Expression and Cell State of Schwann Cells

- during Culture In Vitro. *PLoS One* **10**, e0123278 (2015).
96. López-Álvarez, V. M., Modol, L., Navarro, X. & Cobianchi, S. Early increasing-intensity treadmill exercise reduces neuropathic pain by preventing nociceptor collateral sprouting and disruption of chloride cotransporters homeostasis after peripheral nerve injury. *Pain* **156**, 1812–1825 (2015).
 97. Ma, Y. *et al.* A novel recombinant slow-release TNF α -derived peptide effectively inhibits tumor growth and angiogenesis. *Sci. Rep.* **5**, 13595 (2015).
 98. Maier, M., Berger, P., Nave, K.-A. & Suter, U. Identification of the Regulatory Region of the Peripheral Myelin Protein 22 (PMP22) Gene That Directs Temporal and Spatial Expression in Development and Regeneration of Peripheral Nerves. *Mol. Cell. Neurosci.* **20**, 93–109 (2002).
 99. Mancuso, R. Electrophysiological biomarkers for the study of new therapeutic strategies for motoneuron disease. (2014).
 100. Manuscript, A. & Nanostructures, S. P. C. NIH Public Access. *Nano* **6**, 2166–2171 (2008).
 101. Martini, R. & Willison, H. Neuroinflammation in the peripheral nerve: Cause, modulator, or bystander in peripheral neuropathies? *Glia* **64**, 475–486 (2016).
 102. MC Deeds, JM Anderson, AS Armstrong, DA Gastineau, HJ Hiddinga, A Jahangir, N. & Eberhardt, and Y. K. Single Dose Streptozotocin Induced Diabetes: Considerations for Study Design in Islet Transplantation Models. *Lab. Anim.* **45**, 131–140 (2011).
 103. McElroy, P. D. *et al.* Predicting outcome in malaria: Correlation between rate of exposure to infected mosquitoes and level of Plasmodium falciparum parasitemia. *Am. J. Trop. Med. Hyg.* **51**, 523–532 (1994).
 104. Menorca, R. M. G., Fussell, T. S. & Elfar, J. C. Nerve physiology: mechanisms of injury and recovery. *Hand Clin.* **29**, 317–30 (2013).
 105. Mijatovic, T. *et al.* Tumor necrosis factor-alpha mRNA remains unstable and hypoadenylated upon stimulation of macrophages by lipopolysaccharides. *Eur. J. Biochem.* **267**, 6004–12 (2000).
 106. Misra, U. K., Kalita, J. & Nair, P. P. Diagnostic approach to peripheral neuropathy. *Ann. Indian Acad. Neurol.* **11**, 89–97 (2008).
 107. Mittal, M., Siddiqui, M. R., Tran, K., Reddy, S. P. & Malik, A. B. Reactive oxygen species in inflammation and tissue injury. *Antioxid. Redox Signal.* **20**, 1126–67 (2014).
 108. Mokarram, N., Merchant, A., Mukhatyar, V., Patel, G. & Bellamkonda, R. V. Effect of modulating macrophage phenotype on peripheral nerve repair. *Biomaterials* **33**, 8793–8801 (2012).
 109. Mu, Z.-P. *et al.* Association Between Tumor Necrosis Factor- α and Diabetic Peripheral Neuropathy in Patients with Type 2 Diabetes: a Meta-Analysis. *Mol. Neurobiol.* **54**, 983–996 (2017).
 110. Mueller, M. *et al.* Macrophage Response to Peripheral Nerve Injury: The Quantitative Contribution of Resident and Hematogenous Macrophages. *Lab. Investig.* **83**, 175–185 (2003).
 111. Myers, R. R. *et al.* HHS Public Access. **16**, 277–286 (2015).
 112. Nickols, J. C., Valentine, W., Kanwal, S. & Carter, B. D. Activation of the transcription factor NF- κ B in Schwann cells is required for peripheral myelin formation. *Nat. Neurosci.* **6**, 161–167 (2003).
 113. Nieto-Vazquez, I. *et al.* Insulin resistance associated to obesity: the link TNF-

- alpha. *Arch. Physiol. Biochem.* **114**, 183–194 (2008).
114. Nishimoto, S. *et al.* Neurotrophin attenuates local inflammatory response and inhibits demyelination induced by chronic constriction injury of the mouse sciatic nerve. *Biologicals* **44**, 206–211 (2016).
 115. Nseir, W. Soft drinks consumption and nonalcoholic fatty liver disease. *World J. Gastroenterol.* **16**, 2579 (2010).
 116. O'brien, P. D., Sakowski, S. A. & Feldman, E. L. Mouse models of diabetic neuropathy. *ILARJ.* **54**, 259–272 (2014).
 117. Oliveira Junior, J. O. de *et al.* Inflammatory mediators of neuropathic pain. *Rev. Dor* **17**, 35–42 (2016).
 118. Omura, T. *et al.* Different expressions of BDNF, NT3, and NT4 in muscle and nerve after various types of peripheral nerve injuries. *J. Peripher. Nerv. Syst.* **10**, 293–300 (2005).
 119. Pasnoor, M., Dimachkie, M. M., Kluding, P. & Barohn, R. J. Diabetic neuropathy part 1. Overview and symmetric phenotypes. *Neurol. Clin.* **31**, 425–445 (2013).
 120. Patodia, S. & Raivich, G. Role of Transcription Factors in Peripheral Nerve Regeneration. *Front. Mol. Neurosci.* **5**, 1–15 (2012).
 121. Pavić, R., Pavić, M. L., Tot, O. K., Benšić, M. & Heffer-Lauc, M. Side distinct sciatic nerve recovery differences between rats and mice. *Somatosens. Mot. Res.* **25**, 163–170 (2008).
 122. Peluffo, H. *et al.* CD300f immunoreceptor contributes to peripheral nerve regeneration by the modulation of macrophage inflammatory phenotype. *J. Neuroinflammation* **12**, 145 (2015).
 123. Peluffo, H. *et al.* CD300f immunoreceptor contributes to peripheral nerve regeneration by the modulation of macrophage inflammatory phenotype. *J. Neuroinflammation* **12**, 145 (2015).
 124. Pinheiro, R., Salles, J., Sarno, E. & Sampaio, E. Mycobacterium leprae–host-cell interactions and genet. *Futur. Microbiol* **6**, 217–230 (2011).
 125. Probert, L., Akassoglou, K., Pasparakis, M., Kontogeorgos, G. & Kollias, G. Spontaneous inflammatory demyelinating disease in transgenic mice showing central nervous system-specific expression of tumor necrosis factor alpha. *Proc. Natl. Acad. Sci. U. S. A.* **92**, 11294–8 (1995).
 126. Putko, B. N. *et al.* Circulating levels of tumor necrosis factor-alpha receptor 2 are increased in heart failure with preserved ejection fraction relative to heart failure with reduced ejection fraction: evidence for a divergence in pathophysiology. *PLoS One* **9**, e99495 (2014).
 127. Quintes, S. *et al.* Zeb2 is essential for Schwann cell differentiation, myelination and nerve repair. *Nat. Neurosci.* **19**, 1050–1059 (2016).
 128. Rachana, K. S., Manu, M. S. & Advirao, G. M. Insulin influenced expression of myelin proteins in diabetic peripheral neuropathy. *Neurosci. Lett.* **629**, 110–115 (2016).
 129. Ramesh, G., MacLean, A. G. & Philipp, M. T. Cytokines and chemokines at the crossroads of neuroinflammation, neurodegeneration, and neuropathic pain. *Mediators Inflamm.* **2013**, 480739 (2013).
 130. Rao, S. N. R. & Pearse, D. D. Regulating Axonal Responses to Injury: The Intersection between Signaling Pathways Involved in Axon Myelination and The Inhibition of Axon Regeneration. *Front. Mol. Neurosci.* **9**, 1–28 (2016).
 131. Reichert, F., Saada, a & Rotshenker, S. Peripheral nerve injury induces

- Schwann cells to express two macrophage phenotypes: phagocytosis and the galactose-specific lectin MAC-2. *J. Neurosci.* **14**, 3231–3245 (1994).
132. Rieckmann, P. *et al.* Tumor necrosis factor-alpha messenger RNA expression in patients with relapsing-remitting multiple sclerosis is associated with disease activity. *Ann. Neurol.* **37**, 82–8 (1995).
 133. Rigaud, M. *et al.* NIH Public Access. *Pain* **136**, 188–201 (2008).
 134. Robson, T. & Hirst, D. G. Transcriptional targeting in cancer gene therapy. *J. Biomed. Biotechnol.* **2003**, 110–137 (2003).
 135. Romero, A. Q. Implicación de las citoquinas TNF- α e IL-6 y de las metalotioneínas... (2007).
 136. Salazar, P. M. the Role of Neurotrophins and Neurotrophin Receptors in the Pathogenesis of Neurodegeneration and Neuroregeneration. (2014).
 137. Santos, D., Gonzalez-Perez, F., Navarro, X. & Del Valle, J. Dose-Dependent Differential Effect of Neurotrophic Factors on In Vitro and In Vivo Regeneration of Motor and Sensory Neurons. *Neural Plast.* **2016**, 4969523 (2016).
 138. Sawada, T. *et al.* Spatiotemporal quantification of tumor necrosis factor-alpha and interleukin-10 after crush injury in rat sciatic nerve utilizing immunohistochemistry. *Neurosci. Lett.* **417**, 55–60 (2007).
 139. Scheib, J. L. & H?ke, A. An attenuated immune response by Schwann cells and macrophages inhibits nerve regeneration in aged rats. *Neurobiol. Aging* **45**, 1–9 (2016).
 140. Seijffers, R., Mills, C. D. & Woolf, C. J. ATF3 Increases the Intrinsic Growth State of DRG Neurons to Enhance Peripheral Nerve Regeneration. *J. Neurosci.* **27**, 7911–7920 (2007).
 141. Shamash, S., Reichert, F. & Rotshenker, S. The cytokine network of Wallerian degeneration: tumor necrosis factor-alpha, interleukin-1alpha, and interleukin-1beta. *J. Neurosci.* **22**, 3052–60 (2002).
 142. Shi, X., Chen, Y., Nadeem, L. & Xu, G. Beneficial effect of TNF- α inhibition on diabetic peripheral neuropathy. *J. Neuroinflammation* **10**, 69 (2013).
 143. Shi, X., Chen, Y., Nadeem, L. & Xu, G. Beneficial effect of TNF- α inhibition on diabetic peripheral neuropathy. *J. Neuroinflammation* **10**, 836 (2013).
 144. Shy, M. E. Inherited Neuromuscular Diseases. **652**, 171–181 (2009).
 145. Simmons, R. D. & Willenborg, D. O. Direct injection of cytokines into the spinal cord causes autoimmune encephalomyelitis-like inflammation. *J. Neurol. Sci.* **100**, 37–42 (1990).
 146. Siqueira Mietto, B. *et al.* Role of IL-10 in Resolution of Inflammation and Functional Recovery after Peripheral Nerve Injury. *J. Neurosci.* **35**, 16431–16442 (2015).
 147. Smith, D., Tweed, C., Fernyhough, P. & Glazner, G. W. Nuclear factor-kappaB activation in axons and Schwann cells in experimental sciatic nerve injury and its role in modulating axon regeneration: studies with etanercept. *J. Neuropathol. Exp. Neurol.* **68**, 691–700 (2009).
 148. Sonoda, Y. *et al.* Circulating TNF receptors 1 and 2 are associated with the severity of renal interstitial fibrosis in IgA nephropathy. *PLoS One* **10**, e0122212 (2015).
 149. Steinle, J. J., Sharma, S., Smith, C. P. & McFayden-Ketchum, L. S. Normal aging involves modulation of specific inflammatory markers in the rat retina and choroid. *Journals Gerontol. - Ser. A Biol. Sci. Med. Sci.* **64**, 325–331 (2009).

150. Stoecklin, G., Lu, M., Rattenbacher, B. & Moroni, C. A constitutive decay element promotes tumor necrosis factor alpha mRNA degradation via an AU-rich element-independent pathway. *Mol. Cell. Biol.* **23**, 3506–15 (2003).
151. Stratton, J. A., Kumar, R., Sinha, S., Shah, P. & Stykel, M. Purification and Characterization of Schwann Cells from Adult Human Skin and Nerve. **4**, 1–15 (2017).
152. Stratton, J. A. *et al.* The immunomodulatory properties of adult skin-derived precursor Schwann cells: Implications for peripheral nerve injury therapy. *Eur. J. Neurosci.* **43**, 365–375 (2016).
153. Strickland, I. T. *et al.* Changes in the expression of Nav1.7, Nav1.8 and Nav1.9 in a distinct population of dorsal root ganglia innervating the rat knee joint in a model of chronic inflammatory joint pain. *Eur. J. Pain* **12**, 564–572 (2008).
154. Sulaiman, W. & Gordon, T. Neurobiology of Peripheral Nerve Injury, Regeneration, and Functional Recovery: From Bench Top Research to Bedside Application. *Ochsner J.* **13**, 100–108 (2013).
155. Susuki, K. Myelin: a specialized membrane for cell communication. *Nat. Educ.* **3**, 59 (2010).
156. Suter, U. & Snipes, G. J. Peripheral myelin protein 22: Facts and hypotheses. *J. Neurosci. Res.* **40**, 145–151 (1995).
157. Svehlens, Å. & Dahlin, L. Repair of the Peripheral Nerve—Remyelination that Works. *Brain Sci.* **3**, 1182–1197 (2013).
158. Sykam, A. *et al.* Association of tumor necrosis factor-alpha and interferon gamma gene polymorphisms and their plasma levels in leprosy, HIV and other peripheral neuropathies. *Cytokine* **76**, 473–479 (2015).
159. Tanaka, T. *et al.* Microglia support ATF3-positive neurons following hypoglossal nerve axotomy. *Neurochem. Int.* 1–11 (2017). doi:10.1016/j.neuint.2017.05.007
160. Tao, Y. in *Methods in molecular biology (Clifton, N.J.)* **1018**, 93–104 (2013).
161. Taveggia, C., Feltri, M. L. & Wrabetz, L. NIH Public Access. *Cell* **6**, 276–287 (2011).
162. Thakor, D. K. *et al.* Increased Peripheral Nerve Excitability and Local Nav1.8 RNA Up-Regulation in Painful Neuropathy. *Mol. Pain* **5**, 1744-8069-5-14 (2009).
163. Town, T. *et al.* T-Cells in Alzheimer’s disease. *Neuromolecular Med.* **8**, 175–190 (2006).
164. Tsouni, P. *et al.* Anti-TNF alpha medications and neuropathy. *J. Peripher. Nerv. Syst.* **20**, 397–402 (2015).
165. Tsukahara, R. & Ueda, H. Myelin-related gene silencing mediated by LPA1 ??? Rho/ROCK signaling is correlated to acetylation of NF??B in S16 Schwann cells. *J. Pharmacol. Sci.* **132**, 162–165 (2016).
166. Velanac, V. *et al.* Bace1 processing of NRG1 type III produces a myelin-inducing signal but is not essential for the stimulation of myelination. *Glia* **60**, 203–217 (2012).
167. Verdiyan, E. E., Allakhverdiev, E. S. & Maksimov, G. V. Study of the peripheral nerve fibers myelin structure changes during activation of Schwann cell acetylcholine receptors. *PLoS One* **11**, 1–10 (2016).
168. Verdú, E., Ceballos, D., Vilches, J. J. & Navarro, X. Influence of aging on peripheral nerve function and regeneration. *J. Peripher. Nerv. Syst.* **5**, 191–

- 208 (2000).
169. Wagner, R. & Myers, R. R. Schwann cells produce tumor necrosis factor alpha: expression in injured and non-injured nerves. *Neuroscience* **73**, 625–629 (1996).
 170. Walthers, C. M. & Seidlits, S. K. Gene Delivery Strategies to Promote Spinal Cord Repair. *Biomarkers Insights* **10**, 10–12 (2015).
 171. Watkins, L. R., Goehler, L. E., Relton, J., Brewer, M. T. & Maier, S. F. Mechanisms of tumor necrosis factor-alpha (TNF-alpha) hyperalgesia. *Brain Res.* **692**, 244–250 (1995).
 172. Whitwam, J. G. Classification of peripheral nerve fibres. *Anaesthesia* **31**, 494–503 (1976).
 173. Willem, M. Proteolytic processing of Neuregulin-1. *Brain Res. Bull.* **126**, 178–182 (2016).
 174. Wu, L. M. N. *et al.* Zeb2 recruits HDAC–NuRD to inhibit Notch and controls Schwann cell differentiation and remyelination. *Nat. Neurosci.* **19**, 1060–1072 (2016).
 175. Xie, W., Strong, J. A. & Zhang, J.-M. Active nerve regeneration with failed target reinnervation drives persistent neuropathic pain. *Eneuro* **4**, ENEURO.0008-17.2017 (2017).
 176. Xu, Y. *et al.* 5-Hydroxymethylcytosine Represses the Activity of Enhancers in Embryonic Stem Cells: a New Epigenetic Signature for Gene Regulation. *Cell* **15**, 1–15 (2013).
 177. Ydens, E. *et al.* Acute injury in the peripheral nervous system triggers an alternative macrophage response. *J. Neuroinflammation* **9**, 641 (2012).
 178. Ydens, E. *et al.* The neuroinflammatory role of Schwann cells in disease. *Neurobiol. Dis.* **55**, 95–103 (2013).
 179. Yoshizumi, M., Perrella, M. A., Burnett, J. C. & Lee, M. E. Tumor necrosis factor downregulates an endothelial nitric oxide synthase mRNA by shortening its half-life. *Circ. Res.* **73**, 205–9 (1993).
 180. Young, P. & Sueter, U. Animal models of hereditary neuropathies. *Hered. Peripher. Neuropathies* **22**, 227–236 (2005).
 181. Yu, C. G. Distinct roles for ERK1 and ERK2 in pathophysiology of CNS. *Front. Biol. (Beijing)*. **7**, 267–276 (2012).
 182. Zhang, Y., Li, J., Wang, T. & Wang, J. Amplitude of sensory nerve action potential in early stage diabetic peripheral neuropathy: an analysis of 500 cases. *Neural Regen. Res.* **9**, 1389–94 (2014).
 183. Zhou, Y. & Notterpek, L. Promoting peripheral myelin repair. *Exp. Neurol.* **283**, 573–580 (2016).